

**Proteins under the control
of phospholipase D in
*Arabidopsis thaliana***

Dissertation

zur Erlangung des Doktorgrades (Dr. rer. nat.)
der
Mathematisch–Naturwissenschaftlichen Fakultät
der
Rheinischen Friedrich–Wilhelms–Universität Bonn

vorgelegt von

Guido Ufer

aus Gummersbach, Deutschland

am: 24.11.2015

Bonn, 2015

Erscheinungsjahr: 2016

Promotionsprüfung: 23.02.2016

1. Gutachter: Prof. Dr. Dorothea Bartels
2. Gutachter: Dr. Hans-Hubert Kirch

Acknowledgements	V
Abbreviations	VII
List of tables	IX
List of figures	X
1 Introduction	13
1.1 The phospholipase family	13
1.1.1 Phospholipase D	14
1.2 Phosphatidic acid	16
1.3 Proteins under the control of phospholipase D	19
1.4 The unknown protein At5g39570.1	21
1.5 Phosphorylation of proteins	22
1.6 Intrinsically disordered proteins	23
1.7 Aims of this study	24
2 Materials and methods	25
2.1 Materials	25
2.1.1 Chemicals	25
2.1.2 Equipment	26
2.1.3 Computer programs and databases	26
2.1.4 Enzymes and markers	28
2.1.5 Primer	28
2.1.6 Vectors	31
2.1.7 Kits	31
2.1.8 DNA-sequencing	31
2.1.9 Quantification of proteins and RNA	32
2.2 Plant material	32
2.2.1 Sterilization of seeds	33
2.2.2 Growth conditions	33
2.3 Microorganisms	35
2.3.1 Bacterial and yeast strains	35
2.3.2 Media for microorganisms	35
2.3.3 Generation of rubidium chloride-competent cells	36
2.3.4 Generation of electro-competent <i>A. tumefaciens</i>	36
2.3.5 Glycerol stocks	37
2.4 Cloning methods	37
2.4.1 Electrophoresis of nucleic acids	37
2.4.2 Isolation and purification of plasmid DNA	37
2.4.3 Purification of DNA	38
2.4.4 Restriction digestion	38
2.4.5 Ligation	39
2.4.6 Transformation of rubidium chloride-competent <i>E. coli</i>	39

2.4.7	Transformation of electro-competent <i>A. tumefaciens</i>	39
2.5	Isolation of genomic DNA.....	40
2.5.1	UREA-extraction method.....	40
2.5.2	Quick-extraction method.....	40
2.6	Amplification of DNA fragments by PCR.....	41
2.6.1	Genotyping of T-DNA insertion mutants.....	41
2.6.2	Colony-PCR.....	41
2.7	Extraction of RNA from plant tissue.....	42
2.7.1	RNA extraction with urea.....	42
2.7.2	Phenolic RNA-extraction method.....	42
2.7.3	Extraction of polysomes.....	43
2.8.	Reverse transcription polymerase chain reaction.....	44
2.8.1	DNase treatment.....	44
2.8.2	Synthesis of cDNA.....	44
2.9	Extraction of proteins.....	45
2.9.1	Extraction of total proteins.....	45
2.9.2	Enrichment of phosphoproteins.....	46
2.9.3	Protease inhibitor Assay.....	46
2.10	Quantification of nucleic acids and proteins.....	47
2.10.1	Estimation of nucleic acid concentrations.....	47
2.10.2	Estimation of proteins concentrations.....	47
2.11	Over-expression and isolation of recombinant proteins.....	48
2.12	Electrophoresis of proteins.....	50
2.12.1	Isoelectric focusing (first dimension).....	50
2.12.2	SDS-PAGE (second dimension).....	51
2.12.3	Staining of polyacrylamide gels.....	51
2.13	Protein blot.....	53
2.14	Affinity purification of antibodies.....	54
2.15	Identification of protein-protein interactions.....	55
2.15.1	Co-immunoprecipitation.....	55
2.15.2	Yeast-Two-Hybrid Assay.....	56
2.15.3	Affinity chromatography with spin columns.....	58
2.16	Protein-lipid interactions.....	59
2.16.1	Protein-lipid-overlay assay.....	59
2.16.2	Liposome-binding assay.....	59
2.16.3	Liposome-turbidity assay.....	60
2.17	Transient and stable transformation.....	60
2.17.1	Transient expression analysis via particle gun bombardment ..	60
2.17.2	<i>A. tumefaciens</i> -mediated stable transformation of <i>A. thaliana</i> ..	61
2.18	Generation of the At3g29075 “knock-down” plant.....	62

3.	Results.....	63
3.1	<i>In silico</i> analysis of the protein At5g39570.1	63
3.1.1	Basic characterization of At5g39570.1 and At3g29075	63
3.1.2	Homologs and Orthologs of At5g39570.1.....	66
3.1.3	Protein structure.....	71
3.1.4	Analysis of the promoter region and coding sequence.....	73
3.1.5	Post-translational modifications of At5g39570.1	75
3.1.6	Gene co-expression network of <i>At5g39570.1</i>	75
3.1.7	Protein-protein interactions	76
3.2	Genotyping.....	77
3.2.1	Genotyping of phospholipase D mutants.....	77
3.2.2	Genotyping of the <i>At5g39570.1</i> T-DNA insertion mutant	78
3.3	Production of recombinant proteins.....	78
3.3.1	Amplification and cloning of <i>At5g39570.1</i> into pET28-a	78
3.3.2	Cloning of <i>Ct-At5g39570.1</i> into pET28-a	79
3.3.3	Expression and isolation of At5g39570.1	80
3.4	Generation of monospecific antibodies against At5g39570.1	83
3.5	RNAi-knock-down mutants of <i>At3g29075</i>	84
3.6	Phenotypic analysis of mutant plants.....	86
3.6.1	Phenotypic analysis of <i>At5g39570.1</i> knock-out plants in phosphate-depletion media	90
3.6.2	Phenotypic analysis of <i>At3g29075</i> knock-down plants	91
3.6.3	Phenotypic analysis of the <i>At5g39570.1</i> knock-out/ <i>At3g29075</i> knock-down double mutant	91
3.7	Expression analysis of At5g39570.1 in <i>pld</i> mutants.....	92
3.7.1	Developmental stage-specific expression of At5g39570.1	92
3.7.2	Tissue specific expression of At5g39570.1	92
3.7.3	Expression analysis of At5g39570.1 in <i>pld</i> mutants	93
3.7.4	Expression analysis of At5g39570.1 upon water-limiting conditions.....	94
3.7.5	Expression analysis of the gene <i>At5g39570.1</i>	96
3.8	Identification of At5g39570.1 interacting partners.....	98
3.8.1	Yeast-2-hybrid assay	99
3.8.2	Affinity chromatography assay.....	103
3.8.3	Co-immunoprecipitation assay	105
3.8.4	Tandem-affinity purification	106
3.8.5	Protein aggregation assay	107
3.9	Interaction of PLD α 1 with At5g39570.1	108
3.9.1	Direct interaction of PLD α 1 and At5g39570.1	109
3.9.2	Indirect interaction of PLD α 1 and At5g39570.1	109
3.10	Identification of proteins under the control of phospholipase D	115
3.11	Over-expression of At5g39570.1	118
3.12	Localization of At5g39570.1	119

3.12.1	Intercellular localization of At5639570.1	119
3.12.2	Intracellular localization of At5639570.1	119
4.	Discussion.....	122
4.1	Gene analysis of <i>At5g39570.1</i>	122
4.1.1	Promoter region	122
4.1.2	Protein coding sequence of At5g39570.1	123
4.2	Protein analysis of At5g39570.1 and At3g29075	124
4.2.1	The protein At5g39570.1 is divided into two major regions ...	124
4.2.2	The lysine-rich protein At3g29075.....	125
4.2.3	Comparison of At5g39570.1 and At3g29075.....	126
4.3	At5g39570.1 is intrinsically disordered.....	127
4.4	Phosphorylation of At5g39570.1	128
4.5	Phenotypic analysis of <i>At5g39570.1</i> and <i>At3g29075</i> mutants.....	129
4.6	Regulation of At5g39570.1.....	130
4.6.1	Expression of At5g39570.1 is dependent on PLD α 1	131
4.6.2	Expression of At5g39570.1 is not only dependent on PLD α 1	132
4.6.3	Expression of At5g39570.1 is tissue specific and correlates with PA production.....	134
4.6.4	Regulation of At5g39570.1 upon exposure to stress	135
4.7	Interaction of PLD α 1 and the unknown protein At5g39570.1	139
4.7.1	PLD α 1 does not directly bind to At5g39570.1	140
4.7.2	PLD α 1 mediates interaction with At5g39570.1 by PA.....	140
4.8	Interacting partners of At5g39570.1	143
4.8.1	Identification of RNA-binding proteins as putative interacting partners of At5g39570.1	143
4.8.2	<i>In vitro</i> interaction of At5g39570.1 with MORF proteins suggest an involvement in the RNA-editing complex.....	146
4.8.3	Identification of additional, putative binding partners	148
4.9	Identification of proteins under the control of phospholipase D	149
5.	Outlook.....	150
6.	Summary	152
7.	Supplementary data.....	154
8.	References	171

Acknowledgements

I would like to express my deep gratitude to my advisor Professor Dorothea Bartels, for her professional and enthusiastic guidance and commitment, for her motivation and immense knowledge throughout this research work.

Special thanks should also be given to Dr. Hans-Hubert Kirch and Dr. Horst Röhrig for their valuable advices and critiques of this research work. Thank you for your theoretical and technical support during my research project that incited me to widen my research from various perspectives.

I am particularly grateful to Professor Montserrat Pagès, who invited me to her group and provided me valuable assistance with co-immunoprecipitation techniques. Advice and technical help given by Dr. Zsuzsa Koncz and Dr. Quancau Hou regarding the yeast-two-hybrid assays was greatly appreciated.

I wish to acknowledge the technical help provided by Dr. Dinakar Challabathula, Dr. Francisco Gasulla, Dr. Valentio Giarola, Dr. Jan Petersen, Verena Braun and Barbara von den Driesch. I would like to thank Tobias Dieckmann, Christiane Buchholz and Christa Müller for their invaluable and time-consuming support. Vielen Dank!

I would further like to thank Abdelaziz Nasr, Volkan Cevik and Selvakumar Sukumaran for their help and extension of my project. Barbara Kalisch provided me with lipid strips and useful advice. I would like to offer my special thanks to my working group, the members of the IMBIO and IZMB for valuable criticism, support and assistance during my research work.

I acknowledge the scholarship provided by the COST program that enabled my research stay in the CRAG research center in Barcelona.

Acknowledgements

I wish to thank my family for their support and encouragement throughout my study. I am very grateful to Divykriti for her continuous patience, support and love during the past years. You were and are my source of happiness – thank you so much.

Finally, I would like to thank my friends for the time we shared in our extracurricular activities. Thanks to Niklas, Alex, Jesu, Mike, Georg, Philipp, Birth, Christian, Fleix, Loga, Maria, Pascal, Benji, Robert, Bikram and the ASG Uni Bonn.

Abbreviations

A	adenine	miRNA	micro RNA
AA	amino acid	MOAC	metal oxide affinity chromatography
ABA	abscisic acid	mRNA	messenger RNA
bp	base pair	NO	nitric oxide
BSA	bovine serum albumin	nt	nucleotides
C	cytosine	OD	optical density
Col-0	Columbia-0	PA	phosphatidic acid
cDNA	complementary DNA	PAGE	polyacrylamide gel electrophoresis
CDS	coding sequence	PC	phosphatidylcholine
CRISPR	clustered regularly interspaced short palindromic repeats	PE	phosphatidylethanolamine
d	days	PCR	polymerase chain reaction
Da	Dalton	pH	pondus Hydrogenii
DEPC	diethylpyrocarbonate	pI	isoelectric point
DGK	diacylglycerol kinase	PIP2	phosphatidylinositol 4,5- bisphosphate
dH ₂ O	distilled "milli-Q" water	PLD	phospholipase D
DNA	deoxyribonucleic acid	PM	plasma membrane
dNTPs	deoxyribonucleoside triphosphates	PPI	phosphoinositides
e-value	expectation value	rpm	rounds per minute
<i>et al.</i>	et alii	RNA	ribonucleic acid
G	guanine	ROS	reactive oxygen species
g	gram	RT	room temperature
<i>g</i>	gravity acceleration ($9.81 \frac{m}{s^2}$)	RT-PCR	reverse transcriptase-polymerase- chain reaction
G-protein	guanine nucleotide-binding protein	snoRNA	small nucleolar RNAs
h	hour(s)	T	thymine
His-tag	histidine-affinity tag	Taq	<i>Thermus aquaticus</i>
HsP	heat-shock protein	T-DNA	transfer DNA
IDP	intrinsically disordered protein	TOF	time of flight
LPA	lysophosphatidyl acyltransferases	UV	ultraviolet
M	molar	V	volume
MALDI	matrix-assisted-laser- desorption/ionization	[v/v]	volume/volume
MAPK	mitogen-activated protein kinases	[w/v]	weight/volume
min	minute(s)		

Chemicals and buffers

3-AT	3-amino-1,2,4-triazole	PBS	phosphate-buffered salt solution
APS	ammonium persulfate	NaCl	sodium chloride
CHAPS	3-[3-(cholamidopropyl)dimethylammonio]-1-propanesulfonate	NADPH	nicotinamide adenine dinucleotide phosphate
DOC	sodium deoxycholate	NaOH	sodium hydroxide
EDTA	ethylene diamintetraacetic acid	NTA	nitrilotriacetic acid
EtBr	ethidium bromide	PIPES	piperazine-N,N'-bis (2-ethanesulfonic acid
HCl	hydrochloric acid	SDS	sodium dodecylsulfate
IPTG	isopropyl- β -D-thiogalactopyranoside	SOC	Super Optimal Broth
KOH	potassium hydroxide	TAE	tris-acetate-EDTA
LB	“Lysogeny broth” or “Luria broth”	TBS	tris- buffered salt solution
LiCl	lithium chloride	TCA	trichlor acetic acid
MgCl ₂	magnesium chloride	TEMED	tetramethylethyldiamine
MOPS	3-(N-morpholino)propanesulfonic acid	Tris	tris(hydroxymethyl)-aminomethane
MS-salt	Murashige-Skoog-Medium	TWEEN	polyoxyethylene(20) sorbitan monolaurate

Institutes and databases

1001	1001 Genome Project
BAR	Bio-Analytic Resource for Plant Biology (Toronto, Canada)
EMBL	European Molecular Biology Laboratory (Heidelberg, Germany)
ExpASy	ExpASy Bioinformatic Resources Portal
GABI-KAT	German plant genomics research program. (Bielefeld, Germany)
NASC	Nottingham Arabidopsis Stock Centre (Nottingham, Great Britain)
NCBI	National Center for Biotechnology Information (Bethesda, USA)
SALK	Salk-Institute (La Jolla, USA)
STRING	Known and Predicted Protein-Protein Interaction
TAIR	The Arabidopsis Information Resource (Stanford, USA)
UniProt	Uniprot Protein database

List of tables

Table 1: Properties and requirements of Arabidopsis PLDs	16
Table 2: Gene-specific primers.....	29
Table 3: Actin- and poly(A)-primers.....	30
Table 4: T-DNA-specific primers	30
Table 5: Vector-specific primers.....	30
Table 6: Orthologs of At5g39570.1 with unknown function	67
Table 7: Orthologs and homologs of At5g39570.1 with predicted attributes	68
Table 8: Structural motifs of the protein At5g39570.1	73
Table 9: Prediction of kinase-specific phosphorylation sites in At5g39570.1	75
Table 10: Generation of the <i>At3g29075</i> -specific miRNA	84
Table 11: Interacting partners of At5g39570.1	103

List of figures

Figure 1: Cleavage sites of phospholipases	14
Figure 2: Protein homology of PLDs	15
Figure 3: PLD subfamilies and their domain structures	15
Figure 4: PA formation and degradation pathways in plants	17
Figure 5: Properties of phosphatidic acid in membrane environments	18
Figure 6: The electrostatic/hydrogen bond switch model.	18
Figure 7: Gene model of <i>At5g39570.1</i>	22
Figure 8: BSA calibration line.....	47
Figure 9: Cloning strategy for artificial micro RNAs	62
Figure 10: Nucleotide and protein sequence of <i>At5g39570.1</i>	64
Figure 11: Protein sequences of <i>At5g39570.1</i> and <i>At3g29075</i>	65
Figure 12: Alignment of <i>At5g39570.1</i> and <i>At3g29075</i>	66
Figure 13: Variable amino acids in the sequence of <i>At5g39570.1</i> and <i>At3g29075</i>	66
Figure 14: Blast results for <i>At5g39570.1</i> and <i>At3g29075</i>	69
Figure 15: Phylogenetic tree of <i>At5g39570.1</i>	70
Figure 16: Amino acid composition of <i>At5g39570.1</i> and <i>At3g29075</i>	71
Figure 17: Hydrophobicity plots of <i>At5g39570.1</i> and <i>At3g29075</i>	71
Figure 18: Tandem repeats in <i>At5g39570.1</i> and <i>At3g29075</i>	72
Figure 19: Overview of disordered regions in <i>At5g39570.1</i> and <i>At3g29075</i>	73
Figure 20: Putative promoter region of <i>At5g39570.1</i>	74
Figure 21: Short, conserved nucleotide sequences in <i>At5g39570.1</i>	74
Figure 22: Gene co-expression network of <i>At5g39570.1</i>	76
Figure 23: Predicted functional partners of <i>At5g39570.1</i>	76
Figure 24: Genotyping of <i>pld</i> knock-out mutants	77
Figure 25: Genotyping of the <i>At5g39570.1</i> T-DNA insertion line	78
Figure 26: pET28-a with the His-tagged fragment <i>At5g39570.1</i>	79
Figure 27: pET28-a with the His-tagged fragment <i>Ct-At5g39570.1</i>	80
Figure 28: C-terminal protein fragment of <i>At5g39570.1</i>	80
Figure 29: Induction of the full-size protein <i>At5g39570.1</i>	80
Figure 30: His-tag affinity chromatography of <i>At5g39570.1</i> -full-size	81
Figure 31: Comparison of proteins before and after heat-treatment	82
Figure 32: Induction and detection of <i>Ct-At5g39570.1</i>	82
Figure 33: Test of monospecific antibodies	83
Figure 34: Cloning strategy for the generation of <i>At3g29075</i> -RNAi knock-down mutants	84
Figure 35: Selection of positive plants on MS ^{Kan} -plates	85
Figure 36: Transcript analysis of double <i>At5g39570.1</i> knock-out/ <i>At3g29075</i> knock-down mutants	85
Figure 37: Phenotypic comparison of wild type and mutant plants	86

Figure 38: Six week old Arabidopsis plants after two weeks of dehydration	87
Figure 39: Six week old Arabidopsis plants after two weeks of cold-treatment.....	87
Figure 40: Six week old Arabidopsis plants after salt treatment.....	89
Figure 41: Arabidopsis seedlings grown on MS-phosphate depletion media	90
Figure 42: Phenotypic differences of Arabidopsis seedlings grown on MS-phosphate depletion media	91
Figure 43: Expression of At5g39570.1 in leaves at different developmental stages. ...	92
Figure 44: Tissue-specific analysis of At5g39570.1	92
Figure 45: Immunodetection of PLD α 1 in wild type and <i>At5g39570.1</i> knock-out mutants	93
Figure 46: Protein expression of At5g39570.1 in leaves and seeds of different <i>pld</i> mutants.	93
Figure 47: Protein expression levels of At5g39570.1 in leaf material upon dehydration in <i>pld</i> knock-out mutants	94
Figure 48: Protease inhibitor assay	95
Figure 49: Comparison of total and phosphoproteins upon dehydration in wild-type leaves of <i>A. thaliana</i>	95
Figure 50: Immunodetection of At5g39570.1 in enriched phosphoproteins from <i>A. thaliana</i> leaves	96
Figure 51: Expression of <i>At5g39570.1</i> in response to dehydration.....	96
Figure 52: RT-PCR analysis of the N-terminal <i>At5g39570.1</i> transcript level	97
Figure 53: Transcript analysis of <i>At5g39570.1</i> with full-size primers	97
Figure 54: Transcript analysis of <i>At5g39570.1</i> by RT-PCR	98
Figure 55: Construct of the bait pAS2- <i>At5g39570.1</i> and transformed yeast colonies on SD- _{Trp} depletion media	100
Figure 56: At5g39570.1 yeast-two hybrid test of auto-activation.....	100
Figure 57: Colorimetric β -galactosidase assay.....	101
Figure 58: Construct of the prey pACT2-cDNA library	101
Figure 59: Yeast-two-hybrid screening with At5g39570.1 as bait.....	102
Figure 60: Ni-NTA affinity chromatography of total proteins from leaf extracts.....	104
Figure 61: Ni-NTA affinity chromatography of total proteins from root extracts	104
Figure 62: Protein yield of At5g39570.1 by denaturing and non-denaturing extraction methods.....	105
Figure 63: Co-immunoprecipitation of At5g39570.1.....	105
Figure 64: pnTAPa- <i>At5g39570.1</i> construct (Pandey, 2012)	106
Figure 65: Protein-aggregation assay for At5g39570.1	108
Figure 66: Test of direct interaction between PLD α 1 and At5g39570.1	109
Figure 67: Detection of At5g39570.1 protein fragments in protein-lipid-overlay assays.....	111
Figure 68: Detection of At5g39570.1 protein fragments in protein-lipid-overlay assays	111
Figure 69: Pre-experiment to determine optimal pH-conditions for liposome- binding assays.....	112

Figure 70: Liposome-binding assay with <i>At5g39570.1</i>	112
Figure 71: Liposome-turbidity assay for <i>At5g39570.1</i> with PA and PC	113
Figure 72: Liposome-turbidity assay of <i>At5g39570.1</i> and <i>Nt-At5g39570.1</i>	114
Figure 73: Liposome-turbidity assay of <i>Ct-At5g39570.1</i>	114
Figure 74: Two dimensional analysis of total protein extracts	116
Figure 75: Two dimensional analysis of phospho-enriched protein extracts	117
Figure 76: Constructs for the generation of the <i>At5g39570.1</i> over-expressing line....	118
Figure 77: Microscopic analysis of the intracellular localization of <i>At5g39570.1</i>	120
Figure 78: Construct of <i>At5g39570-GFP</i> and selection of transformed plants.....	121
Figure 79: Comparison of <i>At5g39570.1</i> and <i>At3g29075</i>	126
Figure 80: Model for the regulation of expression of <i>At5g39570.1</i> in response to water-limiting conditions in the absence of <i>PLDα1</i>	139

1 Introduction

Arabidopsis thaliana (*A. thaliana*), a member of the Brassicaceae family, is the most popular model organism in molecular plant biology. Its small size and rapid life cycle of 6-8 weeks from germination to mature seeds renders the plant perfectly suited for laboratory growth. The fully-sequenced, small (157 mega base pairs), diploid genome encodes for approximately 27,000 genes, which are distributed on five chromosomes (The Arabidopsis genome project, 2000). Although its molecular characteristics facilitate research, the functions of nearly 50 % of all *A. thaliana* genes and associated proteins are still unknown. The characterization of unknown proteins and their position in intracellular pathways is of major importance for the understanding of plants growth, development and their stress-adaptation mechanisms. Drought, salinity, pathogens and availability of nutrients challenge plant growth worldwide and cause a global loss of about 1.3 billion tons of food per year, while the world population and associated demands for food rise constantly (Gustavsson *et al.*, 2011). Fundamental research on regulatory pathways and plant stress-adaptation processes has been exploited by scientists to increase and improve crop yields in cultivated plants. However, the regulatory networks of plant adaptation processes towards environmental stresses are complex and intersect with many different physiological pathways. A few signaling pathways have so far been identified as important for plant responses to environmental stresses. In addition to the well researched phytohormone-mediated signaling pathways (especially the central role of abscisic acid (ABA) with regard to dehydration and salinity) (Larrieu & Vernoux, 2015), the role of lipid signaling in plant adaptation attracts growing interest among scientists. One of the key regulators of lipid-mediated stress pathways are phospholipases, which are involved in the abiotic stress-induced production and accumulation of lipid signals such as phosphatidic acid (PA) (Bargmann & Munnik, 2006).

1.1 The phospholipase family

Over the last decades numerous enzymes (> 5000) of the phospholipase family have been identified in a wide range of organisms, including bacteria, viruses, fungi, yeast, animals and plants. Plant phospholipases show the widest diversity and can be grouped into four major groups corresponding to the types of reaction which they catalyze: Phospholipase A (PLA), phospholipase B (PLB), phospholipase C (PLC) and phospholipase D (PLD) (Wang, 1997).

Phospholipase A enzymes can further be classified into phospholipase A1 and phospholipase A2 corresponding to the hydrolysis of the first (PLA₁) or second (PLA₂) acyl-ester bond respectively (**Figure 1**).

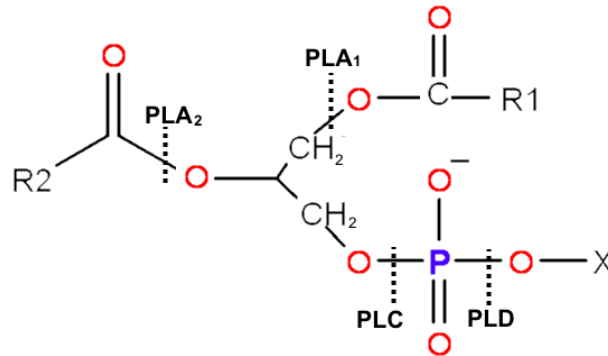


Figure 1: Cleavage sites of phospholipases

The term “phospholipase B” refers to enzymes that are capable of hydrolyzing the phospholipid at any of those acyl-ester bonds. Members of the phospholipase C family hydrolyze the glycerophosphate bond in front of the phosphate, releasing diacylglycerol (DAG) and a phosphate head group. Phospholipase D cleaves behind the phosphate, producing phosphatidic acid and a polar alcoholic head group (Wang, 1997). Phosphatidic acid can also be generated by the sequential action of phospholipase C and a diacylglycerol kinase (DGK) (Singh *et al.*, 2015). This thesis focuses on *A. thaliana* phospholipase D and its enzymatic cleavage product phosphatidic acid which regulates expression of a number of proteins and hence physiological events in the cells (Hong *et al.*, 2010).

1.1.1 Phospholipase D

In plants, PLDs comprise a large and diverse family of enzymes with over 80 described genes. In *A. thaliana*, twelve isoforms of PLDs have been identified and researched in the past years (**Figure 2**) (Bargmann & Munnik, 2006). These can be classified into six major categories (α , β , γ , δ , ϵ , and ζ) based on their protein domain structure and biochemical properties (Li *et al.*, 2009).

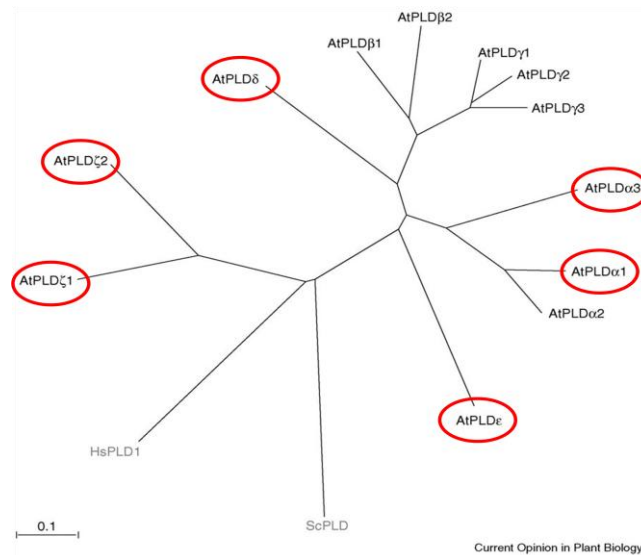


Figure 2: Protein homology of PLDs.

Radial phylogenetic tree with all twelve Arabidopsis PLD proteins, a human (HsPLD1) and a yeast (*Saccharomyces cerevisiae*, ScPLD) PLD protein. Red circles indicate isoforms used in this work. Figure was adapted from Bargmann & Munnik (2006).

Except PLD ζ , all family members contain a C2 (Ca^{2+} /phospholipid-binding) domain near the N-terminus, while the Ca^{2+} -independent PLD ζ is characterized by the presence of PH (Pleckstrin Homology) and PX (Phox Homology) lipid-binding domains (**Figure 3**) (Elias *et al.*, 2002, Qin & Wang, 2002).

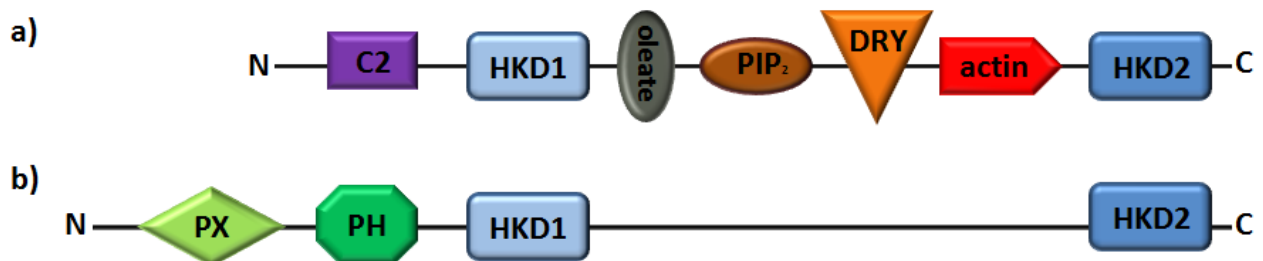


Figure 3: PLD subfamilies and their domain structures.

a) C2-PLDs (α , β , γ , δ , ϵ) b) PLD ζ and mammalian PLDs. C2, Ca^{2+} -dependent phospholipid binding domain; PH, pleckstrin homology domain; PX, Phox homology domain; HKD, HxKxxxxD motif; Binding domains: DRY motif to bind G-proteins; Actin-binding domain; PIP_2 -binding domain; Oblate-binding domain. Model adapted from Wang *et al.* (2014).

The catalytic activity of PLDs bears on the hydrolysis of structural phospholipids such as phosphatidylcholine (PC) and phosphatidylethanolamine (PE) at the terminal phosphodiester bond to generate PA and the corresponding alcoholic head group (Bargmann & Munnik, 2006). Substrate specificity or preference was observed for all PLD isoforms. While members of the PLD ζ class exclusively hydrolyze PC, PE and phosphatidylglycerol serve as substrates for other PLD isoforms (Qin & Wang, 2002). Activity of PLDs varies among different isoforms and their catalytic properties. Differences in substrate specificity, transphosphatidylation potential, pH and temperature profiles as well as requirements of calcium and PIP_2 , small G-proteins or actin, have been reported (**Table 1**) (Bargmann &

Munnik, 2006, Wang *et al.*, 2014). Therefore, different PLD isoforms may generate specific subsets of molecular PA species depending on the physiological environment in the cell.

Table 1: Properties and requirements of Arabidopsis PLDs

PLD Isoform	Ca ²⁺	Requirements			Others	Subcellular location
		PIP2	Oleate	Substrate		
PLD α 1	mM/ μ M	-	-	PC > PE		Cytosol and IM, mostly PM
PLD α 2	mM	-		PC = PE		Cytosol= IM and PM
PLD α 3	mM	-		PC > PE, PG		mostly PM
PLD ϵ	mM/ μ M	-	-/+	PC = PE > PG		PM
PLD β 1	μ M	+	-	PC = PE	actin binding	
PLD β 2		not determined				
PLD γ 1	μ M	+	-	PE > PC	PIP2 and triton effect	mostly IM
PLD γ 2	μ M	+	-			
PLD γ 3		not determined				
PLD δ	μ M-mM	+	+	PE > PC	tubulin binding	PM
PLD ζ 1	no	+	-	PC		PM
PLD ζ 2		not determined			induced by Pi deficiency	IM

(-) indicates no requirement of effectors for PLD activity. (+) indicates promoted PLD activity by selected effectors. PC, phosphatidylcholine, PE, phosphatidylethanolamine, PG, phosphatidylglycerol, PM, plasma membrane, IM, intracellular membrane. Adapted from Wang *et al.* (2014).

1.2 Phosphatidic acid

The polar lipid PA accounts for less than 1 % of total lipids in plants, but it plays a major role in lipid metabolism and signaling (Hong *et al.*, 2010). The importance of PA as a second messenger in plants was thoroughly researched in recent years. It is involved in signal mediation and responses to stress, such as pathogens (Zhao, 2015), freezing (Zhang *et al.*, 2013b), dehydration (Hong *et al.*, 2008), salinity (Munnik *et al.*, 2000, Yu *et al.*, 2010) and nutrient starvation (Yamaryo *et al.*, 2008). PA is implicated in a number of physiological processes like plant growth, development and adaptation to environmental stresses (Hong *et al.*, 2010). By targeting and regulating a wide range of proteins, such as phosphatases, kinases and oxidases, PA affects membrane trafficking, cytoskeletal organization, root hair growth and elongation, ABA and ROS response, stomatal movement and plenty more (Hong *et al.*, 2010).

Besides the role of PA in signaling it also serves as an important intermediate in lipid biosynthesis (Ohlrogge & Browse, 1995). In plants, lysophosphatidyl acyltransferases (LPA) are involved in the generation of PA as a precursor for structural phospho- and galactolipids (Testerink & Munnik, 2011). A signaling role for the LPA-derived PA species has not been reported yet, but cannot be ruled out. Signaling PA is generally produced *via* the hydrolysis of

phospholipids by members of the PLD family, but PA can also be formed in a two-stage process by the sequential action of PLC and DGK (**Figure 4**) (Singh *et al.*, 2015). The molecular species of PA produced *via* both pathways differ in the number of carbons and double bonds, which form the two fatty acid chains. The PLC/DGK pathway is mainly involved in the generation of PA 16:0/18:2 and 16:0/18:3 PA species, whereas PLD generates additional PA species like PA 18:3/18:2 and PA 18:2/18:2 (Vergnolle *et al.*, 2005). Guo *et al.* (2011) hypothesized that these different molecular forms of PA exhibit diverse affinities to proteins. Although the molecular action of PA on target proteins remains unclear, emerging evidence indicates that binding of PA induces distinct downstream responses (Testerink & Munnik, 2011).

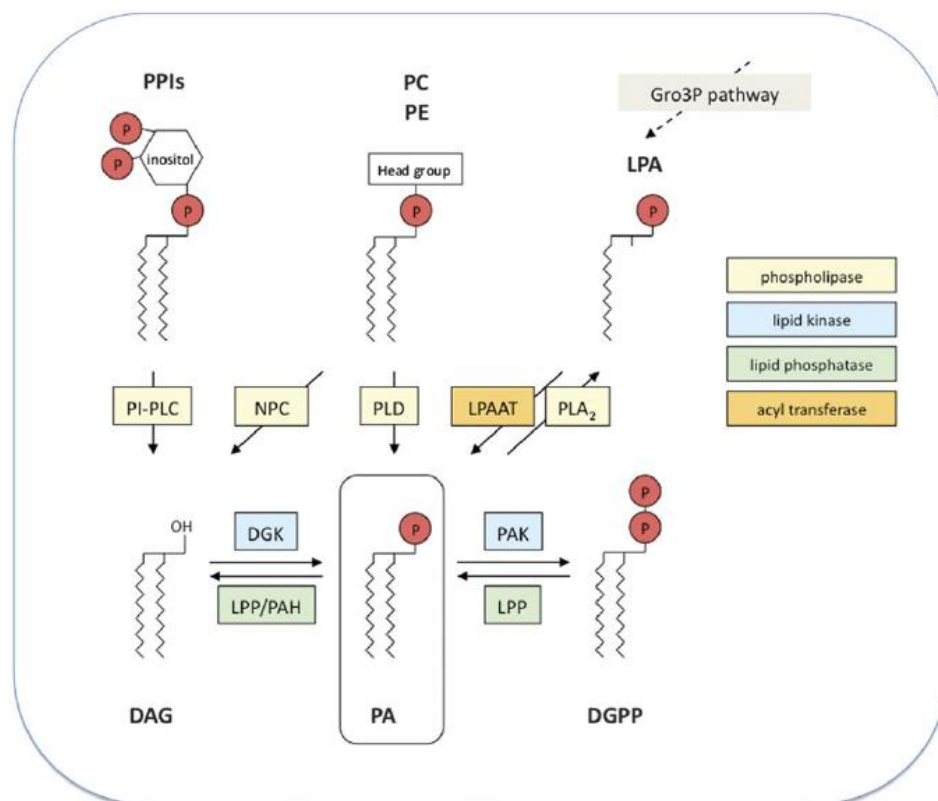


Figure 4: PA formation and degradation pathways in plants.

PE, phosphatidylethanolamine; LPA, lyso-PA; Gro3P, glycerol 3-phosphate; NPC, non-specific phospholipase C; PI-PLC, PPI-hydrolyzing phospholipase C; LPAAT, LPA acyltransferase; PLA₂, phospholipase A₂; DGPP, DAG pyrophosphate; DGK, diacylglycerol kinase. Figure from Testerink & Munnik (2011).

PA itself was shown to affect membrane curvature and surface charge in the vicinity of the plasma membrane (Kooijman *et al.*, 2003). In mammals and yeast, PA is thought to positively influence vesicle fission and sporulation events due to its extraordinary structure (Nakanishi *et al.*, 2006, Yang *et al.*, 2008). The small, highly-negatively charged head group, which is in direct vicinity of its glycerol backbone, provides a special, cone-shaped structure to this lipid.

These unique properties affect curvature and charge of plasma membranes and provide spatial information for protein targets (**Figure 5**) (Testerink & Munnik, 2011).

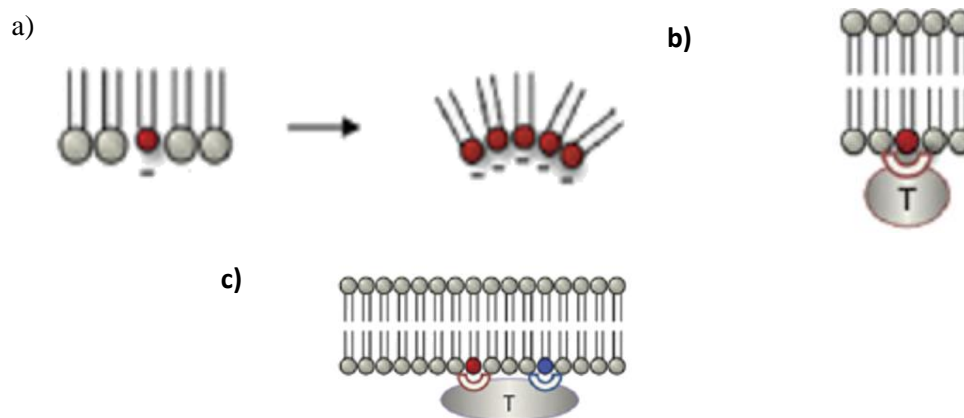


Figure 5: Properties of phosphatidic acid in membrane environments.

a) PA affects membrane curvature and charge. b) PA provides spatial information for target protein recruitment. c) Cooperation with other lipid signals. Lipids with red head groups represent PA, T represents target protein. Figure was adapted from Testerink & Munnik (2011).

The negative charge of PA's phosphate head group may provide crucial information for protein binding. Kooijman *et al.* (2007) described the “electrostatic/hydrogen-bond switch” model which suggests interaction of the negatively-charged PA head group with positively-charged residues (lysine or arginine) of target proteins. Formation of hydrogen bonds may then lead to further deprotonation of the head group, resulting in a positive feedback of additional electrostatic and hydrogen bonds between PA and the target protein (**Figure 6**).

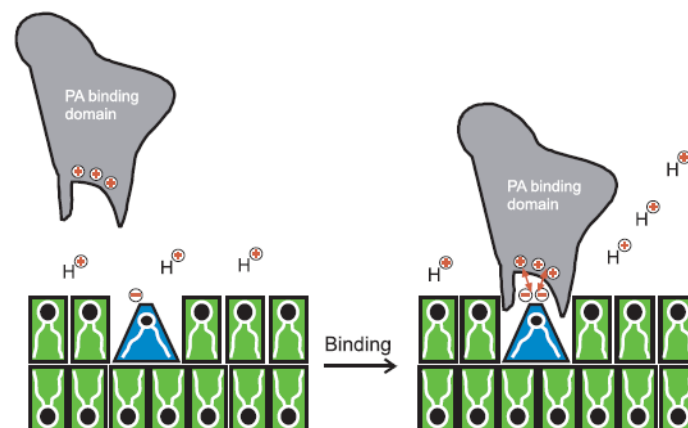


Figure 6: Schematic representation of the electrostatic/hydrogen bond switch model.

The molecular shape of PA (a cone shaped lipid) is shown schematically as is the location of the head group of PA deep into the lipid head group region of a PC bilayer. The electrostatic/hydrogen bond switch is incorporated in this model. Figure and legend was adapted from Kooijman *et al.* (2007).

The model explains the absence of a distinct PA-binding domain and refers to the requirements of domains containing basic amino acids like lysine and arginine as potential interacting sides. Recent studies reported that PA-binding interactions are pH-dependent (Petersen *et al.*, 2012). This is in accordance with the above described model as increased levels of cellular H^+ -ions weaken electrostatic hydrogen bonds. Nevertheless, the model

cannot explain why different molecular forms of PA were reported to share diverse affinities towards proteins and differ in their affect on protein targets (Guo *et al.*, 2011). PA-profiling experiments detected eight molecular PA species in Arabidopsis, namely: 34:6 PA, 34:4 PA, 34:3 PA, 36:6 PA, 36:5 PA, 36:4 PA, 36:3 PA and 36:2 PA (Devaiah *et al.*, 2006). This molecular diversity might explain the distinct regulations of multiple target proteins and the involvement of PA in numerous physiological processes. A second factor for PA's role in countless regulatory processes (Hong *et al.*, 2008) might be its cooperation with other cellular signals (**Figure 5 c**) (Testerink & Munnik, 2011). Lipid signals, such as phosphoinositides (PPI), lysophospholipids and oxylipins accumulate in response to similar abiotic stresses and play important roles in PA-regulated processes, such as the regulation of the water household, synthesis of protective molecules and the control of root system architecture (Hou *et al.*, 2015). In addition, several PA-binding proteins were reported to also bind PPIs directly (e.g. AtPDK1, Deak *et al.*, 1999), illustrating a possible interplay. Synergetic and/or antagonistic regulations of downstream pathways by PA with other cellular signals, including Ca^{2+} , reactive oxygen species (ROS) and nitric oxide (NO) have been reported (Hou *et al.*, 2015). For instance, PA promotes the formation of NO and ROS in response to drought stress, which are implicated in the ABA-mediated response of stomata closure (Distéfano *et al.*, 2012, Guo *et al.*, 2012b). Regulation of PLD activity by intracellular Ca^{2+} concentrations controls PA production upstream of target proteins (Li *et al.*, 2009) and in some cases is required for PA-binding (Domínguez-González *et al.*, 2007). Multiple additional signaling pathways are suggested to intersect and influence the PA-mediated signaling in plants, forming a complex, inscrutable regulatory network that to this day remains enigmatic. The low abundance of PA, its fast turnover in response to environmental changes as well as the difficulty to distinguish molecular PA species impede the disclosure of the molecular interaction networks. Recently, a novel PA biosensor was presented by Potocký *et al.* (2014) to monitor PA dynamics in plant cells, but its inability to discriminate between molecular PA species demands for additional methods and techniques to unravel distinct PA-binding proteins and networks.

1.3 Proteins under the control of phospholipase D

More than 15 years have passed since the first identification of PA-binding proteins in mammals (Jenkins *et al.*, 1994) and plants (Deak *et al.*, 1999), respectively. The list of plant PA targets has grown during the last decades and contains over 30 PA-binding proteins (Hou *et al.*, 2015) that are regulated in response to PA. While the affect of PA binding remains to

be elucidated for a number of proteins, PA was shown to trigger activation, inhibition, translocation and degradation of several targets (Hou *et al.*, 2015). For instance, PLD-derived PA binds and activates the Arabidopsis phosphoinositide-dependent kinase1 (PDK1) and its downstream targets: PINOID and the mitogen activated protein kinase 6 (MPK6) (Anthony *et al.*, 2006, Deak *et al.*, 1999, Zegzouti *et al.*, 2006). Salt stress triggers PLD-derived 16:0-18:2 PA accumulation, which leads to activation of MPK6 and promotes phosphorylation of the Na⁺/H⁺-antiporter salt overly sensitive (SOS1) *in vitro* (Yu *et al.*, 2010). This PLD-dependent signaling cascade is additionally controlled by PA at different stages and regulates root hair growth and development as well as adaptation of plants to water-limiting conditions in Arabidopsis. More than a third of all identified plant PA-binding proteins have been implicated in root growth and response to water-limiting conditions (McLoughlin & Testerink, 2013). In accordance to the promoted PLD activity in response to environmental stresses, PA targets and stimulates dehydrins, proteins involved in pathogen defense, wound and temperature stress response (Hou *et al.*, 2015). Binding of PA to the plant defensin MtDEF4 from *Medicago truncatula* was reported to promote entry of MtDEF4 into cells of the pathogen *Fusarium graminearum in vitro*, where it permeabilizes the fungal plasma membrane (Sagaram *et al.*, 2013). However, no direct evidence for PLD-induced MtDEF4 activation can be deduced from this report. On the other side, PDK1-mediated plant pathogen defense mechanisms can be linked to PLD-generated PA species (Anthony *et al.*, 2006). Transcriptional activation of the wound-responsive calcium-dependent protein kinase from maize (ZmCPK11) is also directly dependent on PLD-derived PA species like PA 16:0 and PA 18:0 (Klimecka *et al.*, 2011).

Besides its role in the activation and promotion of cellular processes, PA regulates activities of proteins by degradation and inhibition of molecular targets. The heterodimeric capping protein from Arabidopsis dissociates from actin filaments and cannot block its polymerization in the presence of PA (Huang *et al.*, 2006). Increased actin polymerization in distinct cellular compartments might be important for pollen tube tip growth (Huang *et al.*, 2006).

Binding of PA to cytosolic glyceraldehyde-3-phosphate dehydrogenases (GAPCs) induces their translocation to the membrane and promotes proteolytic cleavage of GAPC2 in Arabidopsis (Kim *et al.*, 2013b, McLoughlin & Testerink, 2013). Diverse binding affinities of molecular PA species were observed, but cleavage of GAPC2 could not yet be specifically linked to PLD-derived PAs. Interestingly, GAPC was recently reported to directly bind and activate PLD δ in response to water-limiting conditions, resulting in the increased formation of PA (Guo *et al.*, 2012a). PLD δ -derived PA may regulate GAPC degradation to modulate its

PLD activity in a negative feedback loop in order to desensitize the ABA signaling machinery (Kim *et al.*, 2013b). Degradation of GAPC was further reported to be induced by the dissociation of 14-3-3 proteins from GAPC upon sugar deprivation (Demarse *et al.*, 2009). Members of the 14-3-3 protein family were previously also identified as PA targets (Camoni *et al.*, 2012). Taken together sugar and PA signaling might induce dissolution of 14-3-3 scaffold proteins, resulting in the exposure of cleavage sites of GAPCs and their subsequent proteolytic degradation (Kim *et al.*, 2013b).

In some cases PA binding has been linked to the translocation of target proteins similar to the effect of phosphatidylinositol-5-bisphosphate, which promotes translocation of proteins from the nucleus to the cytoplasm and *vice versa* (Alvarez-Venegas *et al.*, 2006, Gozani *et al.*, 2003). For instance, PLD α 1-derived PA binds to ABI1, a negative regulator of ABA response, and promotes its accumulation at the plasma membrane in wild-type *Arabidopsis* plants, whereas ABI1 is translocated to nuclei in *plda1* mutants (Zhang *et al.*, 2004). The PA-promoted membrane retention decreases ABI1s phosphatase activity and thus positively influences ABA signaling. PA binding to the transcription factor WER results in the opposite effect: Despite the absence of a nuclear-localization signal, PA was shown to trigger the nuclear localization of the WER transcription factor to promote root hair formation and elongation (Yao *et al.*, 2013). It is likely that PA's regulatory function largely relies on PAs ability to trigger translocation of proteins and thereby, indirectly controls the activities of its targets.

PA is a versatile stress signal and is involved in numerous physiological pathways. Although some PA targets have been identified in plants, the mechanism of PA binding and its mode of action have not been unraveled yet. Identification of novel PA targets can help to understand PA as a signaling molecule and the regulatory role of PLDs.

1.4 The unknown protein At5g39570.1 from *Arabidopsis thaliana*

Arabidopsis thaliana, the first fully-sequenced plant, contains nearly 27,000 genes coding for up to 34,000 proteins (EMBL, European Molecular Biology Laboratory). While no function has been assigned to half of these proteins, the existence of several thousand proteins remains to be proven. Besides these “putative proteins” a number of proteins have been annotated in protein databases as “unknown proteins” since neither function, nor additional information are known, although the protein has been detected. One of those proteins is At5g39570.1 (gene: *At5g39570.1*gi|24417262) which is listed in the TAIR and NCBI database as “unknown

protein“. The gene encoding for this 43 kDa protein consists of two exons that are separated by a 660 bp long intron towards the 3'-end (**Figure 7**).



Figure 7: Gene model of *At5g39570.1*.

Evidence on protein level for the existence of this protein was first provided in 2005 by Fu *et al.* Jian Shen (2008) and Anke Kuhn (2009) detected a missing protein spot in the *plda1* mutant when compared to the wild-type phosphoproteom of *A. thaliana*. Matrix-assisted laser-desorption/ionization and time-of-flight analysis identified the protein as the unknown protein At5g39570.1. Previous genome-scale proteomic studies (Baerenfaller *et al.*, 2008) confirmed the phosphorylated status of At5g39570.1 under standard conditions and identified a specific phosphorylation site in it. These observations made At5g39570.1 a good candidate for the study of phospholipase-controlled pathways. This work aims at a detailed investigation of At5g39570.1 that in part builds on the results of my Diploma thesis (2011).

1.5 Phosphorylation of proteins

The reversible phosphorylation of proteins by protein kinases and phosphatases is one of the most important post-translational modifications in prokaryotic and eukaryotic organisms. The interplay of phosphorylation and dephosphorylation regulates activities and functions of a large number of proteins that are located at the top of complex physiological signaling pathways. Therefore proteins that are reversibly phosphorylated can act as “regulatory switches” and deserve special attention regarding the analysis of signaling cascades and networks. Protein kinases hydrolyse nucleotide triphosphates and transfer negatively charged γ -phosphate groups (PO_4^{3-}) to the amino acids (AA) serine, threonine or tyrosine, resulting in an induced conformational change (Barford *et al.*, 1991) or altered electrostatic properties (Serber & Ferrell Jr, 2007). In addition to its role in the activation and repression of enzyme activity, phosphorylation of target proteins plays a major role in signal transduction, regulation of biological thermodynamics, mediation of protein-protein interactions and protein degradation *via* the ubiquitin/proteasome pathway (Johnson, 2009). The perception of an external stimulus, such as environmental stress can result in the phosphorylation of plant mitogen-activated protein kinases (MAPK), which are capable of transducing and amplifying

an intracellular signal by activating additional MAPKs further downstream in order to trigger a physiological response (Rodriguez *et al.*, 2010b). The power of phosphorylation to induce conformational changes or even disorder-to-order transitions of proteins by phosphorylation reveals the impact of post-translational modifications on target proteins (Rodriguez *et al.*, 2010b). These observations led to the rediscovery of a group of proteins, which had been neglected so far: Intrinsically disordered proteins.

1.6 Intrinsically disordered proteins

Despite Anfinsen's dogma (Anfinsen, 1972) which states, that the function of a protein is dependent on its fixed three-dimensional structure, numerous proteins which largely lack α -helices and β -sheets upon physiological conditions have been identified and functions have been assigned to some of these "intrinsically disordered proteins" (IDPs) (Wright & Dyson, 1999). The conformational change of IDPs from disorder-to-order in response to phosphorylation and protein-protein interactions respectively, opened a fresh focus on this diverse class of proteins. IDPs are characterized by high amounts of charged, hydrophilic amino acids (Romero *et al.*, 2001). Long stretches of hydrophobic amino acids are rare as a hydrophobic core forms the basis of the three dimensional structure of most globular proteins (Gsponer & Madan Babu, 2009). IDPs have been linked to the occurrence of intrinsic tandem repeats, heat stability, post-translational modifications and structural flexibility (Gsponer & Madan Babu, 2009, Uversky *et al.*, 2008), features that have previously been observed for the unknown protein At5g39570.1 (Ufer, 2011). The introduction of bioinformatic prediction tools for intrinsically disordered regions detected large stretches of amino acids that lack a three-dimensional structure in over 30 % of eukaryotic cells (Gsponer & Madan Babu, 2009), demonstrating the frequent occurrence of IDPs in complex organisms. A large-scale study in *A. thaliana* detected IDP-like stretches of over 50 amino acids in 29 % of the tested proteins (Dunker *et al.*, 2000). On experimental level putative IDPs are analyzed by Circular dichroism (CD)-spectroscopy that measures the absorption of the spin momentum of left and right-handed polarized light to determine the spatial orientation of peptides (Kelly *et al.*, 2005). Specific absorption spectra indicate the existence of secondary structure motifs like α -helices and β -sheets, while randomly-coiled stretches exhibit altered characteristics.

1.7 Aims of this study

The unknown protein At5g39570.1 was detected and identified by comparing phosphoproteoms of wild type and *plda1*-mutant plants in a previous Diploma thesis (Kuhn, 2009). A prime characterization of the protein and production of an antibody against At5g39570.1 is described in my earlier work (Ufer, 2010). This intended to provide a comprehensive, functional characterization of At5g39570.1 based on existing literature and data compiled from *in silico* simulations as well as *in vitro* and *in vivo* experiments. Therefore, three main objectives were followed in this thesis:

First, an extensive characterization of At5g39570.1 was pursued. Numerous bioinformatic prediction tools were exploited and text-mining algorithms were applied to draw a first picture of this enigmatic protein. The extraordinary, unequal composition of the protein's N- and C-terminal regions was in the focus of *in silico* analysis. The identification of the homolog At3g29075.1 and its putative redundant function led to basic characterization of this protein and the generation of double-mutant lines. Work on At3g29075.1 led to a new side project that was followed by a Master student (Nasr, 2015).

Second, At5g39570.1 was chosen as a candidate protein downstream of the PLD-regulated signaling network to gain further insights into the manifold regulatory networks of phospholipases, specifically their role in inducing and mediating signals in response to abiotic stresses. The dependence of At5g39570.1 on different PLD isoforms was analyzed and uni-directional regulation of the protein by PLD was tested. Protein expression of At5g39570.1 upon various environmental stresses was examined in different genetic backgrounds of PLD mutants. To establish a regulating model, it was further tested whether At5g39570.1 is directly (by physical contact) or indirectly (by signaling molecules) influenced by PLDs.

Third, a starting point for the functional characterization of the unknown protein should be allocated in this thesis. First hints for the protein's functions were gathered with the help of *in silico* data analysis and text-mining approaches. *At5g39570.1* and *At3g29075* mutant plants were phenotypically monitored upon different stress conditions. Several protein-protein interacting assays were conducted to detect putative interacting partners of At5g39570.1. Candidate proteins were further examined and putative interactions were evaluated based on bioinformatic predictions and scientific reports.

2 Materials and methods

2.1 Materials

The following lists provide an overview of developers, producers and suppliers from chemicals, equipment, databases and programs used in this thesis. The texts in the subsequent sections refer to the manufacturers and companies listed below and will only provide the manufacturer's name.

2.1.1 Chemicals

- AppliChem GmbH (Darmstadt, Germany)
- Apollo Scientific (Ltd Bledsbury, Czech Republic)
- Avanti Polar Lipids (Alabaster, USA)
- Biomol (Hamburg, Germany)
- Bio-Rad (Munich, Germany)
- Carl Roth GmbH (Karlsruhe, Germany)
- Dushefa Biochemie B.V. (Haarlem, Netherlands)
- Fermentas (St. Leon-Rot, Germany)
- GE Healthcare (Freiburg, Germany)
- Invitrogen (Karlsruhe, Germany)
- Labomedic (Bonn, Germany)
- LMS Consult (Brigachtal, Germany)
- Merck AG (Darmstadt, Germany)
- Sigma-Aldrich Chemie GmbH (Munich, Germany)
- Stratagene (Heidelberg, Germany)
- ZVE (Bonn, Germany)

2.1.2 Equipment

- Binocular microscope: SMZ-800 (Nikon, Düsseldorf, Germany)
- Blotting chamber for proteins: “Criterion Blotter” (Biorad, Munich, Germany)
- Chemiluminescence detector: Intelligent Dark Box II, (Fujifilm, Tokyo, Japan)
- Confocal Laser Scanning Microscope: ZE2000 (Nikon, Düsseldorf, Germany)
- Consumables: Pipette tips and centrifugal tubes (Sarstedt AG, Nümbrecht, Germany)
- Desalting columns: “PD–10” (GE Healthcare, Freiburg, Germany)
- Electroporation system GenepulserII Electroporator (Bio-Rad, Hercules, USA)
- Lyophilisator: “LDC–2” (Christ, Osterode am Harz, Germany)
- Gel electrophoresis chambers:
 - “Minigel” (Biometra, Göttingen, Germany)
 - “EasyCast” (Owl, Portsmouth, USA)
- Isoelectric focuser “Ettan IPGphor II IEF Unit” & IEF–strip holder “Ettan IPGphor Strip Holder” (Amersham, Buckinghamshire, Great Britain)
- Luminescent Image Analyzer LAS 1000 (Fujifilm Life Science, Stamford, USA)
- Nanodrop: Biospec – Nano (Shimadzu Biotech, Japan)
- Particle Gun: Biolistic (Bio-Rad, Hercules, USA)
- PCR–cycler: “T3 Thermocycler” (Biometra, Göttingen, Germany)
- pH–meter (SCHOTT GLAS, Mainz, Germany)
- Rotator: “neoLab–Rotator 2–1175” (neoLab, Heidelberg, Germany)
- Spectrophotometer: “SmartSpec 3000” (Biorad, Hercules, USA)
- Scanner:
 - Typhoon 9200 (Amersham, Piscataway, USA)
 - Image scanner (Amersham, Buckinghamshire, Great Britain)
- Sonification water bath: “Sonorex Super RK102P” (Bandelin electronics, Berlin, Germany)
- T3-Thermocycler, Biometra, Göttingen, Germany
- Centrifuges:
 - Centrifuges: “5415D”; “5417R”, “5810R”; Vacuum centrifuge: “Concentrator 5301” (Eppendorf, Hamburg, Germany)
 - Sorvall centrifuge: “RC50” (DuPont, Hamm–Uentrop, Germany)
 - Ultracentrifuge: “L8-70M” (Beckman Coulter, Brea, USA)

2.1.3 Computer programs and databases

For *in silico* analyses various bioinformatic tools were exploited to predict characteristics of genes and proteins. The “ExpASY Bioinformatics Resource Portal” (<http://expasy.org/tools/>) provides a basic set of prediction and analysis tools. For detailed *in silico* analysis additional computer programs and databases were used in this thesis.

Computer programs and tools:

- AGRIS (<http://www.arabidopsis.med.ohio-state.edu/AtTFDB/>)
- AIDA Image Analyzer 2.11 (Fujifilm Life Science, Stamford, USA)
- APE – A Plasmid Editor v. 1.7
- Blastp – protein blast (<http://blast.ncbi.nlm.nih.gov/Blast.cgi>)
- ClustalW2 (www.ebi.ac.uk/clustalw/)
- cNLS Mapper (http://nls-mapper.iab.keio.ac.jp/cgi-bin/NLS_Mapper_y.cgi)
- Cell eFP browser (http://bar.utoronto.ca/cell_efp)
- CFSSP(<http://cho-fas.sourceforge.net/>)
- Compute pI/Mw (http://web.expasy.org/compute_pi/)
- DisEMBL (<http://dis.embl.de/>)
- GeneMANIA (<http://www.genemania.org/>)
- GlobPlot (<http://globplot.embl.de/>)
- GOR4 (https://npsa-prabi.ibcp.fr/cgi-bin/npsa_automat.pl?page=npsa_gor4.html)
- Interpro (<http://www.ebi.ac.uk/interpro/>)
- Lig-Input: http://www.insilico.uni-duesseldorf.de/Lig_Input.html
- Medor v. 1.4 (<http://www.vazymolo.org/MeDor/>)
- Mega 6 – Molecular evolutionary genetics analysis
- Microsoft Office 2010 (Microsoft, Redmond, USA)
- NetPhos 2.0 (<http://www.cbs.dtu.dk/services/NetPhos/>)
- NetPhosK (<http://www.cbs.dtu.dk/services/NetPhosK/>)
- Kinase Phos 2.0 (<http://kinasephos2.mbc.nctu.edu.tw/>)
- NEBcutter2 (<http://tools.neb.com/NEBcutter2>)
- NucPred (<http://www.sbc.su.se/~maccallr/nucpred/>)
- Photoshop CS and Paint.net
- Primer3 (<http://frodo.wi.mit.edu/primer3/>)
- Protscale (<http://web.expasy.org/cgi-bin/protscale/protscale.pl?1>)
- PONDR-FIT (<http://www.disprot.org/pondr-fit.php>)
- Reverse Complement (www.bioinformatics.org)
- SAM_T08 (http://compbio.soe.ucsc.edu/SAM_T08/)
- SNAPgene
- SOPMA <https://prabi.ibcp.fr/htm/index.php>
- Subnuclear2 (<http://array.bioengr.uic.edu/cgi-bin/subnuclear/subnuclear2.pl>)
- TRANSFAC (<http://www.gene-regulation.com/pub/databases.html>)
- TRUST “Tracking Repeats Using Significance and Transitivity” (<http://www.ibi.vu.nl/programs/trustwww/>)
- TSSP (<http://www.softberry.com/berry.phtml>)
- Vector NTI (Invitrogen, USA)

Databases:

- Arabidopsis 1001 genome project (<http://1001genomes.org/>)
- BAR–Database, Arabidopsis eFP Browser (<http://www.bar.utoronto.ca>)
- European Molecular Biology Laboratory (<http://www.embl.de>)
- German plant genomics research program (<http://www.gabi-kat.de>)
- IuPred (<http://iupred.enzim.hu/>)
- Nottingham Arabidopsis Stock Centre (<http://arabidopsis.info>)
- National Center for Biotechnology Information (<http://www.ncbi.nlm.nih.gov/>)
- Salk–Institute (<http://www.salk.edu>)
- STRING (<http://www.string-db.org>)
- TAIR (www.arabidopsis.org)
- T–DNA Express (<http://signal.salk.edu/cgi-bin/tdnaexpress>)
- Uniprot (<http://www.uniprot.org/>)

2.1.4 Enzymes and markers

- DNA–marker (New England Biolabs, Ipswich, USA)
- Restriction enzymes and Pfu–DNA–polymerase (Fermentas, St. Leon–Rot, Germany)
- Taq DNA–polymerase (Ampliqon, Skovlunde, Denmark)
- Taq DNA–polymerase (isolated and provided by Frederik Faden)

2.1.5 Primer

Primer pairs were designed with the help of the Primer3 program. A primer with a guanine/cytosine (G/C) content of 45-55 % was considered most stable, with a higher ratio of GC in terminal nucleotides. Primer pairs were further selected based on similar melting temperatures (T_M) in the range of 55°C-65°C and low self complementarity of the sequences. For mutagenesis primers, point mutations were avoided when possible. Primers were obtained from Sigma–Aldrich and Eurofins Genomics. All primers were stored at -20°C and 100 mM concentrations. The following primers were designed in this thesis: For a complete list of all primers used see the additional excel file and lab database.

Table 2: Gene-specific primers

<i>Name</i>	<i>Sequence (5' → 3')</i>	<i>Restriction site</i>
Unknown-fwd	AGGAAGGAAGTTACAGGAAACCT	
Unknown-rev	AGCAACAGTTACATGGTGACCCA	
N-At5g39570-rev	AATCAGGGCTTGGATCTGGT	
N-At5g39570-fwd	GCCGTACAGTGGTGGTTACG	
Ct-At3g29075-fwd	AGAGCAGTACAAGGAGCATCA	
Ct-At3g29075-rev	CCCTTGTGGTGCTTATCCTTC	
Ct-At5g39570-fwd	AGGAAGGAAGTTACAGGAAACCT	
At5g39570-full-fwd	GATCAGATCCAAGAAACCAAAAGAG	
At5g39570-full-rev	CTTCCGACGTTGGTGTGTGTTTGT	
Mutagenesis Primers:		
At5g39570-5Fwd	GAAGGAGATATACCATGGCGTACTATACCAGAGA	<i>NcoI</i>
At5g39570-5Rev	AGTGCGGCCGCAAGCTTCCTCGAGTTCTTCAG	<i>XhoI</i>
At5g-full-NCO1-fwd	TCTTCTTAAACCATGGCGTACTAT	<i>NcoI</i>
At5g-full-XHO1-rev	GGGTTTAGTTTACTCGAGGTCTTC	<i>XhoI</i>
Cterm-At5g-fwd-NHE1	GAGTATGCTAGCAGACCTGAATCA	<i>NheI</i>
Cterm-At5g-rev-BAMH1	CAGGGATCCAAACAACACAACAC	<i>BamHI</i>
NCO1-At3g-start-fwd	CCAAAACCATGGCGTATTACACC	<i>NcoI</i>
NCO1-At3g-be-stop-rev	GTCATGTCCCATGGGGTGCTTATC	<i>NcoI</i>
NCO1-At3g-Ct-fwd	GGTGGAACCATGGAGAGCGATTAC	<i>NcoI</i>
XHO1-At3g-bef-end-rev	CATGTCCCTCGAGGTGCTTATCCT	<i>XhoI</i>
NHE1 -At3g-Ct-fwd	GAAGAATTGCTAGCGATTACGTGAAGC	<i>NheI</i>
XHO1-At3g-3'end-rev	CATAAACCTCGAGAGCAGTGTGCTTAG	<i>XhoI</i>
At5g-Y2H-Rev	GCACAGAGAGGGATCCGTTTACTC	<i>BamHI</i>
At5g-Y2H-Fwd	TCTTAAACCATGGCGTACTATAACC	<i>NcoI</i>
Genotyping primers:		
PLD α 1_717f	CCTCTCGCTGGAGGGAAGAAC	
PLD α 1_gene_r	TTAGGTTGTAAGGATTGGAGG	
PLD δ _616_f	GGAAAGGAAAGGGTCTGAGGC	
PLD δ _1200_r	AGCTTACTGCTGGCACGGTAC	
PLD α 4_ATG_f	ATGGAGCTTGAAGAACAGAAG	
PLD α 4_gene_r	ACCTCTTGGCTCCATGTTGC	
PLD α 3_ATG_for	ATGACGGAGCAATTGCTGCT	
PLD α 3_948_rev	ACTTCGTGAGACGTTCTATCG	
PLDZ1-RP	GTGATCGTCTCTGTCTCTCGC	
PLDz1-LP	TGAAAAGCATGGAAATTTTCG	
PLDz2-RP	CGGCATTTACCTCCGGTACAG	
PLDz2-LP	CTTCATGAGCCTTCAGAATGC	
Primer for the generation of At3g29075.1 knock-down mutant		
1-At3g29075-miRs	GATAAATTAGGTCGCTGATACTGCTCTCTTTTGTATTCCA	
2-At3g29075-miRa	AGCAGTATCAGCGACCTAATTTATCAAAGAGAATCAATGA	
3-At3g29075-miR*s	AGCAATATCAGCGACGTAATTTTTCACAGGTCGTGATATG	
4-At3g29075-miR*a	GAAAAATTACGTCGCTGATATTGCTACATATATATTCCTA	

Table 3: Actin- and poly(A)-primers

Name	Sequence (5' → 3')
ATH-ACTIN2_FWD	ATGGCTGAGGCTGATGATATTCAAC
ATH-ACTIN2_REV	GAAACATTTTCTGTGAACGATTCCT
Oligo(dT)18 Primer	TTTTTTTTTTTTTTTTTTTT

Table 4: T-DNA-specific primers

Name	Sequence (5' → 3')
L4	TGATCCATGTAGATTTCCCGGACATGAAG
LBA3	ACCCAACCTTAATCGCCTTGCAGCAC
Fish2	CAGTCATAGCCGAATAGCCTCTCCA
GK-LB	CCCATTTGGACGTGAATGTAGACAC

Table 5: Vector-specific primers

Name:	Sequence (5' → 3')	Restriction site
T7-Promoter	TAATACGACTCACTATAGGG	
T7-Terminator	GCTAGTTATTGCTCAGCGG	
pJET1.2 fwd	CGACTCACTATAGGGAGAGCGGC	
pJET 1.2 rev	AAGAACATCGATTTTCCATGGCAG	<i>NcoI</i>
pAS2-1 fwd	TCATCGGAAGAGAGTAG	
pAS2-1-rev	CTGAGAAAGCAACCTGAC	
P35s-pROK2	CACTGACGTAAGGGATGACGC	
pGJ280_rev	TGTGCCCATTAACATCACCA	
NTAP-a-rev	AAGACCGGCCAACAGGATTC	

2.1.6 Vectors

- pJET1.2/blunt (Fermentas)

This plasmid was used for blunt-end cloning of PCR-fragments.

- pET-28a (Novagen)

This plasmid encodes for N/C-terminal histidine-tags (His-tag) and possesses an inducible promoter. The vector was used for the expression of His-tagged proteins.

- pBIN19 (Novagen)

This plasmid comprises a binary vector system that facilitates replication in *Agrobacterium*.

- pGJ280

This plasmid contains a dual CaMV35S promoter and encodes for the Green Fluorescent Protein (GFP) and was used for over-expression and localization studies. The vector was constructed by Dr. G. Jach (Max-Planck-Institute, Cologne, Germany).

- pRS300

This plasmid contains the miR319a precursor which is used for the generation and expression of miRNAs in stable transformed *A. thaliana* plants. The vector was kindly provided by Prof. D. Weigel (Max Planck Institute for Developmental Biology, Tübingen, Germany).

- pAS2-1

This binary vector system can replicate autonomously in *E. coli* and *S. cerevisiae*. The gene of interest is fused to the GAL4DNA binding domain and was therefore exploited for the generation of bait-fusion construct for the yeast-two hybrid assays. The TRP1 gene allows auxotroph growth on tryptophan-depletion media.

- pACT2

This binary vector system can replicate autonomously in *E. coli* and *S. cerevisiae*. The cDNA library is fused to the GAL4DNA activating domain and was therefore exploited for the amplification of the cDNA library in the yeast-two-hybrid assays. The LEU2 gene allows auxotroph growth on leucine-depletion media.

All plasmid vector maps can be found in the supplementary data.

2.1.7 Kits

- GeneJET Plasmid Miniprep Kit, Fermentas (St. Leon-Rot, Germany)
- CloneJET PCR Cloning Kit, Fermentas (St. Leon-Rot, Germany)
- NucleoSpin Extract II, Macherey-Nagel (Düren, Germany)
- RevertAid First Strand cDNA Synthesis Kit, Fermentas (St. Leon-Rot, Germany)
- Novex Dynabeads kit (ThermoFisher, Waltham, USA)

Kits were used according to manufacturer's instructions.

2.1.8 DNA-sequencing

DNA-sequencing of plasmid DNA (100 ng/μl) and PCR-DNA (50 ng/μl) was performed by Macrogen Inc. (Seoul, South Korea) and Eurofins Genomics (Elbersberg, Germany), respectively.

2.1.9 Quantification of proteins and RNA

Quantification of protein and RNA signals with image J was followed as described by Dr. Daniel Kraus (http://home.arcor.de/d-kraus/lab/ImageJ_Western_blot.html). At first the bands of interest were selected, marked and the signal area was quantified automatically using the tracing tool. The same was repeated for the corresponding housekeeping gene (actin) or protein (RubisCO), respectively. The data was transferred to Microsoft Excel and relative values (%) were calculated based on the reference value (wild type value was set to 100 %). The quotient of gene/protein of interest and its housekeeping gene/protein was determined and the median of three repetitions and associated standard deviations were calculated.

2.2 Plant material

The subject of this study was *Arabidopsis thaliana* (Ecotype Columbia-0). Wild-type plants and the following transgenic lines were used:

- PLD α 1-1 (PLD α 1): SALK_067533
- PLD δ 3: SALK_023247
- PLD ϵ 2: KONCZ_68434
- PLD α 3: SALK_130690
- PLD ζ 1/PLD ζ 2: obtained from Munnik (2010)
- Double and triple Mutants of *pld* “knock-out” mutants
- At5g39570.1: GK-167C05.10
- At5g39570.1/At3g29075: GK-167C05.10/At3g29075 knock-down

Emmanuelle Merquiol generated and provided the transgenic lines *pld α 1-1*, *pld δ 3* and the double-knockout mutant line *pld α 1-1/pld δ 3*. Csaba Koncz generated the *pld δ 2*-line. Crossing of the *pld ϵ* -single mutant with the *pld α 1/pld δ* -double mutant for the creation of the triple mutant *pld α 1/pld δ /pld ϵ* was performed by Dr. Nicolas Sauerbrunn.

The At5g39570.1 knock-out plants were ordered from the “European *Arabidopsis* Stock Centre” (NASC, Nottingham, Great Britain).

2.2.1 Sterilization of seeds

To prevent contamination of seedlings grown on MS-plates, two different sterilization methods have been used.

Sterilization with sodium hypochlorite:

- 12 % (w/v) Sodium hypochlorite (NaOCl)
- 0.1 % (w/v) Sodium dodecylsulfate (SDS)

Seeds were sterilized for two minutes with 70 % (v/v) ethanol and subsequently incubated in sterilization solution for 25 min. Seeds were cleaned by repetitive washing steps in dH₂O.

Sterilization with ethanol:

- 70 % (v/v) EtOH
- 0.01 % (w/v) Polyoxyethylen(20)-sorbitan-monolaurate (TWEEN)

Seeds were sterilized for one minute with 100 % EtOH and subsequently incubated in sterilization solution for 15 min. Seeds were cleaned by repetitive washing steps in dH₂O.

2.2.2 Growth conditions

Sterilized seeds were grown on MS-agar plates supplemented with the appropriate antibiotic. Soil grown seedlings did not require premature sterilization.

2.2.2.1 Breeding on soil

Seeds were sowed on wet, Lizetan® (Bayer, Leverkusen, Germany)-treated soil and vernalized for two days at 4°C. Seedlings were grown under short-day conditions: Photo-periodic cycle of eight hours of light at 22°C and 16 hours of darkness at 20°C. After two weeks seedlings (up to 4) were transferred into separate pots. Plants were harvested after 2-6 weeks, depending on the experimental set-up and stored at -70°C.

Six-week-old plants were grown under long-day conditions (16 hours of light at 22°C and 8 hours of darkness at 20°C) for the production of seeds.

2.2.2.2 Breeding on MS-plates

Vitamin solution

2 mg/l Glycine
 0.5 mg/l Niacin
 0.5 mg/l Pyridoxine–HCl
 0.1 mg/l Thiamine
 in dH₂O sterile filtrated

MS–Media (Murashige & Skoog, 1962)

4.6 g/l MS–salts
 20 g/l Saccharose
 1 ml/l Vitamin solution
 pH 5.8 (KOH)
 8 g/l “Select Agar”
 Media was autoclaved for 20 min (121°C, 1.2 bar)

Seeds were sterilized and stratified (2 d, 4°C) before sowing and growing on MS-media. Single seeds were applied to MS-media under sterile conditions. After two weeks seedlings were transplanted on soil.

2.2.2.3 Stress conditions

Prior to stress treatments, soil-grown seedlings were transferred in pairs of four into separate pots. The pots were placed on Petri dishes, which were watered equally with 50 ml dH₂O per week. For osmotic stress treatments the water was replaced by the appropriate solutions (concentrations from 100 mM-400 mM) of mannitol and sodium chloride respectively. For cold treatments, plants were grown at 4°C. Drought treatment was performed by withholding water till the desired relative water content was reached. The relative water content (RWC) of plants was calculated as described below:

$$RWC (\%) = \frac{\left[\frac{Fwt}{Dwt} - 1 \right]}{\left[\frac{TwT}{Dwt} - 1 \right]} * 100 \%$$

RWC: Relative water content (%). Fwt (Fresh weight); TwT (Turgescent weight): Weight after the rehydration of leaves for 24 h in H₂O. Dwt (drought weight): Drought weight of leaves after 24 h at 80°C.

2.3 Microorganisms

2.3.1 Bacterial and yeast strains

- *Escherichia coli* DH10B (Lorow & Jessee, 1990)
Genotype: F⁻ mrcAΔ(mrr-hsdRMS-mcrBC)φ80d lacZΔ M15 Δ lacX74 endA1 recA1 deoRΔ (ara. leu) 7697 araDD139 galU galK nup6 rpsLλ⁻
This *E. coli* strain was used for cloning.
- *Escherichia coli* BL21(DE3) (Pharmacia, Freiburg, Germany)
Genotype: F⁻. ompT. hsdS(r⁻_B. m⁻_B). gal. dcm. /λDE3 (lacI. lacUV5-T7 gene 1. ind1. sam7. nin5).
This *E. coli* strain was used for the over-expression of proteins.
- *Saccharomyces cerevisiae* Y190 (Durfee *et al.*, 1993)
Genotype: MATa, gal4-542, gal80-538, his3-200, trp1-901, ade2-101, ura3-52, leu2-3,112, URA3:: GAL-LacZ, Lys2::GAL1-HIS3,cyhr
This yeast strain was used for yeast-two-hybrid assays. This strain is auxotroph for tryptophan, leucine, and histidine, which can be used as selection markers.
- *Saccharomyces cerevisiae* containing the cDNA library
Genotype: MATa, gal4-542, gal80-538, his3-200, trp1-901, ade2-101, ura3-52, leu2-3,112, URA3:: GAL-LacZ, Lys2::GAL1-HIS3,cyhr.
This oligo (dT)-primed cDNA library using mRNA from *A. thaliana*, was cloned in the plasmid pACT2 and kindly provided by Dr. Csaba Koncz (Max plank institute for Plant Breeding Research, Cologne, Germany).

2.3.2 Media for microorganisms

- SOC-media: 2 % (w/v) Tryptone, 0.5 % (w/v) yeast extract, 10 mM NaCl, 10 mM MgSO₄, 10 mM MgCl₂
- LB-media: 1 g/l Tryptone, 10 g/l NaCl, 5 g/l yeast extract, pH 7.0
- LB-agar: 15 g/l Select-Agar was added to LB-media
- YEB-media: 5 g Beef extract, 5 g peptone, 5 g sucrose, 1 g yeast extract, pH 7.0. After autoclaving filter-sterilized MgCl₂ solution (final concentration 2 mM) was added
- YPAD-media: 4 % (w/v) Pepton, 2 % (w/v) yeast extract, 10 % (v/v) glucose solution (40 % w/v), pH 6.5
- SD-media: 0.67 % (w/v) YNB, 5 % (v/v) glucose (40 %), 10 % (v/v) drop-out solution, pH 5.8

Media was autoclaved for 20 min at 121°C and 1.2 bar.

Media supplements:

- Ampicillin stock solution: 100 mg/ml in dH₂O. Dilution: 1:1000
- Kanamycin stock solution: 50 mg/ml in dH₂O. Dilution: 1:1000
- Gentamycin stock solution: 25 mg/ml in dH₂O. Dilution 1:1000
- Spectinomycin stock solution: 50 mg/ml in dH₂O. Dilution 1:1000
- Rifampicin stock solution: 50 mg/ml in DMSO (dimethyl sulfoxide). Dilution: 1:500

2.3.3 Generation of rubidium chloride–competent cells

TFBI	TFBII
30 mM Potassium acetate	10 mM MOPS
100 mM Rubidium chloride	75 mM Calcium chloride
10 mM Calcium chloride	10 mM Rubidium chloride
50 mM Manganese chloride	15 % (v/v) Glycerol
15 % (v/v) Glycerol	
pH 5.8 (Acetic acid)	pH 6.5 (KOH)

Generation of rubidium chloride-competent cells was performed as described by (Stiti *et al.*, 2007) with few modifications. A pre-culture (3 ml) of *E. coli* was inoculated and incubated overnight at 37°C on a shaker (200 rpm). The next day, a main culture (100 ml) was inoculated, and grown to an OD₆₀₀ of 0.35 – 0.45. Bacterial cells were centrifuged (4000 g, 10 min, 4°C) and resuspended in 15 ml ice-cold TFBI solution, incubated on ice (10 min) and again centrifuged (4000 g, 10 min, 4°C). The pellet was resuspended in 25 ml ice-cold TFBI solution, incubated on ice (5 min) and re-centrifuged. Finally, the pellet was resuspended in 2 ml TFBII and stored at -80°C.

2.3.4 Generation of electro-competent *A. tumefaciens*

A pre-culture of *A. tumefaciens* was grown in 5 ml YEB medium supplemented with rifampicin overnight at 28°C (250 rpm). A fresh culture of 50 ml YEB medium with rifampicin was inoculated and grown to an OD₆₀₀ of 0.5 and subsequently placed on ice for 30 min. Cells were harvested by centrifugation (10 min, 5000 rpm, 4°C) and the recovered pellet was resuspended in 25 ml ice-cold sterile water. The cells were centrifuged (10 min, 5000 rpm, 4°C) and washed as follows:

1. 25 ml 1 mM Hepes pH 7.5
2. 12.5 ml 1 mM Hepes pH 7.5
3. 10 ml 10 % (v/v) Glycerol, 1 mM Hepes pH 7.5
4. 5 ml 10 % (v/v) Glycerol, 1 mM Hepes pH 7.5
5. 2 ml 10 % (v/v) Glycerol

The cells were finally resuspended in 1 ml 10 % (v/v) glycerol, frozen in liquid nitrogen and stored at -80 °C.

2.3.5 Glycerol stocks

A single colony of the desired clone was transferred to appropriate media, supplemented with the appendant antibiotic and incubated overnight. Equal volumes of the culture and sterile glycerol were mixed in a cryotube, frozen in liquid nitrogen and stored at -70°C.

2.4 Cloning methods

2.4.1 Electrophoresis of nucleic acids (Adkins & Burmeister, 1996)

50 x TAE–Buffer

2 M Tris
50 mM EDTA
pH 8.0 (Acetic acid)

10 x Loading buffer

2.5 mg/ml Bromphenol blue
2.5 mg/ml Xylenxanol
30 % (v/v) Glycerol
2 % (v/v) 50 x TAE–buffer

Nucleic acids were separated by electrophoresis on agarose gels with concentrations ranging from 0.8 % to 1.5 % (w/v) depending on their molecular size. Agarose was added to 1x TAE–buffer, boiled and after cooling down supplemented with ethidium bromide (final concentration 10 µg/ml). A 1 kb GeneRuler was used as a molecular marker. Electrophoresis was performed in 1x TAE–buffer at 90 V and gels were analyzed under UV-light.

2.4.2 Isolation and purification of plasmid DNA (Sambrook *et al.*, 1989)

P1–buffer

50 mM Tris
11 mM EDTA
RNase A (100 µg/µl)
pH 8.0 (HCl)

P2–buffer

200 mM NaOH
1 % (w/v) SDS

P3–buffer

3 M Potassium acetate
pH 5.5 (Acetic acid)

Isolation of plasmid DNA was performed as described by Sambrook *et al.* (1989) in a modified version. A clone was incubated (200 rpm, 37°C) overnight in 2 ml LB-media and supplemented with antibiotics. The overnight culture was centrifuged (16,000 g) and the resulting pellet was resuspended in 100 µl buffer P1. After the addition of 100 µl buffer P2, the solution was mixed carefully and supplemented with 150 µl P3-buffer. The mixture was centrifuged (16,000 g, 10 min, RT) and 700 µl of the supernatant was transferred to an equal volume of phenol-chloroform (1:1 v/v). After centrifugation the upper phase was precipitated

with equal amounts of isopropanol on ice for 15 min. Plasmid DNA was retained by centrifugation (16000 g, 30 min, RT), washed with 70 % (v/v) EtOH and stored at -20°C.

For the extraction of high amounts of pure plasmid the “Plasmid Maxi Kit” (Fermentas) was used according to the manufacturer’s instructions.

2.4.3 Purification of DNA

For the purification of DNA samples (100 µl), equal volumes of phenol were added, shortly vortexed and centrifuged. Equal volumes of chloroform were added to the supernatant and the mixture was supplemented and mixed with two volumes ice-cold 90 % (v/v) ethanol, 0.1 volumes 3 M sodium acetate (pH 4.5) and 20-40 µg glycogen. After centrifugation (20 min, 16,000 g, 4°C) the precipitated DNA was washed twice with 70 % (v/v) ethanol, air-dried and finally dissolved in 20 µl sterile dH₂O.

Extraction and purification of plasmid DNA from agarose gels was done with the NucleoSpin Extract II Kit (Macherey-Nagel) according to the manufacturer’s instructions.

2.4.4 Restriction digestion

A typical restriction digest:

10 x buffer	2 µl
DNA / plasmid	100 ng – 1 µg
Restriction enzymes	Each 5 units
dH ₂ O	Rest
Total:	20 µl

Restriction digests were performed as described by Sambrook *et al.* (1989) at 37°C for 1-3 h or overnight. To avoid spontaneous re-ligation of compatible ends of single-digested, linearized plasmids, dephosphorylation of plasmids was performed after the restriction digest by alkaline phosphatases. The SAP-enzyme (Thermo Fisher Scientific) was added to the restriction digest reaction (final concentration 1 unit/µl) and incubated for 10 min at 37°C. Inactivation of the phosphatases was achieved by heating the samples for 15 min at 65°C.

2.4.5 Ligation (Sambrook *et al.*, 1989)

Prior to cloning DNA amplicons into plasmids, a restriction digest was carried out. The molar insert concentration was at least 3-fold higher than the plasmids. The ligation calculator Lig_Input (University of Düsseldorf) was used for the calculation of molar ratios. Digested plasmids and inserts were ligated at 23°C for 3 h (or at 16°C overnight) by the T4-DNA-ligase. An additional ligase reaction without insert was used as a negative control. The ligation mix was subsequently used for transformation or stored at -20°C.

A typical ligase reaction:

10 x ligase buffer	1 µl
T4-DNA-ligase	1 µl
Plasmid	x ng/µl
Insert	3*x ng/µl
dH ₂ O:	4 µl
Total:	10 µl

2.4.6 Transformation of rubidium chloride-competent *E. coli* (adapted from Hanahan, 1983)

Rubidium chloride-competent cells (50 µl) were supplemented with 2 µl ligation mix (1 pg – 100 ng) and incubated on ice for 30 min. Bacterial cells were transformed at 42°C for 30 s and subsequently cooled on ice for 5 min. After the addition of 950 µl SOC-medium (sterile filtrated), cells were incubated for one hour at 37°C (200 rpm). Regenerated cells were streaked out on LB-plates with the appropriate antibiotic and incubated overnight (37°C). Transformation without the ligation mix was used as a negative control.

2.4.7 Transformation of electro-competent *A. tumefaciens* (adapted from Tung & Chow, 1995)

Plasmid DNA (10-100 ng/µl) was added to electro-competent cells (50 µl) and mixed carefully. The mixture was transferred to a pre-cooled electro cuvette and placed into the electroporation device (Bio-Rad). An electric pulse was applied for 9 seconds (25 µF, 2.5 kV, 400Ω). YEB medium (1 ml) was subsequently added and cells were regenerated at 28°C (3 h, 250 rpm). Regenerated cells were placed on YEB-plates containing appropriate antibiotics and incubated at 28°C for 2 days.

2.5 Isolation of genomic DNA

Plant material was harvested, frozen in liquid nitrogen and grinded with a mortar. Depending on the experiment to be carried out, two different DNA-extraction methods have been applied.

2.5.1 UREA-extraction method (adapted from Sambrook *et al.*, 1989)

2 x Lyses-buffer:

0.6 M NaCl

0.1 M Tris-HCL, pH 8.0

40 mM EDTA, pH 8.0

4 % (w/v) Sarkosyl

1 % (w/v) SDS

Pulverized plant material (50–200 mg) was resuspended in 375 μ l 2x Lyses-buffer and 375 μ l 2 M UREA. After the addition of one volume phenol–chloroform–isoamyl alcohol (25:24:1), the suspension was centrifuged (14,000 rpm, 10 min, RT) and the resulting supernatant was precipitated with 0.7 volumes of isopropanol. The DNA-pellet was obtained by centrifugation (14,000 rpm, 15 min, 4°C) and subsequently washed twice with 1 ml 70 % (v/v) EtOH. The pellet was air-dried and resuspended in 25 μ l resuspension buffer. Genomic DNA was stored at -20°C.

2.5.2 Quick-extraction method (adapted from Edwards *et al.*, 1991)

DNA-extraction buffer:

100 mM Tris-HCL, pH 8.0

100 mM NaCl

10 mM EDTA

1 % (w/v) SDS

The “quick-extraction method” provides genomic DNA in a quality that is sufficient for genotyping PCRs. Plant material from *A. thaliana* was transferred to small tubes containing 250 μ l DNA-extraction buffer and subsequently triturated with a small mortar. After the addition of 100 μ l chloroform–isoamylalcohol (24:1), the suspension was mixed and centrifuged (16,000 g, 10 min, RT). The supernatant was transferred and DNA precipitated by the addition of isopropanol (5 min, RT). After centrifugation (16,000 g, 10 min, RT), genomic DNA was purified in two subsequent washing steps with 70 % (v/v) ethanol. The air-dried pellet was finally resuspended in dH₂O and stored at -20°C.

2.6 Amplification of DNA fragments by PCR (Mullis & Faloona, 1987)

The polymerase-chain-reaction (PCR) was used to amplify specific nucleid sequences by a primer pair and a thermostable DNA-polymerase.

A typical PCR-mixture:

10 x PCR-Buffer	2.0 μ l
Template-DNA (1 μ g/ μ l)	1.0 μ l
dNTPs (10 mM)	1.0 μ l
Fwd.-primer (10 mM)	0.5 μ l
Rev.-primer (10 mM)	0.5 μ l
Taq-polymerase	0.2 μ l
dH ₂ O	14.8 μ l
Total:	20.0 μl

A typical PCR-program:

Initial denaturation	95 °C	5 min	} 25 cycles
Denaturation	95 °C	30 s	
Annealing	T _a	30 s	
Elongation	72 °C	30 s/500 bp	
Final elongation	72 °C	10 min	
Storage	4 °C	∞	

2.6.1 Genotyping of T-DNA insertion mutants

To confirm homozygosity of T-DNA insertion mutants, all plants were genotyped before the experiments were carried out. For each gene, a gene-specific primer pair and a T-DNA specific primer pair was used to reassure the gene knock-out. Wild-type DNA was used as a control for gene-specific PCRs.

2.6.2 Colony-PCR (Sambrook *et al.*, 1989)

A single bacterial colony was inoculated in 50 μ l dH₂O and 2 μ l of this suspension was deployed in a colony-PCR. Gene and vector-specific primers for the construct of interest were used to test successful transformation of the construct.

2.7 Extraction of RNA from plant tissue

2.7.1 RNA extraction with urea (adapted from Missihoun *et al.*, 2011)

RNA extraction buffer:

6 M Urea

3 M Lithium chloride (LiCl)

10 mM Tris-HCl, pH 8.0

20 mM EDTA, pH 8.0

The extraction buffer was autoclaved prior to use (20 min, 121°C, 1.2 bar).

Frozen and pulverized plant material (100 mg) was resuspended and homogenized in 500 µl extraction buffer. After the addition of 500 µl phenol–chloroform–isoamylalcohol (25:24:1), the suspension was centrifuged twice (5 min, 10,000 g, RT) and the upper phase was subsequently transferred to a tube containing equal volume of chloroform-isoamylalcohol (24:1). The mixture was centrifuged (5 min, 10,000 g, 4°C) and the supernatant precipitated with one volume ice-cold isopropanol and 0.1 volume 3 M sodium acetate, pH 5.2. The suspension was incubated on ice for five minutes, centrifuged (10 min, 14,000 rpm, 4°C) and the resulting pellet was washed twice with 70 % (v/v) ethanol. The air-dried pellet was finally dissolved in 25 µl dH₂O or diethyl pyrocarbonate– (DEPC, final concentration 0.1 %) treated water and stored at -80°C.

2.7.2 Phenolic RNA-extraction method (adapted from Valenzuela-Avendaño *et al.*, 2005)

RNA extraction buffer:

38 % (v/v) Phenol

0.8 M Guanidine thiocyanate

0.4 M Ammonium thiocyanate

0.1 M Sodium acetate, pH 5.0

The extraction buffer was autoclaved prior to use (20 min, 121°C, 1.2 bar).

Frozen plant material (100 mg) was subjected to 1.5 ml RNA extraction buffer. The suspension was vortexed, centrifuged (10,000 g, 10 min, RT) and the supernatant was mixed with $\frac{2}{3}$ volumes of chloroform–isoamylalcohol (24:1). After centrifugation (10,000 g, 10 min, 4°C) the upper phase was precipitated with equal volumes of ice-cold isopropanol and 0.8 M sodium citrate/ 1 M sodium chloride solution. The mixture was incubated (10 min, RT) and subsequently centrifuged (12,000 g, 10 min, 4°C). The RNA was air-dried and resuspended in 25 µl dH₂O or DEPC-treated water.

2.7.3 Extraction of polysomes (adapted from Jackson & Larkins, 1976)

Buffer D	Extraction buffer	Dissociation buffer
200 mM Tris-HCL 9.0	200 ml Buffer D	20 mM HEPES, pH 7.2
120 mM Potassium chloride	200 mM Sucrose	10 mM EDTA
50 mM Magnesium chloride	5 mM DTT	1 % (w/v) SDS
Solution was autoclaved (20 min, 121°C, 1.2 bar)		0.5 M NaCl

Sucrose cushion

54 % (w/v) Sucrose
46 % (w/v) Buffer D

Pulverized plant tissue (1 g) was affiliated in 40 ml extraction buffer, centrifuged (10 min, 4000 g, 4°C) and the supernatant was transferred to a fresh reaction tube. To exclude insoluble debris an additional washing step was carried out (10 min, 10000 g, 4°C) prior to the collection of polysomal RNA (30 min, 38,000 g, 4°C). The polysomal pellet was subsequently resuspended in 15 ml isolation buffer, washed (30 min, 38,000 g, 4°C) and the suspension transferred into a centrifugal tube containing a sucrose cushion (2 ml). The final centrifugation was carried out in an ultra-centrifuge (3 h, 100,000 g, 4°C) and the resulting pellet was resuspended in dissociation buffer.

2.8. Reverse transcription polymerase chain reaction

2.8.1 DNase treatment (adapted from Innis *et al.*, 2012)

The “RevertAid H Minus First Strand cDNA Synthesis Kit” (Fermentas) was used according to manufacturer’s instructions for DNase treatment of RNA.

A typical DNase treatment reaction:

10 x reaction buffer (Fermentas)	1 μ l
DNase I, RNase-free (Fermentas)	1 μ l
RNA (500 ng/ μ l)	2 μ l
DEPC-treated dH ₂ O	6 μ l
Total	10 μ l

The reaction was incubated for 30 min at 37°C. Subsequently the DNase was inactivated by the addition of 1 μ l 50 mM EDTA for 10 min at 65°C.

2.8.2 Synthesis of cDNA (adapted from Innis *et al.*, 2012)

The “RevertAid H Minus First Strand cDNA Synthesis Kit” (Fermentas) was used according to manufacturer’s instructions for the generation of cDNA.

A typical reaction mix:

5 x reaction buffer (Fermentas)	4 μ l
RiboLock (Fermentas)	0.5 μ l
dNTPs (10 mM)	2 μ l
Template RNA (1000 ng/ μ l)	1 μ l
Oligo(dT) ₁₈ primer (10 mM)	0.5 μ l
Transcriptase (Fermentas)	0.5 μ l
DEPC-treated dH ₂ O	rest
Total	20 μ l

The reaction was incubated for 60 min at 42°C and finally terminated by heating for 10 min at 70°C. Reverse transcription reaction product was stored at -20°C or directly used in PCR.

2.9 Extraction of proteins

To avoid degradation of proteins, all steps were carried out on ice, whenever possible.

2.9.1 Extraction of total proteins from *A. thaliana*

2.9.1.1 Extraction of total proteins (Röhrig *et al.*, 2008).

Quality of extracted proteins was sufficient for subsequent phosphoprotein enrichment.

Dense SDS

30 % (w/v) Sucrose

2 % (v/v) SDS

0.1 M Tris-HCl, pH 8.0

5 % (v/v) 2-Mercaptoethanol

Pulverized plant material (3 ml) was transferred to a 15 ml reaction tube, containing 10 ml ice-cold acetone. The suspension was vortexed, centrifuged (4,000 g, 5 min, 4°C) and washed again with acetone. The resulting pellet was resuspended in 10 ml 10 % (w/v) TCA solution and sonicated in an ice-cold water bath (10 min). After centrifugation (4,000 g, 5 min, 4°C), the resulting pellet was successively washed with 10 % (w/v) TCA in acetone (3 times), 10 % (w/v) TCA and twice with 80 % (w/v) acetone. The acetone-wet pellet was thoroughly resuspended in 5 ml Dense SDS and 5 ml phenol, centrifuged and the upper phase was transferred to new reaction tubes. Proteins were precipitate by the addition of 0.1 M ammonium acetate in methanol for 30 min at -20°C. The protein pellets were washed twice with ice-cold 0.1 M ammonium acetate and once with ice-cold 80 % acetone (w/v). Proteins were stored at -20°C prior to use.

2.9.1.2 “Direct-method” (Laemmli, 1970)

Pulverized plant material (200 mg) was affiliated in 100 µl 1 x SDS-sample buffer (2 % (w/v) SDS, 10 % (w/v) glycerol, 60 mM Tris-HCl, pH 6.8, 0.01 % (w/v) bromphenol blue, 0.1 M DTT), boiled at 95°C for 10 min and centrifuged (2,000 g, 10 s, RT). Samples were directly used for gel-electrophoresis (SDS-PAGE) or stored at -20°C.

2.9.2 Enrichment of phosphoproteins (Röhrig *et al.*, 2008).

IB-A	IB-B	IB-200
30 mM MES–HCL, pH 6.1	30 mM MES–HCL, pH 6.1	30 mM MES–HCL, pH 6.1
0.25 % CHAPS	0.25 % CHAPS	0.25 % CHAPS
7 M Urea	7 M Urea	7 M Urea
2 M Thiourea	2 M Thiourea	2 M Thiourea
	0.23 M Sodium glutamate	0.2 M Sodium glutamate
	0.23 M Potassium aspartate	0.2 M Potassium aspartate
	30 mM Imidazol	20 mM Imidazol

EB-300: 7 M Urea, 2 M Thiourea, 0.3 M Potassium pyrophosphate, pH 9.0

A pellet of total proteins was resuspended in IB-A (final protein concentration 3 mg/ml), sonicated in a water bath (5 min, 4°C) and stored at 10°C overnight. After the addition of two volumes IB-B (final protein concentration 1 mg/ml) the solution was stored at -20°C.

Aliquots of 120 mg aluminium hydroxide were washed twice in 2 ml tubes with IB-200 (1 min, 12,000, RT). The stored protein solution was centrifuged (10,000 g, 10 min, 4°C) and the clear supernatant was transferred to the prepared aluminium hydroxide. The mixture was incubated on a rotating wheel for 60 min at 10°C. Aluminium-bound phosphoproteins were washed six times with IB-200 (10,000 g, 1 min, 4°C) and finally affiliated in EB-300 (1 ml). After elution of phosphoproteins on a rotator (30 min, RT), the mixture was centrifuged (20,000 g, 5 min, RT) and the clear supernatant was transferred to an Amicon Ultra-4 Centrifugal Filter (Ultracel-10K, Milipore). Proteins were concentrated to a final volume of 100 µl by centrifugation (7,000 g, 30 min, 4°C) and the retentate was transferred to a reaction tube containing 500 µl dH₂O and 7 µl 2 % (w/v) sodium deoxycholate (DOC). The mixture was vortexed and incubated on a rotator for 120 min at 4°C. Precipitated proteins were recovered by centrifugation (20,000 g, 10 min, 4°C) and washed sequentially with 1 ml 25 % (w/v) TCA-solution (4°C) and 1 ml ice-cold 80 % acetone/ 20 % Tris–HCl (50 mM, pH 7.5). After a final washing step (1 ml 80 % (w/v) acetone) the protein pellet was recovered and air-dried. Phosphoproteins were stored at -80 °C.

2.9.3 Protease inhibitor Assay

The proteasome inhibitor cocktail P9599 (Sigma) was used according to manufacturer's instructions to prevent protein degradation. The treatment was conducted as described by (Speranza *et al.*, 2001). The inhibitor solution was added to protein extracts (final concentration 0.2 % (w/v)), while control samples were not treated with the inhibitor cocktail.

2.10 Quantification of nucleic acids and proteins

2.10.1 Estimation of nucleic acid concentrations

Concentration of DNA and RNA was estimated with a spectrophotometer (Biospec–Nano, Shimadzu Biotech). The concentration (c) can be calculated with the optical density at 260 nm (OD_{260}) in combination with the dilution factor (V) and a DNA/RNA– specific multiplication as follows:

Double-stranded DNA: $c [\mu\text{g/ml}] = OD_{260} \times V \times 50$

RNA: $c [\mu\text{g/ml}] = OD_{260} \times V \times 40$

The OD_{260}/OD_{280} quotient describes the purity of the solution. A value between 1.8 and 2.0 indicates pure nucleic acids.

2.10.2 Estimation of proteins concentrations (adapted from Bradford, 1976)

Proteins (100 μl) were dissolved overnight in 7 M urea/2 M thiourea. 20 μl of the protein solution was transferred to a reaction tube containing 0.8 ml dH_2O and 0.2 ml Bradford reagent (section 2.10.2). The mixture was incubated at RT for 5 min and the absorbance at 595 nm was measured. The protein concentration was estimated with a calibration line from BSA (**Figure 8**).

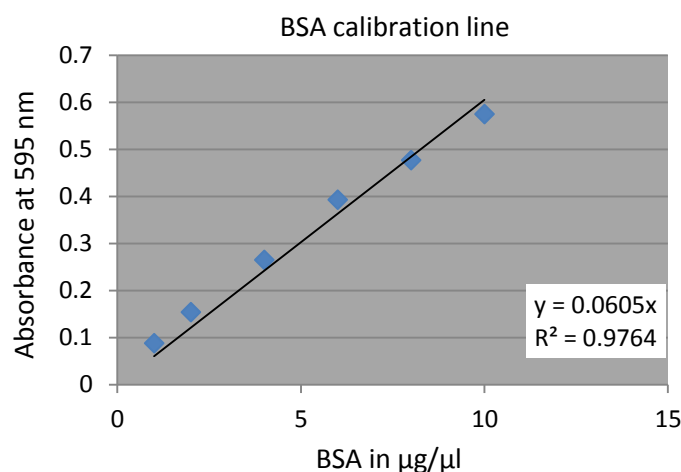


Figure 8: BSA calibration line

2.11 Over-expression and isolation of recombinant proteins

The pET-28 expression system in the *E. coli* BL21 strain was used for the over-expression of recombinant proteins.

Buffer A

50 mM Sodium dihydrogenphosphate
0.3 M NaCl
5 mM Imidazol
10 % (v/v) Glycerol
0.1 % (v/v) Triton X-100
pH 8.0 (NaOH)

Buffer C

50 mM Sodium dihydrogenphosphate
0.3 M NaCl
0.25 M Imidazol
10 % (v/v) Glycerol
0.1 % (v/v) Triton X-100
pH 8.0 (NaOH)

Buffer B

50 mM Sodium dihydrogenphosphate
0.3 M NaCl
20 mM Imidazol
10 % (v/v) Glycerol
0.1 % (v/v) Triton X-100
pH 8.0 (NaOH)

Regeneration buffer

0.1 M EDTA
0.5 M NaCl
20 mM Tris-HCL, pH 7.9

Charge buffer

50 mM Nickel sulfate

A pre-culture of the bacteria of interest was grown in 2 ml LB-medium supplemented with the appropriate antibiotic at 37°C overnight. The next day the main culture (100 ml) was inoculated and grown (37°C, 200 rpm) till an OD₆₀₀ of 0.5. The culture was subsequently incubated at 26°C for 15 min in the dark and a sample of the not-induced bacteria was collected (sample 0 h). Expression of proteins was induced by the addition of isopropyl-β-D-thiogalactopyranoside (IPTG) (final concentration 1 mM) and bacteria were grown for 3 h at 26°C. Bacterial samples (1 ml) were taken every hour and stored at -20°C. Main cultures (100 ml) were centrifuged (4,000 g, 20 min, 4°C) and bacterial pellets were stored at -20°C.

Over-expression of recombinant proteins often results in the precipitation of insoluble proteins, so called “inclusion bodies”. To test for the formation of inclusion bodies, the collected 1 ml samples were treated as described by (Palmer & Wingfield, 2001). The samples were centrifuged (4,000 g, 5 min, 4°C) and resuspended in 200 µl ice-cold PBS. The mixture was sonicated (4 x 20 s) after the addition of $\frac{1}{10}$ volumes of 10 % (v/v) Triton X-100. Bacterial cells were centrifuged (12,000 g, 10 min, 4°C) and pellets and supernatants were separated and resuspended in SDS-sample buffer prior to electrophoretic analysis.

The mixture was incubated on ice for 30 min and subsequently sonicated (6x 20 sec). An optional heat-treatment step (10 min, 100°C) was included for heat-stable proteins. Inclusion bodies were obtained by centrifugation for 30 min (14,000 rpm, 4°C) and stored at -20°C. The supernatant was purified through a filter (\approx 0.45 μ m) and a control sample (1 ml) was taken prior to loading the culture on a Ni-NTA column. Before the protein solution was loaded, the column was sequentially washed with dH₂O (3 ml), charge buffer (5 ml) and buffer A. After 2 ml of the protein solution ran through the column, 20 μ l of the flow through (sample Ft) was collected and frozen at -20°C. The Ni-NTA-bound proteins were washed by the addition of buffer A (10 ml) and buffer B (8 ml) to exclude unspecific binding of proteins. His-tagged proteins were eluted by the sequential addition of buffer C (six times 500 μ l). The eluted protein fractions were collected in reaction tubes (F1-F6) and stored at -20°C. The Ni-NTA column was regenerated by the addition of dH₂O (3 ml), regeneration buffer (3 ml) and 20 % (v/v) ethanol (3 ml). The regenerated column was stored in 20 % (v/v) ethanol at 4°C.

Recombinant proteins were loaded onto PD10-desalting columns (GE Healthcare) to remove remaining salts from the solution. The desalting columns were used according to the manufacturer's instructions and the buffer was exchanged to 100 mM ammonium bicarbonate (NH₄HCO₃). Ammonium bicarbonate is a volatile organic compound that is commonly used in protein lyophilization. Proteins were lyophilized for 2-3 days in a lyophilizer (LDC-2, Christ) and stored at -20°C.

2.12 Electrophoresis of proteins

2.12.1 Isoelectric focusing (first dimension)

IPG strips: Immobiline DryStrip, pH 3–10, 7 cm (GE Healthcare)

Equilibration buffer	Rehydration solution	IEF–agarose
50 mM Tris–HCl, pH 6.8	7 M Urea	0.5 % (w/v) Agarose
2 % (w/v) SDS	2 M Thiourea	0.002 % (w/v) Bromphenol blue
6 M Urea	2 % (w/v) CHAPS	in 1x running buffer
Bromphenol blue	Bromphenol blue	melted at 100°C, stored at 60°C
30 % (v/v) Glycerol	Prior to usage:	
	0.2 % (w/v) DTT	
	0.5 % (v/v) IPG buffer pH 3–10 (GE Healthcare)	

Protein samples (20–40 µg) were completely dissolved in 130 µl rehydration solution (>1h, RT). Insoluble particles were removed by centrifugation (12,000 g, 10 min, RT) and 125 µl of the protein solution was then transferred to an IPG strip in a focusing tray. To prevent evaporation during the rehydration process (12–16 h, 20°C), the IPG strip was overlaid with mineral oil. Proteins were separated according to their isoelectric point in the IPGphor II isoelectric focusing system (GE Healthcare).

Typical focusing conditions for the first dimension used in this work:

14 h Rehydration
 30 min 500 V
 30 min 1000 V
 100 min 5000 V

Prior to separating the proteins in the second dimension, IPG strips were equilibrated in SDS-containing buffers to reduce and alkylate cysteine residues, which might interfere with staining of two-dimensional gels. IPG strips were incubated for 15 min in 5 ml equilibration buffer, supplemented with 50 mg DTT. Subsequently, IPG strips were transferred to 5 ml equilibration buffer with 125 mg iodacetamide. Finally IPG strips were put on SDS-PAGE gels and sealed with IEF agarose.

2.12.2 SDS-PAGE (second dimension) (adapted from Laemmli, 1970)

SDS-sample buffer (2x)	Polyacrylamide gels	Separating gel (12 %)	Stacking gel (4 %)
4 % (w/v) SDS	dH ₂ O	2.88 ml	2.16 ml
20 % (w/v) Glycerol	1.5 M Tris-HCl, pH 8.8	2.34 ml	-
120 mM Tris-HCl, pH 6.8	1 M Tris-HCl, pH 6.8	-	375 µl
Bromphenol blue	Rotiphorese gel 30	3.60 ml	405 µl
0.2 M DTT (added freshly)	10 % (v/v) SDS	90 µl	30 µl
	10 % (w/v) APS	90 µl	30 µl
	TEMED	3.6 µl	3 µl
1 x running buffer			
25 mM Tris			
192 mM Glycine			
0.1 % (w/v) SDS			

Protein pellets (1-fold) and solutions (2-fold) were dissolved in SDS-sample buffer and boiled at 95°C for 10 min prior to loading on SDS-PAGEs. For the separation of proteins in the second dimension, IPG strips were directly transferred to SDS-PAGEs. Electrophoresis was performed in 1 x running buffer at 20 mA for 2 h.

2.12.3 Staining of polyacrylamide gels

2.12.3.1 Coomassie Staining (adapted from Zehr *et al.*, 1989)

Fixation solution	Staining stock solution	Staining solution
10 % (v/v) Acetic acid	10 % (w/v) Ammonium sulfate	80 % (v/v) Staining stock solution
40 % (v/v) Methanol	1 % (v/v) Phosphoric acid	20 % (v/v) Methanol
	0.1 % (w/v) Coomassie G250	

Polyacrylamide gels were fixed in 100 ml fixation solution for one hour or overnight. Subsequently, the gel was washed three times for 10 min with dH₂O. Finally the gels were incubated in 50 ml staining solution on a shaker overnight. Gels were washed several times with dH₂O for destaining. The sensitivity limit of Coomassie stain is about 10-50 ng protein per band.

2.12.3.2 Silver staining (adapted from Chevallet *et al.*, 2006)

Fixation solution	Incubation solution	Staining solution
10 % (v/v) Acetic acid	6.8 % (w/v) Sodium acetate	0.1 g Silver nitrate
50 % (v/v) Ethanol	0.2 % (v/v) Sodium thiosulfate	30 µl 37 % (v/v) Formaldehyde
	30 % (w/v) Ethanol	in 100 ml H ₂ O
	0.5% (w/v) Glutardaldehyde	
Developer solution	Stop solution	
2.5 % (w/v) Sodium carbonate	0.8 g Glycine in 200 ml H ₂ O	
15 µl 37 % (v/v) Formaldehyde		

Polyacrylamide gels were fixed for one hour or overnight in fixation solution and subsequently for two hours in incubation solution. Proteins were visualized by the addition of developer solution and this reaction was stopped by the exchange with stop solution.

2.12.3.3 Phosphoprotein staining (adapted from Röhrig *et al.*, 2008)

The staining of phosphoproteins was carried with the Pro-Q Diamond phosphoprotein gel stain (Molecular Probes) which specifically binds to phosphate groups that are attached to serine, threonine and tyrosine residues.

Fixation solution	ProQ-Diamond	Destain Solution
10 % (v/v) Acetic acid	Ready to use staining solution	20 % (v/v) Acetonitrile
50 % (v/v) Methanol	Dilutions up to 1:3 with dH ₂ O (up to 30 ml per gel)	50 mM Sodium acetate, pH 4.0 in 100 ml H ₂ O

Polyacrylamide gels were fixed for 30 min (RT) by shaking or overnight without shaking. The gels were washed three times with dH₂O (10 min, RT) and subsequently incubated in the dark by gentle agitation in the staining solution for 90 min. To avoid illumination of the gel, all following steps were carried out in the dark: The gel was washed shortly with water (3 x 5 min) and three times thoroughly with destain solution (30 min). Short washing cycles (2 x 5 min) with dH₂O were performed to remove any remaining destain solution. The Typhoon 9200 scanner (GE Healthcare) was used for the visualization of phosphoproteins (excitation wavelength: 532 nm, band pass emission filter: 610 nm).

2.13 Protein blot (adapted from Towbin *et al.*, 1979).

The protein blot enables transfer of proteins from polyacrylamide gels to membranes and subsequent immunological detection of specific proteins.

Towbin–buffer	TBS	TBST
25 mM Tris	20 mM Tris, pH 7.5	0.1 % (v/v) Tween–20 in TBS
0.2 M Glycine	0.15 M NaCl	
20 % (v/v) Methanol		

Proteins were transferred at 70 V for 1-3 h (4°C) as described by Towbin *et al.* (1979). Successful transfer of proteins to nitrocellulose membrane (Whatman) was confirmed by staining with Ponceau red for 10 min. The membrane was destained with dH₂O.

Ponceau Red	Blocking solution
0.2 % (w/v) Ponceau S	4 % (w/v) low-fat milk powder in TBST
3 % (w/v) TCA	

The membrane was blocked in 4 % (w/v) low-fat milk powder in TBST for 1 hour (RT) or overnight (4°C) to minimize unspecific detection of the antibody. Afterwards the membrane was incubated with the first antibody (concentration 1:1000 – 1:5000 in blocking solution, depending on the antibody used) for 1 h (RT) or overnight (4°C).

The membrane was washed with TBST for a total of 30 min (1x 15 min; 3x 5 min) and subsequently incubated at RT for 45 min with the second antibody (1:5000 in blocking solution). The membrane was again washed as described above. The “ECL Western Blotting Detection Reagent” kit (GE Healthcare) was used for the detection of signals according to manufacturer’s instructions. The secondary antibody is coupled to a horseradish peroxidase and binds the primary antibody. By the addition of its substrate, the enzyme generates chemiluminescence signals, which were detected with the “Intelligent Dark Box II” (Fujifilm Corporation).

Alternative detection was done with photo-sensitive membranes. The blot was incubated with detection reagents as described above and subsequently transferred onto Whatman papers. The set-up was placed into photo-incubation cassettes and covered with photo-sensitive membranes (Fujifilm Corporation). Photo-membranes were incubated in the dark for 2 to 20 minutes and subsequently incubated in fixation solution. Development of the screens was done according to manufacturer’s instructions. The protein blots were stored at 4°C.

Overview of different antibodies used in this thesis:

Antibody	Antibody	Antibody
Anti-PLD α :	Anti-At5g39570.1:	Anti-At5g39570.1:
Rabbit antiserum	Rabbit antiserum	Rabbit antiserum
Animal 6636 (31)	Animal 1114 (Heat-treated)	Animal 1115
Final bleeding (19.10.2004)	Final bleeding (10.02.2011)	Final bleeding (10.02.2011)
Dilution: 1:1000	Dilution: 1:5000	Dilution: 1:5000
Antibody	Secondary antibody	
Anti-His	Anti-IGG Peroxidase:	
Rabbit antiserum	Goat antiserum	
GE-Healthcare	Sigma-Aldrich Chemie GmbH	
Dilution: 1:1000	Dilution: 1:5000	

2.14 Affinity purification of antibodies

The polyclonal antibody against At5g39570.1, which I produced during my diploma thesis, was used for the generation of a monospecific antibody to improve the signal in protein blots and for co-immunoprecipitation assays.

High concentrated, recombinant At5g39570.1 protein was loaded on a polyacrylamide gel and blotted on a nitrocellulose membrane. The blot was stained with Ponceau S, and the At5g39570.1 protein band was cut, destained and incubated in 4 % (w/v) dry milk powder in TBS for 1 hour at RT. The strip was washed five times in TBS prior to incubation with 2 ml anti-At5g39570.1 at 4°C overnight. On the next day, the serum was removed and the strip was washed once with TBST and thrice with TBS. The antibodies were eluted from the strip with 100 mM glycine pH 2.5 for 30 min. Subsequently, the eluate was neutralized by the addition of 0.5 ml 100 mM Tris pH 8.8. Antibodies were checked on protein blots and stored at -20°C.

2.15 Identification of protein-protein interactions

To identify putative binding partners of At5g39570.1 a subset of different identification methods has been used in this thesis.

2.15.1 Co-immunoprecipitation (adapted from Klenova *et al.*, 2002)

The co-immunoprecipitation (Co-IP) enables the detection of protein complexes. A selected antibody targets a known protein (e.g. At5g39570.1) that binds to other proteins in a complex. To detect these putative interacting partners, the intact protein complex has to be retrieved from the solution without destroying protein bonds of the known protein to candidate interacting partners. However it is difficult to detect weak protein-protein interactions because the protein complex is separated from the solution by different washing steps that prevent identification of unspecific binding partners. Co-IP can be carried out in denaturing and non-denaturing conditions. The latter one prevents loss of disulfide bonds in protein complexes.

A. thaliana wild-type plants were grown on MS-media and used for sample preparation according to (Karlova *et al.*, 2006) with the addition of 10 % (v/v) glycerol (denaturing conditions). For native protein extractions the non-denaturing extraction method described by Klenova *et al.* (2002) was followed. The magnetic-based Co-IP Kit (Novex) was used for antibody coupling and elution of protein complexes as described in the manufacturer's instructions. In addition, denaturing Co-IPs were conducted as described by Röhrig *et al.* (2006).

Denaturing immunoprecipitation (Röhrig *et al.*, 2006)

Wash buffer 1

50 mM Tris-HCl, pH 7.5
1 mM EDTA
0.5 M NaCl
0.1 % (w/v) Nonidet P40

Wash buffer 2

50 mM Tris-HCl, pH 7.5
1 mM EDTA
0.5 M NaCl
0.1 % (w/v) Nonidet P40

Wash buffer 3

10 mM Tris-HCl, pH 7.5
0.1 % (w/v) Nonidet P40

Lyses buffer

50 mM Tris-HCl, pH 8.0; 1 % (v/v) SDS; 1 mM EDTA

Pulverized plant tissue (100-200 µg) was supplemented with 200 µl lyses buffer and boiled at 95°C for 5 min. Samples were cooled on ice for 10 min and subsequently incubated in 1.8 ml wash buffer 1 on ice for 10 min. After centrifugation (16,000 g, 10 min, 4°C), 0.9 ml of the

supernatant was transferred into a new reaction tube and affiliated with anti-At5g39570.1 (10-50 μ l) on a rotator for one hour (4°C). Subsequently, 40 μ l of a protein-A-agarose suspension was added and the solution was again incubated (3 h, 4°C). The solution was centrifuged as above and the protein complex on agarose beads was obtained. The beads were washed (12,000 g, 1 min, 4°C) with wash buffer 1 (2 times), wash buffer 2 (2 times) and wash buffer 3 (1 time) prior to analysis on polyacrylamide gels.

2.15.2 Yeast-Two-Hybrid Assay (adapted from Gietz & Schiestl, 2007)

Transformation

Transformation of yeast strains was done according to Gietz and Schiestl (2007).

2 x YPAD medium	Drop-out solution (10 x)	1 x SD medium
4 % (w/v) Peptone	Amino acid solution was	0.67 % (w/v) YNB
2 % (w/v) Yeast extract	prepared without histidine,	5 % (v/v) Glucose (40 % w/v)
10 % (v/v) Glucose (40 % w/v)	leucine and uracil according	10 % (v/v) Drop-out solution
pH 6.5 (H ₂ SO ₄)	to Gietz <i>et al.</i> , 2007	pH 5.8 (NaOH)
(2 % w/v Agar for plates)		(2 % w/v Agar for plates)

Yeast colonies (\varnothing 2 mm) were selected and grown in 25 ml 2x YPAD medium in a 500 ml flask and incubated at 30°C under agitation (16-20 h, 250 rpm) to an OD₆₀₀ of \sim 1.0 (1×10^7 cells/ml). The culture was centrifuged (3 min, 3,000 g, RT) and the resulting pellet was subsequently resuspended in 50 ml warm 2 x YPAD medium and transferred to a fresh Erlenmeyer flask. The mixture was grown at 30°C for 3-5 hours until an OD₆₀₀ of 2.0. The cells were centrifuged (3 min, 3000 g, RT) and washed with sterile dH₂O. Finally the suspension was resuspended in 25 ml sterile dH₂O.

For the generation of bait-constructs, yeast cells were centrifuged (3 min, 3,000 g, RT), resuspended in 1 ml sterile water and transferred in aliquots of 100 μ l to ten 1.5 ml centrifugal tubes. The cells were centrifuged for 30 s at maximum speed and the supernatant was completely discarded. In case of the big scale 10 x transformation (used for the cDNA library) the cells were washed in 50 ml centrifugal tubes (3 min, 3,000 g, RT) and the pellet was stored on ice prior to further procedure. Master mixes for both, small scale and big scale transformations were prepared as follows:

	Small scale (10 x)	Large scale (single transformation)
50 % PEG	2.64 ml	2.4 ml
1 M Lithium acetate	396 μ l	360 μ l
SS-DNA (2 mg/ml)	550 μ l	500 μ l
Transforming DNA	x μ l (100 – 1000 ng)	340 μ l of library preparation (10 μ g)
Sterile dH ₂ O	up to 3.6 ml (10 x 360 μ l)	

The mixtures were freshly prepared and added to each tube containing the yeast cells. After vortexing the suspensions thoroughly (1 min), the transformation mixes were incubated at 42°C for 40 min in a water bath. To provide optimal transformation efficiencies, tubes were inverted every 5 minutes. Cells were harvested by centrifugation (small scale: 30 s, 16,000 rpm, RT; large scale: 2 min, 16,000 rpm, RT) and resuspended in 1 ml sterile water (small scale transformation), respectively 10 ml (large scale transformation).

Resuspended cells (200 μ l) from the small scale transformations were transferred with sterile disposal loops to plates (\varnothing 92 mm) containing selective SD-media. A full-media plate (YPAD medium) was inoculated with 10 μ l yeast cells as a control.

For big scale transformations 500 μ l cells were spread on plates containing SD_{-Trp-Leu-His} depletion media supplemented with different concentrations of 3-Amino-1,2,4-triazole- (3-AT). To calculate the transformation efficiency, 10 μ l of this suspension was diluted in a total volume of 100 μ l dH₂O and spread on SD_{-Trp} and SD_{-Trp-Leu} plates. The yeast plates were incubated at 30°C for 3-7 days.

Screening

Yeast colonies with putative bait-constructs that have grown on SD_{-Trp} plates were deployed in yeast colony PCRs by using gene-specific primers. Bait expression of positive clones was verified by western blotting. Extraction of yeast proteins was followed according to Gietz & Schiestl (2007) with modifications. Cracking buffer (8 M urea, 5 % (v/v) SDS, 40 mM Tris pH 6.8, 0.1 M EDTA, 0.4 mg/ml bromphenol blue) was used for protein extraction. Positive colonies were tested for autonomous reporter-gene activation with the colorimetric β -galactosidase activity assay.

Z-Buffer

- 16.1 g/l Na₂HPO₄x 7H₂O
- 5.5 g/l NaHPO₄x 7H₂O
- 0.75 g/l KCL
- 0.246 g/l MgSO₄x 7H₂O
- 2.7 ml/l β -Mercaptoethanol
- 1 mg/ml X-Gal (20 mg/ml in DMF)

A nylon filter (WH10311897, Whatman) was placed onto selected yeast colonies grown on selective media and incubated at 30°C (2-3 days). The filter was lifted from the plates and directly frozen in liquid nitrogen for 30-60 s. Whatman paper (3MM Chr) was soaked in 3 ml Z-Buffer and placed into a fresh Petri dish. The nylon filter was placed (yeast facing up) onto two layers of the prepared Whatman paper without introducing air bubbles or folds. The plates were incubated at 37°C for 24 hours and monitored. To avoid auto-activation of bait-constructs, a yeast colony that did not produce the blue compound after 24 hours was chosen. It was confirmed that the selected bait cannot grow on SD-depletion media with high concentrations (> 50 mM) of 3-AT.

After transformation of the expression library into yeast containing the selected bait, clones were selected on SD-depletion media supplemented with different concentration of 3-AT as described above. Positive colonies were picked and activation of the reporter gene was tested in another β -galactosidase assay. Colonies that grew on SD-depletion media with 50 mM 3-AT and that generated the blue indigo colorant were selected for further analysis.

2.15.3 Affinity chromatography with spin columns

Affinity chromatography assays using the 0.2 ml His-Pur Ni-NTA spin columns (Thermo Scientific) were conducted according to manufacturer's instructions. Lyophilized, recombinant protein was incubated with plant material (15 min, RT) and resuspended in equal volume of Buffer A (see section **2.11**). Ni-NTA spin columns were cut open and placed into 1.5 ml reaction tubes. The storage buffer was removed by centrifugation (2 min, 700 g, RT). Spin columns were equilibrated by two subsequent washing steps with Buffer A. Finally the columns were loaded with the protein suspensions and washing and elution was performed as described in section **2.11** with down-scaled bed volumes of 0.2 ml. Eluates were diluted with 2 x Laemmli buffer and stored at -20°C prior to analysis.

2.16 Protein-lipid interactions

2.16.1 Protein-lipid-overlay assay (adapted from Deak *et al.*, 1999)

Immobilization of lipids on nitrocellulose filters in the protein-lipid-overlay assay is the method of choice to identify whether a protein can bind to a lipid but it does not take into account the cellular environment where the lipids occur. The immobilized lipids (each 5 μg) on nitrocellulose membranes were kindly provided by Barbara Kalisch (IMBIO, University of Bonn, Germany). After blocking the membranes overnight in 5 % (w/v) BSA in TBS-T at 4°C, the membranes were washed four times with TBS-T (5 min) and incubated in the primary antibody (1 h, RT). Washing steps were repeated and the membrane was incubated for 45 min with the secondary antibody prior to analysis.

2.16.2 Liposome-binding assay (adapted from Zhang *et al.*, 2004)

Liposome-binding buffer A	Liposome-binding buffer B
20 mM MES	20 mM MES
30 mM Tris-HCl (pH 7)	30 mM Tris-HCl (pH 7)
100 mM NaCl	0.5 mM NaCl
1 mM DTT	2 M Urea
	0.5 % CHAPS
pH 5–9 was used	1 mM DTT

Phosphatidic acid (PA) and Phosphatidylcholine (PC), were dissolved in chloroform/methanol (2:1) solution (final concentration 4 $\mu\text{g}/\mu\text{l}$) and stored separately at -20°C. For each assay 250 μg lipids (150 μg PC & 100 μg of the tested lipid) was transferred to fresh glass tubes. Solvents were evaporated under the fume hood and resuspended in liposome-binding buffer A or B (0.5 μl $\mu\text{g}/\mu\text{l}$). The mixture was incubated at 37°C on a shaker (1 h, 250 rpm) and the resulting liposomes were vortexed (5 min) and subsequently centrifuged (10 min, 20,000 g, 4°C). Liposomes were stored at -20°C for no longer than two days or directly used for further analysis.

Prepared liposomes were resuspended in liposome-binding buffer A or B containing 0.1 $\mu\text{g}/\mu\text{l}$ of the protein of interest. The mixture was incubated at 30°C for 30 min and subsequently spun down (10 min, 10,000 g, 4°C). Supernatants and pellets were analyzed on polyacrylamide gels.

2.16.3 Liposome-turbidity assay (adapted from Roston *et al.*, 2011)

The liposome-turbidity assay was used for the time-dependent analysis of PA-binding proteins. Liposomes were prepared as described for the liposome-binding assay. The production of unilamellar liposomes was done by filtering liposome solutions through the Avanti Mini-Extruder (Avanti). Liposomes were extruded repetitively till the solution became clear. Unilamellar liposomes were transferred to UV-cuvettes and the OD₃₅₀ was determined. The protein of interest (5 µg) was added to the solution, mixed and directly analyzed by a spectrophotometer. The OD₃₅₀ was measured every two seconds for 5 – 8 minutes and values were transferred into excel sheets for further analysis.

2.17 Transient and stable transformation

2.17.1 Transient expression analysis via particle gun bombardment (adapted from Sanford *et al.*, 1993)

Microcarriers (30 mg gold particles, ø 1.6 µm) were washed thoroughly for 5 min with 1 ml ethanol followed by three washing steps with 1 ml sterile dH₂O. Gold particles were resuspended in 500 µl sterile 50 % (v/v) glycerol, distributed to fresh reaction tubes and stored at 4°C for further procedure. For coating of microcarriers 25 µg plasmid DNA, 50 µl 2.5 M CaCl₂ and 20 µl 100 mM spermidine was added in the indicated order to the gold suspension and mixed thoroughly by vortexing for 5 min. The microcarriers were centrifuged shortly and subsequently washed with 140 µl 70 % (v/v) ethanol and 100 % ethanol. A microcarrier disk was loaded with 25 µl of the prepared DNA-coated microcarrier suspension and placed into the metal holder. A metal grid was placed on top and the complete set-up was placed into the assembly unit of the particle gun. A ½ MS-media plate was loaded with fresh leaves from *A. thaliana* and placed in the center of the particle gun. By the application of vacuum (27 mm Hg, 3.6 MPa), the pressure was rising till the desired value (1150 psi) and was then released to shoot the DNA-coated gold particles with high velocity into the leaves. The leaves were incubated on the ½ MS plate for 12-48 h and analyzed under a confocal laser scanning microscope.

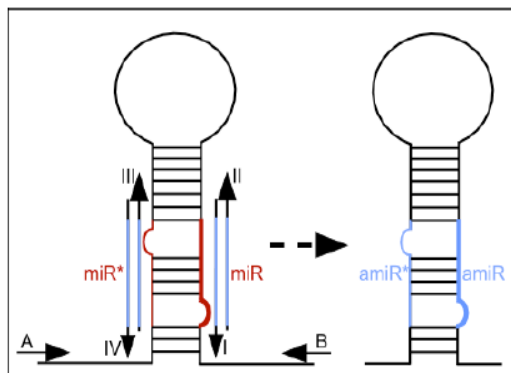
2.17.2 *A. tumefaciens*-mediated stable transformation of *A. thaliana* adapted from Clough & Bent, 1998)

A confirmed positive *A. tumefaciens* clone carrying the construct of interest was incubated in 20 ml YEB-medium supplemented with appropriate antibiotics (50 µg/ml kanamycin and 50 µg/ml rifampicin) at 28°C (24 h, 250 rpm). This subculture was used to inoculate a 250 ml culture of YEB medium with antibiotics and grown until an OD₆₀₀ of ~0.8 was reached. Prior to transformation, siliques were removed from flowering plants. The Agrobacterium culture was transferred to a 500 ml beaker and 0.05 % (v/v) of the surfactant Silwet Gold L-77 was added. The flowering plants were carefully immersed in the medium and dipped with gentle agitation for 30 s. After Agrobacterium-infiltration, plants were covered with perforated plastic bags and grown under long-day conditions. After one week of recovery, the infiltration was repeated to increase transformation efficiency. Putatively transformed seeds were collected and sown on MS-media supplemented with the appropriate antibiotics.

2.18 Generation of the At3g29075 “knock-down” plant (Schwab *et al.*, 2006)

Artificial microRNAs (miRNAs) are small RNAs of 21 bp, that can be genetically engineered and function to specifically silence a gene of interest in *A. thaliana* (Schwab *et al.*, 2006). The generation of the At3g29075-specific miRNA and subsequent cloning steps were done as described by Schwab *et al.* (2006). The artificial miRNA vector pRS300 was kindly provided by Prof. Weigel (Max Planck Institute for Developmental Biology, Tübingen, Germany).

To identify an appropriate miRNA against At3g29075, the web MicroRNA Target Search tool (<http://wmd3.weigelworld.org/cgi-bin/webapp.cgi>) was used. A suitable oligo sequence to express the small RNA from endogenous miRNA precursors was selected based on the listed recommendations. In order to engineer the artificial miRNA into the endogenous miR319a precursor by site-directed mutagenesis, four primers were designed with the help of the MicroRNA design tool. In a next step, three overlapping PCRs (**Figure 9** a-c), using the plasmid pRS300 which contains the miR319 precursor, were conducted for the generation of the template for the fusion PCR (**Figure 9** d).



I: microRNA forward
 II: micro RNA reverse
 III: micro RNA* forward
 IV: micro RNA* reverse

	Forward oligo	Reverse oligo	Template
(a)	A	IV	pRS300
(b)	III	II	pRS300
(c)	I	B	pRS300
(d)	A	B	(a)+(b)+(c)

Figure 9: Cloning strategy for artificial micro RNAs (Adapted from Schwab *et al.*, 2006)

In following cloning steps the generated miRNA was sub-cloned behind a 35S-promoter of the PGJ280 vector and finally cloned into the binary vector pBIN19 for *Agrobacterium* transfer.

3. Results

The role of phospholipases in plant growth, development and adaptation to stress has gained wide attention in the past years. A special significance has been attributed to phospholipase D and its enzymatic product phosphatidic acid (Bargmann *et al.*, 2009, McLoughlin & Testerink, 2013). The identification of various proteins under the control of PLDs and PA emphasizes the importance of research in this field. Cellular and physiological effects, such as stomatal movement, ABA response, production of ROS and the organization of the cytoskeleton are crucial PA-mediated responses of plants and have major impacts on plants growth and development (Hou *et al.*, 2015). Nevertheless, knowledge about detailed actions of PLD and PA is scarce, demanding more targets to be analyzed. This work characterizes At5g39570.1, a novel downstream target of PLD and shortly describes its putative homolog At3g29075 isolated from the model plant *A. thaliana*.

3.1 *In silico* analysis of the protein At5g39570.1

Computer simulations and *in silico* analysis of proteins and their interaction partners has gained rising interest in the past decades. The improvement of computer-based algorithms, availability of sequenced genomes and public databases facilitated bioinformatic studies. Recently, researchers used the protein docking algorithm EADock to successfully identify potential inhibitors of an enzyme which mediates an immune-escape in several cancer types (Röhrig *et al.*, 2010). However, *in silico* analyses can only provide hints for a molecular process and identify putative interacting partners. Experimental studies *in vitro* and *in vivo* are indispensable for the elucidation of biological processes. The collection and evaluation of previous findings and large-scale studies can help to understand biological mechanisms and protein interactions. In this study a subset of bioinformatic tools, databases and large-scale studies was exploited for the characterization of At5g39570.1 and At3g29075.

3.1.1 Basic characterization of At5g39570.1 and At3g29075

The gene *At5g39570.1* encodes for the amino acid sequence of the protein At5g39570.1 **Figure 10**. As depicted in **Figure 10** the protein At5g39570.1 has previously been identified by mass spectrometry analysis (Baerenfaller *et al.*, 2008, Kuhn, 2009). I have previously

shown by protein blot analysis that At5g39570.1 is expressed by At5g39570.1 (Ufer, 2011). The existence of a second, annotated (<http://www.uniprot.org/>) reading frame that putatively encodes for the protein At5g39570.2 has not been verified and the protein does not exist.

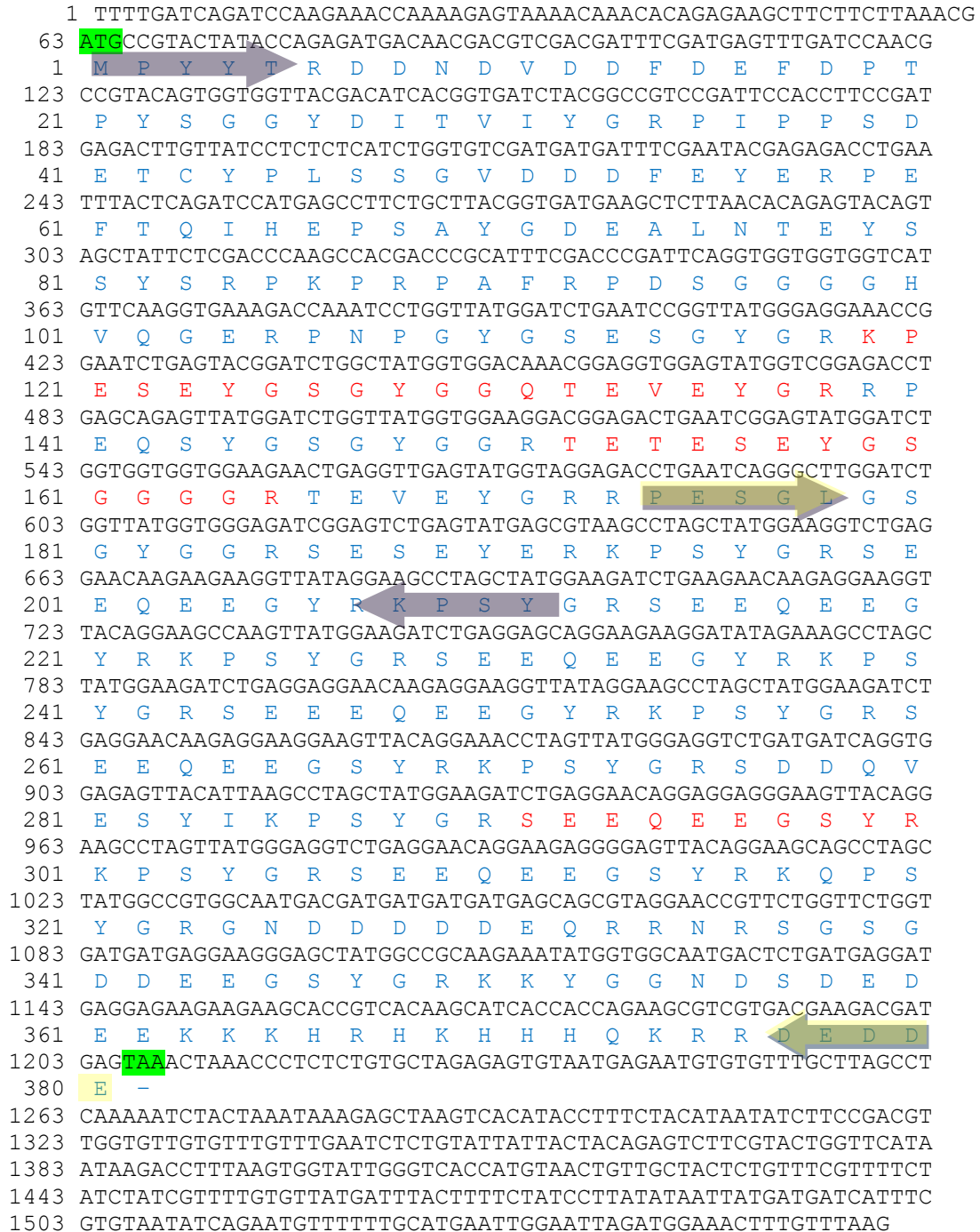


Figure 10: Nucleotide and protein sequence of *At5g39570.1*. Green: Start and stop codon of the gene *At5g39570.1*; Blue: At5g39570.1; Red: Peptides identified by MS-analysis (Baerenfaller *et al.*, 2008, Kuhn, 2009). Purple arrows: Primers for the generation of the N-terminal fragment. Yellow arrows: Primers for the generation of the C-terminal fragment.

The updated TAIR database (arabidopsis.org) lists the protein At5g39570.1 and its best protein match At3g29075 on two distinct gene models: *At5g39570.1* and *At3g29075*. Both proteins have not been described previously and little is known about their structure, expression and function. In accordance to the nomenclature of glycine-rich proteins by (Sachetto-Martins *et al.*, 2000), these proteins can be classified as glycine-rich. The typical motifs “GXGX”, “GGX” and “GGGX” are highlighted in **Figure 11**.

a)

MPYYTRDDNDVDDDFDEFDPTPYS **GGY**DITVIYGRPIPPSDETCYPLSSGVDDDDFEYERPEFTQI
 HEPSAYGDEALNTEYSSYSRPKPRPAFRPDS **GGGG**HVQGERPNP **GYGSES** **GYGR**KPESEY **GSG**
YGGQTEVEYGRRPEQSYGS **GYGG**RTETESEYGS **GGGG**RTEVEYGRRPES **GLGSGYGG**RSESE
 YERKPSYGRSEEQEEGYRKPSYGRSEEQEEGYRKPSYGRSEEQEEGYRKPSYGRSEEEQEEGY
 RKPSYGRSEEQEEGSYRKPSYGRSDDQVESYIKPSYGRSEEQEEGSYRKPSYGRSEEQEEGSY
 RKQPSYGRGNDDDDDEQRRNRS **GSGD**DEEGSYGRKKYGGNDSDEDEEKKKHRHKHHHQR
 RDEDDE

b)

MPYYTNDNDVDDDFTEYDPMPYS **GGY**DITVITYGRSIPPSDETCYPLSSLSGDAFEYQRPNFSS
 NHDSSAYDDQALKTEYSSYARPGPV **GSGS**DFGRKPNS **GYGG**RTEVEYGRKTESEH **GSGYGG**
 RIESDYVKPSY **GGH**EDDGDDGHKKHSGKDYDDGDEKSKKKEKEKDKKKDGNNSDDEF
 KKKKKKEQYKEHDDDDYDEKKKKKKDYNDDEKSKKKKHYNDDDEKSKKKKHYNDDDD
 DEKSKKKKEYHDDDEKSKKKKHYNDDDEKSKKKKDKHRDDDEKSKKKKDKHHKGH

Figure 11: Protein sequences of At5g39570.1 and At3g29075.

a) Protein sequence of At5g39570.1. b) Protein sequence of At3g29075. Green: Sequence motif of glycine-rich proteins.

At5g39570.1 consists of 381 amino acids and exhibits a theoretical pI of 4.71 (Compute pI/Mw). While the calculated molecular weight is approximately 43.5 kDa (Compute pI/Mw), the protein was observed to run at ~55 kDa in polyacrylamide gels (Ufer, 2011). The smaller protein At3g29075 contains 294 amino acids and has a theoretical molecular weight of 34.4 kDa and a pI of 5.73. An antibody against this protein is being produced in the context of a Master thesis (Nasr, 2015). Despite their sequence differences, both proteins clearly share high sequence identities in the N-terminal half, while the C-terminal region is more variable (**Figure 12**).

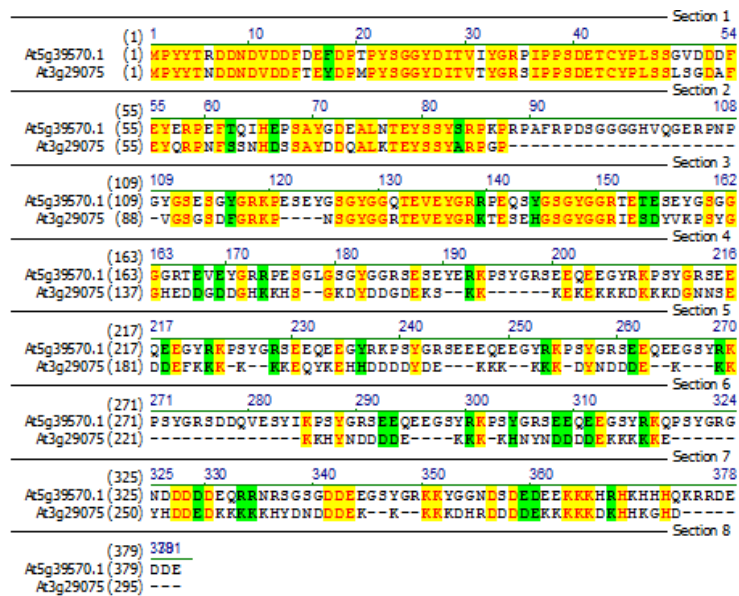
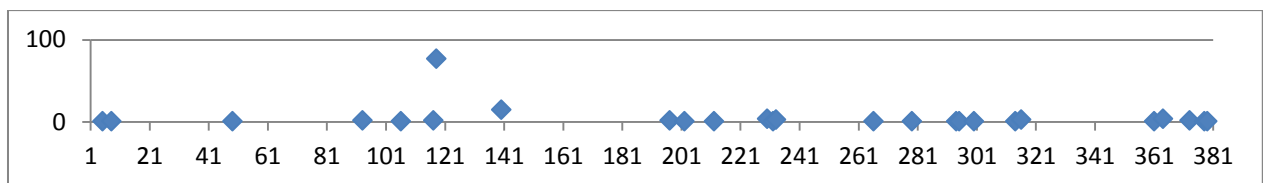


Figure 12: Alignment of At5g39570.1 and At3g29075.

3.1.2 Homologs and Orthologs of At5g39570.1

The Arabidopsis 1001 genome project provides detailed sequence data of different wild-type strains from *A. thaliana*. The project enables insights into the evolution of genes and proteins in order to understand their functions and importance for the organism. Protein sequences of 854 *Arabidopsis* ecotypes were aligned and analyzed to detect variable amino acids in the sequences of At5g39570.1 and At3g29075 (**Figure 13 a**).

a)



b)

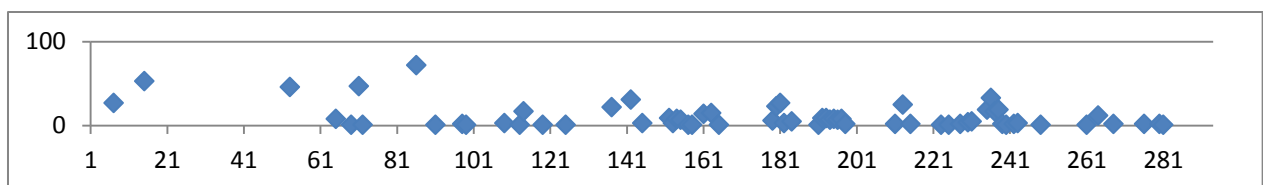


Figure 13: Variable amino acids in the sequence of At5g39570.1 and At3g29075.

The position of the variable AA in a) At5g39570.1 and b) At3g29075 is highlighted. The ordinate lists the number of ecotypes where the AA change occurred (rate of variability).

A total of 24 variable amino acids (6.3 %) were detected in At5g39570.1, most of them (66.6 %) in the C-terminal region of the protein (detailed values can be found in the supplementary data files). The N-terminal region of At5g39570.1 harbors less variable amino

acids, but R₁₁₈, P₁₄₀ and G₁₉₇ show significantly higher rates of variability. The amino acid R₁₁₈ was evolutionary converted into S₁₁₈ in 77 out of 750 different *Arabidopsis* ecotype strains. For At3g29075 a total of 775 complete data sets were analyzed and 64 variable amino acids (22.1 %) were detected (**Figure 13** b). Interestingly, the first 150 N-terminal amino acids, that show high sequence similarity to At5g39570.1 revealed only 19 (12.6%) variable sites, while the C-terminal half contains 45 variable sites (31.2 %) (supplementary data files). These prominent differences between the N- and C-terminal half of both proteins can be highlighted by the analysis of At5g39570.1 by protein blasts using the NCBI database.

The annotation of At3g29075 as the closest *Arabidopsis* homolog of At5g39570.1 (Query coverage: 40 %, amino acid identities: 60 %, expectation value: $3 \cdot 10^{-46}$) is confirmed by pblast analysis. The amino acid sequence identity is, especially in the first 200 N-terminal amino acids, very high (60 %). The overall sequence identity of both proteins covers 35.7 %. No further reliable homologs (expectation value $E < 10^{-10}$) can be identified in *A. thaliana*. However, protein blasts of At5g39570.1 revealed the existence of multiple orthologous proteins in various plant species, such as *Arabidopsis lyrata*, *Capsella rubella*, *Ricinus communis*, *Populus trichocarpa*, *Eutrema salsugineum*, *Vitis vinifera* and a number of crops (e.g. *Oryza sativa*, *Theobroma cacao*, *Citrus sinensis*). Proteins with high expectation values ($E < 10^{-10}$) can be considered as orthologs of At5g39570.1 (**Table 6**).

Table 6: Orthologs of At5g39570.1 with unknown function

Locus	Organism	Q-value	AA	E-value
XP_002870774.1	<i>Arabidopsis lyrata</i>	100 %	93 %	0
XP_006283824.1	<i>Capsella rubella</i>	100 %	90 %	0
XP_006405620.1	<i>Eutrema salsugineum</i>	100 %	75 %	0
XP_002530006.1	<i>Ricinus communis</i>	94 %	44 %	$8 \cdot 10^{-48}$
XP_002332006.1	<i>Populus trichocarpa</i>	100 %	46 %	$1 \cdot 10^{-45}$
XP_002283932.1	<i>Vitis vinifera</i>	99 %	47 %	$8 \cdot 10^{-45}$
KDO36694.1	<i>Citrus sinensis</i>	49 %	59 %	$8 \cdot 10^{-44}$
XP_007032610.1	<i>Theobroma cacao</i>	83 %	48 %	$2 \cdot 10^{-39}$
NP_001057224.1	<i>Oryza sativa Japonica Group</i>	97 %	33 %	$4 \cdot 10^{-21}$
NP_ACF88189.1	<i>Zea mays</i>	41 %	42 %	$1 \cdot 10^{-23}$

Q-value: Query coverage of At5g39570.1; E-value: The expectation value defines the likeliness that the sequence identity is based on chance, rather than homology. A low e-value ($E < 10^{-10}$) represents a significant sequence identity. AA: Amino acid sequence identity.

Related proteins can be identified in various plant families, such as Brassicaceae, Fabaceae, Lycophytes and partial sequence identities ($E < 10^{-5}$) even exist in Cyanobacteria (**Supplementary table 1**). While none of the putative orthologs is characterized, *in silico* analysis and computational tools have been exploited to predict characteristics for selected proteins (**Table 7**).

Additional blast analyses against the Craterodb database (Rodriguez *et al.*, 2010a) that comprises most genes from the drought-tolerant plant *Craterostigma plantagineum*, identified two successive contigs that share high sequence similarities within the N- and C-terminus of At5g39570.1, respectively: Contig 04106 (E-value: 2×10^{-8} ; Q-value 34 %) and Contig 04107 (E-value: 2×10^{-20} ; Q-value: 27 %). The major sequence identities for all identified putative orthologs could be detected within the N-terminal region of the protein (**Figure 14**).

Table 7: Orthologs and homologs of At5g39570.1 with predicted attributes

Locus	Description	Organism	Q-value	AA	E-value
KEH25017.1	pro-resilin precursor	<i>Medicago truncatula</i>	92 %	47 %	2×10^{-64}
At3G29075	glycine-rich	<i>A. thaliana</i>	40 %	60 %	3×10^{-46}
XP_007032610	nucleus-like protein	<i>Theobroma cacao</i>	83 %	48 %	2×10^{-39}
AAP46157	latex abundant	<i>Hevea brasiliensis</i>	27 %	52 %	2×10^{-26}
ACG32088.1	pro-resilin precursor	<i>Zea mays</i>	89 %	35 %	4×10^{-18}
BAD16110.1	glycine-rich-like protein	<i>Oryza sativa Japonica Group</i>	30 %	35 %	1×10^{-10}

Selected orthologs and homologs of At5g39570.1 with predicted attributes from the NCBI database. Q-value: Query coverage of At5g39570.1; E-value: The expectation value defines the likeliness that the sequence identity is based on chance, rather than homology. A low e-value ($E < 10^{-10}$) represents a significant sequence identity. AA: Amino acid sequence identity.

Sequence alignments of the top 40 blast hits for At5g39570.1 (**Figure 14**) and subsequent construction of a family tree based on the neighbor-joining method by MEGA 6, revealed the phylogenetic relationship of At5g39570.1 towards putative orthologs (**Figure 15**).

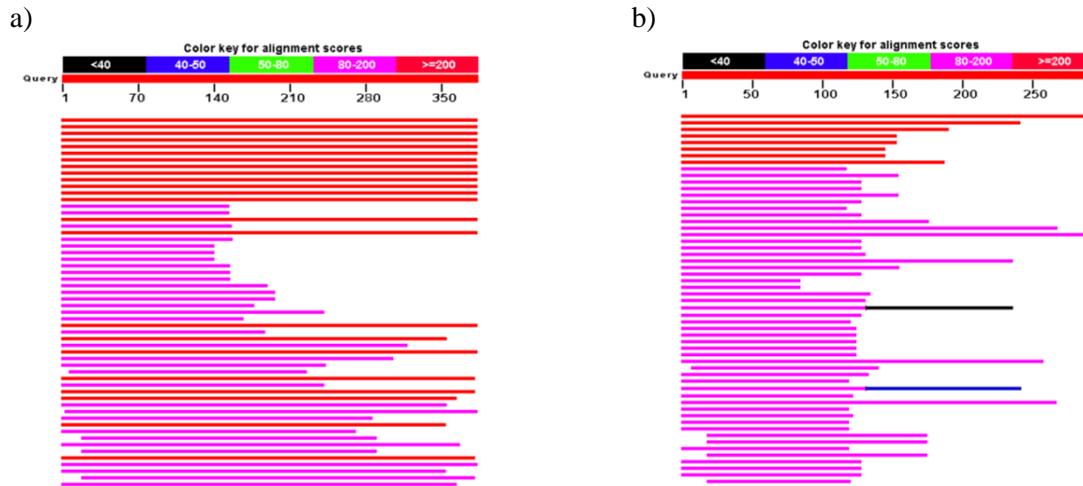


Figure 14: Blast results for At5g39570.1 (a) and At3g29075 (b). Colored lines indicate sequence coverage of candidate proteins.

While the high bootstrap values support the close relation of the proteins within the Brassicaceae (e.g. *A. lyrata*, *E. salsugineum*, *B. rapa*), it is evident that the protein has undergone radical changes in more distant species. Nevertheless, the combination of pblast (see **Supplementary table 2**), the phylogenetic analysis (**Figure 15**) and multiple sequence alignments (see supplementary data) show the wide distribution of At5g39570-like proteins throughout various families in plant species (see **Supplementary table 1**). Proteins with partially overlapping protein sequences to At5g39570.1 could even be identified in the far distant Lycophytes. In accordance with the more conserved N-terminal half of At5g39570.1, multiple sequence alignment of the top 40 blast hits, revealed a strong correlation of the N-terminal protein part to other species, while analysis of the C-terminal protein end results in low consensus sequences. Interestingly, the last C-terminal 50 amino acids show a similar conservation level like the N-terminal protein part (see supplementary data files; polymorphism).

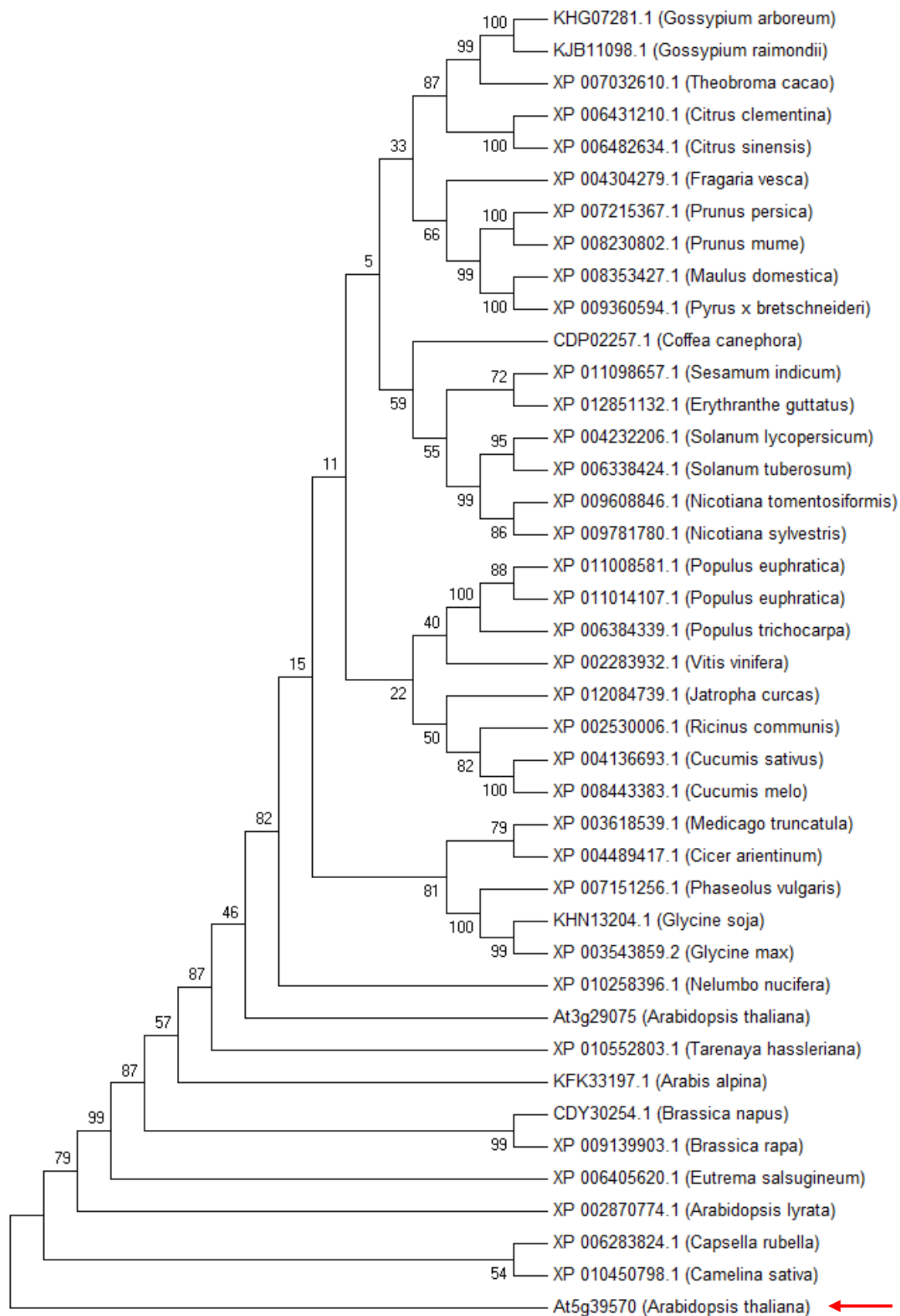


Figure 15: Phylogenetic tree of At5g39570.1.

The phylogenetic tree was constructed with MEGA 6 using the bootstrap method with 500 replications. The red arrow marks At5g39570.1 as the root sequence. Bootstrap values are provided.

3.1.3 Protein structure

The composition of At5g39570.1 and At3g29075 reveals interesting features. Both proteins contain a single cysteine residue, so that no intramolecular disulfide bonds can be formed within the protein. While At5g39570.1 has a high content of glutamic acid (16.3 %) and glycine (14.9 %), At3g29075 displays a high content of the charged amino acids aspartic acid (19.3 %) and lysine (21.1 %), when compared to average values from *A. thaliana* (**Figure 16**).

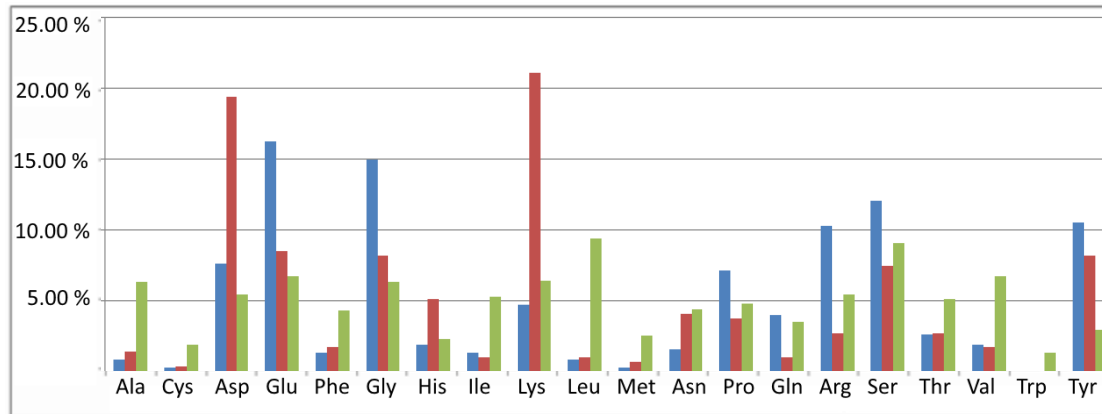


Figure 16: Amino acid composition of At5g39570.1 and At3g29075. Blue: At5g39570.1. Red: At3g29075. Green: Average values from *A. thaliana* proteins.

The high content of the acidic amino acids (glutamic acid and aspartic acid) provide the acidic backbone for both proteins. Polar amino acids (>70 %) contribute to the overall hydrophilic properties. The N-terminal region of At5g39570.1 (first 200 N-terminal AA) is characterized by a high content of glycine (17.5 %), while the C-terminal end (last 181 AA) is dominated by glutamic acid (20.5 %) and arginine (12.2 %) (**Supplementary figure 1**). The unusual high amounts of lysine (38.6 %) and aspartic acid (26 %) in the C-terminal half of At3g29075.1 (**Supplementary figure 1**) give the protein a strong hydrophilic character (**Figure 17**).

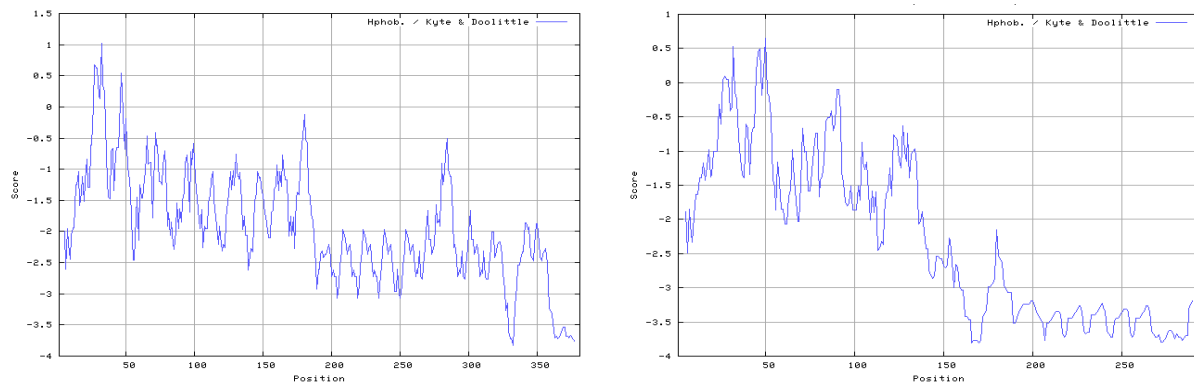


Figure 17: Hydrophobicity plots of At5g39570.1 and At3g29075. Hydrophobicity of At5g39570.1 (left panel) and At3g29075 (right panel) according to ProtScale (Kyte & Doolittle, 1982). Isoleucine is considered the most hydrophobic AA with a score of 4.5. Arginine is the most hydrophilic AA with a score of -4.5.

The distribution of hydrophobicity supports the previous observation of a separation of both proteins into two major regions. Besides differences in the grade of conservation, amino acid composition and hydrophobicity, both proteins exhibit prominent imperfect tandem repeats in their C-terminal region (**Figure 18**). The repetitive sequences overlap with the least conserved amino acids. The amino acid sequence “YGRSEEQEEGYRKPS” occurs (with minor alterations) up to ten times in the C-terminal half of At5g39570.1. Five aspartic acid and lysine-rich tandem repeats in At3g29075 provide numerous, charged amino acids (**Figure 18**) to the protein.

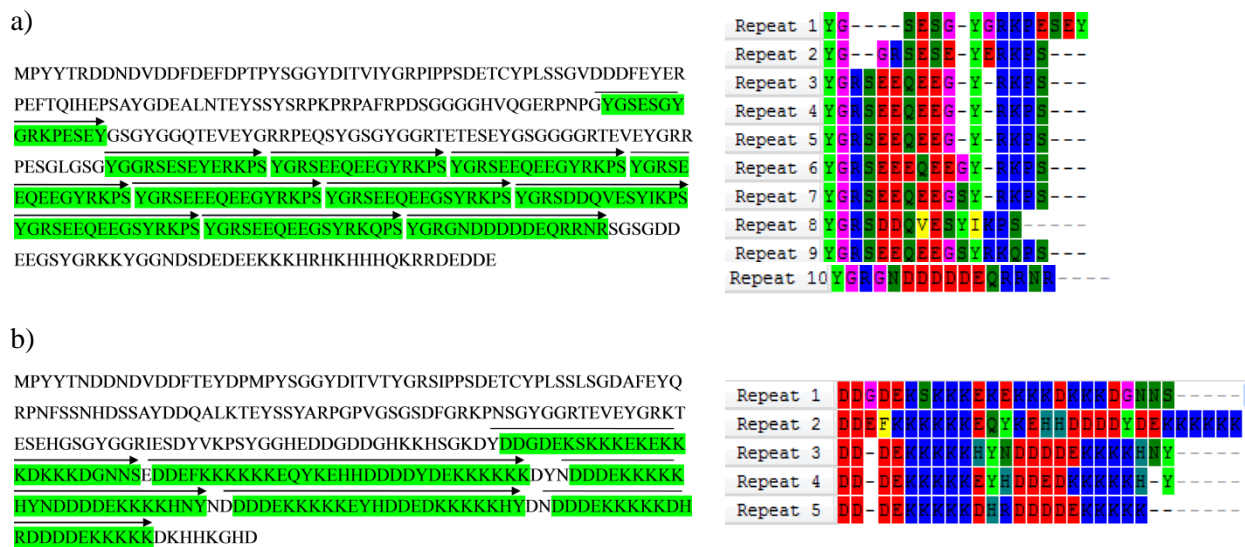


Figure 18: Tandem repeats in At5g39570.1 (a) and At3g29075 (b). Left: Amino acid sequence with tandem repeats marked in green. Black arrows: Length of motifs. Right: Alignments of identified sequence motifs by TRUST (see section 2.1.3).

The unequal amino acid composition and hydrophobicity of both proteins in combination with the exclusive occurrence of tandem repeats in their C-terminal regions point to a structural division within these proteins. Sequence analysis of tandem repeats (marked green in **Figure 18** a) by protein blast detected a very low conserved ($4 \cdot 10^{-4}$), putative protein domain (PRK12678: “transcription termination factor Rho”) for At5g39570.1. Similar tandem-repeat structures were exclusively observed in orthologs of At5g39570.1, but not in other proteins. This observation is even more prominent for At3g29075, where protein blast analysis of tandem repeats (marked green in **Figure 18** b) did not detect any matches to other proteins. Both repetitive domains appear unique.

The prominent tandem repeats in both proteins may influence protein folding and thus the secondary protein structure. Bioinformatic tools predict a highly unstructured protein conformation for At5g39570.1 (see **Table 8**).

Table 8: Structural motifs of the protein At5g39570.1

Program (%)	α -helix		β -turn		Random-coil		Others	
GOR4	12.6	36.4	-	-	75.6	53.7	11.8	9.9
SOPMA	4.2	20.4	-	8.8	92.4	62.6	3.4	8.2
CFSSP	19.7	47.6	21.5	20.1	58.8	32.3	-	-

Predicted structural motifs in At5g39570.1 (blue) and At3g29075 (red). Values are given in % according to the prediction tools. For program details see section 2.1.3.

As tandem repeats often occur in intrinsically disordered proteins (IDPs), disorder prediction tools were exploited to confirm previous observations. *In silico* analysis by the meta-predictor PONDR-FIT (Xue *et al.*, 2010) predicted a highly disordered structure of the C-terminal end of both proteins, as indicated by values above 0.5 (**Figure 19** a & b). Additional sequence analysis by DisEMBL, GlobPlot and IuPred support these findings by the identification of multiple disordered regions, mainly in the C-terminal part of both proteins. However, the prediction of secondary structures of proteins is difficult and may only serve as a hint for the genuine protein structure.

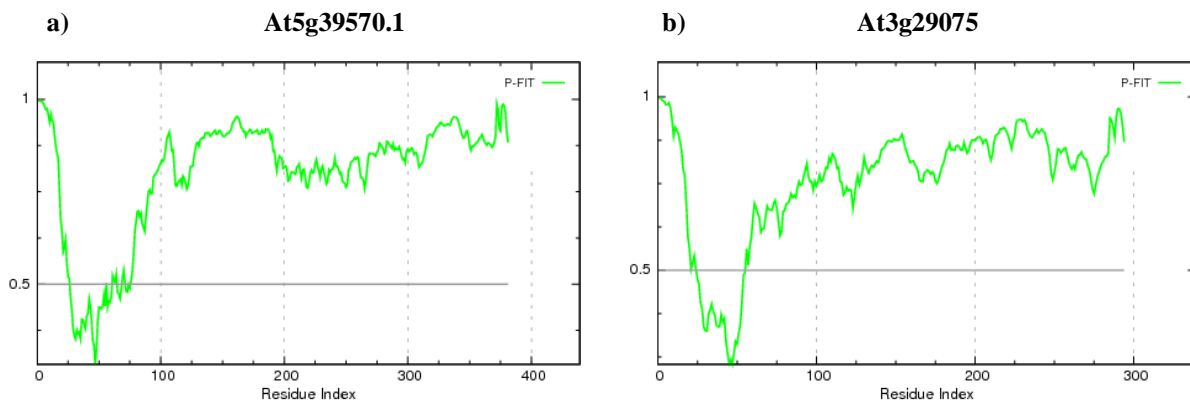


Figure 19: Overview of disordered regions in At5g39570.1 (a) and At3g29075 (b). The prediction tool PONDR-FIT (Xue *et al.*, 2010) was used to predict disordered regions within the protein structures. For program details see section 2.1.3.

3.1.4 Analysis of the promoter region and coding sequence

The promoter region of *At5g39570.1* is suggested to be located in the 1000 bp upstream of the translation start point and seems to contain a number of cis-regulatory elements. A putative TATA-box 25 bp upstream of the coding sequence has been identified by TSSP (section 2.1.3). Besides the detection of numerous MYB and WRKY binding sites, putative cis-regulatory elements coding for heat-stress transcription factors and drought-responsive elements were detected (**Figure 20**).

```
TACATATCTAAATATTGTGGACATAATTAGTTGTGGTGTCAAAAAAAAAAAAAAAAAAATTAGTTGTAGTC
ATTCATTGTCCAAGATTTGTTTATAGACATAAATCATAGCTTATAAGATTTTTTTTCTAAAGTAAATA
ATGGTTATAGTTTATAAATAAATAAATAAAGATCTACAAGGCTTAAAAATAAAAAATCAAAAGGAAAT
TAAATCTACAAAATAAACCTAAATGTA AAAACATAAAAACAAAAAATCAAGATACACTAATCAATTG
CATTAATTCATAAATTTATCCTTATTTTAAATATATTAATTTCTTTTGTAAAGGTAACAATGGTTATA
AATAATTTAAATTTGAAATAAAGGACCTTAAAAATAAAGATATACAAAAACCTTAAAAAGCCTCATATC
AAAAGGAAATTTAAATCTACAAAATAAACCTAAATTTAAAAACCATAAA CCAAA AATATGAGGCACATTT
TCTTCTTTT CCAAATCATAAA CCAAAATTCAAGACACAATAATTCATAAATTATATTCGTTTTGTAA
TATAGTCCCTTAAATGATTATTAATTAATCATATCTTCTCCCATGGTTTGGTCCCGGTTAAATCACTCGGCAA
TTGGTACAATCAAAATTGGTTATTACCAATTAAGATAACCCACGTGGCATAGCTTGCCCGAATCGTAGTGG
TCTCCATGTAACAGCAGGAAGATGGGATCCACAATTATTCATTCAAACCGCAACGTTTTTAAACTCTTCG
TCTTCTCTCCCGCGTATAAATTCTCATTCTGTCAITTTGTATCAGATCCAAAGAAACCAAAAGAGTAA
AACAAACACAGAGAAGCTTCTTCTTAAACGATGCCGTAATAACCAGA
```

Figure 20: Putative promoter region of *At5g39570.1*. Blue: Putative cis-regulatory elements. Brown: Putative cis-elements coding for heat-shock transcription factors. Orange: Putative cis-element coding for drought-responsive elements. Red: Putative TATA-Box. Grey: cDNA sequence. Yellow: Start codon of *At5g39570.1*. TRANSFAC and AGRIS were used for predictions (2.1.3).

In silico analysis of *At5g39570.1* confirmed differences in the conservation status of the 5'- and 3'-region. Although DNA-specific blast did only identify *At3g29075* with a reliable expectation value (e-value $3 \cdot 10^{-46}$), plenty proteins in Arabidopsis share similar DNA-sequences in their 5'-end (**Supplementary table 3**). Analysis of *At5g39570.1* additionally detected short (19–48 bp), highly conserved, nucleotide stretches in the 3'-end of *At5g39570.1* (**Figure 21**).

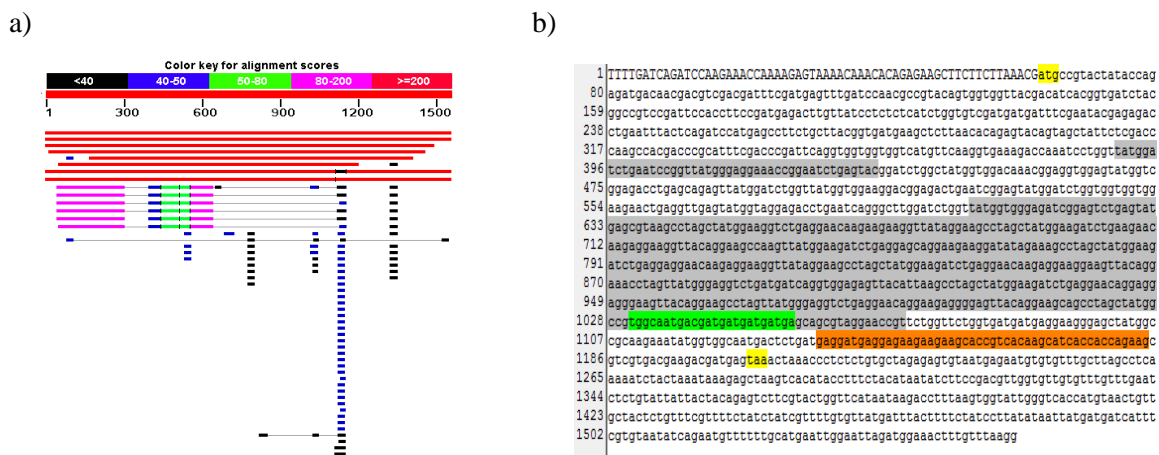


Figure 21: Short, conserved nucleotide sequences in *At5g39570.1*. a) Occurrence of the conserved fragments in *A. thaliana* by blastn b) Position of conserved nucleotide sequences in *At5g39570.1*: Grey: Repetitive region. Yellow: Start/stop codon. Green: Fragment 1. Orange: Fragment 2.

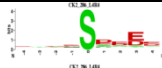

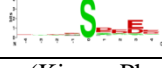
Protein blast against these fragments identified identical nucleotide stretches in other species, like *Drosophila melanogaster* (**Supplementary tables 4 & 5**). Genes with known function like the scaffolding protein *LN161904.1* from *Spirometra erinaceieuropaei* (24 of 24 identities), the 28S ribosomal gene *FJ966018.1* from *Eustacus armatus* (39/48), the ribosomal assembly protein *NM_001199520.1* from *Gallus gallus* (31/35) and various RNA-binding proteins, like *LOC101845137* from *Aplysia californica* share the identical sequence of 24 and more consecutive nucleotides to fragment 1 or fragment 2, respectively (**Figure 21**). Both fragments share high similarities to RNA-associated genes. A specific blast of these

against the *A. thaliana* genome identified a wide range of genes encoding for phosphatases, phospholipases, translation-initiation factors and RNA-binding proteins (**Supplementary tables 6 & 7**).

3.1.5 Post-translational modifications of At5g39570.1

After the generation of polypeptide chains in ribosomes, newly synthesized proteins may undergo post-translational modifications to form a mature and functional protein. Post-translational modifications comprise the addition of functional groups such as phosphate or acetate, carbohydrates or even lipids (Reinders & Sickmann, 2007). The interplay of phosphorylation and dephosphorylation of a protein is known to regulate protein activity and function, and therefore is in the focus of research since many years (Reinders & Sickmann, 2007). It has been shown previously that At5g39570.1 contains at least one phosphorylation site at position S₃₃₉ (Laugesen *et al.*, 2006). Different prediction tools identified two additional, putative phosphorylation sites in At5g39570.1, using a support vector machine algorithm (**Table 9**)

Table 9: Prediction of kinase-specific phosphorylation sites in At5g39570.1

AA position	Kinase Phos 2.0	NetPhos 2.0	NetPhosK	Kinase	
48	0.922	0.968	-	CK2	
339	0.984	0.998	0.57	CK2	
357	0.982	0.997	0.71	CK2	

Values in the range of 0.000-1.000 represent possibilities of phosphorylation sites (Kinase Phos 2.0 and NetPhos 2.0) and kinase-specific phosphorylation sites (NetPhosK). For detailed program information see section **2.1.3**.

All sites are predicted to be phosphorylated by a casein kinase. The protein At5g39570.1 was recently shown to be phosphorylated by a VH1-interacting kinase (Braun, 2015) and a CPK3 kinase (Mehlmer, 2008) *in vitro*. Exploitation of various protein prediction tools (**2.1.3**) could not identify additional post-translational modifications with high probability scores (> 90%).

3.1.6 Gene co-expression network of At5g39570.1

In combination with *in silico* co-localization data, gene networks might lead to the detection of putative interaction partners of a protein of interest. *In silico* analysis of the At5g39570.1 network identified *PLDα1* and *At3g29075* as two of the top three candidate genes (**Figure 22**). The BSD domain-containing protein *At1g03350* showed high co-expression with

At5g39570.1. Spiral 1 (SPR1) displayed a similar co-expression profile and co-localization. Further putative targets comprise a GDP-regulator protein (*AT3g59920*) and several stress genes (e.g. dehydrin *LTI29*, LEA-protein *AT2G44060* and *Cor47*).

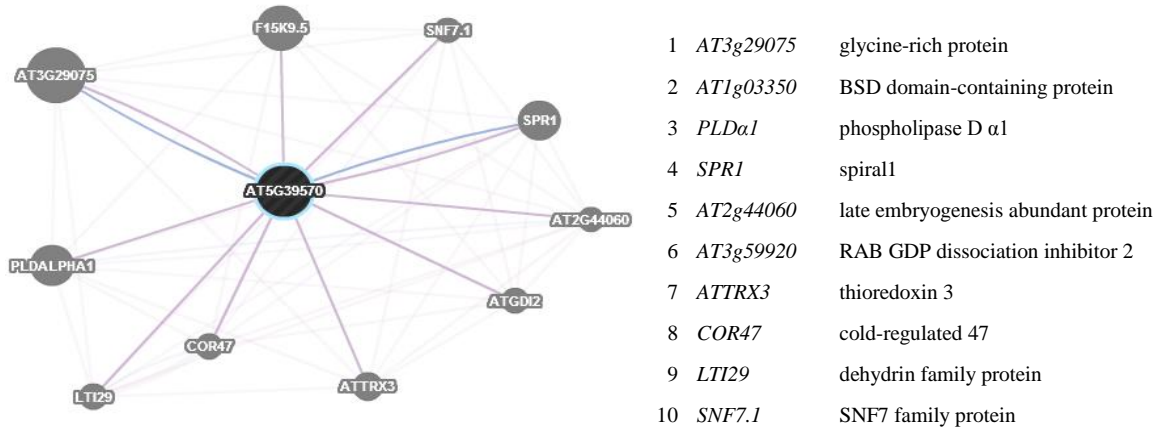


Figure 22: Gene co-expression network of *At5g39570.1*. Purple line: Predicted co-expression. Blue line: Predicted co-localization. Gene co-expression network was generated by geneMANIA (section 2.1.3).

3.1.7 Protein-protein interactions

A recent experiment using affinity capture-MS to identify ubiquitylation targets in Arabidopsis, detected an interaction between *At5g39570.1* and polyubiquitin3 (*AT5g03240*) as the first putative interacting partner of the unknown protein (Kim *et al.*, 2013a). Further interacting molecules have been predicted by text mining methods and remain to be verified (**Figure 23**).

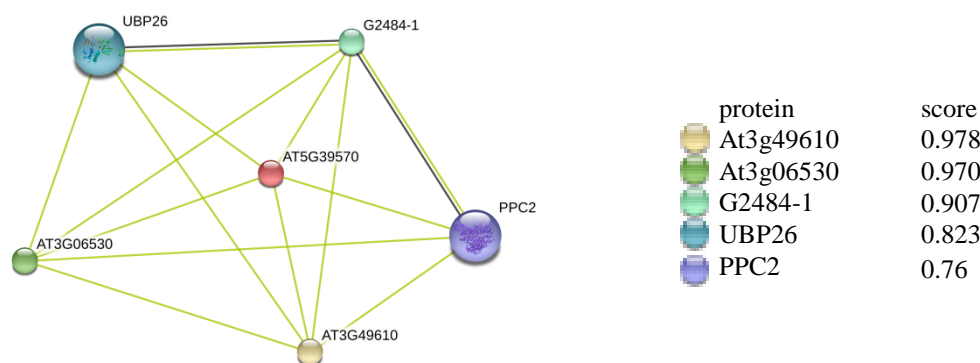


Figure 23: Predicted functional partners of *At5g39570.1*. The protein-interaction network shows predicted protein interactions based on text mining analyses. A score value of 1 represents a confirmed interaction. String10 (section 2.1.3) was used to create the interaction network. PPC2, phosphoenol pyruvate carboxylase 2; UBP26, ubiquitin carboxyl-terminal hydrolase 26.

At3g06530, a small U3-nucleolar RNA-associated protein and phosphoenolpyruvate carboxylase 2 (PPC2) were identified as putative interacting partners of *At5g39570.1*. The function of the remaining candidate proteins is unknown.

3.2 Genotyping

Before working with plant material, genotyping of all available mutant plants (see section 2.2) was conducted by PCR. Genotyping was carried out by the use of gene and vector-specific primers. Primer sequences are listed in section 2.1.5.

3.2.1 Genotyping of phospholipase D mutants

Plants with a T-DNA insertion for all tested genotypes (*PLD α 1*, *PLD α 3*, *PLD ϵ* , *PLD δ -3*, *PLD ζ 1*, and *PLD ζ 2*) have been confirmed, although not all mutants were homozygous. The putative “knock-out” line *pld α 3* “SALK_122059” amplified a fragment with gene-specific primers and thus was not used for further analysis. A few mutant plants were only weakly detected by T-DNA specific primer analysis (e.g. **Figure 24** a line 2) and thus have been excluded. Homozygous plants have been detected for all investigated *pld* mutants (**Figure 24**). Double and triple mutants have been genotyped separately for each of the genes.

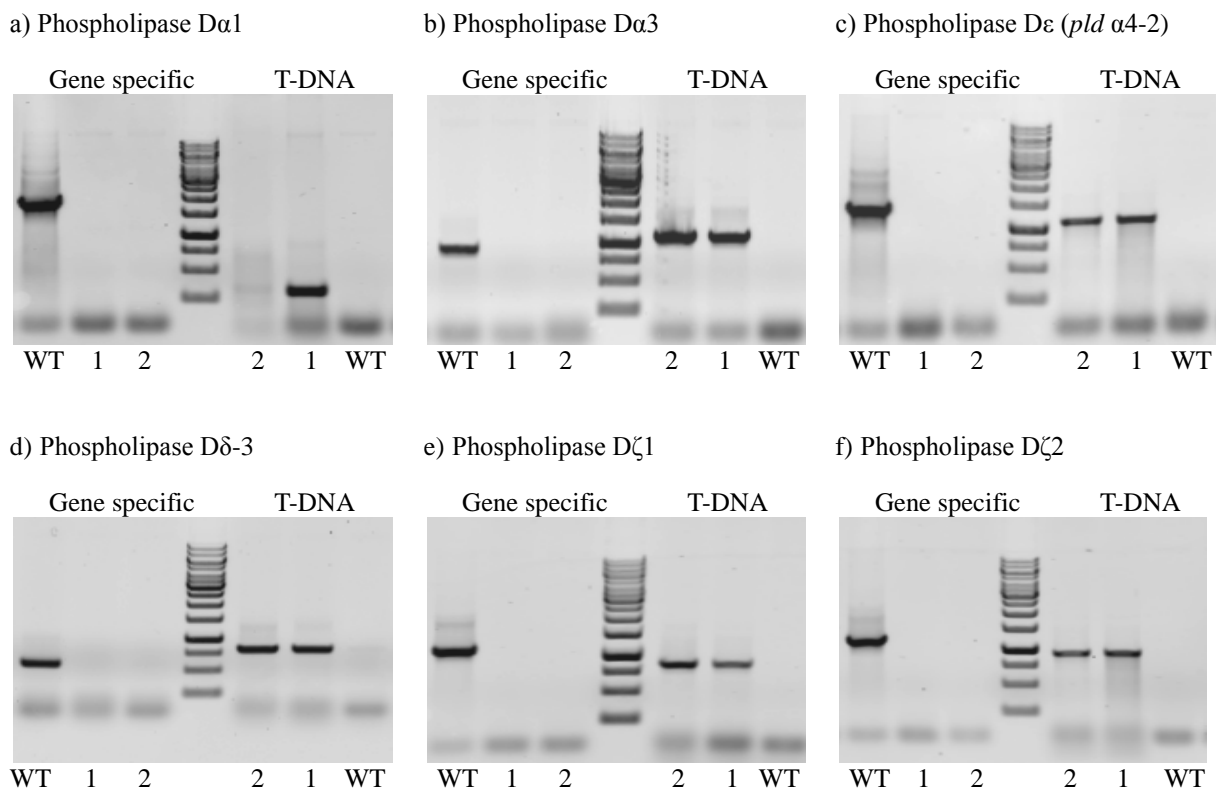


Figure 24: Genotyping of *pld* knock-out mutants.

WT: wild type; 1 & 2: Homozygous knock-out plants. Primer combinations: a) gene specific: PLD α 1_717f & PLD α 1_gene_r (1923 bp), T-DNA: LBb1 & PLD α 1_gene_r (309 bp) b) Gene specific: PLD α 3_ATG_for & PLD α 3_948_rev (950 bp), T-DNA: Lba1 & PLD α 3_ATG_for (1187 bp); c) Gene specific: PLD α 4_ATG_f / PLD α 4_gene_r (1438 bp), T-DNA: Fish1 & PLD α 4_gene_r (1200 bp) d) Gene specific: PLD δ _616_f & PLD δ _1200_r (584 bp), T-DNA: Lba1 & PLD δ _616_f (791 bp) e) Gene specific: PLD ζ 1-RP & PLD ζ 1-LP (1134 bp), T-DNA: PLD ζ 1-LBA1 & PLD ζ 1-RP (1350 bp) f) gene specific: PLD ζ 2-RP & PLD ζ 2-LP (1205 bp), T-DNA: PLD ζ 2-LBA1 & PLD ζ 2-RP (1350 bp).

3.2.2 Genotyping of the *At5g39570.1* T-DNA insertion mutant

As exemplarily depicted in **Figure 25**, genotyping of the *At5g39570.1* knock-out mutant was successful. Amplification with gene specific primers resulted in an amplicon of 1234 bp. The T-DNA specific primer combination could only amplify a fragment (573 bp) in mutant plants.

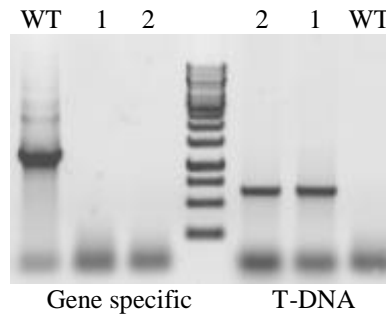


Figure 25: Genotyping of the *At5g39570.1* T-DNA insertion line.

WT: wild type; 1 & 2: Homozygous T-DNA insertion lines. Primer combinations: Gene specific: *At5g_fwd* & *At5g_rev* (1234 bp); T-DNA: *At5g_fwd* & GK-LB (573 b).

3.3 Production of recombinant proteins

For detailed analysis of *At5g39570.1* an antibody against the N-terminal half of the protein (Nt-*At5g39570.1*, **Supplementary figure 2**) has previously been produced (Ufer, 2011). For further research the recombinant full-size protein *At5g39570.1* and the recombinant C-terminal protein fragment (Ct-*At5g39570.1*) were generated in this work (**Supplementary figure 2**).

3.3.1 Amplification and cloning of *At5g39570.1* into pET28-a

In a first step an amplicon of 1167 bp, containing the complete coding sequence of *At5g39570.1* was amplified by RT-PCR. By using the mutagenesis primers *At5g-full-NcoI-fwd* and *At5g-full-XhoI-rev*, the restriction sites *NcoI* and *XhoI* were introduced into the transcript and exploited for subsequent cloning steps into the expression vector pET28-a (see supplementary data). After restriction digests of the fragment and the empty pET28-a vector, the amplicon was ligated into the expression vector (**Figure 26**). Successful ligation was confirmed by sequencing with T7-promoter and T7-terminator primers. The use of *NcoI* as the N-terminal restriction site for *At5g39570.1* leads to the change of the second amino acid from proline to alanine. No other changes have been observed.

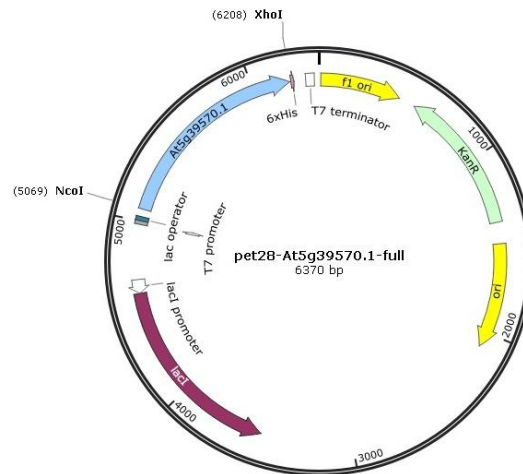


Figure 26: Expression vector pET28-a bearing the His-tagged fragment *At5g39570.1*. The blue arrow represents the full-size *At5g39570.1*-fragment (1139 bp) that is fused on the 3'-end to six consecutive histidine residues. The resulting fusion protein consists of 387 amino acids.

3.3.2 Cloning of *Ct-At5g39570.1* into pET28-a

The C-terminal fragment of *At5g39570.1* (*Ct-At5g39570.1*) was generated in accordance to the full-size clone with minor changes: The mutagenesis primers Cterm-At5g-fwd-Nhe and Cterm-At5g-rev-BamHI were used to generate a DNA fragment of 782 bp, containing the restriction sites *NheI* and *BamHI*. The enzyme *BamHI* possesses star activity and might cut the DNA unspecifically, when the incubation time exceeds a threshold. Therefore, a sub-cloning step with blunt ends into pJET 1.2 (supplementary data) was performed as a backup with 1 μ l of the transcript. The remaining fragment was digested (767 bp) and ligated into the expression vector pET28-a (**Figure 27**).

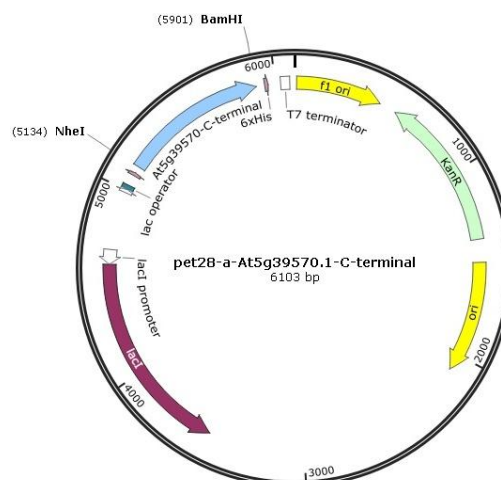


Figure 27: Expression vector pET28-a bearing the His-tagged fragment *Ct-At5g39570.1*. The blue arrow represents the C-terminal *At5g39570.1*-fragment (767 bp) that is fused on the 5'-end to six consecutive histidine residues. The resulting fusion protein consists of 234 amino acids.

The His-tag was introduced at the 5'-end of *Ct-At5g39570.1* to avoid interference of histidines at the C-terminal end of the expressed protein with putative binding partners. Successful ligation was confirmed by sequencing with T7-promoter and T7-terminator primers. The use of employed restriction sites in combination with the use of the partial fragment of *At5g39570.1*, results in a few changes in the 3'-end (extra nucleotides between his-codons and gene are introduced). The 208 amino acids at the expressed C-terminal region are not altered (**Figure 28**).

Met G S S H H H H H H S S G L V P R G S H M A S R P E S G L G S G Y G G R S E S E
Y E R K P S Y G R S E E Q E E G Y R K P S Y G R S E E Q E E G Y R K P S Y G R S E E
Q E E G Y R K P S Y G R S E E E Q E E G Y R K P S Y G R S E E Q E E G S Y R K P S Y
G R S D D Q V E S Y I K P S Y G R S E E Q E E G S Y R K P S Y G R S E E Q E E G S Y
R K Q P S Y G R G N D D D D D E Q R R N R S G S G D D E E G S Y G R K K Y G G N
D S D E D E E K K K H R H K H H H Q K R R D E D D E

Figure 28: C-terminal protein fragment of At5g39570.1. Grey area: 208 C-terminal amino acids in At5g39570.1. The His-tag is highlighted in green.

3.3.3 Expression and isolation of At5g39570.1

The sequenced constructs pET28a-*At5g39570.1* (**Figure 27**) and pET28a-*Ct-At5g39570.1* (**Figure 26**) were transformed into *E. coli* BL21 cells. The T7 promoter was induced by the application of IPTG (final concentration 1 mM) for three hours (**Figure 29 a**). For detailed analysis, small samples (1 ml) were taken and processed as described in section 2.11. Soluble protein fractions (S0, S1, S2 and S3) and insoluble proteins (P0, P1, P2 and P3) were separated on SDS-PAGEs (**Figure 29**).

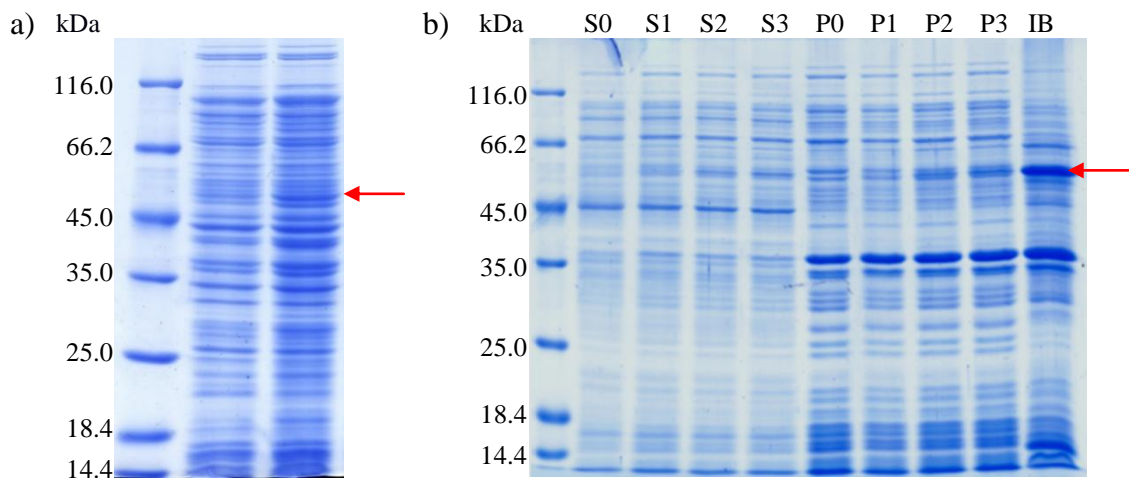


Figure 29: Induction of the full-size protein At5g39570.1. Red arrow: At5g39570.1 a) Induction of bacteria for 3 h. Not-induced (-) and induced (+) fractions. b) Detailed analysis of protein synthesis upon induction. S0-S3: Soluble protein fractions before and after induction. P0-P3: Insoluble protein fractions before and after induction. IB: Purified inclusion bodies.

A protein fraction containing precipitated proteins (IB), so called “inclusion bodies” from the main culture (see section 2.11), was purified and loaded on the gel (**Figure 29**). The full-size fragment of At5g39570.1 shows an increase in soluble fractions (S0 to S3) at 55 kDa after three hours of induction. This effect can also be observed in the insoluble fractions (P0 → P3), although the overall protein content is at a higher level and additional protein bands appear. The fraction of purified inclusion bodies displays a strong signal at 55 kDa. The main culture of soluble protein fractions and inclusion bodies were prepared as described in section 2.11. As depicted in **Figure 30**, the protein fraction F0 contains all proteins, while only unbound proteins (Ft) are eluted from the column by mild washing steps. The At5g39570.1-containing protein fractions F1-F6 display a strong protein band at 55 kDa. The Bradford test (section 2.10.2) enabled the quantification of the proteins for each eluted protein fraction F1-F6. Isolation and purification of the recombinant protein At5g39570.1 by His-tag affinity chromatography was followed as described in section 2.11.

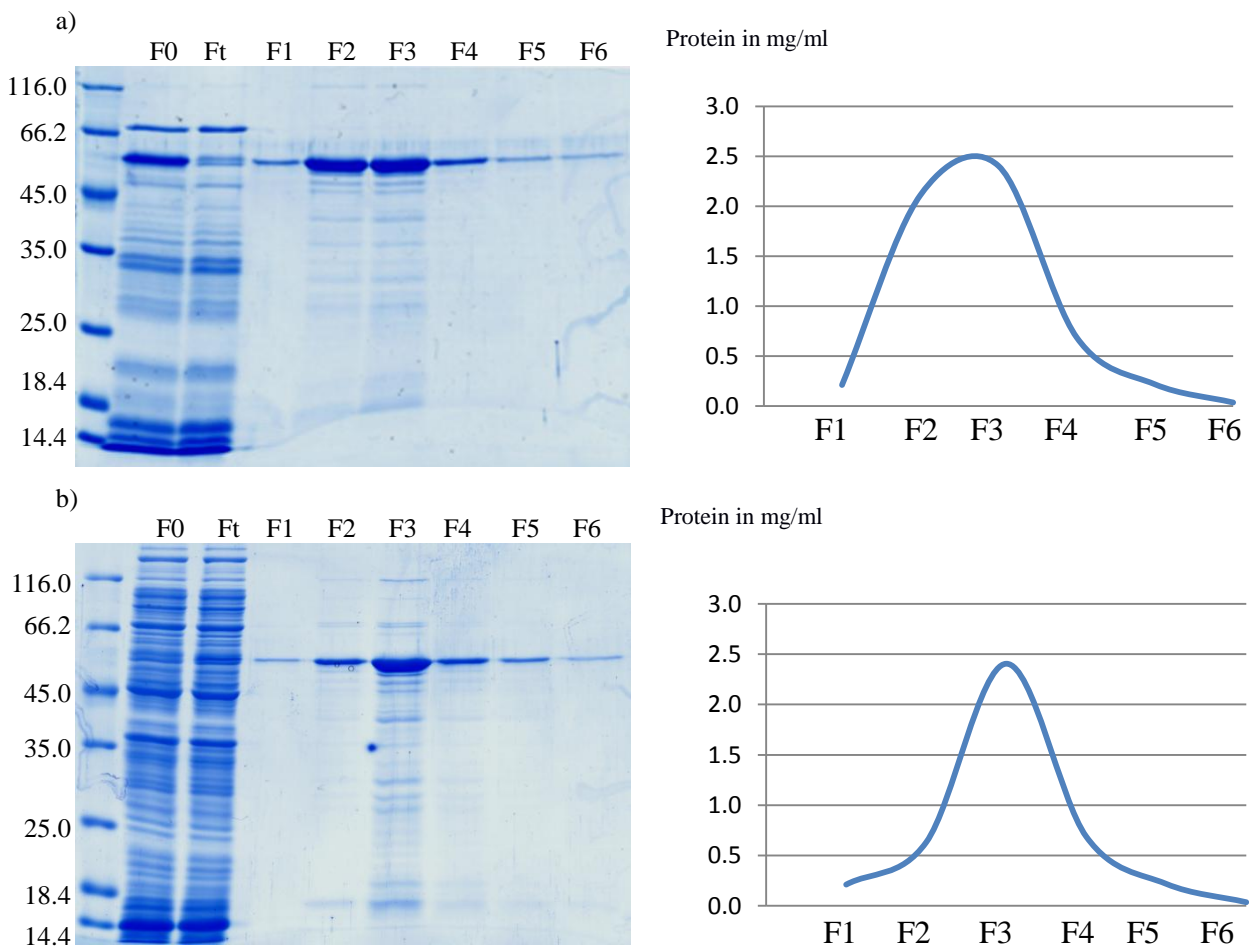


Figure 30: His-tag affinity chromatography of At5g39570.1-full-size.

a) Soluble protein fractions. b) Inclusion bodies. F0: Total proteins before loading onto the column; Ft: Flow-through; F1–F6: Eluted His-tag fractions. Right panels: Elution profile of fraction F1–F6 according to protein contents determined by the Bradford assay.

The elution profiles show maximum protein contents in the fractions F2 and F3. Although At5g39570.1-protein bands are highly enriched after the purification, few unspecific proteins can be detected. A comparison of the purification of At5g39570.1 by His-tag affinity chromatography of soluble proteins (**Figure 30 a**) and inclusion bodies (**Figure 30 b**) revealed a more specific purification in the soluble fractions. The introduction of a heat-treatment step (100°C for 10 min), prior to the affinity chromatography, resulted in a decrease of unspecific bands (**Figure 31**).

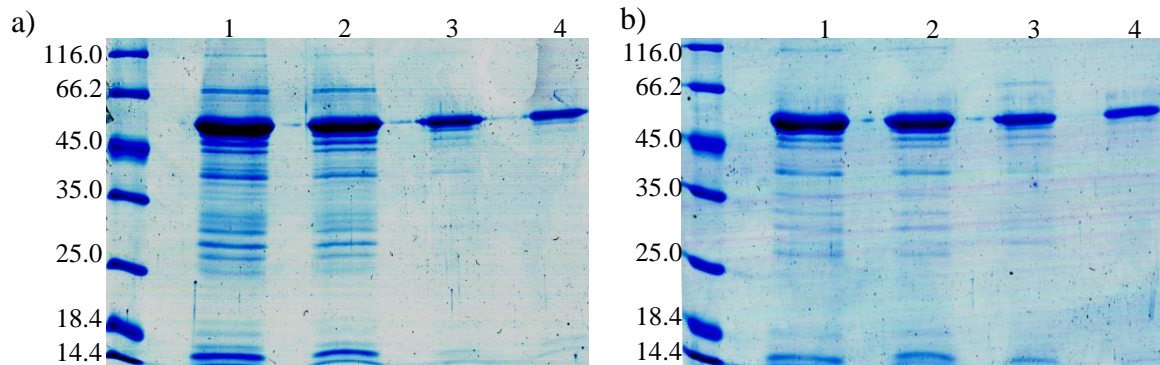


Figure 31: Comparison of proteins before and after heat-treatment. Dilutions of 100 µg protein (1) to 10 µg protein (4) were loaded. a) Standard purification by affinity chromatography. b) Heat-treatment was performed at 100°C for 10 min prior to purification.

Binding of unspecific proteins could be further reduced by demineralization of protein samples with PD-10 desalting columns (GE Healthcare).

The C-terminal protein fragment of At5g39570.1 was induced and purified as shown for the At5g39570.1-full-size protein (**Figure 32**). The previously generated antibody (Ufer, 2011) is targeted against the N-terminal half of the protein and thus cannot identify the C-terminal protein fragment (**Supplementary figure 3**). For further analysis of the C-terminal fragment the anti-His antibody (GE-Healthcare) was used (**Figure 32**).

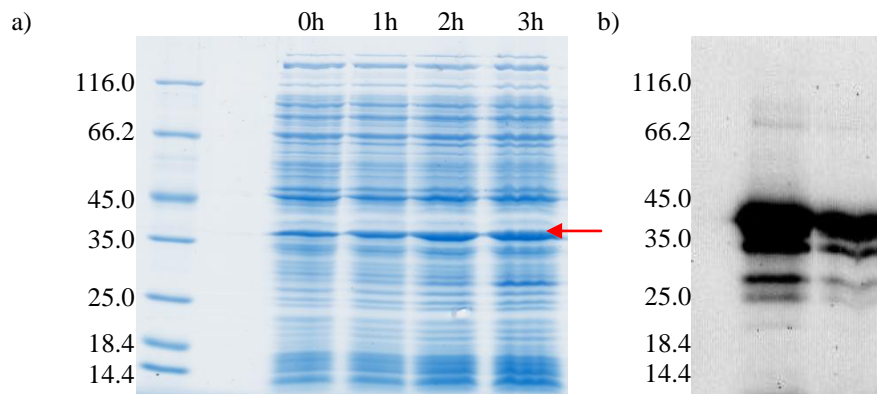


Figure 32: Induction and detection of the C-terminal protein fragment of At5g39570.1. a) Protein induction for 3 h. b) Detection of recombinant Ct-At5g39570.1 with the anti-histidine antibody

3.4 Generation of monospecific antibodies against At5g39570.1

To increase the binding specificity of the anti-At5g39570.1 antibody, monospecific antibodies against At5g39570.1 were produced as described in section 2.14. **Figure 33** shows the specific signal band for At5g39570.1 in a protein blot.

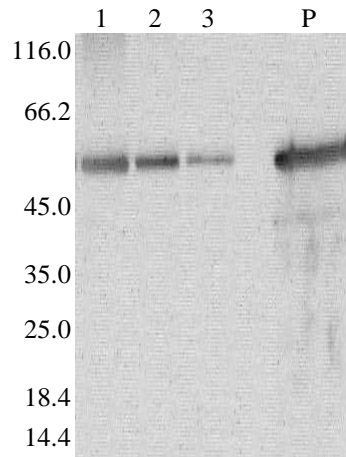


Figure 33: Test of monospecific antibodies.
Plant material (1-3), P: Recombinant protein At5g39570.1.

The purified antibodies bind more specific to the plant and recombinant proteins. Only few unspecific bands are visible on the tested protein blot. Monospecific antibodies were used for further experiments (e.g. co-immunoprecipitation, see section 2.15.1).

3.5 RNAi-knock-down mutants of *At3g29075*

Homozygous T-DNA insertion mutants do not express a protein of interest and are therefore widely used to observe phenotypic differences, triggered by a specific gene of unknown function. The gene knock-down by RNA interference (RNAi) does not completely prevent the expression of a protein, but reduces gene expression by mRNA degradation (Fire *et al.*, 1998). A T-DNA insertion line for *At5g39570.1* was ordered and confirmed in my previous work (Ufer, 2011). The putative homolog *At3g29075* shows high sequence similarities with *At5g39570.1* (**Figure 12**) and might influence the function of *At5g39570.1*. Unfortunately, no T-DNA insertion line for *At3g29075* was available. Thus a knock-down mutant for *At3g29075* and a double *At5g39570.1* knock-out/ *At3g29075* knock-down mutant was generated in this work, as described in section 2.18. Four primer combinations were used to engineer the artificial microRNA “TAAATTAGGTCGCTGATACTG” from the template plasmid pRS300 (supplementary data) (**Table 10**), which was kindly provided by Prof. Weigel (Max Planck Institute for Developmental Biology, Tübingen, Germany).

Table 10: Generation of the *At3g29075*-specific miRNA

	Forward oligo	Reverse oligo	Template
a)	A	4- <i>At3g29075</i> -miR*a	pRS300
b)	3- <i>At3g29075</i> -miR*s	B	pRS300
c)	1- <i>At3g29075</i> -miRs	2- <i>At3g29075</i> -miRa	pRS300
d)	A	B	(a)+(b)+(c)

The resulting amplicon (750 bp) was digested with *Bam*HI and *Eco*RI, gel eluted (430 bp) and cloned into pGJ280. Transformation into DH10B *E. coli* cells was confirmed by colony-PCR (P35S-prok2 & 2-*At3g29075*-miRa, 300 bp). Restriction digest by *Hind*III and subsequent ligation into the pBIN19 vector was confirmed by DNA sequencing (**Figure 34**).

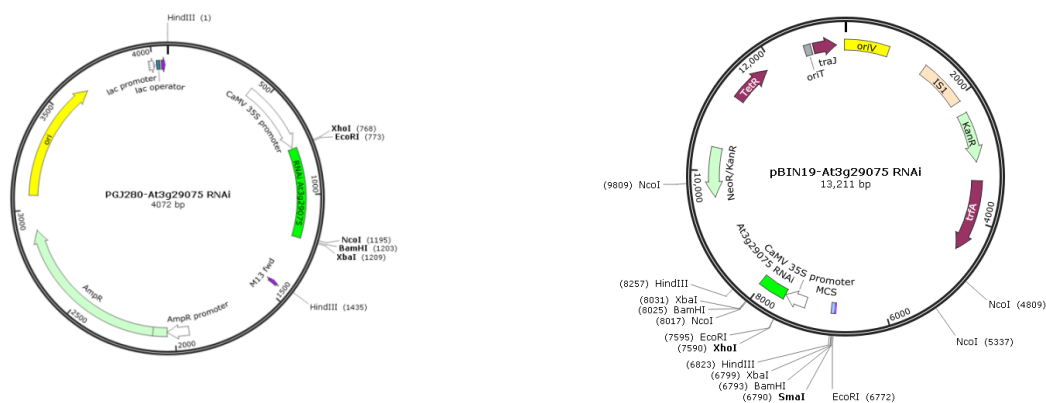


Figure 34: Cloning strategy for the generation of *At3g29075*-RNAi knock-down constructs.

The construct *pBIN19-At3g29075-RNAi* was transformed into *Agrobacterium* and checked by colony-PCR. Wild-type and *At5g39570.1* knock-out plants were transformed by floral dip (section 2.17.2). Successfully transformed plants carry a kanamycin-resistant gene and were selected on MS-Kan^R plates (Figure 35).

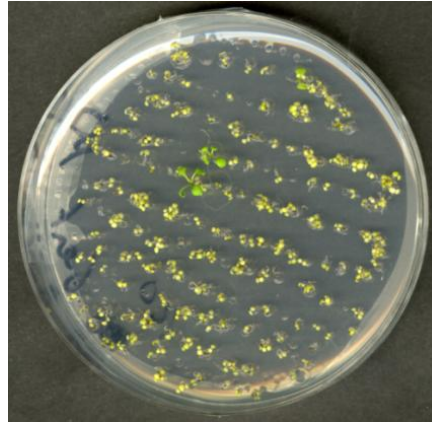


Figure 35: Selection of positive plants on MS-plates supplemented with 80 mM kanamycin.

Semi-quantitative analysis by RT-PCR confirmed the successful generation of four double *At5g39570.1* knock-out/ *At3g29075* knock-down lines with altered expression levels of *At3g29075* (Figure 36).

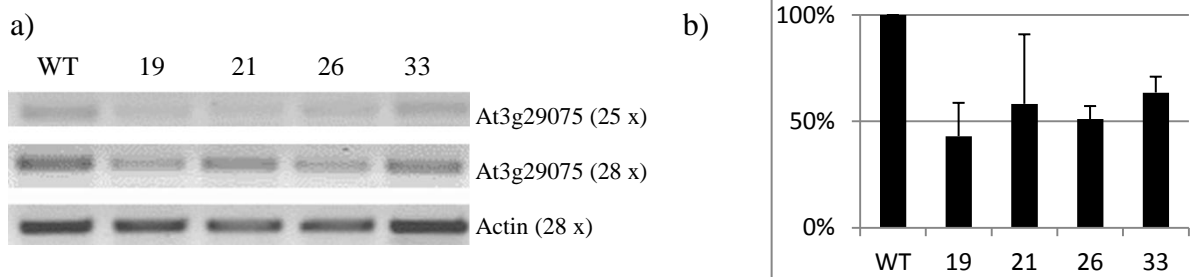


Figure 36: Transcript analysis of double *At5g39570.1* knock-out/ *At3g29075* knock-down mutants

a) RT-PCR results by Ct-*At3g29075*-fwd & Ct-*At3g29075*-rev b) Mean values of transcript levels (%) upon three-fold repetition of RT-PCR with 28 cycles. The mean value for WT is set to 100 %. Values were calculated as described in section 2.1.9 and are given in the supplementary data files.

Single *At3g29075* knock-down mutants were checked and analyzed in the context of a Master thesis (Nasr, 2015).

3.6 Phenotypic analysis of mutant plants

For phenotypic analysis, seeds of all mutant plants and the wild type were harvested at the same day and subjected to uniform conditions (for detailed information see section 2.2.2). Morphology and developmental stage of mutants and wild type was monitored under standard conditions and upon abiotic stresses. Besides macroscopic analyses, mutant plants were screened using a stereomicroscope and a microscope. No prominent phenotypic differences were observed for *At5g39570.1* mutants upon standard conditions (**Figure 37**).



Figure 37: Phenotypic comparison of wild type and mutant plants.

a) Wild type b) *plda1* knock-out mutant c) *At5g39570.1* knock-out mutant d) *At5g39570.1* knock-out/*At3g29075* knock-down mutant.

When subjected to mild, abiotic stress, such as dehydration **Figure 38**, cold (**Figure 39**) or salinity (**Figure 40**) mutant plants displayed no changes in growth or development compared to the wild type. The *plda1* mutant appeared slightly more vulnerable to water-limiting conditions. Interestingly, salt-stressed *At5g39570.1* knock-out mutant plants displayed an altered phenotype after two to three weeks of salt treatment (**Figure 40** b - c).



Figure 38: Six week old Arabidopsis plants after two weeks of dehydration.

a) Wild type b) *plda1* knock-out mutant c) *At5g39570.1* knock-out mutant d) *At5g39570.1* knock-out/
At3g29075 knock-down mutant.

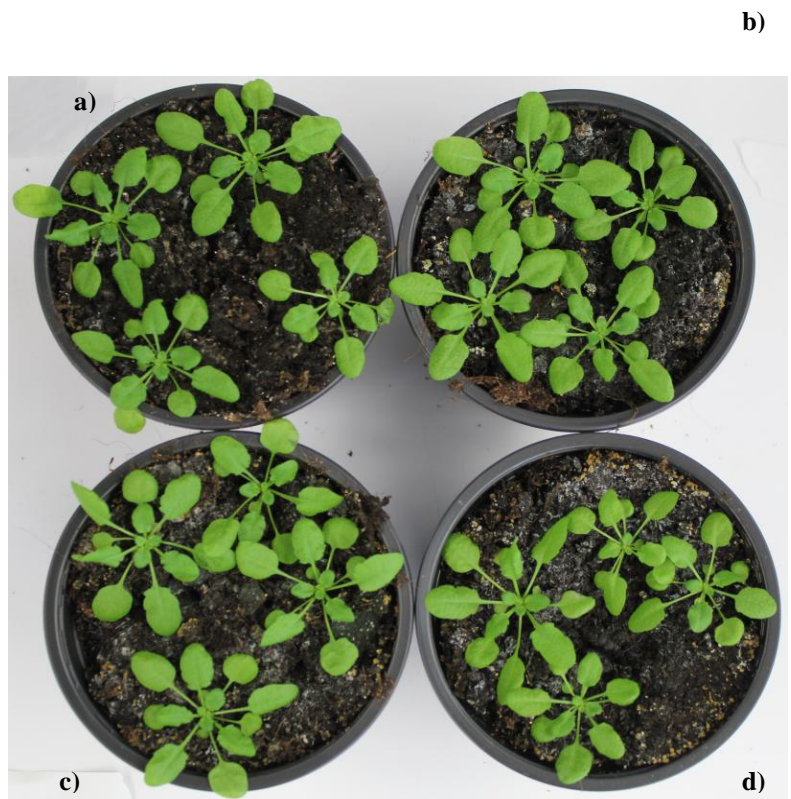
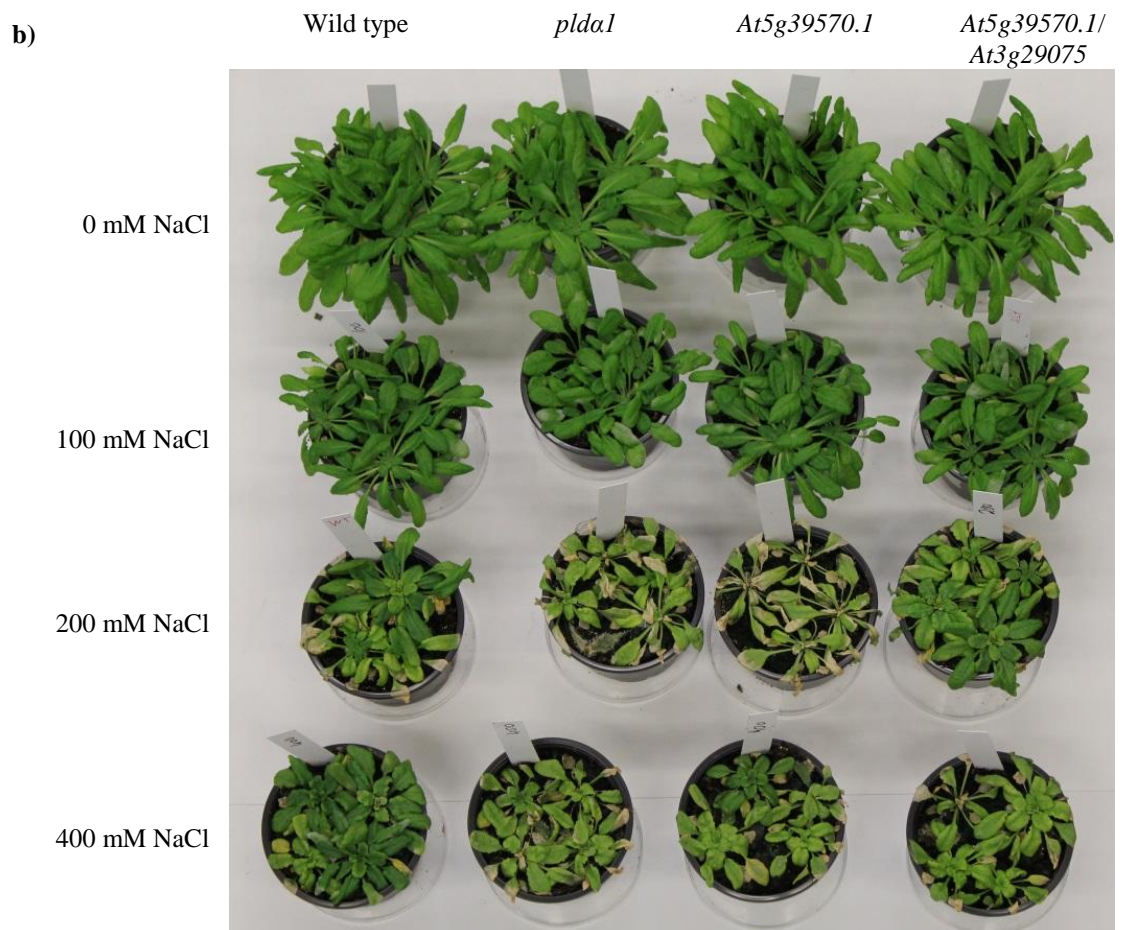
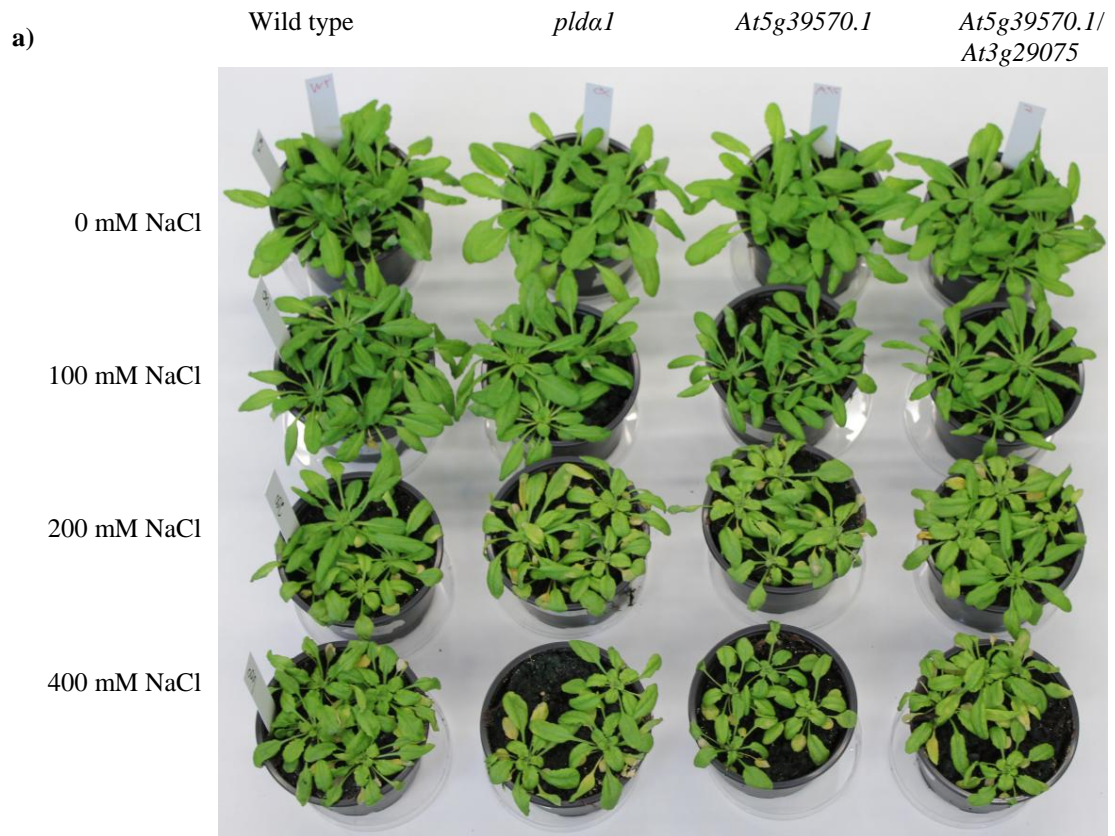


Figure 39: Six week old Arabidopsis plants after two weeks of cold-treatment.

a) Wild type b) *plda1* knock-out mutant c) *At5g39570.1* knock-out mutant d) *At5g39570.1* knock-out/
At3g29075 knock-down mutant.



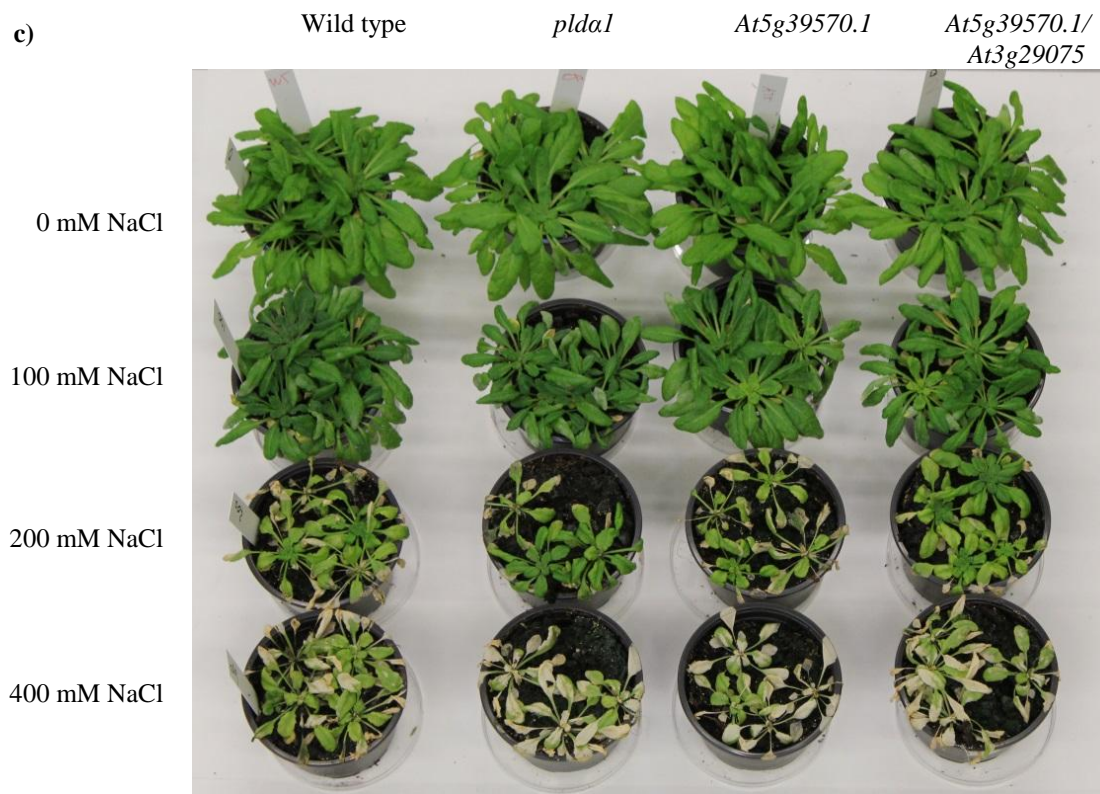


Figure 40: Six week old *Arabidopsis* plants after salt treatment.

a) Wild-type and mutant plants after salt treatment for 1 week. b) Wild-type and mutant plants after salt treatment for 2 weeks. c) Wild-type and mutant plants after salt treatment for 3 weeks.

While *At5g39570.1* and *At5g39570.1/At3g29075* knock-out mutants showed no prominent phenotypic differences compared to the wild type when subjected to NaCl concentrations of 100 – 400 mM for seven days, continuous salt-treatment for 14-21 days resulted in a *plda1*-like phenotype for these mutants. The *At5g39570.1*-mutant and the *plda1* mutant were strongly impacted by 200-400 mM NaCl, displaying growth inhibition and chlorophyll loss. The double knock-out mutant *At5g39570.1/At3g29075* did not result in a more prominent phenotype.

3.6.1 Phenotypic analysis of *At5g39570.1* knock-out plants in phosphate-depletion media

Several T-DNA insertion lines of *At5g39570.1* were obtained from the SALK institute and subsequently genotyped (Ufer, 2011). None of these lines has shown a prominent phenotype upon standard conditions (e.g. **Figure 37**). For further analysis, the homozygous T-DNA insertion line GK-167C05.09 was selected. Wild-type and mutant plants were subjected to drought stress conditions (**Figure 38**), cold stress (**Figure 39**) and salt treatment (**Figure 40 a**). However, only minor phenotypic differences have been observed, which could not be solely connected to these abiotic stress conditions. Continuous salt-stress treatment revealed a PLD- α 1-like phenotype for *At5g39570.1* knock-out mutants. Depletion of phosphate level in the media triggered altered plant growth and development (**Figure 41**). *At5g39570.1* knock-out plants and *plda-1* knock-out mutants displayed reduced growth and decreased production of chlorophyll (**Figure 42 a-b**). The root length of mutant plants was affected in the same manner as the wild type, when subjected to altered phosphate concentrations (**Figure 42 c**). Immunodetection of *At5g39570.1* could detect a minor shift in protein level depending on the phosphate concentration *At5g39570.1* in wild-type and *plda1* mutants (**Figure 42 d**).

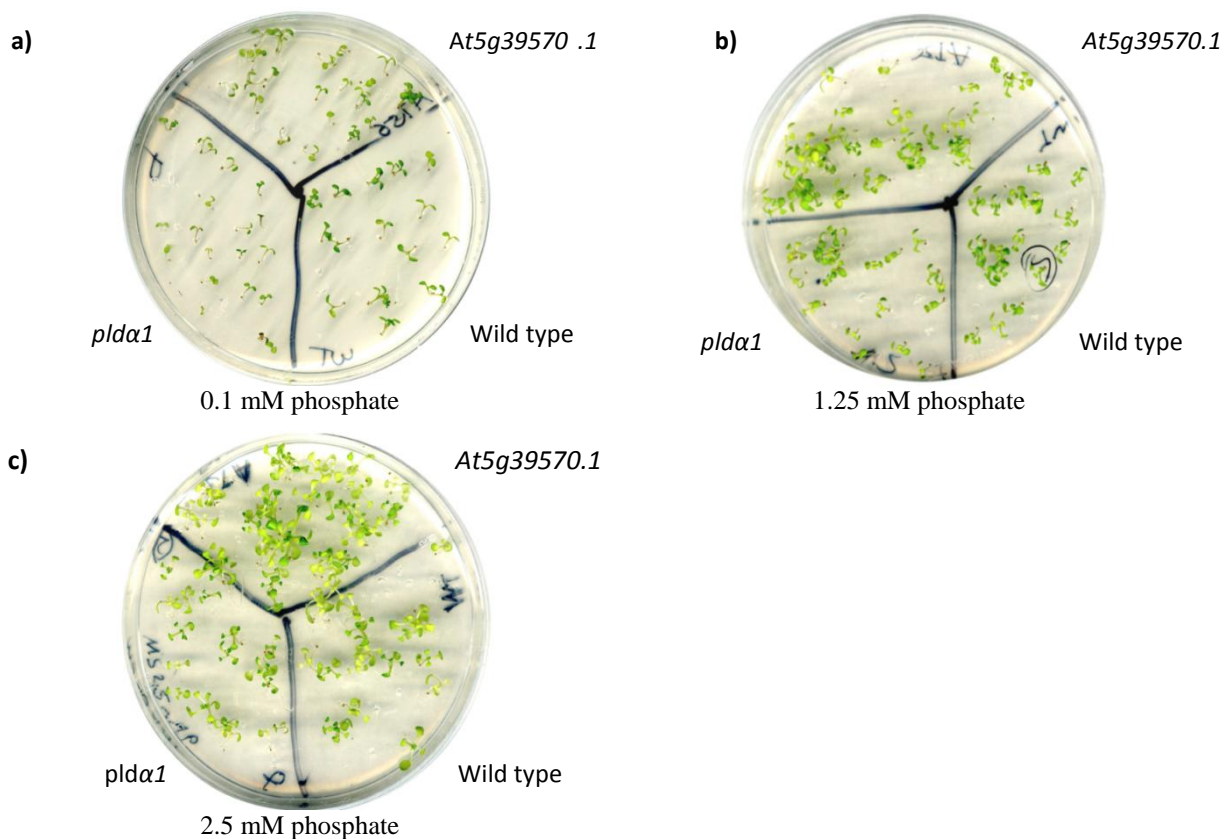


Figure 41: 10-day old seedlings grown on MS-phosphate depletion media.

a) Low phosphate concentration (0.1 mM) b) Standard phosphate concentration (1.25 mM) c) High phosphate concentration (2.5 mM).

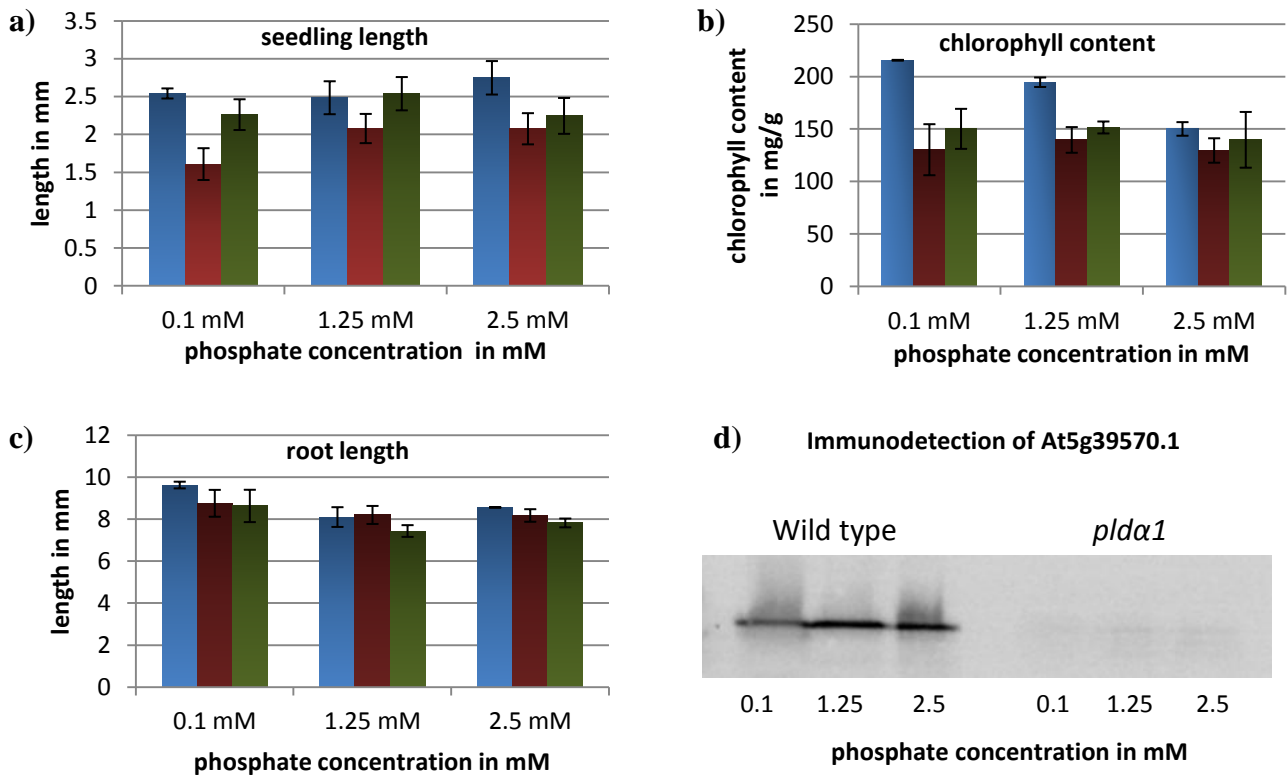


Figure 42: Phenotypic differences of 10-day old Arabidopsis seedlings on MS-phosphate depletion media. Low (0.1 mM), standard (1.25 mM) and high (2.5 mM) phosphate concentrations. Blue: Wild type; Red: *plda1* mutant; Green: *At5g39570.1* mutant. a) Growth of seedlings b) Chlorophyll content c) Root length a)-c): Mean values of repetitions d) Immunodetection of At5g39570.1 in wild type and *plda1* knock-out mutants under phosphate stress.

3.6.2 Phenotypic analysis of *At3g29075* knock-down plants

In this work, wild-type and *At3g29075* mutant plants were grown under standard conditions and monitored daily, but no prominent phenotypic difference was observed (**Figure 37**). Further stress experiments will be carried out in the context of a Master thesis (Nasr, 2015).

3.6.3 Phenotypic analysis of the *At5g39570.1* knock-out/ *At3g29075* knock-down double mutant

Wild type and mutant plants were monitored daily, but no prominent phenotypic difference could be observed (**Figure 37**). Mild stress treatments, such as short term dehydration (**Figure 38**) and cold stress (**Figure 39**), could not trigger a prominent phenotype. Long-term stress treatments with high concentrations of NaCl resulted in a *plda1*-like phenotype (**Figure 40**). However, no difference between the double mutant and the *At5g39570.1* knock-out mutant were observed. Further stress experiments will be carried out in the context of a project work (Sukumaran, 2015).

3.7 Expression analysis of At5g39570.1 in *pld* mutants

Gene and protein expression pattern vary in different developmental stages of a plant, in different plant tissues and can be changed upon stress treatments. For the characterization of gene and protein regulatory networks, it is required to study their expression profiles. Microarray data (**Supplementary figure 4**) can provide first hints for possible expression patterns of unknown genes.

Previous studies (Shen, 2008, Kuhn, 2010) suggested a control of At5g39570.1 expression by PLD α 1. To reveal interdependences between both genes, respectively proteins further studies focusing on expression analyses of transcripts, proteins and phosphoproteins have been carried out in this thesis.

3.7.1 Developmental stage-specific expression of At5g39570.1

In accordance to microarray studies (**Supplementary figure 4**) it has been shown that the protein level of At5g39570.1 increases in senescent leaves (**Figure 43**). While the protein content in 7-14 days old seedlings is low, the amount of At5g39570.1 increases rapidly in 3-5 weeks old plants.

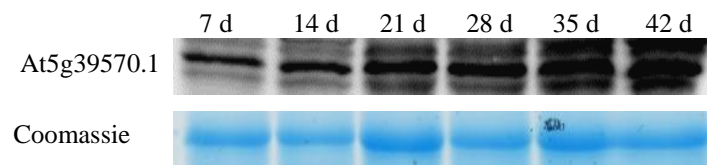


Figure 43: Expression of At5g39570.1 in leaves at different developmental stages.

3.7.2 Tissue specific expression of At5g39570.1

Protein blots revealed differences at the protein level of At5g39570.1 in different plant tissues. While the protein expression in leaves (rosette, cauline) is equivalent, their expression in roots, plant stems and flowers is increased (**Figure 44**).

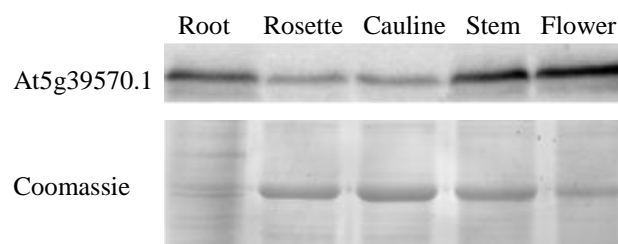


Figure 44: Tissue-specific analysis of At5g39570.1.

3.7.3 Expression analysis of At5g39570.1 in *pld* mutants

A previous study (Ufer, 2010) has shown, that the protein expression level of At5g39570.1 is dramatically decreased in *plda1* knock-out mutants and thus confirmed previous suggestions of a dependence of At5g39570.1 and PLD α 1 (Shen, 2008, Kuhn, 2010). To test whether both proteins are regulated mutually, immunodetection of PLD α 1 was carried out in wild type and *At5g39570.1* knock-out mutants. No down-regulation of PLD α 1 was observed in *At5g39570.1* knock-out mutants (**Figure 45**).

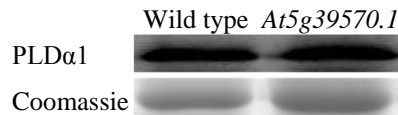


Figure 45: Immunodetection of PLD α 1 in wild type and *At5g39570.1* knock-out mutants.

The protein expression of At5g39570.1 was not only decreased in *plda1* knock-out mutants, but also in further mutants of the phospholipase D family, such as *plda3*, *plde*, and the double mutants *pld ζ 1/ ζ 2* all of which displayed reduced protein levels in leaves and seeds (**Figure 46**).

The strongest decrease can be observed for the single and double knock-mutant of *plda1*, but also the double knock-out mutant *pld ζ 1/ ζ 2* reveals a strong down-regulation. An additional decrease of At5g39570.1 in the *plde* knock-out mutant is prominent in the seeds, although the overall protein level is reduced in seeds as well.

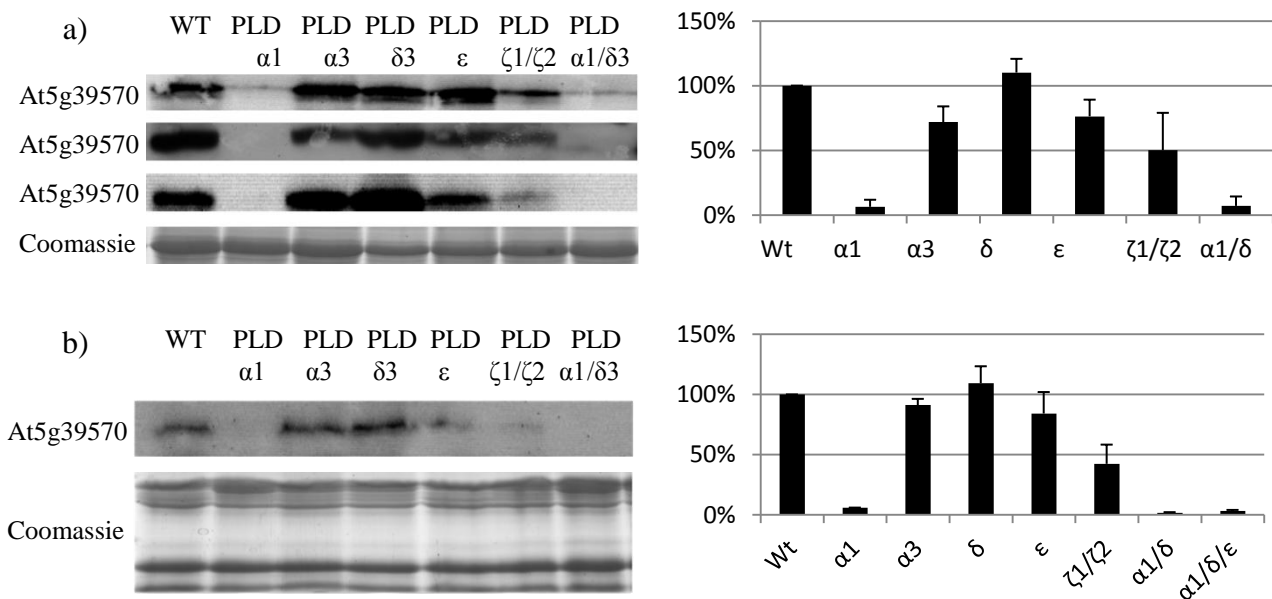


Figure 46: Protein expression of At5g39570.1 in leaves (a) and seeds (b) of different *pld* mutants. Left panel: Examples for protein expression. Right hand side: Mean values of protein levels (%) upon three technical repetitions of protein blots. Values were calculated as described in section 2.1.9. The mean value for the wild type is set to 100 %.

3.7.4 Expression analysis of At5g39570.1 upon water-limiting conditions

To determine whether expression of At5g39570.1 is regulated in response to water stress, fully-turgescient *A. thaliana* plants were compared to dehydrated (relative water contents of 75-35 %) plants (**Figure 47**).

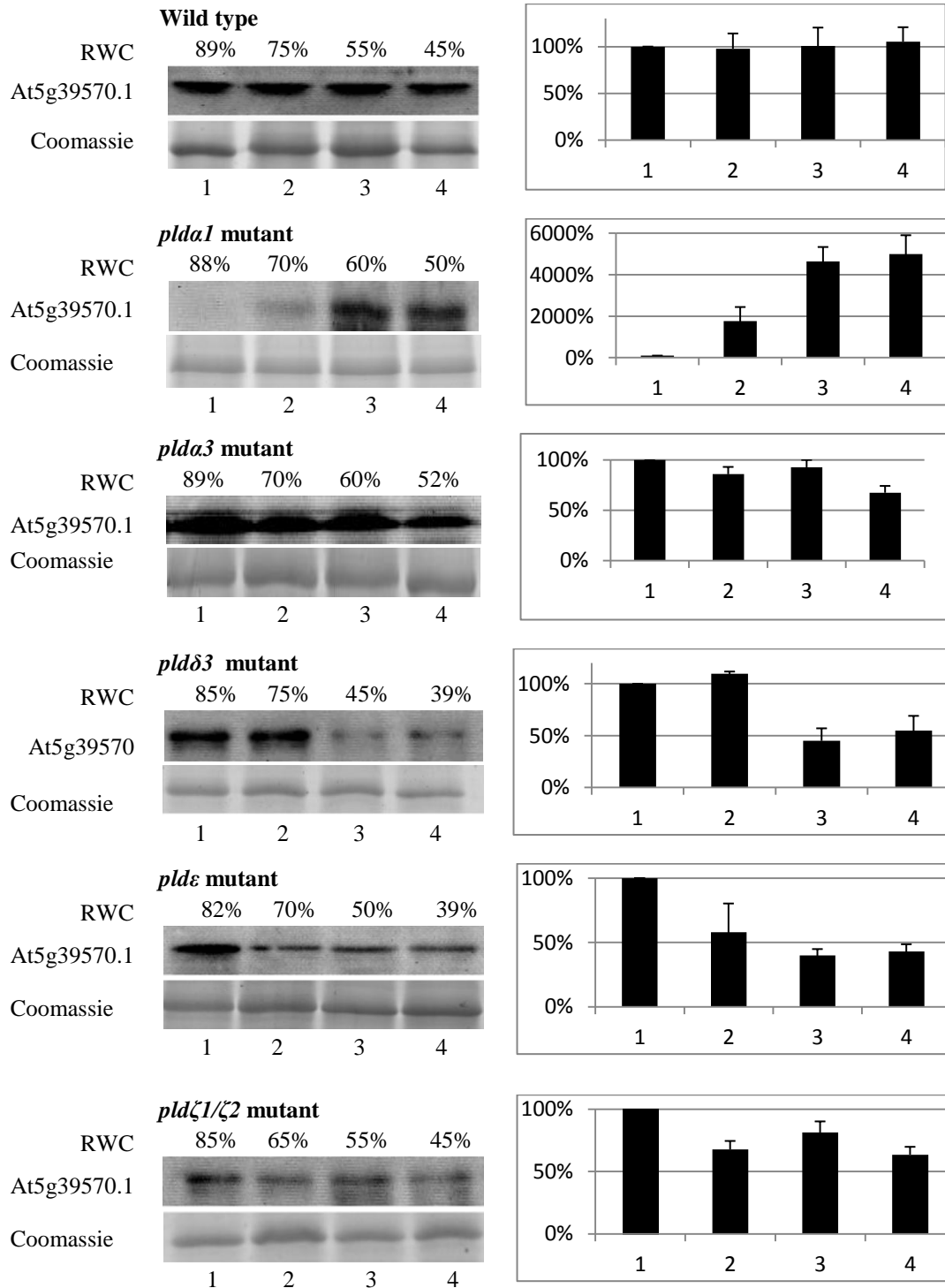


Figure 47: Protein expression levels of At5g39570.1 in leaf material upon dehydration in *pld* knock-out mutants. Left hand side: Exemplified protein blots; RWC: Relative water content. Right hand side: Mean values of protein levels (%) of three technical repetitions. Values were calculated as described in section 2.1.9 and are given in the supplement. The mean values for fully turgescient plants (line 1) are set to 100 % for each individual experiment.

As shown in **Figure 47**, dehydration did not significantly affect the protein content in leaves of wild-type plants. In contrast, strong induction of At5g39570.1 upon dehydration was observed in *plda1* knock-out mutants, which supports earlier findings of increased At5g39570.1 levels upon salt stress treatments (Jandl, 2012). The *pld* knock-out mutants *pldδ3* and *pldε* showed decreased protein levels upon severe dehydration stress (RWC <50 %), while expression levels of At5g39570.1 increased under comparable conditions in the *plda1* knock-out mutant. However the protein At5g39570.1 could not be detected in the *plda1* knock-out mutant upon extreme drought conditions (RWC <20 %) (data not shown).

A subsequently performed protease inhibitor assay could not detect any post-transcriptional differences in protein stability in wild type and *plda1* knock-out mutants (**Figure 48**).

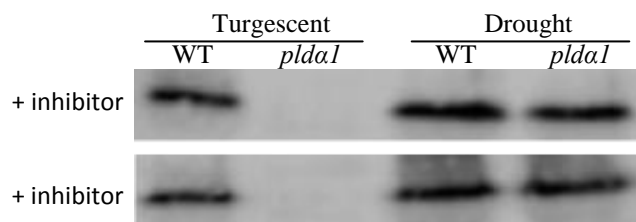


Figure 48: Protease inhibitor assay.
For details see section 2.9.3.

Besides stress-induced changes in the protein level, post-translational modifications, such as the phosphorylation of proteins, are of crucial importance for proteins functions (Reinders & Sickmann, 2007). Laugesen *et al.* (2006) identified a phosphorylation site at position S₃₃₉ in At5g39570.1 in the context of a large scale study. While the At5g39570.1 protein level remained constant upon drought stress conditions in wild-type plants, dehydration induced a slight phosphorylation of the protein (**Figure 49**).

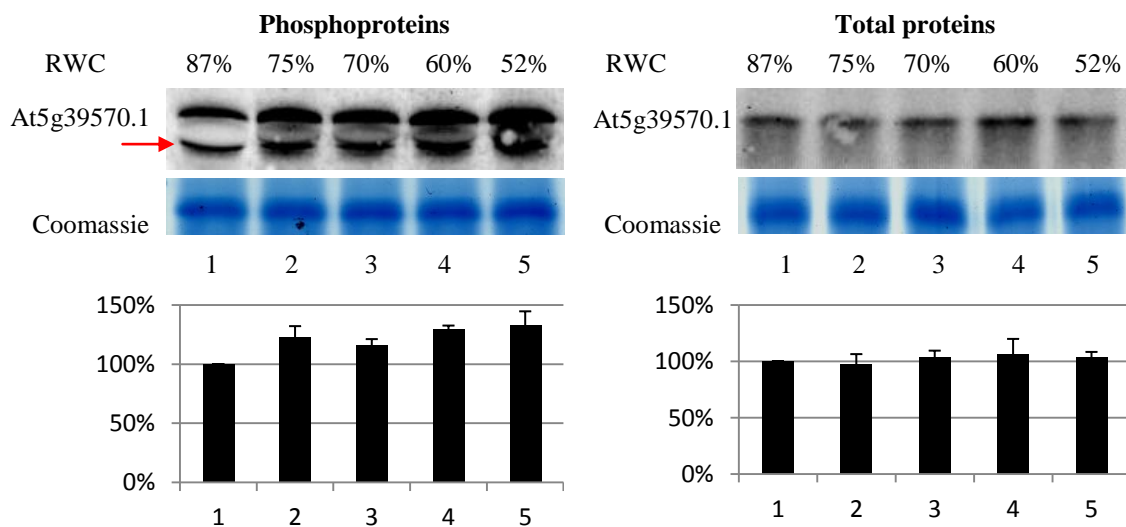


Figure 49: Comparison of total and phosphoproteins upon dehydration in wild-type leaves of *A. thaliana*. Top panels: Exemplified protein blots. Red arrow: Additional protein band in phospho-enriched proteins. Bottom panels: Mean values of protein levels of three fold repetitions. Values were calculated as described in section 2.1.9. The mean values for fully turgescent plants (line 1) are set to 100 % for each individual experiment.

Severe water-limiting conditions (RWC < 60 %) resulted in increased phosphorylation of At5g39570.1.

Immunodetection of At5g39570.1 in phospho-enriched plant protein extracts identified an additional, smaller protein which cannot be detected in the total protein fraction (red arrow in **Figure 49**). The comparison of phosphoproteins in fresh plant material of wild type, *plda1* knock-out mutant and *At5g39570.1* knock-out mutant, shows the presence of this unspecific protein band in wild type and mutants (**Figure 50**). The protein band appears less abundant, because fewer proteins have been loaded. **Figure 50** additionally displays the detection of low amounts of phosphorylated At5g39570.1 in the *plda1* knock-out mutant.

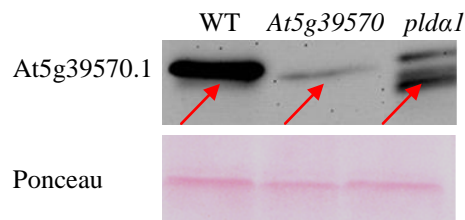


Figure 50: Immunodetection of At5g39570.1 in enriched phosphoproteins from *A. thaliana* leaves. Red arrow indicates unspecific protein bands (Ufer, 2011).

3.7.5 Expression analysis of the gene *At5g39570.1*

The repetitive structure of *At5g39570.1* impeded the transcript analysis of the gene by RT-PCR and led to different results, depending on the primers used for transcript analysis. Primer pairs that amplify the 5'-region of the gene (N-terminal fwd & N-terminal rev, see section **2.1.5**) could not identify differences in transcript levels of turgescient wild-type and *plda1* mutants (**Figure 51**) while the protein levels have shown strong differences (**Figure 46**).

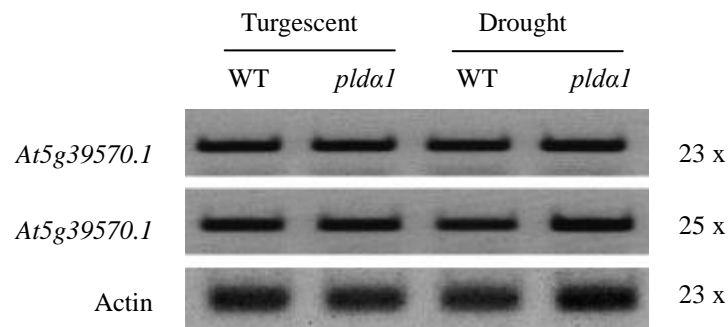


Figure 51: Expression of *At5g39570.1* in response to dehydration. RT-PCR analysis of the 5'-region of *At5g39570.1* transcript in 1 μ g total RNA extracted from WT and *plda1-1* mutant (upper panels). Actin transcripts served as loading control (lower panel). The number of RT-PCR cycles is indicated for each PCR. Primers are listed in section **2.1.5**.

For further analysis, polysomal RNA was extracted and analyzed by RT-PCR (section 2.8). As depicted in **Figure 52** the polysomal RNA level is reduced in *plda1* mutants.

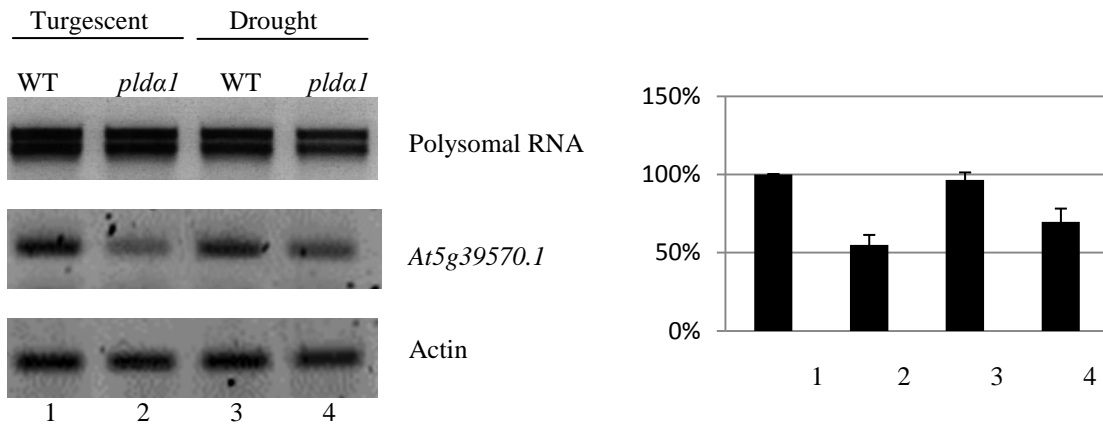


Figure 52: RT-PCR analysis of the N-terminal *At5g39570.1* transcript level. Polysomal RNA (1 µg), extracted from WT and *plda1-1* KO was loaded. Left panel: Exemplified RT-PCR analysis with N-terminal-fwd & N-terminal-rev (section 2.1.5). Right panel: Mean values of polysomal levels (%) of two technical repetitions. Values were calculated as described in section 2.1.9. The mean value for the wild type (line 1) is set to 100 %.

Especially fresh tissue of knock-out mutants revealed strong down-regulations of polysomal *At5g39570.1*-RNA. These reduced polysomal RNA levels face constant transcript levels for total RNA in the *plda1* knock-out mutant in case of amplification of the 5'-region (**Figure 51**). Surprisingly, transcript analysis of the full-length gene *At5g39570.1* resulted in different expression patterns (**Figure 53**). Here the transcript levels in the leaves of turgescent *plda*- mutant plants have shown a drastically decreased expression level compared to the wild type. Unlike the observed transcript level of the 5'-region of *At5g39570.1*, this observation is in accordance with the protein levels (**Figure 46**).

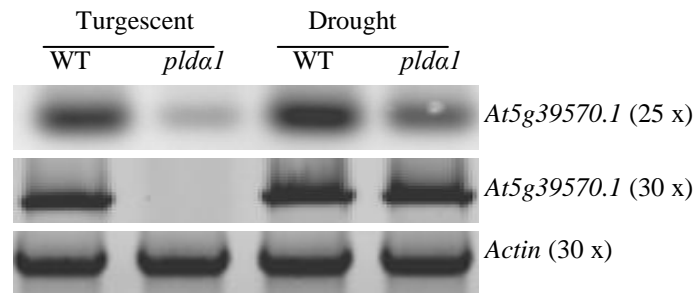


Figure 53: Transcript analysis of *At5g39570.1* with full-size primers.

Not only *pld α 1*-, but also the *pld α 3* knock-out mutant revealed decreased expression of *At5g39570.1*, while transcript levels remained constant in other PLD isoforms (**Figure 54**).

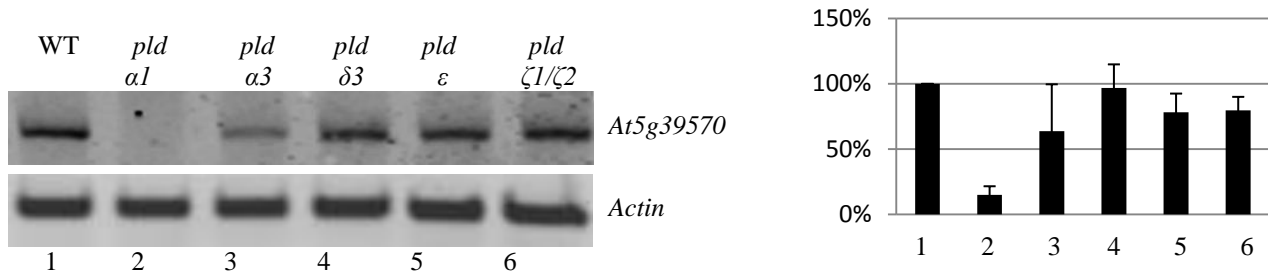


Figure 54: Transcript analysis of *At5g39570.1* by RT-PCR.

Left hand side: Exemplified RT-PCR analysis with full-size primers (section 2.1.5). Right hand side: Mean values of transcript levels (%) of two technical repetitions. Values were calculated as described in section 2.1.9 and are given in the supplement. The mean value for the wild type (line 1) is set to 100 %.

3.8 Identification of *At5g39570.1* interacting partners

The knowledge of putative *At5g39570.1* interacting partners is limited to data obtained from *in silico* analysis and large scale studies (**Supplementary table 8**). The degradation-marker protein, polyubiquitin3 was the only experimentally-detected binding partner of *At5g39570.1* and cannot provide any information of the putative function of the protein. The results of sections 3.1 and 3.7 indicate that *At5g39570.1* is dependent on PLD α 1 and acts downstream of this phospholipase. Co-expression of *At5g39570.1* further suggests a putative interaction with stress proteins (**Figure 22**). The identification of a phosphorylation site (Laugesen *et al.*, 2006), combined with the detection of multiple, imperfect tandem repeats and highly disordered regions (**Figure 18 & Figure 19**) render *At5g39570.1* as an interesting molecule in the signal-transduction pathway downstream of phospholipase D. Intrinsically disordered proteins have gained special attention in the past years, for challenging the traditional structure-function paradigm, which states that the function of proteins solely depends on their three-dimensional structure. Numerous proteins without an intrinsic globular structure under physiological conditions have been described in the past decades (Wright & Dyson, 1999). In fact, IDPs form a large and functionally diverse class of proteins and highlight the importance of protein dynamics for crucial molecular processes, such as allosteric signaling and enzyme catalysis (Bu & Callaway, 2011, Fraser *et al.*, 2009). The knowledge of how IDPs exert their functions is mostly unknown. The absence of a stable three-dimensional structure impedes the identification of protein-protein interactions.

The arrangement of *At5g39570.1* into an N- and C-terminal half is interesting and provides additional aspects for protein-binding assays. Binding of proteins suggest an interaction in

similar cellular processes and thus the identification of interacting partners of At5g39570.1 can indicate an involvement of the protein in distinct cellular pathways. In this work a variety of different protein-protein interacting methods with different advantages and disadvantages was applied to reveal the putative function of At5g39570.1: Yeast-2-hybrid screening, co-immunoprecipitation, affinity chromatography assays and protein-aggregation assays were carried out to discover interacting partners of At5g39570.1.

3.8.1 Yeast-two-hybrid assay

The yeast-two-hybrid system is a frequently used technique for the identification of protein-protein interactions *in vivo*. It is based on the activation of downstream reporter genes by binding of a specific transcription factor (e.g. GAL4) to an upstream activating sequence (UAS) (Keegan *et al.*, 1986). The transcription factor is composed of two (or more) domains: A DNA-binding domain (BD) that interacts with the UAS and an activator domain (AD) that promotes interaction with the RNA polymerase (Keegan *et al.*, 1986). Generation of a bait construct that expresses the protein of interest fused to the BD and a cDNA library encoding putative interacting partners fused to the AD (prey), respectively allows spatial separation of transcription factor fragments, preventing the expression of reporter genes. Interaction of bait and prey leads to merging of AD and BD, which can exert their function in close vicinity of each other without direct binding. The reconstitution of the functional transcription factor activates downstream reporter genes that can be monitored.

In this study, the GAL4 transcriptional activator system (Fields & Song, 1989) of the *Saccharomyces cerevisiae* strain Y190 was used and complementation of the transcription factor was monitored by the reporter genes *HIS3* and *LacZ*. The yeast strains and vectors were kindly provided by Dr. Zsuzsa Koncz (Max Planck Institute for Plant Breeding Research, Cologne).

3.8.1.1 Generation and transformation of the *At5g39570.1*-bait construct

The coding sequence of *At5g39570.1* was amplified from *A. thaliana* Columbia-0 cDNA using the primers At5g-Y2H-rev and At5g-Y2H-fwd. The PCR product (1157 bp) was digested with the restriction enzymes *NcoI* and *BamHI* and cloned into the digested pAS2-1 vector to express the fusion construct *At5g39570.1*-GAL4-BD. The generated plasmid was sequenced and subsequently transformed into the yeast strain Y190 (**Figure 55**).

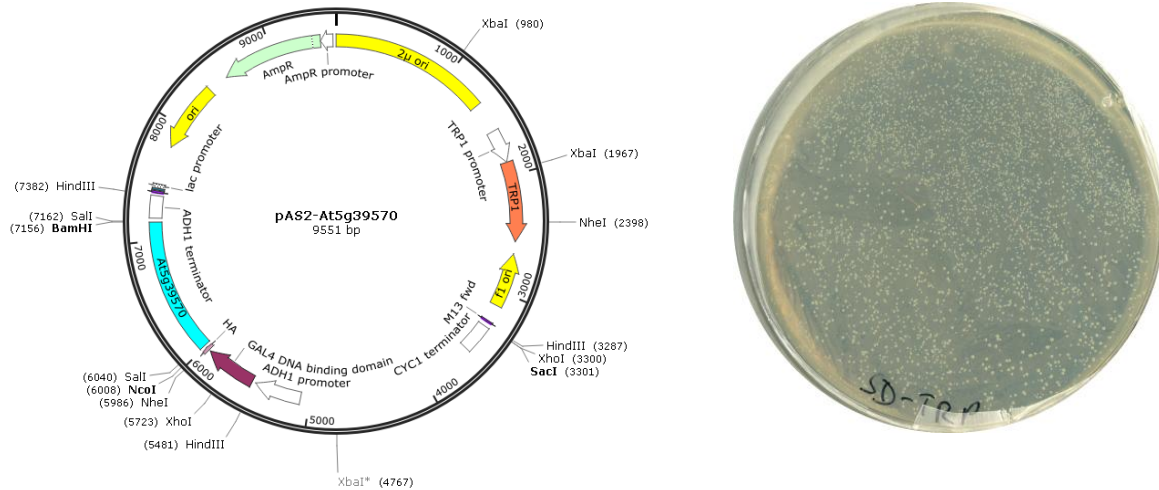


Figure 55: Construct of the bait pAS2-*At5g39570.1* and transformed yeast colonies on SD_{-Trp} depletion media.

Positive colonies were selected from SD_{-Trp} media and confirmed by PCR using the primers pAS2_1fwd and pAS2_1rev. Positive clones were diluted in sterile H₂O and applied on SD_{-Trp}-His plates supplemented with 3-amino-1,2,4-triazole (3-AT) (0-100 mM) to test for an auto-activation of the *HIS3* reporter gene. While yeast colonies grew on SD_{-His}-Trp media, their growth was strongly inhibited by 15 mM 3-AT (**Figure 56**). At concentrations of 50 mM 3-AT, yeast growth was completely inhibited.



Figure 56: *At5g39570.1* yeast-two-hybrid test of auto-activation.

Left hand side: Yeast strains grown on SD_{-Trp}-His media after 5 d of incubation at 30°C. Right hand side: Growth of yeast colonies after 5 d on SD_{-Trp}-His media containing 15 mM of 3-AT.

3.8.1.2 Calorimetric β -galactosidase assay

The colorimetric β -galactosidase assay (section 2.15.2) was used to confirm the absence of auto-activation of the *LacZ* reporter in positive clones. After 24 hours incubation no β -galactosidase activity has been observed, indicating the absence of auto-activation activity within the clones. Incubation times of more than 72 hours led to weak activation of the *LacZ* reporter (Figure 57).



Figure 57: Colorimetric β -galactosidase assay.

Left: Positive control with sucrose non-fermenting 1 (SNF1) and SNF2. Right: *At5g39570.1*-bait construct.

For further experiments a colony without auto-activation activity and inhibited growth at 25 mM 3-AT was selected.

3.8.1.3 Generation and transformation of the prey construct

A clone containing the oligo (dT)-primed cDNA library in the plasmid pACT2 was kindly provided by Dr. Zsuzsa Koncz (Figure 58). The cDNA library was obtained using mRNA from an *A. thaliana* cell suspension (Németh *et al.* 1998).

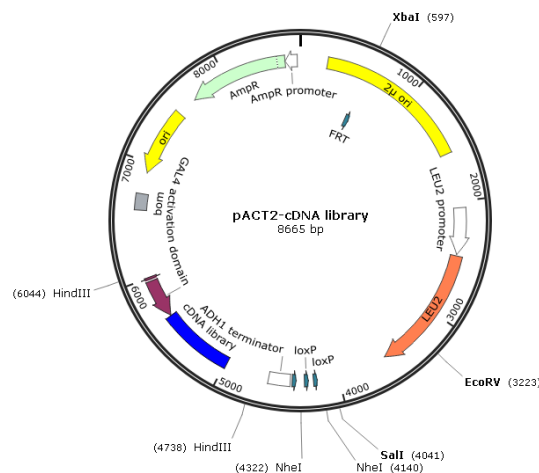


Figure 58: Construct of the prey pACT2-cDNA library.

3.8.1.3 Transformation and protein-protein interaction

The bait strain was transformed with 150 μ g pACT2 plasmid harboring the cDNA library in the plasmid pACT2. Transformed cells were inoculated on SD_{-Trp-His-Leu} plates supplemented with 25 mM 3-AT, incubated at 30°C for five days and screened by the colorimetric β -galactosidase assay (section 2.15.2). Blue colonies indicate β -galactosidase activity triggered by the interaction of bait and prey. Positive clones were replicated on SD_{-His-Trp-Leu} plates containing different concentrations of 3-AT (15-100 mM) to screen for true activation of the *His3* reporter gene (**Figure 59**).

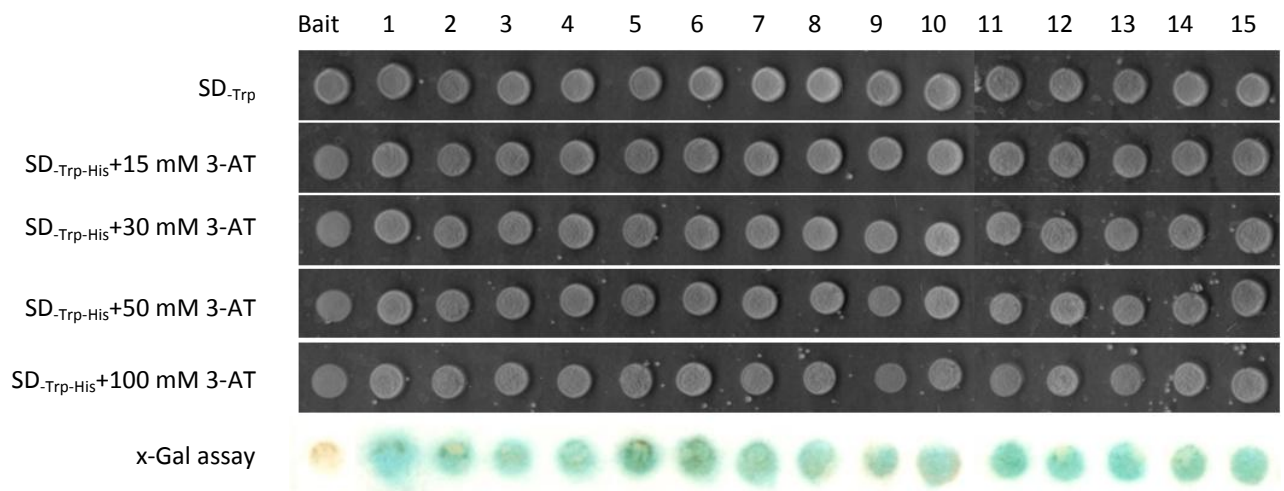


Figure 59: Yeast-two-hybrid screening with At5g39570.1 as bait.

Top five rows: Growth of yeast colonies, containing putative interacting preys on different SD media after 5 d of incubation at 30°C. Bottom row: Results of the β -galactosidase assays after 12 h incubation at 37°C. This screen was kindly provided by Dr. Quancan Hou.

Positive genes were amplified by yeast-colony PCR using the primers pACT2_fwd and pACT2_Gal4AD. A total of 23 clones were sequenced and identified by blast, resulting in the detection of 15 different, putative interaction partners of At5g39570.1 (**Table 11**). Additional positive clones were detected by the β -galactosidase assay, but not sent for DNA-sequencing as the repetitive detection of targets indicates the identification of the most likely interaction partners of At5g39570.1. Nine out of 23 clones were identified as proteins involved in RNA-processing: MORF 6, MORF 2 and U1-70K. The other putative interacting partners range from transcription factors to protein kinases. Two proteins of unknown function were detected. The identification of these proteins by additional, independent methods is required to confirm these target candidates.

Table 11: Interacting partners of At5g39570.1 identified by yeast-two-hybrid assays

Nr.	Protein	Name	Suggested function	Occurrence
1	AT2G35240	MORF 6	mitochondrial mRNA modification	4
2	AT2G33430	MORF 2	rRNA processing	3
3	AT1G10590	OB-fold-like protein	nucleic acid-binding	1
4	AT1G80460	GLI1	similar to glycerol kinase	1
5	AT3G05050	Protein kinase superfamily protein	protein kinase	1
6	AT4G24780	Pectin lyase-like superfamily protein	pectate lyase activity	1
7	AT3G49120	PRXCB	class III peroxidase	1
8	AT3G16640	TCTP	homologous to translationally controlled tumor protein (Drosophila)	1
9	AT3G50670	U1-70K	mRNA splicing	2
10	AT2G01650	PUX2	peripheral membrane protein	1
11	AT1G53170	ATERF-8	transcription factor	2
12	At4g23885	Unknown protein	unknown	1
13	At5g63350	Unknown protein	unknown	2
14	AT2G05220	Ribosomal protein S17	ribosomal protein	1
15	AT1G33120	Ribosomal protein L6	ribosomal protein	1

3.8.2 Affinity chromatography assay

A quick and simple method to screen for protein-protein interaction is the affinity-based isolation of interaction partners. The generation of the His-tagged recombinant protein as bait is described in section **2.11**. Plant extracts containing proteins of leaf or root extracts represent putative binding partners “prey”. The mixture was incubated with an affinity resin containing bound bivalent nickel ions and a NTA-chelating complex that binds with micromolar affinity to poly-histidine tags (Porath *et al.*, 1975). The protein of interest and putative binding and interacting proteins remain in the column upon washing with mild concentrations of imidazol (10-20 mM), while unspecifically-bound proteins are excluded. High concentrations of imidazol (≥ 100 mM) displace the protein bonds and co-elute the protein of interest. The eluted fractions (E1-E3) were loaded on SDS-PAGEs and stained by Coomassie or silver stain (section **2.12.3**). Plant protein extracts without the His-tagged At5g39570.1 served as a negative control, to exclude direct binding of plant proteins to the Ni-NTA columns. Coomassie stain and immunodetection identified At5g39570.1 to be the most prominent protein in the eluted column-bound fractions of leaf extracts (red arrow in **Figure 60**). Few additional protein bands that were not present in the negative control have been detected (black arrows in **Figure 60**). Unfortunately, the signal strength of these putative interacting partners was very low and the protein content was insufficient for MS-analysis.

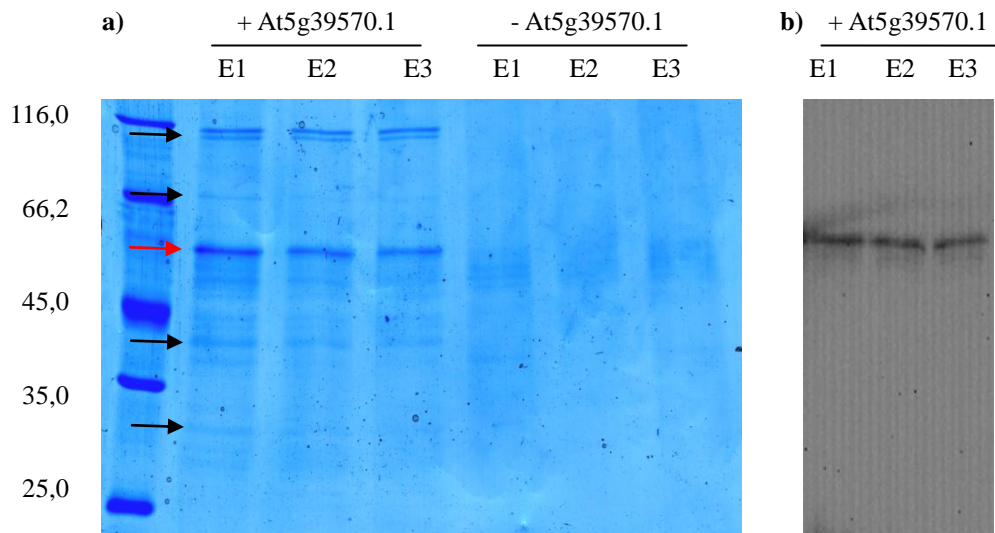


Figure 60: Ni-NTA affinity chromatography of total proteins from leaf extracts.

Leaf extracts were incubated with (+At5g39570.1) and without (-At5g39570.1) bait protein a) Coomassie stain of eluted proteins 1-3. Red arrow: At5g39570.1. Black arrows indicate putative interacting partners of At5g39570.1 b) Immunodetection with anti-At5g39570.1 on a protein blot.

When using total protein extracts from root material as prey for the detection of putative interacting partners of At5g39570.1, no additional protein bands were identified (**Figure 61**). Although the same amount of protein was applied to the column, less protein was eluted in the fractions E1, E2 and E3. A few, unspecific protein bands appeared, but no putative interacting protein was identified. Silver staining revealed additional protein bands, but the very low signal strength suggests unspecific proteins or staining artifacts (**Supplementary figure 5**).

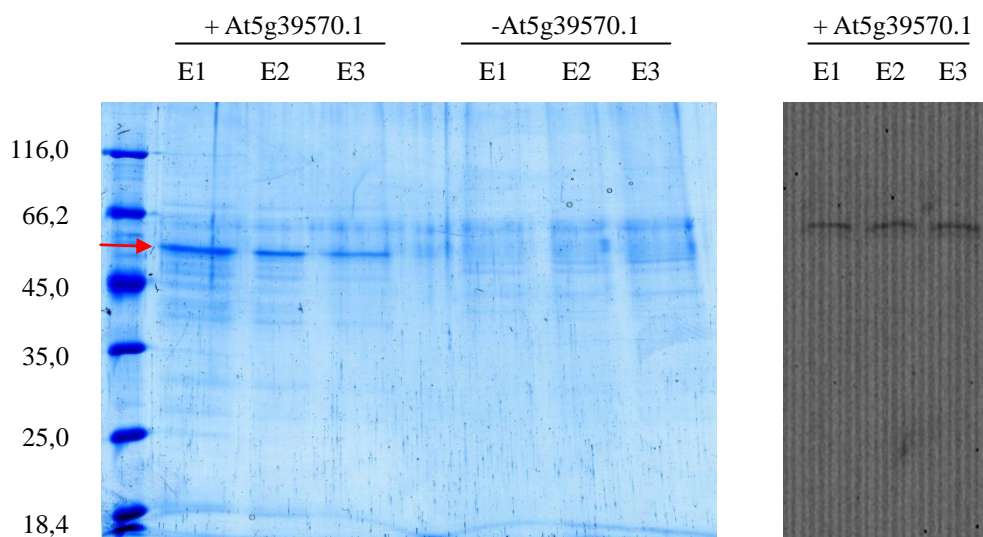


Figure 61: Ni-NTA affinity chromatography of total proteins from root extracts.

Root extracts were incubated with (+At5g39570.1) and without (-At5g39570.1) bait protein a) Coomassie stain of elutions 1-3. Red arrow: At5g39570.1. b) Immunodetection with anti-At5g39570.1 on a protein blot.

3.8.3 Co-immunoprecipitation assay

Co-immunoprecipitation enables the identification of protein-protein interactions by using antibodies directed against the protein of interest. Putative interacting partners of the protein of interest can be indirectly captured in a protein complex, co-eluted and subsequently analyzed (Klenova *et al.*, 2002). Protein-protein interactions depend on a wide range of parameters, such as protein concentrations and the presence of other proteins, nucleic acids and ions (Golemis, 2002). The protein conformation is of major importance for protein-binding. Disruption of the secondary, tertiary or quaternary structure of proteins by denaturing-experimental conditions might influence binding properties of complex proteins. Previous results suggested At5g39570.1 to be intrinsically disordered. Therefore, a denaturing and a non-denaturing method were used for the extraction of plant proteins (section 2.15.1). The protein At5g39570.1 was identified in both cell lysates, with a slightly higher protein yield in the denaturing extract (**Figure 62**). Both extracts were used for subsequent analyses.

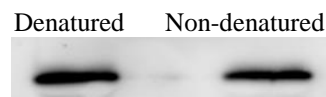


Figure 62: Protein yield of At5g39570.1 by denaturing and non-denaturing extraction methods.

For increased specificity, monospecific antibodies (section 2.14) were used for co-immunoprecipitation assays. Antibody coupling and co-immunoprecipitation was performed as described in section 2.15.1. In a first experiment, 200 mg of plant protein was used and equally split for protein blot and silver staining analysis. Both methods could only identify the At5g39570.1 protein faintly in the eluate. Epoxy beads eluted with Laemmli buffer, revealed two protein bands at 55 kDa and 50 kDa (**Figure 63a**).

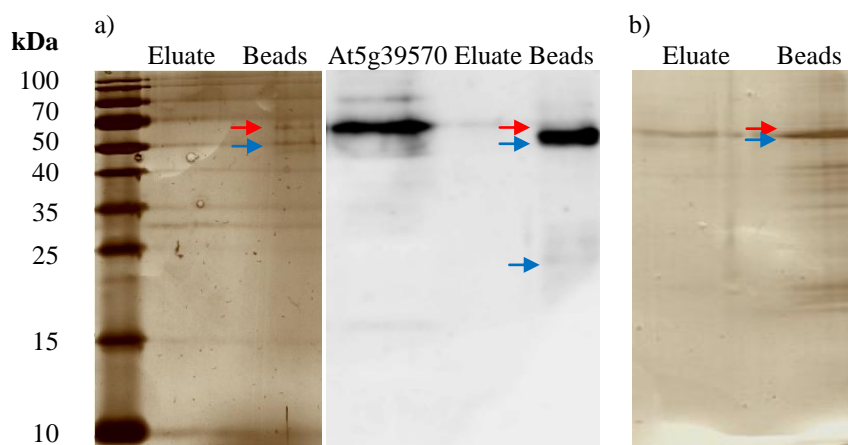


Figure 63: Co-immunoprecipitation of At5g39570.1.

Red arrow: At5g39570; Blue arrows: IgGs a) Co-IP with low amounts of denatured total protein extracts and antibody b) Co-IP with increased amounts of denatured total protein extracts and antibody. Eluate: Eluted fractions from epoxy beads. Beads: Epoxy beads in Laemmli buffer.

While the upper band (red arrow in **Figure 63**) represents At5g39570.1, the lower band (blue arrow) shows the heavy chain of the immunoglobulin at ~50 kDa. A faint band of the light-immunoglobulin chain was visible on the blot (25 kDa). No putative interacting proteins were detected by silver stain. In a following experiment the deployed amount of epoxy beads (2-fold), antibody (3-fold) and plant material (5-fold) was increased to gain higher protein yields (**Figure 63 b**). However, only the “beads fraction” displayed weak protein signals of putative binding partners of At5g39570.1. It was not possible to identify novel binding partners *via* MS-analysis because of the very low yield of these proteins.

3.8.4 Tandem-affinity purification

The tandem-affinity purification is a technique for protein complex purification and identification of novel protein interacting partners based on affinity-chromatography purification steps that are performed in series (Golemis, 2002). A protein of interest is fused to affinity tags (bait) and expressed in a natural organism (*A. thaliana*). Cell extracts of this organism containing bait and prey are prepared and used for the recovery of the target protein and its putative interacting partners. Distinct washing and serial purification steps prevent contaminants of binding to the protein of interest. Finally, putative binding partners are co-eluted from the extract. In a previous project work (Pandey, 2012) a fusion construct for *At5g39570.1* was generated in the Gateway cloning vector pDONR201 and was subsequently transformed and sequenced in the entry vector pnTAPa, encoding for IgG, His-tag and Myc-tag (**Figure 64**).



Figure 64: pnTAPa-*At5g39570.1* construct (Pandey, 2012)

In this work, wild-type and *At5g39570.1* knock-out plants were transformed with pnTAPa-*At5g39570.1* by floral dip (section 2.17.2) and selected on MS-plates supplemented with gentamycin. Positive plants were selected, checked by colony PCR and grown on soil. Unfortunately, the His-tagged protein could not be identified by anti-At5g39570.1. The anti-His antibody detected the protein at a much lower molecular weight as expected (data not shown). A repetition of the previous DNA sequencing (Pandey, 2012) revealed a frame shift of the *At5g39570.1* gene in the pnTAPa-*At5g39570.1* construct; therefore this construct was not used further.

3.8.5 Protein aggregation assay

Subsequently after synthesis the hydrophobic effect forces proteins into their final three-dimensional conformation (Anfinsen, 1972). Intrinsically disordered proteins form a special group of proteins that do not underlie this process and do not exhibit typical features of secondary, tertiary or quaternary structures (Wright & Dyson, 1999). Many IDPs function *via* binding to a partner protein and undergo a disorder-to-order transition. As described previously, At5g39570.1 exhibits typical features of IDPs, such as imperfect tandem repeats and unstructured amino acid segments. While protein aggregation is typically referred to as a biological phenomenon in which miss-folded proteins form aggregates and complexes, IDPs have been implicated in protein aggregation and diseases (Uversky *et al.*, 2008). IDPs expose unfolded, hydrophobic protein stretches, which are not buried in the core of the protein and thus may interact with other exposed hydrophobic patches, leading to protein aggregation. Structural analysis of At5g39570.1 in the lab of P. Harryson and S. Eriksson (University of Stockholm, personal communication) by circular dichroism failed due to an observed aggregation of recombinant At5g39570.1 proteins. Therefore, detailed analysis of the protein solubility in a wide range of different buffers was conducted (**Figure 65**). Aliquots of 100 mg lyophilized, recombinant At5g39570.1 proteins were dissolved in 100 µl of different buffers and centrifuged at low (10,000 g) and subsequently at high speed (20,000 g). The pellet fractions were dissolved in 100 µl Laemmli buffer and 20 µl of each fraction was analyzed on a SDS-PAGE (**Figure 65**). Only the buffers containing urea and CHAPS solubilized majority of the protein. Classical buffers, such as MOPS or phosphate buffers failed to solubilize At5g39570.1 completely. These results indicate that At5g39570.1 forms aggregates *in vitro*, which can be disrupted upon severe, denaturing conditions.

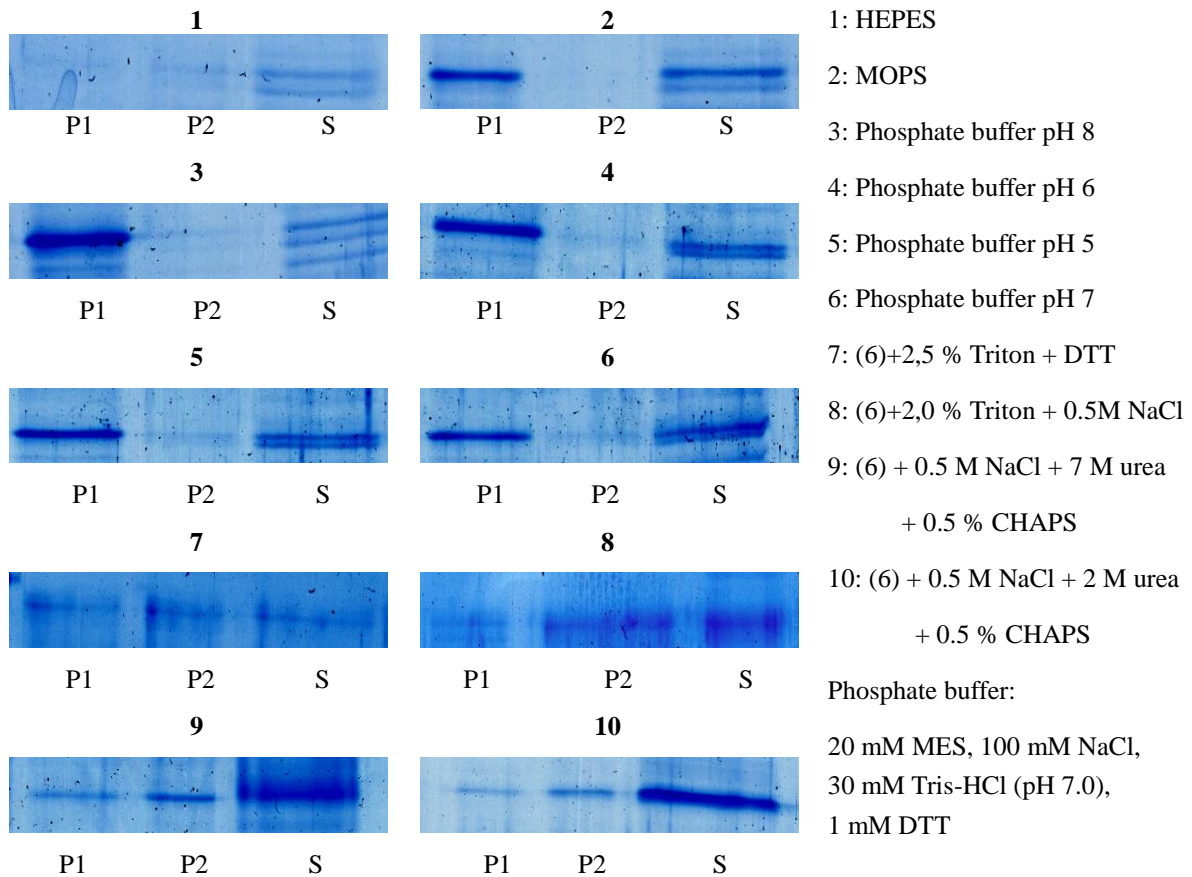


Figure 65: Protein-aggregation assay for At5g39570.1. P1: First pellet fraction after low speed centrifugation (10,000 g); P2: Second pellet fraction after high speed centrifugation (20,000 g). S: Supernatant. For more information about the phosphate buffer see section 2.16.2.

3.9 Interaction of PLD α 1 with At5g39570.1

Indirect interactions of PLD α 1 *via* the signaling molecule phosphatidic acid have been widely researched (Hou *et al.*, 2015), but also direct interactions of phospholipases have been described in plants and animals (Jang *et al.*, 2012). The interacting partners comprise a wide range of target molecules, such as kinases, structural proteins, transporters, proteases, lipases, transcription factors or phospholipids (Hou *et al.*, 2015, Jang *et al.*, 2012).

The downstream regulation of At5g39570.1 by PLD α 1, *in silico* data and co-expression patterns of both proteins suggest an involvement in the same signal-transduction pathway and might indicate a direct or indirect interplay of both proteins.

3.9.1 Direct interaction of PLD α 1 and At5g39570.1

Previous results indicate that At5g39570.1 is regulated by PLD α 1 and acts downstream of this phospholipase. As shown previously, At5g39570.1 does not affect expression of PLD α 1 (**Figure 45**). Thus, a direct interaction of both proteins seems unlikely, but cannot be excluded. Ni-NTA affinity chromatography was used to confirm previous assumptions. In accordance to the affinity chromatography assay (section **2.11**), protein extracts from *Arabidopsis* leaves were incubated with recombinant At5g39570.1 and applied to Ni-NTA columns. After several mild washing steps, a putative binding of PLD α 1 to At5g39570.1 was checked by PLD α 1-specific antibodies (**Figure 66**). The anti-PLD α 1 antibody only detected the protein in the control plant material, but not in the eluted fractions. In accordance to these findings, a co-immunoprecipitation assay could not identify the PLD α 1 protein in the eluted protein fractions (data not shown).

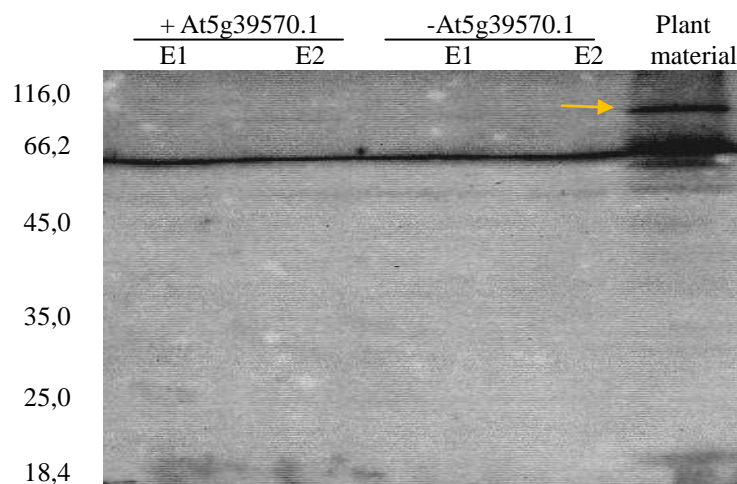


Figure 66: Test of direct interaction between PLD α 1 and At5g39570.1. Immunodetection of PLD α 1 in eluted samples from Ni-NTA affinity chromatography of total proteins from leaf extracts with (+At5g39570.1) and without (-At5g39570.1) bait protein. Orange arrow: PLD α 1.

3.9.2 Indirect interaction of PLD α 1 and At5g39570.1

PLD α 1 is the main enzyme for the production of the signaling molecule phosphatidic acid. PA is known to be involved in multiple cellular pathways, affecting crucial biological processes in plants, such as root hair growth, stomata closure and adaptation to environmental stress (Hou *et al.*, 2015). In the past years a number of PA-binding proteins have been identified, but a genuine binding domain for PA has not been detected and might not exist. Thus, it is difficult to identify further PA-binding targets in order to understand the regulatory PLD-network and the plants adaptation to environmental stresses. Recently, a workflow to identify

novel PA-target proteins has been suggested (Hou *et al.*, 2015). Generally, proteins of interest are tested to bind to a wide spectrum of lipids in protein-lipid-overlay assays. This *in vitro* technique is also used to test whether a protein can bind to a specific lipid (e.g. PA) (Deak *et al.*, 1999). However, the protein-lipid-overlay assay neglects the cellular state of lipids that in cells occur in form of liposomes. The liposome-binding assay (Zhang *et al.*, 2004) considers the intracellular environment and therefore is used to confirm previous findings. To analyze time-dependent binding events of proteins and liposomes, the liposome-turbidity assay is used (Roston *et al.*, 2011).

3.9.2.1 Protein-lipid interactions on nitrocellulose membranes

The exclusion of a direct interaction between PLD α 1 and At5g39570.1 suggests an indirect interaction of both proteins *via* PA. The protein-lipid-overlay assay is the quickest method to check binding of a target protein to a range of different lipids (Deak *et al.*, 1999).

In this work, binding of At5g39570.1 to monogalactosyldiacylglyceride (MGDG), digalactosyldiacylglyceride (DGDG), phosphatidylglycerin (PG), phosphatidylethanolamin (PE), cardiolipin (CL), phosphatidylcholine (PC), phosphatidic acid (PA), diacylglycerol 16:0 (DAG16) and diacylglycerol 18:3 (DAG18) was tested. The lipid-protein interaction was visualized using antibodies directed against the His-tag of target proteins. A His-tagged protein (NusA, *E. coli*) was used as a negative control. A strong signal for the full-size-At5g39570.1 protein binding to phosphatidic acid has been detected (**Figure 67**). While the N-terminal fragment of At5g39570.1 (**Supplementary figure 2**) displays slightly decreased signal strength for PA binding, the C-terminal fragment (**Supplementary figure 2**) reveals a very weak affinity to PA. The His-tagged Nus-protein shows a very faint signal. An additional assay with the At5g39570.1-specific antibody was carried out to identify lipid binding of the full-size protein and the N-terminal fragment of At5g39570.1 (**Figure 68**). These results support the previous findings of PA binding to the full-size protein and a reduced affinity of PA to the N-terminal protein fragment. The antibody was raised against the N-terminal part of At5g39570.1 and thus cannot identify the C-terminal protein part.

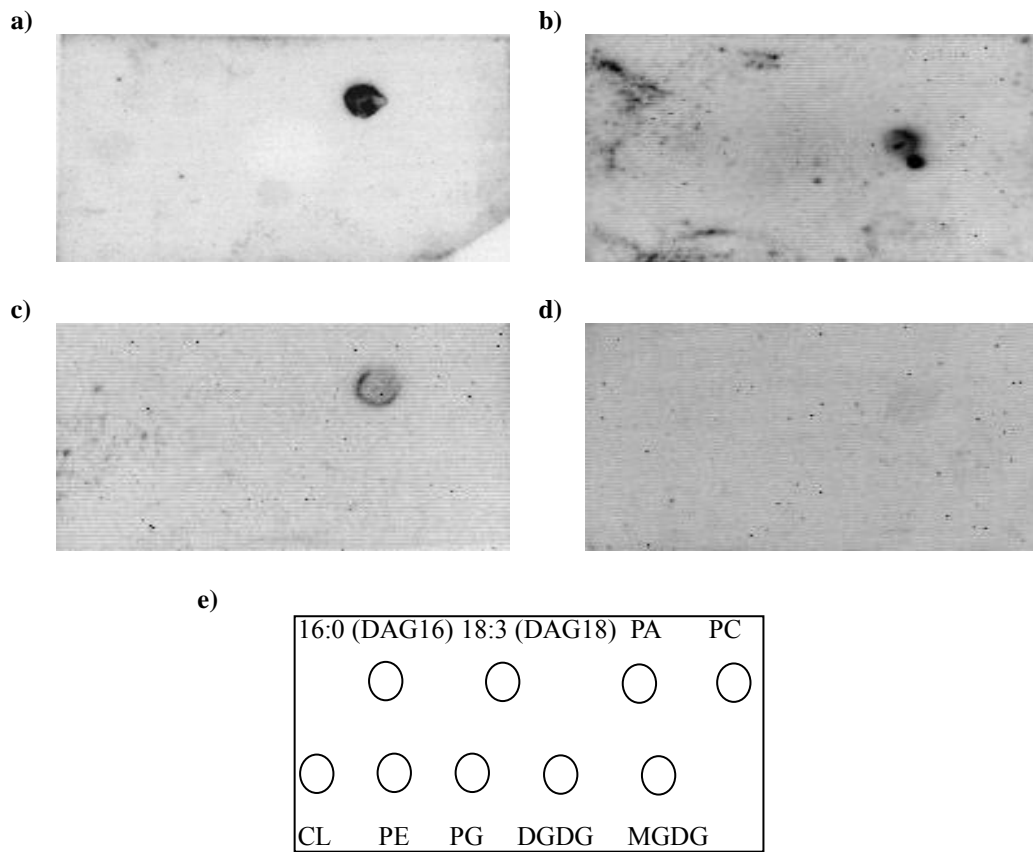


Figure 67: Detection of At5g39570.1 protein fragments in protein-lipid-overlay assays.

The anti-His antibody was used and blots were detected for 10 min. a) Full-size At5g39570.1 b) N-terminal fragment of At5g39570.1 c) C-terminal fragment of At5g39570.1. Here only PA and PC were applied on the membrane. d) Nus-protein with His-tag e) Loading scheme of lipids used for all proteins except the C-terminal fragment.

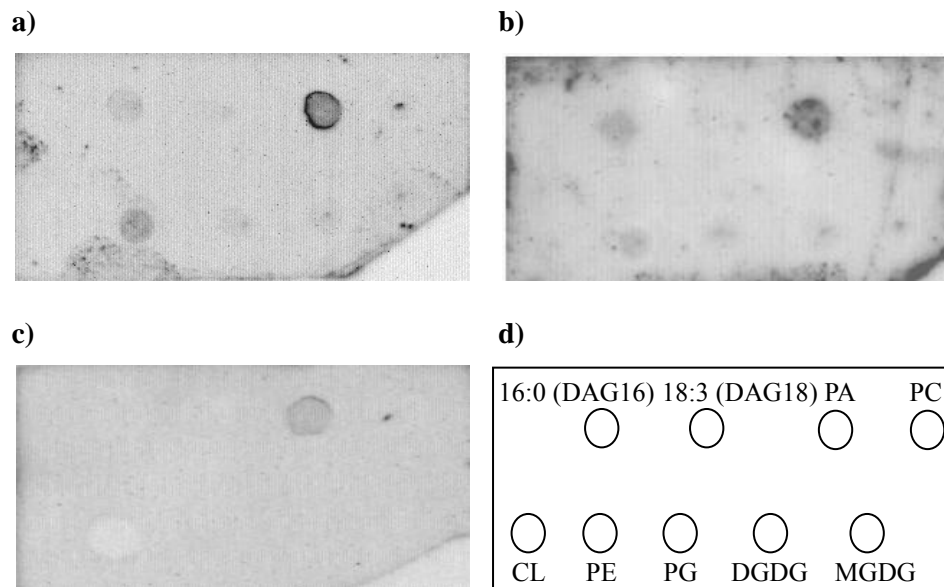


Figure 68: Detection of At5g39570.1 protein fragments in protein-lipid-overlay assays.

The anti-At5g39570.1 antibody (a & b) and the anti-His antibody (c) were used and blots were detected for 10 min. a) Full-size At5g39570.1 b) N-terminal fragment of At5g39570.1 c) Nus-protein with His-tag e) Loading scheme of lipids used for all proteins.

3.9.2.2 Liposome-binding assay

In contrast to protein-lipid-overlay assays, liposome-binding assays take the cellular state of lipids as liposomes into account and thus reflect a more natural environment of lipids. Lipid binding depends on a variety of factors, such as protein conformation and pH of the environment (Ruano *et al.*, 1998). To determine the best *in vitro* conditions for PA binding, a pre-experiment was carried out using different pH-values (**Figure 69**). Liposome-binding assays were conducted as described in section 2.16.2. While unbound proteins are detected in the supernatant, the liposome-bound protein complexes were retained in the pellet fractions.

Incubation of At5g39570.1 with phosphatidylcholine retains proteins in the unbound supernatant fractions, whereas PA-bound proteins can be detected in the pellet fraction at pH 7. Deviant pH-values towards the acidic, respectively basic site indicate a decrease of PA binding. Liposome-binding buffer (pH 7) displayed best binding affinities and was chosen for all following experiments.

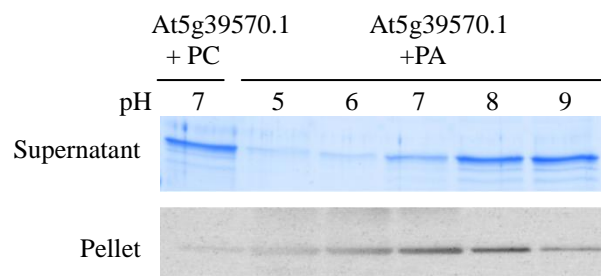


Figure 69: Pre-experiment to determine optimal pH-conditions for liposome-binding assays. Binding of At5g39570.1 to PA was tested for pH 5-9. Control binding of At5g39570.1 to PC was tested at pH 7.

To confirm previously observed binding of PA to At5g39570.1 and the N-terminal region of At5g39570.1, respectively, additional PA-binding assays were carried out (**Figure 70**).

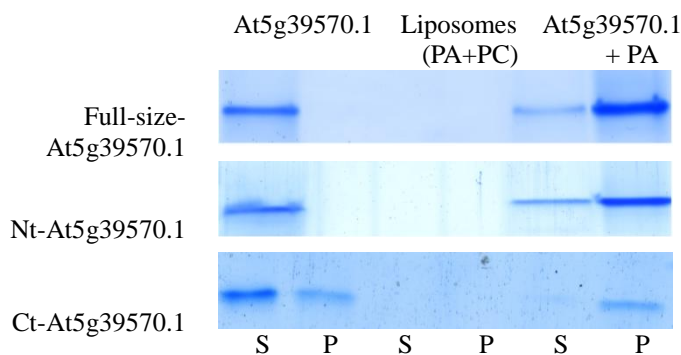


Figure 70: Liposome-binding assay with At5g39570.1. Binding of PA to At5g39570.1 and Nt-At5g39570.1 was tested. Pure protein and pure liposomes were used as binding controls. S: Supernatant, P: Pellet.

The purified recombinant protein samples were dissolved and retained in the supernatant, indicating that the proteins were dissolved. Liposomes cannot be detected by Coomassie stain and were applied as a negative control. Strong binding of PA to the full-size protein and decreased binding to the N-terminal fragment were observed. Only faint binding was seen for the C-terminal protein. In addition, the C-terminal protein showed a weak signal in the pellet fraction, indicating insufficient solubilization of this protein fraction. Complete solubilization of the C-terminal protein was not possible.

3.9.2.3 Liposome-turbidity assay

The liposome-turbidity assay enables the investigation of lipid-binding affinities to proteins in real time. Increasing absorbance at 350 nm indicates protein-liposome cross-linking events. The altered absorbance is a result of fusion or aggregation of proteins and lipids. Previous results indicated PA-specific binding affinity for the full-size At5g39570.1 protein, its N- and C-terminal protein fragment. In a pre-experiment unilamellar liposomes of PA and PC were generated and incubated with At5g39570.1 (**Figure 71**). Before At5g39570.1 was added to the liposome solution, the OD₃₅₀ was reset. Subsequently the protein was added, mixed and the change in absorbance was monitored for 8 minutes at OD₃₅₀. While At5g39570.1 showed weak affinity towards PC liposomes, incubation with 75 % PC/ 25 % PA drastically increased the absorbance. This indicates a stronger affinity of At5g39570.1 towards PA. Both graphs reveal high values for the time point “0”, the first reading point after the addition of the protein. This indicates rapid interaction (or bonding) of proteins and liposomes. In contrast, no increase in absorbance was observed after the first 5 minutes. Therefore all following experiments were monitored for 5 minutes.

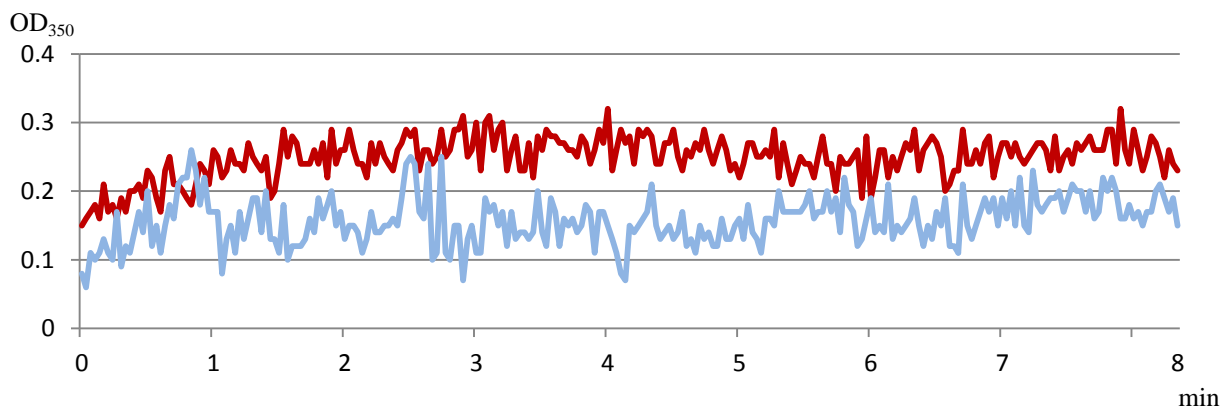


Figure 71: Liposome turbidity assay for At5g39570.1 with PA and PC. At the time point “0” At5g39570.1 was added to the solution. Red line: (75 % PC/ 25 % PA), Blue line: 100 % PC. Binding of PA and PC to At5g39570.1 was monitored in a spectrophotometer at OD₃₅₀ for 8 minutes.

In further experiments the 75 % PC/ 25 % PA mixture was used to investigate time-dependent binding effects in At5g39570.1 and the protein fragments. The His-tagged Nus protein from *E. coli* was used as a negative control. Full-size protein and N-terminal fragment of At5g39570.1 showed a similar time-dependent increase in PA-affinity, while the negative control displayed no binding events (**Figure 72**).

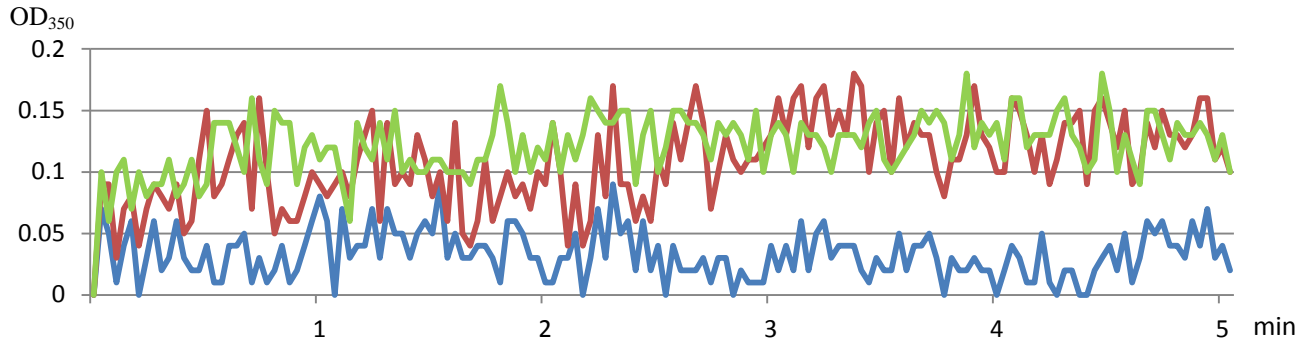


Figure 72: Liposome turbidity assay of At5g39570.1 and Nt-At5g39570.1 with 75 % PC/ 25 % PA. At the time point “0” the protein of interest was added to the solution. Red line: At5g39570.1 full-size, Green line: Nt-At5g39570.1, Blue line: Nus protein. Binding of PA is monitored in a spectrophotometer at OD₃₅₀ for 5 minutes.

Surprisingly, the C-terminal fragment of At5g39570.1 displayed a more prominent OD₃₅₀ shift when incubated with PA for 5 minutes (**Figure 73**). Incubation with 100 % PC could not trigger a similar binding event.

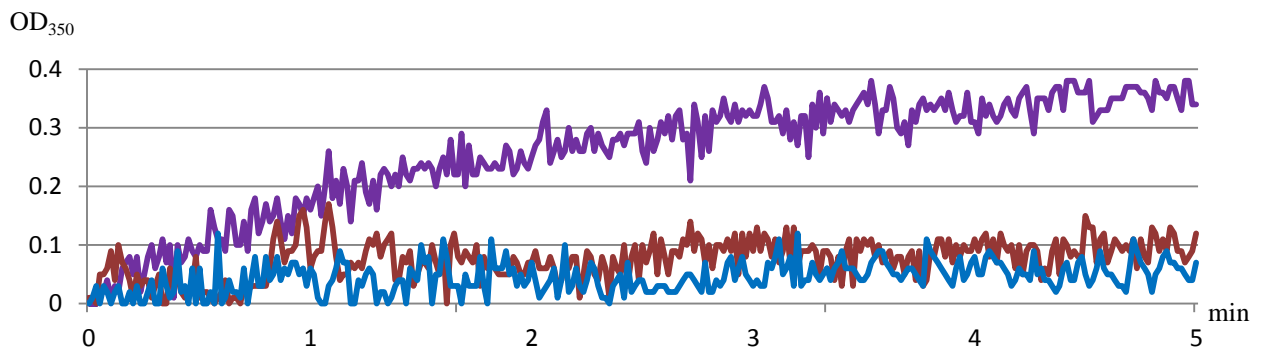


Figure 73: Liposome turbidity assay of Ct-At5g39570.1. At the time point “0” the protein of interest was added to the solution. Purple line: Ct-At5g39570.1 with 75 % PA/ 25 % PC, Red line: Ct-At5g39570.1 with 100 % PC, Blue line: Nus protein with 75 % PA/ 25 % PC. Binding of lipids is monitored in a spectrophotometer at OD₃₅₀ for 5 minutes.

3.10 Identification of proteins under the control of phospholipase D

The first hint of the control of At5g39570.1 expression levels by PLD α 1 was gained by the comparison of total proteins from wild-type and a *plda1* knock-out mutant on two dimensional gels by Shen (2008). The missing protein spot in the mutant proteome was later identified as At5g39570.1 (Kuhn, 2010). To check for further proteins that might be regulated by isoforms of the phospholipase D family, a comparative study of phospholipase D knock-out mutants (*plda1*, *plda3* and *plde*) with the wild type was conducted. Total proteins and phospho-enriched proteins of the selected mutants and the wild type were extracted and isolated as described in section 2.9. Two-dimensional gel analysis was performed to identify putative changes within the proteome of the mutants. The comparison of the proteomes of total proteins did not reveal prominent changes that could certainly be assigned to the knock-out of one of the PLD isoforms (**Figure 74**). Comparative analysis of phospho-enriched proteins confirmed earlier findings of the diminished abundance of At5g39570.1 in the *plda1* knock-out mutant, while the phosphorylated protein was detected in other knock-out mutants (**Figure 75**). The difficulty of equal loading in two dimensional gels limits quantitative analysis of At5g39570.1. No prominent, additional changes in the proteome of *plda3* or *plde* knock-out mutants were detected.

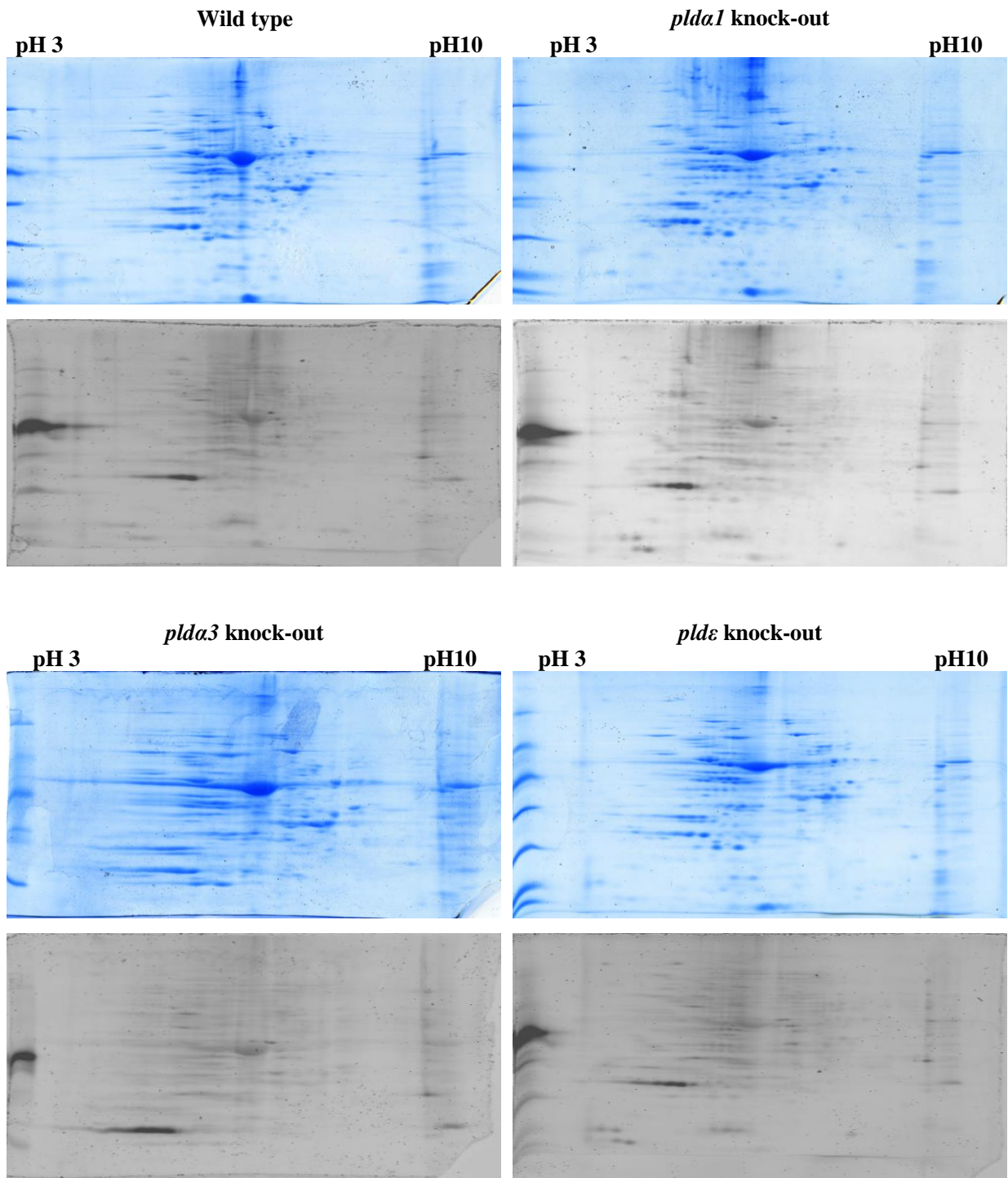


Figure 74: Two dimensional analysis of total protein extracts from *A. thaliana*. Total proteomes of wild type and *pld* mutants are stained by Coomassie and phospho-stain.

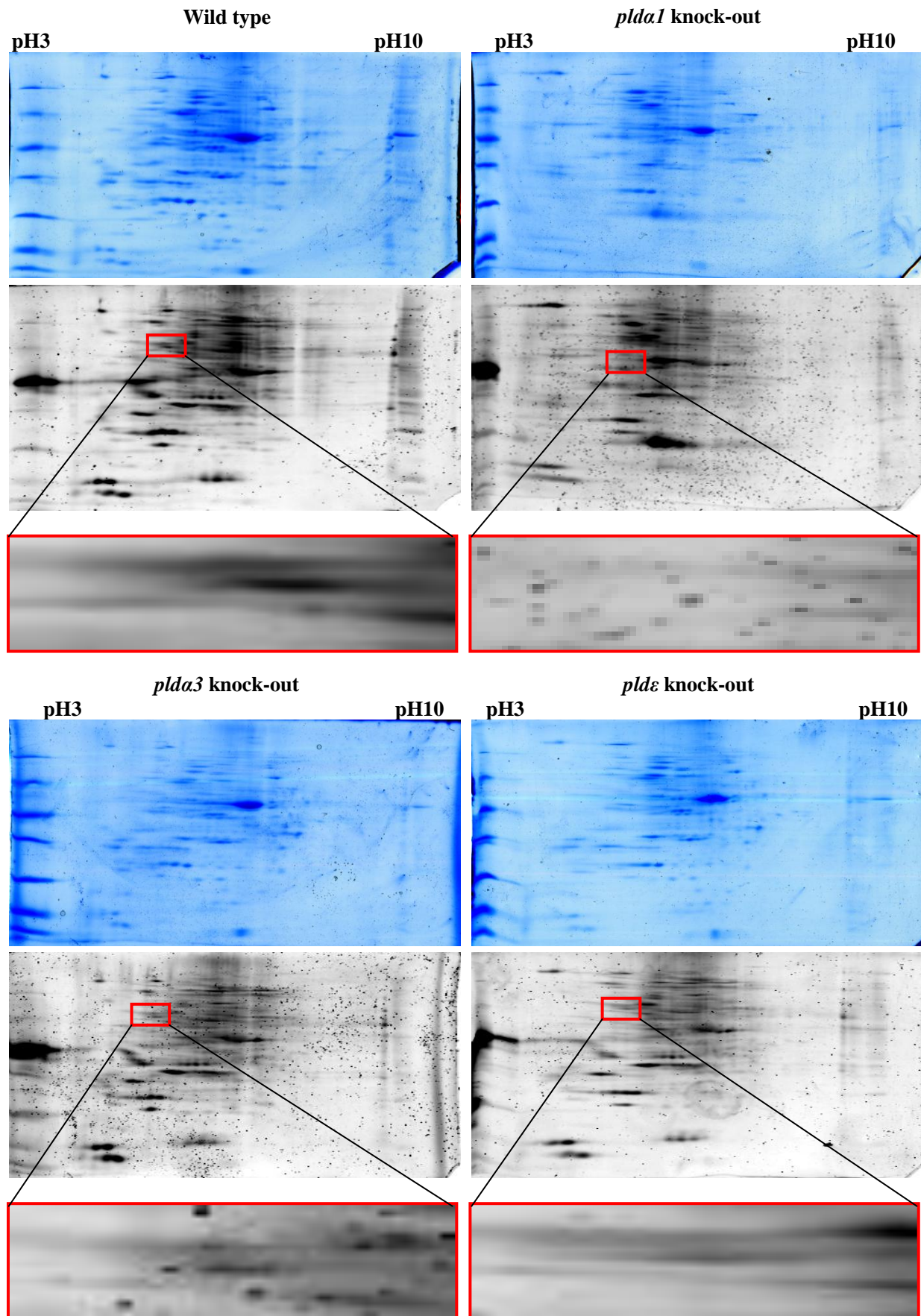


Figure 75: Two dimensional analysis of phospho-enriched protein extracts from *A. thaliana*. Phosphoproteoms of wild type and *pld* mutants are stained by Coomassie and phospho-stain. Red Box: Magnification of At5g39570.1 protein spot on the gel.

3.11 Over-expression of At5g39570.1

Neither the knock-out mutant *At5g39570.1*, nor the *At5g39570.1* knock-out/*At3g29075* knock-down double mutant displayed a prominent phenotype under standard conditions (**Figure 37**). The over-expression of a gene in *A. thaliana* can lead to severe defects in growth and development of plants. Thus, it can help to unravel the function of a gene or protein. Over-expression lines of *pld* mutants have been analyzed previously and revealed the involvement of specific PLD isoforms in distinct physiological responses (Li *et al.*, 2009).

In a first step a cDNA from *A. thaliana* was used as a template for mutagenesis PCRs, generating a full-size fragment of *At5g39570.1* with the primers At5g-Y2H-rev and At5g-Y2H-fwd. 1 μ l of the PCR product (1157 bp) was sub-cloned into the pJET vector as a backup. The remaining fragment was digested with *NcoI* and *BamHI* and cloned downstream of the 35S-promoter of PGJ280 (**Figure 76**). The construct was digested by *HindIII* and the fragment (2289 bp), containing 35S-promoter and full-size *At5g39570.1* was cloned into the binary expression vector pBIN19 (**Figure 76**).

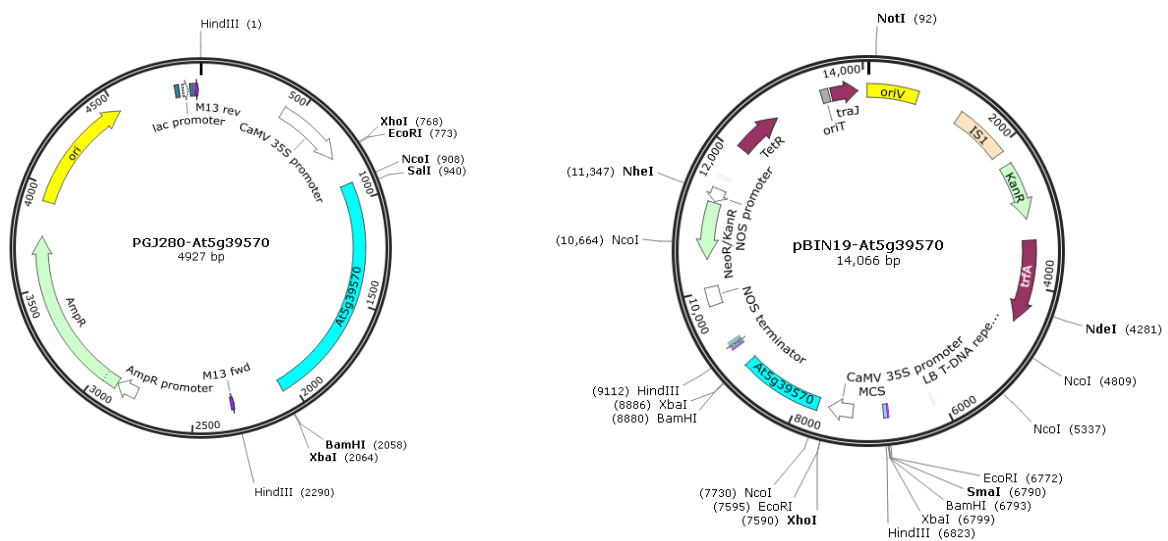


Figure 76: Constructs for the generation of the *At5g39570.1* over-expressing line.

The final construct was checked by DNA sequencing and transformed into *Agrobacterium tumefaciens*. Subsequently, *A. thaliana* wild-type and mutant plants were transformed by floral dip. Positive plants were selected on MS^{Kan}-media and recovered on soil. So far only one transformed Arabidopsis plant was obtained that did not show any phenotypic alterations compared to the wild type upon standard conditions. *Agrobacterium*-dependent transformation was repeated recently and seedlings are being selected on MS^{Kan}-media to

date. Positive plants (F1 and F2 generations) will be phenotypically monitored in the next months. Stress treatments and RNA-Seq of confirmed over-expressing lines will be conducted and compared to the wild type.

3.12 Localization of At5g39570.1

Not only the abundance of a protein, but also its inter- and intracellular distribution is of major importance for the characterization of a protein. The intracellular localization can point to potential interacting partners and indicate the function of a protein of interest.

3.12.1 Intercellular localization of At5g39570.1

Tissue-specific expression pattern of At5g39570.1 (**Figure 44**) have shown an uneven expression of the protein in dependence of its plant tissue. Previous β -glucuronidase-promoter studies supported these findings and identified increased expression of *At5g39570.1* in trichome-neighboring socket cells (Jandl, 2012).

3.12.2 Intracellular localization of At5g39570.1

Most plant proteins are encoded in the nuclear genome and synthesized in the cytosol before they are translocated with the help of their signal sequences to reach their final destination (Blobel & Dobberstein, 1975). In order to fulfill their function, proteins must be localized at their appropriate subcellular compartment. The intracellular localization of a protein can therefore help to understand the proteins function within the cell. The development of powerful bioinformatic tools enabled the fast and accurate identification of protein localizations. For instance, the Cell eFP (section **2.1.3**) browser exploits a subset of twelve independent algorithms to predict the subcellular localization of a protein and suggests a wide intracellular distribution of At5g39570.1, ranging from the cytosol to chloroplasts (**Supplementary figure 6**). Nevertheless, experimental evidence is indispensable for the detection of the genuine subcellular localization.

3.12.2.1 Transient transformation of *At5g39570.1* into *A. thaliana*

In a previous Diploma thesis (Jandl, 2012) a fusion construct expressing *At5g39570.1*-GFP was generated to investigate its intracellular localization. Unfortunately, no clear pictures have

been taken for the explicit identification of the intracellular localization of At5g39570.1, but the data suggested a cytosolic expression of the protein. To confirm these findings the construct PGJ280-*At5g39570.1* was used in a repetitive transient transformation assay by particle gun bombardment (see section 2.17.1) in co-operation with Selva Sukumaran.

The expression of PGJ280-*At5g39570.1* resulted in similar patterns like the free GFP that is localized in cytoplasm and nucleus of plant cells (Tsien, 1998) In accordance to bioinformatic predictions, a wide subcellular distribution with accumulation of At5g39570.1 in the cytosol and nucleus was observed (**Figure 77**).

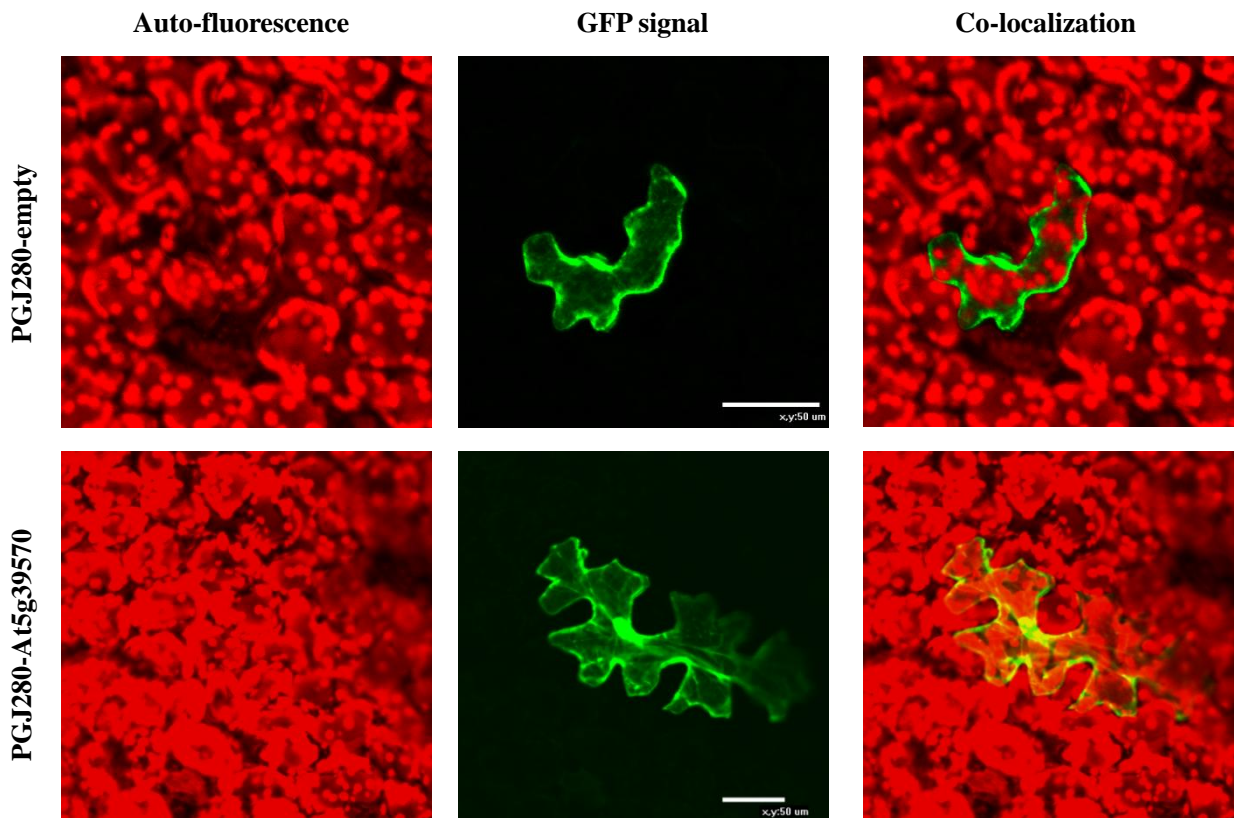


Figure 77: Microscopic analysis of the intracellular localization of At5g39570.1 after particle bombardment. Top panels display the localization of free GFP from the empty vector PGJ280. The panels at the bottom show the localization of At5g39570.1. The white bar represents 50 μm .

3.12.2.2 Generation of a stable-transformed *At5g39570.1*-GFP line

The stable expression of a fluorescent protein enables the identification of its subcellular localization in a variety of different cell types and environmental conditions. Recently a PA-binding protein has been identified that was shown to translocate upon salt-stress conditions (Julkowska *et al.*, 2015). PA-induced translocation of At5g39570.1 might provide insights in the proteins function.

Results

The previously generated construct PGJ280-*At5g39570*-full-GFP (Jandl, 2012) was digested by *HINDIII* (2880 bp) and cloned into the binary expression vector pBIN19 (**Figure 78**). The construct was transformed in electro-competent *E. coli* cells and verified by DNA sequencing. The construct was transformed in *Agrobacterium tumefaciens* and subsequently used for floral dip transformation of *A. thaliana* wild-type plants. Successfully transformed seedlings were selected on MS media supplemented with kanamycin (**Figure 78**) and verified by colony PCR with Ct-*At5g-fwd* and *HindIII*-rev (1331 bp).

Unfortunately no GFP-signal has been observed in the stable-transformed lines. Analysis of the previously generated fusion construct (Jandl, 2012) revealed that the translational enhancer was removed by the digestion of the plasmid with *NcoI* and *XhoI*. While the transient transformed leaves still contain a few transformed cells, there was no evidence for successful stable transformation of *At5g39570.1*. Therefore no further experiments to identify a putative translocation of *At5g39570.1* under stress conditions were carried out.

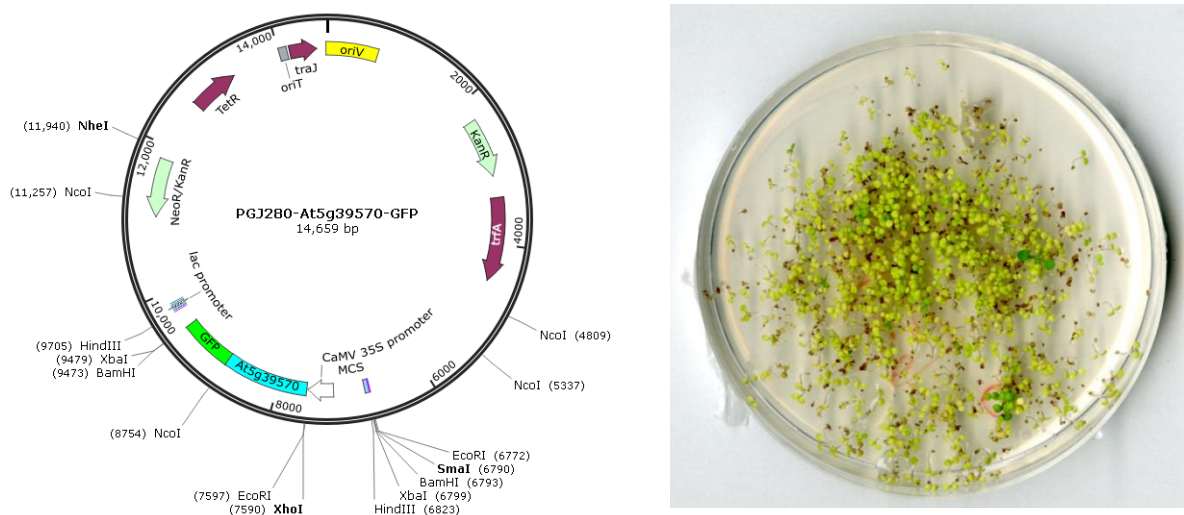


Figure 78: Construct of *At5g39570*-GFP and selection of transformed plants.

4. Discussion

The aim of this work was to contribute to the understanding of the complex network of phospholipases and their signaling pathways in response to abiotic stress by characterizing At5g39570.1, a downstream target of phospholipase D α 1. The data show that the expression of At5g39570.1 depends on PLD α 1 and links its expression to water-limiting conditions. The deduced At5g39570.1 protein has a very unusual amino acid composition. Structure predictions suggest that the At5g39570.1 protein belongs to the intrinsically disordered protein family. Further results suggest a regulation of At5g39570.1 by phosphatidic acid, the breakdown product of the PLD-pathway. Protein interaction studies indicate a possible involvement of At5g39570.1 in RNA-editing processes.

4.1 Gene analysis of *At5g39570.1*

The gene *At5g39570.1* is located on chromosome five in *A. thaliana* and describes a gene model of two exons that comprise a region of 1559 bp (**Figure 7**). The TAIR database lists the gene model *At3g29075* as the best *A. thaliana* protein match for *At5g39570.1*.

4.1.1 Promoter region

Baerenfaller *et al.* (2008) identified a second open reading frame down-stream of *At5g39570.1* that putatively encodes the protein At5g39570.2 (**Supplementary figure 2**). The presence of a ribosome-binding site for the translational initiation of *At5g39570.1* (but not for *At5g39570.2*) (Ufer, 2011) and the presence of a putative TATA-box 25 bp upstream of the transcribed region, suggest that At5g39570.1 is the correct expressed protein. This is supported by the fact that the protein product of this open reading frame has been found previously (Ufer, 2011). Leaky scanning of the mRNA by the 40S ribosomal subunit can lead to initiation of translation downstream of the start codons (Andrews & Rothnagel, 2014). However, no evidence on protein level exists for At5g39570.2, making a translation of this putative reading frame unlikely. The identification of a number of putative cis-regulatory elements involved in heat and drought responses in the promoter region of *At5g39570.1* (**Figure 20**) suggests a highly regulated gene expression that is dependent on various abiotic signals.

4.1.2 Protein coding sequence of At5g39570.1

At5g39570.1 exhibits interesting features in its coding sequence, such as the occurrence of short (19-48 bp), highly conserved nucleotide stretches in its 3'-end (**Figure 21**) that can be found in a variety of RNA-associated genes (**Supplementary tables 4 & 5**). The highly conserved sequences of these small nucleotide stretches within the plant and animal kingdom point to an ancient role of these RNA segments. For a long time, a central hypothesis in molecular biology was that every RNA sequence is the exact copy of its coding DNA and is translated into its associated protein. However, the discovery of numerous RNA species, such as small nuclear RNAs (Thore *et al.*, 2003), micro RNAs (Lin *et al.*, 2006) and small interfering RNAs (Ahmad & Henikoff, 2002) challenged this view. In fact, the importance of small RNAs is just beginning to be unraveled. In the past decades, novel forms of non-functional RNA subclasses have been identified, including the CRISPR RNA in Bacteria and Archaea (Barrangou *et al.*, 2007) and small nucleolar RNAs in Eukaryotes (He *et al.*, 2014). The latter ones comprise a class of small RNA molecules that are encoded in introns of proteins, intergenic regions and open reading frames of protein coding genes. They are involved in chemical modifications of other RNAs that result in altered RNA folding and interaction with ribosomes (Bachellerie *et al.*, 2002). For specific binding, snoRNAs exhibit a stretch of ~20 nucleotides that are complementary to the sequence of the target RNA. The 19-nt long conserved RNA fragment 1 in *At5g39570.1* (**Figure 21**) shares 100 % sequence identity with the minus strand of different, putative target genes in *Arabidopsis* (**Supplementary table 9**), which points to a putative antisense function. These highly conserved RNA-stretches match the minus strand of several members of the phospholipase C family as well as various pentatricopeptide repeat proteins (PPR proteins) that are involved in RNA editing. However, snoRNPs require additional conserved sets of small RNA recognition sites “C/D-box” elements that enclose the antisense element and guide post-transcriptional modifications (Bachellerie *et al.*, 2002). Although a subset of putative C-/D-box elements can be identified in the cDNA of *At5g39570.1* (**Supplementary figure 7**), their position does not comply with the requirements (antisense RNA must be located precisely five nucleotides upstream of the D-box) to guide putative antisense elements (Bachellerie *et al.*, 2002). Therefore it is unlikely that these RNA stretches function as snoRNP recognition sites, but they might be molecular fossils or relics from last universal ancestors and as such play a role in the regulation of protein-biogenesis pathways (Jeffares *et al.*, 1998).

4.2 Protein analysis of At5g39570.1 and At3g29075

Characterization and analysis of At5g39570.1 and At3g29075 have shown a separation of both proteins into N- and C-terminal regions. In this work, the N- and C-terminal protein fragments of both proteins were thoroughly analyzed and revealed crucial differences in their amino acid composition (**Supplementary figure 1**), protein structure (section **3.1.3**) and conservation rate (section **3.1.2**).

4.2.1 The protein At5g39570.1 is divided into two major regions

The N-terminal half of At5g39570.1 is dominated by glycine, while the C-terminal region is unusual rich in charged amino acids, such as glutamic acid or arginine. Despite the two-fold higher content of basic amino acids in the C-terminal region, the N-terminal protein half of At5g39570.1 has a higher overall hydrophobicity (**Figure 17**). The occurrence of ten glutamic acid and aspartic acid-rich tandem repeats in the C-terminal half of At5g39570.1 (**Figure 18**) provides a strong acidic character to this protein region. The repetitive stretches of up to 20 amino acids are almost exclusively present in the C-terminal part of At5g39570.1 and cannot be found in other proteins from plants or animals by pblast. A recent study hypothesized that such a repeat perfection points to recent evolutionary events rather than to functional importance of the repetitive residues (Jorda *et al.*, 2010). However, it cannot be excluded that the repeats provide important information with regards to structural features and thereby indirectly influence the function of At5g39570.1. Besides these differences in their primary structure, both protein regions differ strongly in their secondary structure: While α -helical structures are predicted in the N-terminal protein region of At5g39570.1, the C-terminal end of the protein is highly disordered (**Figure 19**). A separation of both regions can also be observed in regards to protein conservation. The full-size protein carries a total of 24 variable amino acids (**Figure 13**) within the Arabidopsis ecotypes. A look at the separate protein regions revealed that the C-terminal end contains $\frac{2}{3}$ of all variable amino acids, whereas the N-terminal end is more conserved. Multiple sequence alignments of putative At5g39570.1 orthologs detected conserved AA only in the N-terminal protein region (supplementary data files). This observation is supported by pblast results for At5g39570.1 that identified all putative orthologs and homologs with maximum sequence identities within the N-terminal region.

At3g29075, the only putative homolog of At5g39570.1, shares high sequence identities in the N-terminal part, but lacks any consensus sequence with the C-terminal region (**Figure 12**).

The last 30 C-terminal amino acids of both proteins are more similar. This led to the hypothesis that their intermediate C-terminal protein part of At5g39570.1 (AA₂₀₀-AA₃₅₀) might be more recently evolved and inserted into a conserved ancient sequence. This C-terminal protein region seems unique and cannot be found in any other Arabidopsis proteins or even in other species. A closer look at the putative homolog At3g29075 supports the hypothesis of a novel structure: The C-terminal half of At3g29075 contains 45 variable sites within the Arabidopsis ecotypes (31.2 % of the C-terminal part) rendering this protein fragment susceptible for mutations. Another hint pointing to a novel evolutionary origin of the C-terminal part in both proteins is provided by their similar and specific primary structures (**Figure 11**).

The wide occurrence of putative orthologous proteins of At5g39570.1 in Brassicaceae, Fabaceae and even in the far distant Lycophytes emphasizes the importance of this protein within the plant family. Although very low sequence identities (e-value $<10^{-5}$) have also been detected in Cyanobacteria, Cnidaria and even in Mammals, the protein At5g39570.1 seems to be exclusively present in plant species. Orthologs of At5g39570.1 have been experimentally identified in different Brassicaceae, but also in a variety of crop plants such as *Solanum lycopersicum* (Silva *et al.*, 2012), Cucumber (Li *et al.*, 2013), *Glycine max* (Lee, 2013) and *Theobroma cacao* (Niemenak *et al.*, 2015). This might enable research in crop plants since the protein expression of At5g39570.1 positively correlates with high crop yield in *Clementine mandarine* plants (Muñoz-Fambuena *et al.*, 2013).

4.2.2 The lysine-rich protein At3g29075

The putative homologous protein At3g29075 shares high sequence similarities with At5g39570.1, especially in its N-terminal half. It displays similar protein features, like tandem repeats (**Figure 18**), an acidic pI (**section 3.1.1**) and an unusual amino acid composition (**Figure 16**).

At3g29075 contains unusual high contents of charged amino acids (e.g. aspartic acid; 19.3 % lysine 21.1 %). Lysine is one of the essential amino acids that cannot be synthesized in animals and hence must be ingested in the form of lysine-containing proteins from plants or animals. The expert committee of the world health organization recently recommended a daily uptake of up to 30 mg lysine per kilogram of body weight for humans (Joint, 2007). While these requirements are easily met by most adults that consume common food proteins with sufficient lysine concentrations, infants are more susceptible to lysine-deficiency when fed a

diet of proprietary formula (Young & Pellett, 1994). As lysine is much lower concentrated in most plant-food proteins than in animals and represents the limiting amino acid in most cereal grains and rice (Young & Pellett, 1994), it is likely people with insufficient or unbalanced diets and some vegans who do not have additional lysine sources like pulses, have the need for additional lysine up-take. Deficiency of lysine has also been reported for professional athletes (Young & Pellett, 1994).

The majority of industrial produced lysine is used for animal feeding to supplement the low lysine concentration in cereals (Izumi *et al.*, 1978). In this context, research on a number of lysine proteins was conducted and recombinant high lysine-rich proteins were produced in cereals to artificially increase the lysine content (Hejgaard & Boisen, 1980, Jia *et al.*, 2013). Recombinant high lysine-rich proteins contained up to 17 % lysine in stable-transformed barley (Hejgaard & Boisen, 1980). In contrast, the native At3g29075 protein from *A. thaliana* obtains 20 % lysine. This very high amount of the essential amino acid lysine makes At3g29075 an interesting object of further research and is now in the center of interest of a beginning PhD work by Abdelaziz Nasr (2015) in our lab.

4.2.3 Comparison of At5g39570.1 and At3g29075

At3g29075 is the best pblast match for At5g39570.1. The high sequence similarity in their N-terminal ends points to a homology of both proteins. **Figure 79** displays a similar organization of *At5g39570.1* and *At3g29075*.

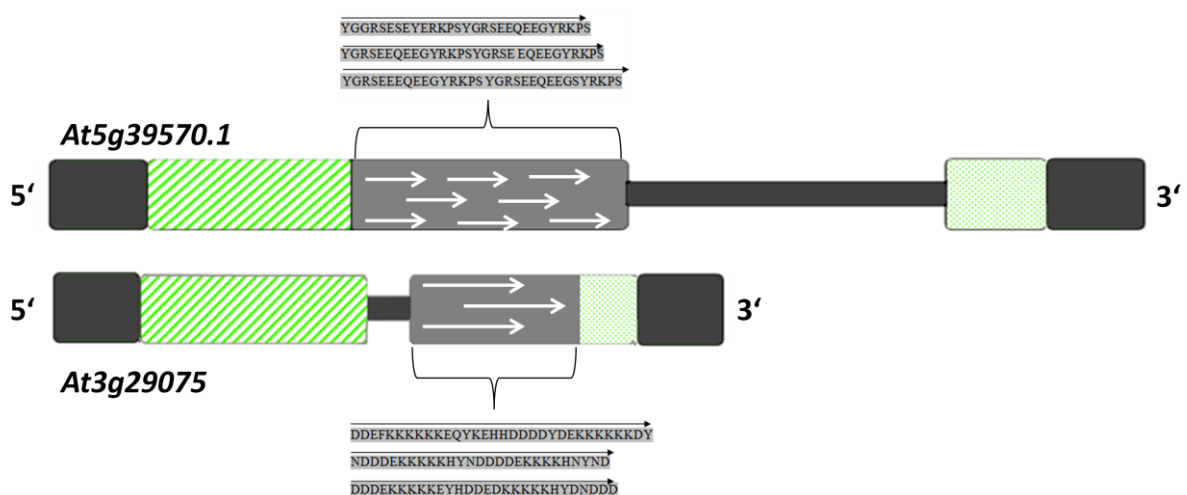


Figure 79: Comparison of *At5g39570.1* and *At3g29075*. The model only sketches the sizes of both genes for a better comparison. *At5g39570.1* encodes for a protein of 381 AA, while *At3g29075* encodes a protein of 294 AA. The intron region is longer in *At5g39570.1*. Both genes share high sequence similarities in the first 500 nucleotides (hatched area in green). The 3' end of both genes codes for unique tandem repeat structures that are rich in charged amino acids (grey area with white arrows). The last 60 nucleotides share some sequence similarity (checked area in green-white).

The N-terminal regions of At5g39570.1 and At3g29075 are more conserved (**Figure 12**, **Figure 13** & **Figure 14**) and therefore suggested to be responsible for the proteins function. The C-terminal protein regions in both proteins are variable and share nearly no sequence similarities. Analog protein sequences cannot be found in other plants by protein blast analysis. However, the C-terminal protein regions of At5g39570.1 and At3g29075 exhibit similar structural features, such as tandem repeats with unusual amino acid compositions (**Figure 18** & **Supplementary figure 1**). Similar protein structures were hypothesized to represent recent evolutionary events rather than functional importance (Jorda *et al.*, 2010). Gene duplications arise from unequal crossing-over events that possibly result in the formation of repetitive genetic elements (Zhang, 2003). High sequence similarities of genes that are located on separate chromosomes (e.g. At5g39570.1 and At3g29075) promote gene duplication processes at duplication breakpoints in plants (Zhang, 2003) and may therefore explain the origin of the unique tandem repeats in both proteins. However, the repetitive structures may provide novel functions to the proteins. Besides sequence similarities no direct connection between At5g39570.1 and At3g29075 has been identified, yet. In contrast to At5g39570.1, At3g29075 was not identified by comparing proteomes of *pld* mutants with the wild type. Also gene knock-down did not provide valuable information about the function of the protein, or its connection to At5g39570.1. An assumed complementary or redundant function of both proteins could not be confirmed. For detailed analysis of both proteins an antibody is being produced in the context of a Master thesis (Nasr, 2015).

4.3 At5g39570.1 is intrinsically disordered

Immunodetection of total- and phosphoprotein extracts displayed At5g39570.1 at a higher Mw of ~51 kDa in comparison to the calculated theoretical Mw (theoretical Mw 43.5 kDa) (Laugesen *et al.*, 2006). The altered migration speed of the protein in SDS-PAGEs could be the result of its unusual, inherent amino acid composition and structure. It has been reported that (due to their special AA composition) intrinsically disordered proteins bind less SDS than structured proteins and often migrate at a 1.2-1.8 fold higher molecular weight than calculated from their sequences (Tompa, 2002). The protein has ten imperfect tandem repeats in its C-terminal region (**Figure 18**). Jorda *et al.* (2010) identified a co-relation between unstructured proteins and repeat perfection: The increasing perfection of tandem repeats typically, results in a loss of protein structure. The absence of extensive hydrophobic motifs in combination with the prediction of a highly disordered structure of At5g39570.1 (**Figure 19**) points to an

intrinsically disordered protein structure. At5g39570.1 exhibits additional characteristics of IDPs, such as phosphorylation sites (**Table 9**) (Laugesen *et al.*, 2006) and heat-stability (**Figure 31**) (Tompa, 2002). The function of IDPs might be controlled by post-transcriptional modifications, which induce disorder-to-order transitions. Phosphorylation as a regulatory switch of these conformational stages has been observed for IDPs (Bah *et al.*, 2015). Unfortunately, no clear structure for At5g39570.1 could be detected by circular dichroism spectroscopy in the lab of P. Harryson and S. Eriksson (University of Stockholm, personal communication) since the protein aggregated *in vitro* (**Figure 65**). Evidence for IDPs involved in protein aggregation has been reported previously (Zhang *et al.*, 2013a) and supports the classification of At5g39570.1 as intrinsically unstructured.

4.4 Phosphorylation of At5g39570.1

The protein At5g39570.1 consists of 381 amino acids (theoretical Mw 43.5 kDa), is very acidic (pI 4.7) and carries a phosphorylation site at position S₃₃₉ (Laugesen *et al.*, 2006). Analysis of phospho-enriched proteins confirmed phosphorylation of At5g39570.1. Identification of phosphorylation of At5g39570.1 by a VH1 kinase (Braun, 2015) and a CPK3 (Mehlmer, 2008) kinase suggests non-specific activation of the protein by different kinases (e.g. depending on the developmental stage) of *A. thaliana*. Phosphorylation as one of the most common post-translational modifications of proteins plays a crucial role in a number of cellular processes, regulating and signaling networks. Therefore it is possible, that phosphorylation of At5g39570.1 influences its function and affects downstream targets. While water-limiting conditions did not result in increased At5g39570.1 levels in wild-type plants, dehydration triggered phosphorylation of At5g39570.1 (**Figure 49**). Mutation of the confirmed phosphorylation site S₃₃₉ might alter the function of At5g39570.1 and thus help to understand its physiological role. Further analyses of the phosphorylation state of At5g39570.1 upon changing conditions, environmental stages and different tissues in wild type and mutant plants may help to understand its activity in response to phosphorylation.

4.5 Phenotypic analysis of *At5g39570.1* and *At3g29075* mutants

Screening of T-DNA-insertion mutants is a powerful method for the detection of morphological or developmental changes in plants due to the knock-out of a gene of interest. In the context of my Diploma thesis I received and confirmed T-DNA knock-out mutants (section 3.2) to be homozygous for the gene knock-out of *At5g39570.1*. Genotyping experiments confirmed the depletion of the gene (**Figure 25**), but no prominent phenotypic differences were observed under standard conditions (**Figure 37**).

Various proteins function synergetically or share redundant roles in molecular processes and are therefore able to partially complement a gene knock-out of a related protein. For instance, *TPK1* and *TPK2*, two structurally conserved isoforms of the protein kinase A family were reported to suppress each other's defects, resulting in similar phenotypes of single knock-out plants (Bockmühl *et al.*, 2001). The previously described existence of the homologous protein *At3g29075* in *Arabidopsis thaliana* may complement the knock-out of *At5g39570.1* in a similar matter. The generation of a double knock-out mutant for both homologs was not possible, since no T-DNA-insertion line for *At3g29075* has been available until to date. Therefore, I generated an *At5g39570.1* knock-out/ *At3g29075* knock-down double mutant. Positive plants did not show a prominent phenotype under standard growth conditions (**Figure 37**).

Different studies reported that protein expression levels of *At5g39570.1* were affected upon different abiotic stresses and environmental conditions, such as salinity, dehydration, temperature and light stress (**Supplementary table 8**). No phenotypic differences were observed in mutant plants upon exposure to dehydration (**Figure 38**), cold (**Figure 39**) or short term salt treatment (**Figure 40a**). Microscopic comparison of mutant and wild-type plants could not detect any prominent changes. Only the *plda1* mutant showed an impaired phenotype upon dehydration, which is in accordance to the observations of increased water loss in mutant plants lacking *PLDα1* (Zhang *et al.*, 2004). Interestingly, long-term salt-treatment triggered a *plda1*-like phenotype in *At5g39570.1* and *At5g39570.1/At3g29075* knock-out mutants (**Figure 40 b-c**). After two to three weeks of salt-treatment (see section 2.2.2) the wild-type plants remained viable, while all mutants were strongly affected or not-viable after stress treatments. The double mutant *At5g39570.1/At3g29075* was affected in the same manner as the single *At5g39570.1* knock-out mutant, highlighting the importance of *At5g39570.1* in the context of stress signaling and adaptation. In conclusion, *At5g39570.1* could possibly be involved in the late downstream response of *PLDα1* to severe water-limiting conditions.

Alterations of phosphate levels in the media are known to trigger phenotypic effects in plants, as phosphorous is an important macronutrient and is required to sustain the energy household in plants. Under phosphate deprivation, production of phospholipids decreases whereas generation of non-phosphorous lipids is promoted (Wang *et al.*, 2014). Different PLD isoforms, such as PLD ζ 1 and PLD ζ 2 are reported to be implicated in the plants response to phosphate deprivation (Li *et al.*, 2006). Low phosphate availability influences root growth architecture in Arabidopsis to increase phosphate-uptake (Williamson *et al.*, 2001). However, no prominent phenotype in the primary root length or in the lateral root growth has been observed between wild-type and *At5g39570.1* knock-out mutant plants grown in high or low phosphate concentrations (**Figure 41**). Seedling growth in *A. thaliana* is negatively affected by altered phosphate concentrations (Goldstein *et al.*, 1989) and was therefore monitored in wild-type and mutant plants. Only the *plda1* mutant displayed an impaired seedling growth upon phosphate starvation conditions, but no prominent effects were observed for the *At5g39570.1* knock-out mutants (**Figure 41**). The severe reduction of leaf-area as a result of phosphate starvation faces slightly reduced chlorophyll synthesis levels and was therefore reported to trigger the accumulation of chlorophyll in leaves (Wartenberg & Blumöhr, 1966). The chlorophyll content in the *plda1* and *At5g39570.1* knock-out mutants was slightly lower compared to the wild type, upon phosphate starvation and partly in standard growth conditions. In agreement with this, expression of *At5g39570.1* was slightly reduced upon phosphate starvation. These results point to a putative direct, respectively indirect dependence on phosphorous of *At5g39570.1*. The observation that *At5g39570.1* expression levels are dependent on PLD α 1 underlines these findings. An involvement of *At5g39570.1* in chlorophyll synthesis or photosynthetic reactions cannot be excluded.

4.6 Regulation of *At5g39570.1*

The function of a protein is tightly linked to its expression in different tissues, developmental stages and sub-cellular compartments. These diverse expression patterns are highly regulated within the protein biosynthesis process and take place on transcriptional, post-transcriptional, translational and post-translational level. Export and degradation of proteins counteract the synthesis process and delineate a counterbalance in these complex regulatory networks. The interplay of different proteins in both control mechanisms of the protein biosynthetic pathway, results in dependencies from one protein of the other. Here I describe the regulation of *At5g39570.1* by members of the phospholipase D family. *In silico* analysis of co-expression

patterns have shown a closely linked co-expression of *At5g39570.1* and *PLD α 1* (**Figure 22**). The co-expression of two genes indicates similar transcriptional regulation, a possible functional relationship, or involvement in the same protein complex or pathway (Weirauch, 2011) and therefore enables further investigations of the relationship of both proteins.

4.6.1 Expression of *At5g39570.1* is dependent on *PLD α 1*

In our laboratory, the protein *At5g39570.1* was detected and identified by the comparison of phosphoproteoms of *A. thaliana* wild-type and *pld α 1* knock-out mutants (Kuhn, 2010, Shen, 2008). A one-sided dependence of *At5g39570.1* on *PLD α 1* has been shown in this thesis. While the *PLD α 1* expression level is not affected in the absence of *At5g39570.1* (**Figure 45**), protein levels of *At5g39570.1* are drastically decreased in *pld α 1* knock-out mutants (**Figure 46**). Expression of *At5g39570.1* in the *pld α 3* and *pld δ* knock-out mutants underlines the specific dependence on the *PLD α 1* isoform. Nevertheless, no direct interaction between *At5g39570.1* and *PLD α 1* was detected (**Figure 66**). The enzymatic product of *PLD α 1*, phosphatidic acid is a well known signaling molecule in plants that binds and regulates a wide range of proteins and associated pathways (Munnik, 2001). This suggests a downstream regulation of *At5g39570.1* by phosphatidic acid. *PLD α 1* is the most abundant member of the PLD family, and therefore leads to the maximum production of PA under non-stress conditions (Wang *et al.*, 2014). Surprisingly the absence of *PLD α 1* does not result in reduced PA levels in *A. thaliana* leaves (Devaiah *et al.*, 2006). This indicates a takeover of PA production by other PLD isoforms or generation of PA *via* the PLC-pathway. However, the majority of PA produced in the cell is not involved in signaling pathways and serves as components for the biosynthesis of structural phospholipids (Munnik, 2001). PLD and PLC/DGK pathways generate different molecular species of PA and activate different targets (Arisz *et al.*, 2009, Li *et al.*, 2009, Ruelland *et al.*, 2002). “The PA species differ in the number of carbons and double bonds forming two fatty acid chains. It has been suggested that different molecular forms of PA exhibit diverse affinities to proteins. While PA produced *via* the PLC/DGK pathway is mainly composed of PA 16:0/18:2 and PA 16:0/18:3 species, PLD generates additional PA species like PA 18:3/18:2 and PA 18:2/18:2” (Hou *et al.*, 2015, Vergnolle *et al.*, 2005). Devaiah *et al.* (2006) identified slightly reduced lipid levels for 16:0/18:2 PA and 16:0/18:3 PA in leaves of *pld* knock-out mutants in *A. thaliana*. It was recently shown that the PA species 16:0/18:2 binds and activates the mitogen-activated protein kinase MPK6 in order to regulate downstream pathways (Yu *et al.*, 2010). PA-

mediated regulation of the abundance and activity of transcription factors was reported previously (Klimecka *et al.*, 2011, Yao *et al.*, 2013). A similar activation by 16:0/18:2 PA or 16:0/18:3 PA on the pathway, regulating the expression of At5g39570.1 could explain the drastic down-regulation of *At5g39570.1* in *plda1* knock-out mutants. As a signaling molecule, minor concentrations of PA may trigger broad downstream responses. Binding of PA was previously shown to induce cleavage of target proteins (Kim *et al.*, 2013b). The PA species 16:2/18:2 and 16:3/18:3 have not been detected in wild-type leaf extracts of *A. thaliana*, but only in the *plda1* mutants (Devaiah *et al.*, 2006) and thus were investigated thoroughly. Although the degradation-marker protein, polyubiquitin3 was experimentally confirmed to bind At5g39570.1 (Kim *et al.*, 2013a), protein-inhibitor assays have shown that At5g39570.1 is not post-translationally degraded by proteases in the *plda1* mutant (**Figure 48**). A negative regulation of expression levels of *At5g39570.1* by PA 16:2/18:2 and PA 16:3/18:3 is unlikely, but cannot be excluded.

To unravel this complex PA-mediated regulating mechanism, specific PA-profiling data for all PLD isoforms are required. The very low abundance of PA in leaves (<0.2 %) in combination with the occurrence of multiple isoforms and the fast turnover of PA species impedes the genuine profiling of PA contents in the cell. In addition to this, PLD activity is strongly regulated during different developmental stages and in response to stress (Qin *et al.*, 2006, Wang *et al.*, 2014), which prevents the identification of a correlation between distinct PA species and downstream effects. However, development-specific analysis revealed altered expression levels of At5g39570.1 in leaf extracts of 1 to 6 week old wild-type plants (**Figure 43**) that may be explained by altered PA levels or PA compositions. A recent study revealed development-specific expression of a putative At5g39570.1-like protein in *Camellia sinensis* (Li *et al.*, 2015).

4.6.2 Expression of At5g39570.1 is not solely dependent on PLD α 1

Protein blot analysis of leaf extracts from different PLD isoforms (**Figure 46**) revealed strongly decreased expression of At5g39570.1 in *plda1* knock-out mutants. Reduced protein levels were also found in *plda3*, *plde* and *pld ζ 1/ ζ 2* mutants. Surprisingly, the genetically more distant *pld ζ 1/ ζ 2* double knock-out mutants expressed very low amounts of At5g39570.1. To confirm this observation additional biological repeats with single *pld ζ* knock-out mutants should be carried out. The absence of PA-profiling data for *pld ζ* mutants, and the fact that only a double knock-out mutant but no single mutant was available in this study, further

impedes the evaluation of these results. However, PLD ζ isoforms exhibit some unique properties that may explain their special role regarding the expression of At5g39570.1.

The production of PA by members of the phospholipase D family is strongly regulated in plant cells and requires special physiological conditions and components, such as pH, Ca²⁺ concentration, PIP₂-availability or free fatty acids (Bargmann & Munnik, 2006). In contrast to all other PLD isoforms, PLD ζ acts independent from Ca²⁺ and does not require any additional divalent cation for its activity (Qin & Wang, 2002). PLD ζ contains two domains that are not found in other PLDs in *A. thaliana*: A PX-domain, capable of binding phosphoinositides (Cheever *et al.*, 2001) and a pH domain that non-specifically binds phosphoinositides (Lemmon & Ferguson, 2000) and is suggested to function in membrane targeting (Qin & Wang, 2002). Furthermore, PLDs share different preferences for substrates (Pappan *et al.*, 1998) and are localized to distinct membranes (Wang *et al.*, 2014). In contrast to other family proteins, PLD ζ selectively hydrolyzes PC (Pappan *et al.*, 1998) and is localized at the tonoplast membrane (Yamaryo *et al.*, 2008). These unique properties of PLD ζ render PLD ζ -isoforms to be candidate proteins for the involvement of PA-mediated regulation of At5g39570.1 expression levels. Due to their different structure and requirements, PLD ζ -isoforms might be involved in a PLD α 1-independent regulation of At5g39570.1, maybe by the production of unique PA species, which target *At5g39570.1*.

Emerging evidence supports the hypothesis that different members of the PLD and PLC families generate specific but also redundant PA species that are involved in distinct cellular signaling pathways. For instance, PA binding to SPHK, ABI1 and RbohD was reported to be dependent on specific molecular PA species. While all three proteins exhibited strong binding affinities towards PA 18:1/18:1, only RbohD displayed a similar strong affinity to PA 18:2/18:2, whereas SPHK and ABI1 showed strongly decreased, respectively no affinity to this PA species (Guo *et al.*, 2011, Hou *et al.*, 2015, Zhang *et al.*, 2004, Zhang *et al.*, 2009). It seems that only a specific subset of PA species is capable of activating distinct targets and pathways. In this context, knock-out of both *PLD ζ* genes might lead to absence of specific PA species that are (in high levels) exclusively expressed in *pld ζ* mutants and may contribute to the At5g39570.1-regulating pathway.

The generation of PLD α 1-derived PA species may not be sufficient to compensate the abrogation of PLD ζ isoforms in *pld ζ* knock-out mutants and result in a reduced expression of At5g39570.1. In the same manner, production of PLD ζ -derived PA species may not be sufficient to compensate the absence of *PLD α 1* in *pld α 1* knock-out mutants. The PLD-derived PA species may synergetically promote expression of At5g39570.1. The cooperation of

different PLD isoforms was previously reported e.g. for PLD α 1 and PLD δ in response to ROS (Bargmann & Munnik, 2006). Abrogation of one or more PLDs would therefore result in reduced amounts and altered compositions of PA species that are involved in the regulation of At5g39570.1.

Other PLD isoforms, (e.g. PLD α 3, PLD δ and PLD ϵ) share more similar requirements with PLD α 1 for their enzymatic activities, such as Ca²⁺ dependence (Pappan *et al.*, 1998) and are also localized at the plasma membrane. Although they are believed to share more similar expression patterns with PLD α 1, knock-out of the corresponding genes did only partially effect expression of At5g39570.1. Therefore it is possible that PLD α 3, PLD δ and PLD ϵ are not (or only partly) involved in the production of PA species, targeting the biosynthetic At5g39570.1 pathway. Hence, distinct PLD isoforms might not (or only partly) influence expression levels of At5g39570.1.

4.6.3 Expression of At5g39570.1 is tissue specific and correlates with PA production

Prominent down-regulation of all protein levels has also been observed in seeds (**Figure 46 b**). The tendency of reduced At5g39570.1-protein levels in mutant plants remained comparable. A recent study identified a two-fold higher expression of the At5g39570.1-like protein in buds from *Camellia sinensis* compared to their young expanding leaves (Li *et al.*, 2015). Activity of PLD isoforms is tissue specific (Bargmann & Munnik, 2006) and thus contributes to different PA concentrations and compositions. Tissue specific expression patterns for At5g39570.1 displayed increased protein levels in roots, stems and flowers (**Figure 44**). Profiling of tissue-specific lipid concentrations in wild-type *A. thaliana* plants displayed PA levels that are in agreement with these findings (Devaiah *et al.*, 2006): The highest relative concentration of PA is found in stalks (~2 %) and roots (~10 %), while the lipid share of PA in leaves (0.2 %) is drastically reduced (Devaiah *et al.*, 2006). Devaiah *et al.* (2006) also identified similar distribution patterns for individual PA species in tissue-specific analyses. This indicates that not the composition, but the concentration of PA is altered in different plant tissues. As reported previously, different molecular forms of PA exhibit diverse affinities to proteins (Guo *et al.*, 2011), which activate or inhibit distinct signaling pathways. It seems that both, PA concentration and PA composition can influence expression levels of At5g39570.1.

In some cases, PA acts synergistically with other signaling lipids, such as DAG or phosphatidylinositol. For instance activation of the C ϵ kinase requires binding of PA and DAG for its full activation (Jose Lopez-Andreo *et al.*, 2003). Other enzymes require simultaneous activation by PA and phosphatidylinositol (Karathanassis *et al.*, 2002, Lindsay & McCaffrey, 2004). The interplay of different PA-molecular species, their abundance and interaction with target proteins in combination with various additional lipid-signaling molecules and plant second messengers indicates a more complex regulation mechanism than previously reported.

4.6.4 Regulation of At5g39570.1 upon exposure to stress

Different studies reported differential expression levels of At5g39570.1 and its homologs upon biotic and abiotic stress treatments (**Supplementary table 8**). Light and especially water-limiting conditions were shown to affect protein expression of At5g39570.1 orthologs in various plant species (Chang *et al.*, 2012, Li *et al.*, 2013, Yin *et al.*, 2014). The observation of necrotic and dead leaves in *At5g39570.1* mutant plants upon water-limiting conditions (**Figure 40 c**) demanded a detailed analysis of the effect of water loss for the expression of At5g39570.1 in wild type and *pld* mutants.

Transcript analysis of *At5g39570.1* was challenging and resulted in different patterns, depending on the applied primer combinations (**Figure 51** and **Figure 53**). The N-terminal primer pair did not detect a down-regulation for *At5g39570.1*-transcript levels and only displayed a minor post-transcriptional down-regulation of *At5g39570.1* in turgescient plant tissues. On the other hand, full-size primers revealed a down-regulation of *At5g39570.1* in in turgescient leaves of *plda1* and partly *plda3* mutants (**Figure 54**). The high sequence identity of the homologous protein *At3g29570* seems to impair gene-specific binding and thus prevents a genuine identification of transcript levels for *At5g39570.1*. The occurrence of tandem repeats prevented a gene-specific detection of expression levels in the C-terminal protein part. These repeats also made sequencing of the gene challenging. Use of gene-specific full-size primers enabled the detection of severely decreased transcript levels of *At5g39570.1* in turgescient leaves of *plda1* mutants and their up-regulation upon dehydration (**Figure 53**). These findings are in accordance with previous observations of decreased gene expression in *plda1*-mutant plants in an *At5g39570.1*-specific GUS-assay (Jandl, 2012). However, only a weak up-regulation upon salt treatment was observed in these assays.

plda1 mutants displayed a strong, relative up-regulation of decreased At5g39570.1 protein levels in response to salt and drought treatment (**Figure 47** & **Figure 48**), while the expression level of At5g39570.1 remained constant in the wild type (**Figure 47** & **Figure 49**). This indicates that water-limiting conditions trigger a compensatory effect of protein expression in *plda1* mutants. Surprisingly, decreased expression levels of At5g39570.1 in response to drought conditions were identified in *plde*, *pldd3* and the *pldζ1/ζ2* mutant (**Figure 47**). However, these plants were severely dehydrated (RWC < 50 %) and displayed a partially non-viable phenotype. The same observation was found in extremely dehydrated *plda1*-mutant plants. They should therefore not be considered in this analysis. Water-limiting stress promotes ABA formation, generation of signaling molecules, such as PA, oxylipins and ROS and activation of complex signaling cascades that eventually result in the up-regulation of protective stress-enzymes and physiological defense mechanisms, such as stomata closure (Hou *et al.*, 2015). The strong physiological impact on the cellular environment might trigger the production of altered PA concentrations and PA compositions in the cell and its subcellular compartments, which were previously shown to affect expression of downstream targets. A protein-inhibitor assay did not show any post-translational degradation of the protein (**Figure 48**), suggesting that no regulation takes place on post-translational level. These data indicate a stress-dependent transcriptional and partly post-transcriptional regulation of At5g39570.1 in the absence of the up-stream regulator PLDα1. The observed effect of different PLD isoforms on the expression of At5g39570.1 points to a regulatory role of phosphatidic acid. Absence of PLDα1, the main contributor of PA, reduces the expression of At5g39570.1. Dehydration and salinity-induced water-loss leads to the activation of numerous stress-signaling pathways, through increased production of NOS, ROS, ABA, inositolphosphates and lipid-signaling molecules (Hou *et al.*, 2015). Also phospholipase C, and distinct PLD isoforms are activated upon water-limiting conditions (Hirayama *et al.*, 1995, Wang *et al.*, 2008, Wang *et al.*, 2014), resulting in the increased production of specific PA species and thus activation of dehydration-associated signaling pathways (Hong *et al.*, 2008, Munnik *et al.*, 2000, Yu *et al.*, 2010). The physiological environment in the cell changes rapidly (e.g. pH-shift and altered Ca²⁺ levels) and favors the activation of stress genes, heat shock proteins, protective molecules, repair mechanisms and essential cellular processes, while non-vital activities are reduced to a minimum (Hou *et al.*, 2015). The plants adaptation to water-limiting stress is a complex cellular and physiological response and requires a subset of different PA-producing enzymes that partly share overlapping functions in providing dehydration tolerance to plants (Wang *et al.*, 2008, Wang *et al.*, 2014), which

indicates some redundancy of *pld* mutants under specific conditions. Activities of PLD isoforms are strongly connected to calcium levels and the intracellular pH. While PLD α 1 requires millimolar Ca²⁺ concentrations and an acidic pH (5.5-6.5) for optimal activity, other PLD isoforms require only micromolar Ca²⁺ concentrations and a neutral pH (6.5-7.5) (Pappan *et al.*, 1998, Pappan & Wang, 1999). Altered environmental conditions could therefore trigger the expression of different *PLD* genes, resulting in the complementation of reduced PA levels as a result from abrogated PLD α 1.

In plants, PA is also indirectly generated *via* the PLC/DGK pathway (Munnik, 2001). In contrast to the PLD isoforms, PLCs are considered to hydrolyze PI(4,5)P₂ *in vivo*, although this phospholipid is extremely scarce in plants (Wang *et al.*, 2014). Water-limiting conditions were shown to drastically increase PI(4,5)P₂ synthesis (Darwish *et al.*, 2009, DeWald *et al.*, 2001, Konig *et al.*, 2008) and thus provide plethora of substrates for the generation of IP₃ and PA. Up-regulation and activation of PLC levels in response to water-limiting conditions (Hirayama *et al.*, 1995, Kocourková *et al.*, 2011, Peters *et al.*, 2010, Tasma *et al.*, 2008) suggests an involvement of PLC in the boosted production of PA upon abiotic stresses. Exogenous application of PA was found to complement phenotypic effects of *plc* knock-out plants in response to water-limiting conditions (Peters *et al.*, 2010), illustrating the importance of PA availability for downstream protein expressions. Despite the main production of PA 16:0/18:2 and PA 16:0/18:3 species via the PLC/DGK pathway in comparison to the more diversely PLD-generated PA species (Vergnolle *et al.*, 2005), an involvement of PLCs in plant signaling pathways is emerging. For instance, salt stress triggers the accumulation of the PLC-derived PA species 16:0-18:2 that binds and activates the MPK6 kinase (Yu *et al.*, 2010). As salinity promotes PLD and PLC activity that results in the production of this PA species, an involvement of PLC in PA signaling cannot be excluded. However, the regulating mechanisms of PLC activity are unknown. Certainly PLCs require micro to millimolar concentrations of Ca²⁺ (Kopka *et al.*, 1998) and are activated by Ca²⁺ Influx (Vaultier *et al.*, 2006). Presumably other factors, such as phosphorylation and interaction with G-proteins additionally contribute to the mode of action (Wang *et al.*, 2014). Elevated Ca²⁺ levels, interaction with G-proteins and increased phosphorylation levels as a response to osmotic stress might therefore trigger PLC activity and raise local PA concentrations independent from PLDs. Although PLD and PLC are suggested to act upstream of two distinct signaling pathways (Vergnolle *et al.*, 2005), they are activated upon similar environmental conditions like salinity and dehydration (Hou *et al.*, 2015, Testerink & Munnik, 2011). These findings point to an overlap of functions in both gene families in response to environmental stresses.

The identification of the relative contribution of the PLD and PLC pathway in modulating responses to water-limiting conditions is one of the important future tasks (Testerink & Munnik, 2011).

The PLC gene family is suggested to have functional redundancy (Munnik, 2014). Members of the PLD family were reported to act cooperatively in response to water-limiting conditions (Uraji *et al.*, 2012). Elevated PA levels originating from other PLD isoforms or PLC-derived PA could therefore compensate the absence of PA produced by a specific PLD isoform like PLD α 1, during dehydration.

The potential of PA to activate, degrade or inhibit expression of target genes and proteins has been reported elaborately (Hou *et al.*, 2015). A putative inhibition of *At5g39570.1* gene-expression levels in the absence of PA and transcriptional activation in response to drought-induced PA levels could explain the observed expression patterns. In the presence of PLD α 1 native, cellular PA levels may already be sufficient for maximal expression of *At5g39570.1* and therefore cannot be increased by osmotic stress.

The recent identification of additional signaling lipids in plants, such as sphingolipids, lysophospholipids, oxylipins, *N*-acylethanolamines, free fatty acids and others, broadens the spectra of candidate signaling molecules that might transduce and regulate expression of *At5g39570.1* in response to dehydration in a PLD-independent manner. The regulatory networks of plant signaling molecules is complex and most signaling lipids are directly, or indirectly up-regulated in response to water-limiting conditions (Hou *et al.*, 2015, Zhu, 2002). Also NO, ROS, ABA and Ca²⁺, which are partly dependent on PLD and PLC activity, exhibit elevated levels in osmotic stress conditions that have the potential to affect gene expression of target genes (Hou *et al.*, 2015).

Taken together, altered environmental conditions could promote the expression of *At5g39570.1* in a PLD(α 1)-independent manner. A possible model for the regulation of the processes is depicted in **Figure 80**.

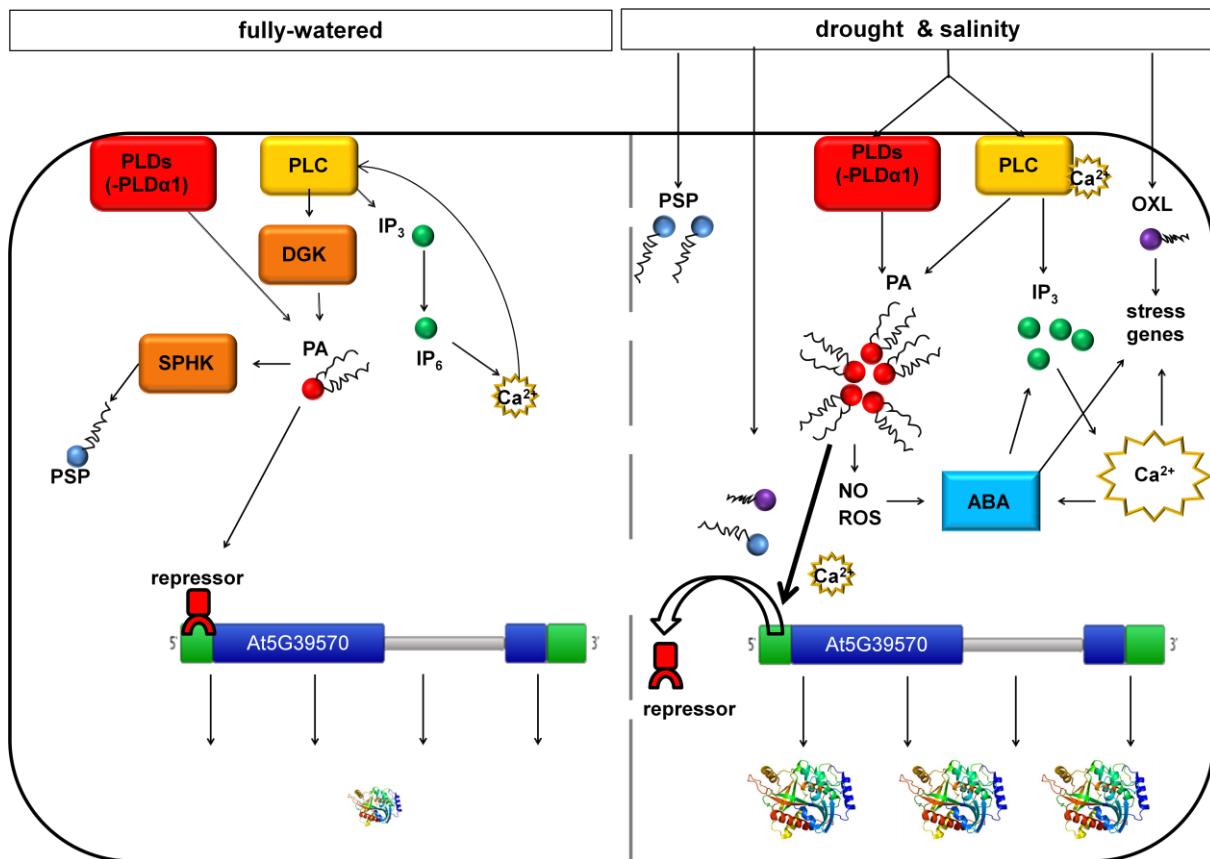


Figure 80: Model for the regulation of expression of *At5g39570.1* in response to water-limiting conditions in the absence of *PLDα1*.

Under turgescence conditions, a repressor prevents transcription of *At5g39570.1*. In the absence of *PLDα1*, the production of PA species is impaired and PA-generated *via* the PLC pathway is insufficient to replace the repressor from the gene. Water-limiting conditions promote PLC and PLD activity, resulting in the increased production of PA species. Additionally, production of other signaling molecules, such as OXL, PSP, NO, ROS and IP_3 is promoted by oxidative stress and has a positive feedback on the generation of PA and stress genes. Elevated levels of distinct PA species in combination with other signaling molecules displace the repressor from *At5g39570.1*, resulting in increased protein biosynthesis. Arrows indicate positive regulatory events. The role of other signaling molecules is indicated to keep the figure simple. ABA, abscisic acid; DGK, Diacylglycerol kinase; IP_3 , inositol trisphosphate; NO, nitric oxide; OXL, oxylipins; PA, phosphatidic acid; PLC, phospholipase C; PLD, phospholipase D; PSP, phytosphingosine phosphate; ROS, reactive oxygen species; SPHK, sphingolipid kinase.

4.7 Interaction of *PLDα1* and the unknown protein *At5g39570.1*

The one-sided downstream regulation of *At5g39570.1* by members of the phospholipase D family, especially *PLDα1*, emphasizes the control hierarchy and the importance of phospholipases in plants regulatory functions. The list of processes affected by PLD isoforms includes a plethora of physiological activities, such as ABA response, stomatal movement, ROS production, root hair growth, membrane trafficking and cytoskeletal changes (McLoughlin & Testerink, 2013). Phosphatidic acid, the enzymatic break-down product of all PLD isoforms, acts as a lipid signaling molecule and thus plays a major role in the

transduction of intracellular signals (Munnik, 2001). However, also direct interactions of PLDs with target proteins have been reported in plants and animals (Jang *et al.*, 2012, Selvy *et al.*, 2011). How PLDs and PA exert their functions in detail remains enigmatic. Identification of target proteins can help to improve our understanding of these processes.

4.7.1 PLD α 1 does not directly bind to At5g39570.1

A number of direct interactions between phospholipase D and target proteins have been described in plants and animals (Jang *et al.*, 2012, Selvy *et al.*, 2011). In animals, interacting partners of PLDs comprise a wide variety of proteins, such as transporters, adaptor proteins, transcription factors, kinases, phosphatases and GTPases (Jang *et al.*, 2012). The regulatory G-proteins have also been implicated in the activation of PLDs in plants. The G α -subunit GPA1 was shown to bind PLD α 1 *via* a DRY-motif in *A. thaliana* and *Nicotiana tabaccum* (Zhao & Wang, 2004). The combination of high PLD activity in early stages of dehydration and the ability of the G-protein activator mastoparan to induce dehydration-tolerance in *Craterostigma plantagineum*, indicates a G-protein-mediated activation of PLD pathways (Frank *et al.*, 2000). Besides binding to G-proteins, a direct interaction of PLD with actin molecules has been demonstrated (Kusner *et al.*, 2003).

To test for direct interaction of PLD α 1 with At5g39570.1 an affinity-based chromatography assay was conducted using At5g39570.1 as bait in a plant extract (**Figure 60**). A PLD α 1-specific antibody was used to detect a putative co-elution of PLD α 1 with the affinity-bound At5g39570.1. While anti-PLD α 1 specifically detected PLD α 1 in plant extracts, the protein could not be immunologically detected in co-eluted fractions of the affinity chromatography assay. Detection of putative interacting partners by the less sensitive Coomassie stain, points to the absence of PLD α 1 in the eluted fractions, rather than an insufficient sensitivity of the anti-PLD α 1 antibody. In the same manner, anti-PLD α 1 could not detect PLD α 1 in At5g39570.1 co-immunoprecipitated fractions (data not shown), while silver-stain of these fractions detected a subset of putative binding partners (**Figure 63**). These results demonstrate that At5g39570.1 does not directly bind to PLD α 1 *in vitro* or *vivo*.

4.7.2 PLD α 1 mediates interaction with At5g39570.1 by PA

PLD α 1 is one of the key enzymes for the control of plant development, growth and adaptation to abiotic stress as it generates the signaling molecule phosphatidic acid in plants which is involved in the regulation of plant development, growth and adaptation to abiotic stress (Hou

et al., 2015, McLoughlin & Testerink, 2013, Munnik, 2001). The signaling role of phosphatidic acid in various physiological processes has been researched thoroughly in plants and animals over the past years and led to the identification of numerous PA-binding proteins (Capelluto, 2013, Hou *et al.*, 2015, Jang *et al.*, 2012, McLoughlin & Testerink, 2013, Munnik, 2001). Nevertheless no consensus PA-binding motif has been identified and it might not exist. Recently an “electrostatic/hydrogen-bond switch” model (Kooijman & Testerink, 2010), which explains the molecular basis of PA binding based on the unique properties of PA has been suggested: Residues of the basic amino acids lysine and arginine were found to increase the charge of PA by binding to its phosphate group. By switching the electrostatic properties, the phosphate of PA turns into a preferred docking site for basic amino acids. The conical shape of PA provides less stability to the plasma membrane than the cylindrical shape of structural phospholipids (Kooijman *et al.*, 2003, Testerink & Munnik, 2011). Therefore, PA is a suitable membrane lipid for the insertion into positively charged membrane protein domains (Kooijman *et al.*, 2007). The absence of a genuine PA-binding motif impedes the identification of putative binding sites in proteins of interest. Therefore, independent lipid-binding assays have been exploited to test binding of PA to At5g39570.1 (section **3.9.2**). Protein-lipid-overlay assays revealed strong PA-specific binding affinity of At5g39570.1, whereas its N- and C-terminal protein fragments displayed decreased, respectively faint affinities towards PA (**Figure 67** & **Figure 68**). No binding affinity towards zwitterions and uncharged lipids were detected, emphasizing the binding specificity to bind PA. These findings were confirmed by liposome-binding assays that consider the cellular state of lipids as liposomes (**Figure 70**). With regards to the proposed “electrostatic/hydrogen-bond switch” model, it seems unlikely that the overall negatively charged proteins At5g39570.1 (pH 4.7) and Nt-At5g39570.1 (pH 4.7) (**Supplementary figure 2**) bind to a negatively charged lipid under physiological conditions (pH 7). However, PA-binding to negatively charged proteins was observed previously (Petersen *et al.*, 2012) and might be explained by the high number of basic amino acid stretches in the protein sequences. Emerging evidence suggests that arginine and lysine residues are important for the PA-binding process (Kooijman & Testerink, 2010, Kooijman *et al.*, 2007, Petersen *et al.*, 2012). While At5g39570.1 exhibits high numbers of these AA, Nt-At5g39570.1 has a strongly reduced lysine concentration (**Supplementary figure 1**). This observation is in accordance with the observed higher binding affinity of the full-size protein compared to its N-terminal fragment (**Figure 67**, **Figure 68** & **Figure 70**).

The positive correlation of PA formation in response to drought (Katagiri *et al.*, 2001, Testerink & Munnik, 2011) and up-regulation of At5g39570.1 in *plda1* knock-out plants upon dehydration (**Figure 47**) indicate a PA-specific interaction *in vivo*. The slight increase in the phosphorylation level of At5g39570.1 in wild-type leaves (**Figure 49**) and the observed PA-binding specificity *in vitro*, support an interaction of PA and At5g39570.1 *in vivo*.

Real-time analysis of PA-binding by liposome-turbidity assays measures the change in absorbance of large unilamellar liposomes as a result of fusion or aggregation (Roston *et al.*, 2011). The hydrophobic effect promotes protein folding and insertion of hydrophobic protein residues into non-polar lipid environments (Hong, 2014). Independent experiments revealed increasing protein-lipid interactions within the first two minutes after the addition of the N-terminal fragment of At5g39570.1 and the full-size protein, respectively. The observed two-fold change in absorbance at OD₃₅₀ indicates a PA-specific binding affinity compared to the weak effect of PC-supplemented samples (**Figure 71**). Comparison of the PA-binding affinity with the His-tagged NUS protein as a negative control shows that the binding event is independent of the His-tag (**Figure 67**, **Figure 68**, & **Figure 72**). The combination of lipid-binding methods shows the ability of At5g39570.1 and partially Nt-At5g39570.1 to specifically bind PA *in vitro*.

Despite its strong basic character, PA-binding experiments (**Figure 67** & **Figure 70**) have shown that the C-terminal fragment of At5g39570.1 does bind PA with strongly reduced affinity. The C-terminal protein fragment harbors extraordinary high amounts of lysine and arginine (18.5 %), but is also very rich in acidic amino acids (24.5 %), which may influence protein binding to the phosphate group of PA. In addition to this, lipid binding is also dependent on additional factors, such as protein conformation, time, temperature, physiological and environmental conditions (Ruano *et al.*, 1998). Alterations of these parameters in previous experiments but also its unusual AA composition with very high amounts of acidic amino acids may prevent PA binding in the C-terminal region of At5g39570.1. Surprisingly, the liposome-binding assay displayed a 4-fold increase of binding effects, such as fusion or aggregation for Nt-At5g39570.1 when incubated with PA (**Figure 73**). It has to be taken into account, that the turbidity of the solution was used as a direct indication of lipid-binding affinity. As observed previously, Ct-At5g39570.1 could not be completely dissolved in phosphate buffer and partially precipitated in liposome-binding assays (**Figure 70**). The unusual composition of Ct-At5g39570.1, consisting of ten imperfect units of tandem repeats lacking a secondary structure, might induce a time-dependent aggregation of the proteins *in vitro* and thus trigger the OD₃₅₀ shift. A similar increase of

turbidity at OD₃₅₀ for sole proteins without the addition of lipids has been observed e.g. for the MOMP protein in *Chlamydia trachomatis* (Cai *et al.*, 2009). The tendency of At5g39570.1 to aggregate *in vitro* has been described previously (**Figure 65**). However, a similar effect could not be observed when Ct-At5g39570.1 was incubated with PC only. PA as a signaling molecule possesses the ability to induce conformational changes in target proteins (Hou *et al.*, 2015), which may induce disorder-to-order transitions in IDP and trigger thereby trigger the gain of β -sheets or similar light-absorbing structures. A minor interaction of PA with Ct-At5g39570.1 could therefore trigger a major change in absorbance. Due to these observations the role of Ct-At5g39570.1 in PA-binding remains to be elucidated. Ct-At5g39570.1 needs to be completely dissolved to continue further research.

4.8 Interacting partners of At5g39570.1

Physical interactions occur between most proteins in order to trigger a variety of different functions in the cell. For instance, proteins enzymatically function in a complex, transport target proteins across membranes or transduce extra- and intracellular signals along the interior of cells. Knowledge of the interatomic networks of protein-protein interactions is essential for the understanding of plants growth, development and adaptation to environmental changes. Sequencing of the Arabidopsis genome (The Arabidopsis genome project, 2000) facilitated the analysis of genes and encoded proteins in *A. thaliana*. The TAIR10 database contains 27,416 protein-coding genes (in total 33,602 genes) of *A. thaliana* but over 50 % lack experimentally confirmed annotations regarding the proteins function. Decryption of an unknown function is difficult, but identification of protein-binding partners and interaction networks can provide useful starting points for this task. Intracellular localization of a protein and identification of its up-stream regulators is useful for the characterization of an unknown protein and may help to establish regulatory models.

4.8.1 Identification of RNA-binding proteins as putative interacting partners of At5g39570.1

A yeast-two-hybrid screen displayed *in vitro* binding of a member of the protein kinase superfamily (At3g05050) and a GLI1 kinase (At1g80460) to At5g39570.1 (**Figure 59**). The latter one is involved in the glycerol metabolism and was shown to be required in defense responses to bacteria (Li *et al.*, 2005). However, phosphorylation of At5g39570.1 by either of

these kinases remains to be elucidated. In contrast, *in vitro* phosphorylation by the VH1-kinase AT1G14000.1 and CPK3 (AT4G23650.1) was previously discussed. Arabidopsis CPK3 was reported to be involved in plants adaptation to dehydration, salinity and cold stress as well as in the response to biotic stresses (Arimura & Sawasaki, 2010).

Besides the identification of these kinases, a transcription factor, a peripheral membrane protein and multiple nucleic acid-binding proteins, namely MORF6 (AT2G35240), MORF2 (AT2G33430.1), U1-70K (AT3G50670) and AT1G10590 were detected in this assay. Interestingly, the proteins MORF6, MORF2 and U1-70K were detected multiple times and are involved in RNA-processing events. The identification of two conserved RNA-stretches within the sequence of At5g39570.1 that can be found in different RNA-associated proteins in *A. thaliana* (**Supplementary tables 6 & 7**) support these findings. *In silico* analysis of putative binding partners predicted an interaction of At5g39570.1 with At3g06530, a small U3-nucleolar RNA-associated protein. It is noteworthy that both proteins have been detected (and their gene model was described) in the same proteomic analysis in *A. thaliana* (Baerenfaller *et al.*, 2008), pointing to similar expression patterns and thus a putative interaction. Despite its acidic character, At5g39570.1 appears disordered (**Figure 19**) and possesses large hydrophobic, conserved patches in its C-terminal end (**Figure 17**) which could enable an interaction with acidic RNA molecules or RNA-processing molecules.

As observed for At5g39570.1, many RNA-binding proteins contain multiple tandem repeats that consist of few basic domains to fulfill their diverse functional requirements (Lunde *et al.*, 2007). RNA-binding proteins have revealed enormous differences in their RNA-binding affinities, which contribute to their specific cellular functions (Glisovic *et al.*, 2008). In the past decades a number of RNA recognition motifs and domains, which promote RNA-binding to a protein of interest have been identified (Lunde *et al.*, 2007). However, prediction of RNA-binding sites based on the primary structure of candidate proteins remains challenging as RNA-binding motifs are variable, influenced by a number of molecules and rely on the existence of hydrophobic stretches, rather than on distinct amino acids. Blast analysis identified a RNA binding motif in the C-terminal half of the protein which could be targeted by the provisional, transcription termination factor Rho “PRK12678-domain”. In accordance with this discovery, several homologous RNA-binding proteins have been identified for At5g39570.1, by the domain-enhanced lookup time accelerated BLAST (**Supplementary table 10**) (Boratyn *et al.*, 2012). The high abundance of these RNA-associated proteins indicates a possible involvement of At5g39570.1 in RNA-processing.

By cross-referencing the BLAST results (**Supplementary table 10**) with the candidate proteins from the yeast-two-hybrid screen (**Figure 59**), the mRNA splicing protein U1-70K was identified in both approaches. Although the expectation value of U1-70K is below the threshold to be considered a homologous protein (e-value: 0.12, positives 30 %), identification of an interaction of this protein with At5g39570.1 *in vitro* and detection of homologous sequences *in silico*, point to a protein interaction. The 70K gene (*U1-70K*) encodes for a small nuclear ribonucleoprotein particle that has been implicated in basic and alternative splicing of pre-mRNAs (Golovkin & Reddy, 1996). U1-70K was found to interact with different plant-specific proteins in their serine/arginine-rich C-terminal region to form the spliceosomal complex (Tanabe *et al.*, 2009). At5g39570.1 exhibits high amounts (>10 %) of serine and arginine, but no additional binding motif was identified. Interestingly, the DELTA-Blast analysis for At5g39570.1 revealed further mRNA-splicing proteins, with high e-values (above the threshold), such as the THO complex subunit 2 (e-value: $6 \cdot 10^{-10}$) and the pre mRNA-splicing factor F5A9.21 (e-value: $2 \cdot 10^{-9}$) (**Supplementary table 10**).

Further *in silico* matches code for proteins that belong to the class of RNA-binding proteins with various specific functions. In the cell, RNA-binding proteins take part in important biochemical reactions, such as RNA splicing, RNA editing, polyadenylation and export of mRNA (Ciuzan *et al.*, 2015, Lunde *et al.*, 2007). Recently, a group of glycine-rich RNA-binding proteins has been suggested to be involved in the adaptation of organisms to biotic and abiotic stresses (Ciuzan *et al.*, 2015). Similar glycine-rich motifs have also been identified in At5g39570.1 (**Figure 11**). Glycine-rich proteins form a diverse class of proteins that are involved in numerous physiological events, such as RNA binding and stabilization of cell walls (Sachetto-Martins *et al.*, 2000).

The detection of a cytosolic and putative nuclear localization (**Figure 77**) supports a function of At5g39570.1 in RNA processing as RNA-binding proteins are generally found in the cytoplasm and nucleus (Lunde *et al.*, 2007). The cytosolic localization of the protein appeared in a cytoplasmic network, connecting the cell walls with each other (**Figure 77**). Although the identification of a putative bipartite nucleus-locating signal in At5g39570.1 (Ufer, 2011) could not be confirmed by GFP-fusion analysis (Jandl, 2012), a nuclear localization could also not be excluded for this acidic protein. In spite of their acidic character, multiple acidic proteins are transported into the nucleus and were shown to bind negatively charged nucleic acids with small stretches of hydrophobic AA (Cameron, 2012, Matilla *et al.*, 1997).

4.8.2 *In vitro* interaction of At5g39570.1 with MORF proteins suggest an involvement in the RNA-editing complex

The two, several times identified targets in the yeast-two-hybrid screen, MORF2 and MORF6, are members of the RNA editing-interacting protein (RIP) family that are located in the plastid and mitochondrion, respectively (Bentolila *et al.*, 2013). Like 95 % of plants the mitochondrial proteins MORF2 and MORF6 are encoded in the nucleus, synthesized in the cytosol and are post-translationally transported into the target organelles. They are involved in the post-transcriptional C-to-U editing of organelle mRNA transcripts (Bentolila *et al.*, 2013, Braun & Schmitz, 1999, Law *et al.*, 2015). The MORF-gene family encodes nine, exclusively in plants occurring, editing factors with distinct cellular functions (Takenaka *et al.*, 2012). While MORF2 was shown to control the editing of multiple plastid genes, MORF6 was reported to affect a small number of mitochondrial editing sites (Bentolila *et al.*, 2013). This finding is reflected by the phenotypes of the corresponding mutated plants. While the *morf2* mutant displays a complete lack of chlorophyll synthesis in light, no phenotypic difference has been observed for *morf6* mutants (Takenaka *et al.*, 2012). Altered expression levels of At5g39570.1 and its homologs have been identified in the context of different “light”-studies (Baerenfaller *et al.*, 2015, Brar, 2013, Fox *et al.*, 2015, Lee, 2013, Ray *et al.*, 2015), indicating a putative connection to the plastid-localized MORF2 protein. For instance, knock-out of four major important photoreceptors (*phyA*, *phyB*, *cry1* and *cry2*) was shown to severely affect plant growth and development, but also reduced chlorophyll levels in *A. thaliana* (Fox *et al.*, 2015). While proteins involved in the Calvin cycle and electron transport were found to be reduced in this quadruple mutant, At5g39570.1 and a set of different proteins involved in signaling and stress response were up-regulated upon white-light conditions (Fox *et al.*, 2015). Differential expression levels of At5g39570.1 were also observed in dark harvested *Glycine max* (Lee, 2013) and *A. thaliana* grown under long-day conditions (Baerenfaller *et al.*, 2015). Increased transcript levels of At5g39570.1 were reported in etiolated seedlings of *Vicia faba* (Ray *et al.*, 2015). Bioinformatics analysis by MASS (Mapping and alignment with short sequences) considered At5g39570.1 a candidate gene for UVB-induced root-growth arrest in *A. thaliana* plants, lacking the DNA-damage response kinase ATR (Brar, 2013). Although knock-out of At5g39570.1 did not result in a chlorophyll-lacking phenotype under standard conditions in soil, mutant plants grown on phosphate depleted media revealed decreased levels of chlorophyll compared to the wild type (**Figure 41**). Analysis of the *morf9* mutant showed a similar behavior: Soil-grown *morf9* mutants displayed an autotrophic

growth, whereas plants grown on agar medium supplemented with sugar, exhibited partial lack of chlorophyll synthesis (Takenaka *et al.*, 2012).

Analysis of further *morf* mutants revealed a strong, altered phenotype for MORF8 (dwarf phenotype), while plant growth was unchanged in other MORF family members, including MORF6 (Bentolila *et al.*, 2013). Neither did the *At5g39570.1*-mutant plants display any phenotypic alteration in standard conditions. Therefore an upstream regulation of *At5g39570.1* of MORF2 or MORF8 can be excluded.

The lack of growth and developmental phenotypes as a result of the knock-out of different pentatricopeptide repeat (PPR) genes, which are involved in organelle editing has been reported previously (Takenaka *et al.*, 2010, Zehrmann *et al.*, 2009). It has to be considered, that RNA-editing proteins might have specific but redundant functions. Different MORF isoforms were shown to synergistically affect RNA-editing events (e.g. MORF2 & MORF9 in plastids) and thus were considered to act in the same editing complex (Bentolila *et al.*, 2013). Interaction and functional overlaps of MORF proteins and additional RNA-binding proteins (e.g. PPR-proteins) have been reported (Takenaka *et al.*, 2012). Similar to *At5g39570.1* these proteins inherit a tandem-repetitive amino acid sequence. The presence of a degenerated PPR-motif within the repeats classifies these proteins as pentatricopeptide repeat proteins, which are involved in RNA-editing processes (Lurin *et al.*, 2004). MORF isoforms that physically interact with PPR-MEF (mitochondrial editing factor) proteins were detected by yeast-two-hybrid screens and pull-down assays (Takenaka *et al.*, 2012). The MORF protein family was shown to interact specific, yet fluid with different MEF proteins (Takenaka *et al.*, 2012). MEF proteins appear to have specific and redundant functions, regarding the RNA-editing process. *At5g39570.1* (and its homolog *At3g29075*) may be involved in similar processes. However, assembly and process of the RNA-editing machinery in higher plants remains enigmatic and is suggested to require a number of additional protein factors for its function (Takenaka *et al.*, 2012). Besides the formation of heterodimeric complexes, MORF proteins were shown to interact with themselves in homodimeric structures (Takenaka *et al.*, 2012). Interestingly, also *At5g39570.1* was shown to form aggregates upon physiological conditions *in vitro* (**Figure 65**). Harsh chemical conditions were required to dissolve the protein complexes.

The above-described consensus of *At5g39570.1* and the MORF proteins in the context of biochemical features and phenotypic observations in combination with their exclusive abundance in plant proteins and their observed interaction *in vitro*, render *At5g39570.1* a good candidate protein for an involvement in RNA processes. No involvement of *At5g39570.1* in the mitochondrial or plastid genome has been reported, but MORF proteins,

such as the plastid-targeted MORF2, have been shown to interact with MEF and MORF proteins despite their different designated localization (Takenaka *et al.*, 2012). Bentolila *et al.* (2013) therefore suggested an indirect effect of MORF2 on mitochondrial editing. At5g39570.1 could indirectly affect the RNA-editing machinery or be involved in other RNA metabolic processes in the same way, as suggested for MORF7 (Bentolila *et al.*, 2013). Unfortunately, neither co-immunoprecipitation experiments, nor affinity chromatography-based pull-down assays identified specific binding partners of At5g39570.1. Further experiments are required to confirm the binding of At5g39570.1 to MORF family members.

4.8.3 Identification of additional, putative binding partners

The yeast-two-hybrid assay additionally identified the peripheral membrane protein PUX2 (AT2G01650), the pectin lyase-like protein AT4G24780 and the unknown proteins At4g23885 and At5g63350 as putative binding partners of At5g39570.1. PUX2 (Plant ubiquitin regulatory x domain-containing protein 2) is a negative, transcriptional regulator of a powdery mildew that infects *A. thaliana* (Chandran *et al.*, 2009). Orthologs of At5g39570.1 revealed decreased expression levels in response to the mildew *Fusarium oxysporum* in *Solanum lycopersicum*, or when challenged by competitive neighboring plants in *Centaurea maculosa*. However, an interaction of At5g39570.1 with these proteins is unlikely, as they were only identified once by the yeast-two-hybrid assay and do not reveal further connection to the protein. Also the identification of the ribosomal proteins S17 and L6 in the yeast-two-hybrid assay has to be considered carefully, as they were only identified once. Ribosomal proteins, transcription factors (e.g. AtERF-8) and heat shock factors are the most common false-positive identifications in yeast-two-hybrid assays (Hengen, 1997) as they are directly involved in generation of the target proteins and their stabilization. TCTP (AT3G16640) was previously identified as a putative false-positive protein in our lab by using an aldehyde dehydrogenase bait protein (Hou, 2015), suggesting a false-positive identification in this screen. Verification of all candidate proteins by independent methods is required to establish genuine At5g39570.1-binding proteins.

4.9 Identification of proteins under the control of phospholipase D

The comparison of total and phosphoproteoms of two-dimensional gels from wild-type and *pld*-mutant plants could not identify additional proteins under the control of the phospholipase D family (**Figure 74** & **Figure 75**). Two dimensional screening for putative downstream targets of PLD is difficult, as protein spots might appear as complexes, migrate at unexpected molecular weights or are not phosphorylated. The complex regulatory network of phospholipases in combination with their overlapping functions in producing phosphatidic acid species impedes the detection of downstream targets. However, a number of plant PA-binding proteins that are indirectly regulated by PLD have been identified (Hou *et al.*, 2015). Generation of PA *via* the PLC/DGK pathway mainly results in the formation of PA 16:0/18:2 and PA 16:0/18:3 species. Additional PA species like 18:3/18:2 PA and 18:2/18:2 PA are commonly generated by PLDs (Vergnolle *et al.*, 2005). Therefore, the spectrum of proteins regulated by members of the PLD family may be wider. The assignment of distinct, molecular PA species to specific regulation processes is one of the future tasks that might disclose PA-binding and interacting mechanisms.

5. Outlook

The extensive characterization of At5g39570.1 in this thesis provides insights in the regulation and function of a novel target of phospholipase D and its cleavage product phosphatidic acid.

A regulation model has been suggested, but additional transcriptional and post-transcriptional data is required to support the suggested expression profiles of At5g39570.1 in response to abiotic stresses. The impact of salinity and osmotic stress on the expression of At5g39570.1 should be further investigated. Wound-stress was shown to induce the expression of PLD α 1 and is therefore a possible expansion of stress-treatments in order to study expression profiles of At5g39570.1.

The expression of At5g39570.1 is dependent on PLD α 1 and partly on other PLD isoforms. To unravel the upstream targets of At5g39570.1, protein expression should be compared in single-mutant lines of the twelve Arabidopsis PLD isoforms, which generate unique sets of PA species and concentrations. External applications of PA may help to uncover concentration and PA species-specific requirements of At5g39570.1. While binding of PA to At5g39570.1 was confirmed in this study, no PA-binding domain has been identified. The identification of a genuine PA-binding domain is in the center of research since many years, but it remains unclear how PA binds to target proteins and exerts its function. The results obtained in this thesis suggest, that PA-binding takes place in the N-terminal half of the protein. However, complete solubilization of the C-terminal fragment was not yet possible and should be repeated. The generation of constructs with partial sequences of At5g39570.1 and subsequent testing of PA-binding affinities may help to identify the PA-binding domain of this protein. To assign distinct PA-species to the observed PA-binding events, lipid-binding assays should be repeated with specific PA species.

Distinct PA-species were previously reported to affect target proteins by translocation and disorder-to-order transitions (Hou *et al.* 2015). Stress-induced up-regulation of PA species may therefore result in the translocation of At5g39570.1 in water-limiting conditions. Stable transformation of *At5g39570.1-GFP* and subsequent *in vivo* monitoring of the protein At5g39570.1 in response to abiotic stress may reveal a translocation of the protein and help to unravel its function. To uncover putative PA-induced disorder-to-order transitions, the protein needs to be completely dissolved and analyzed by circular dichroism (CD) analysis. CD

analysis will dissolve the proteins structure and may confirm At5g39570.1 to be intrinsically disordered.

The highly similar primary structures and homologous N-terminal regions of At5g39570.1 and At3g29075, points to a redundant function of both proteins. However, the role of At3g29075 has not been elucidated in this work and will be in the focus of a new doctoral project. It is unclear whether At3g29075 interacts with At5g39570.1 and is involved in PLD-mediated pathways. The generation of At3g29075-specific antibodies will enable expression studies of At3g29075 in response to various stresses and allow testing for an interaction of At3g29075 with At5g39570.1 and PLDs, respectively. Monitoring of At3g29075 knock-down mutants upon environmental stress conditions may further support to uncover its physiological role. To functionally characterize At5g39570.1, over-expression lines that were generated in this study will be monitored upon standard and stress conditions. RNA sequencing will reveal altered gene-expression levels in mutant plants and may hint to a potential involvement of the protein in physiological pathways. Yeast-two-hybrid analyses identified various RNA-binding proteins as candidate interaction partners of At5g39570.1. Further protein-protein interaction assays, such as bimolecular fluorescence complementation assays or tandem affinity purifications will be applied to confirm these interactions. RNA-binding assays will be conducted to support an involvement of At5g39570.1 in RNA-processing events. It will be further investigated whether a potential PA-induced conformational change of At5g39570.1 affects its function.

Phosphoproteoms of the twelve *Arabidopsis pld* single-mutants will be analyzed by two-dimensional gel-electrophoresis to detect further downstream targets of PLDs.

6. Summary

Previous work on phospholipases led to the discovery of altered phosphoproteoms in *plda1*-mutant lines (Shen, 2008, Kuhn, 2009). A prominent phosphoprotein in wild-type plants that was missing in *plda1* mutants was identified as the unknown protein At5g39570.1. After a first, short characterization of this protein during my Diploma thesis (Ufer, 2010), I continued and expanded its characterization in the context of PLD-regulatory networks in this thesis.

Orthologs of the full-size protein At5g39570.1 were identified in nearly all plant families. *In silico* analysis revealed extraordinary features of the protein At5g39570.1 that incorporates ten imperfect tandem repeats in its C-terminal end. Amino acid composition, hydrophobicity and secondary structure of the protein suggests a separation of At5g39570.1 into two major regions with distinct properties. Blast analysis further supported the division of At5g39570.1 into a conserved N-terminal region and a more variable C-terminal protein half. The homologous protein At3g29075 shares high sequence similarities in the N-terminal protein half, whereas its C-terminal region is unique. A redundant function of the homologous protein At3g29075 could not be identified by the generation and analysis of double knock-out/knock-down mutant plants.

At5g39570.1 was confirmed to be a downstream target of the PLD-regulated signaling network by protein blot analysis using antibodies directed against PLD α 1 and At5g39570.1. It was demonstrated that the abundance of At5g39570.1 is dependent on different members of the PLD family whereat PLD α 1 is the key regulator for the expression of At5g39570.1. Drought and partially salinity were shown to induce expression of At5g39570.1 in the absence of PLD α 1. A regulatory model for At5g39570.1 was constructed based on its transcript and protein expression levels in response to water-limiting conditions. A repressor was hypothesized to block the transcription of *At5g39570.1* in the absence of PLD α 1. Drought-induced accumulation of lipid-signaling molecules, such as PA may displace the repressor from the gene and enable protein production.

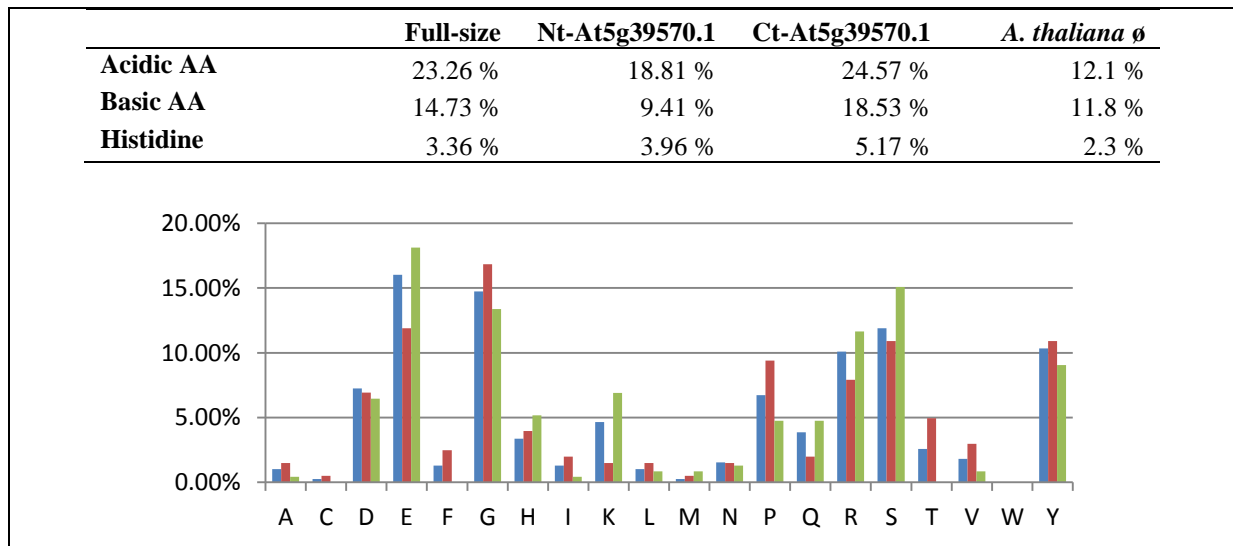
A direct interaction of PLD α 1 and At5g39570.1 was not observed and is unlikely. However, an indirect interaction of both proteins *via* the second messenger phosphatidic acid was shown, especially in the N-terminal protein region. PA-binding does not trigger post-translational regulations of At5g39570.1, but might induce a disorder-to-order transition of this intrinsically disordered protein, which eventually results in gain of function. To further functionally characterize the protein, wild-type and mutant plants were grown and

phenotypically monitored upon different abiotic stresses. At5g39570.1 knock-out mutants displayed a necrotic phenotype similar to *plda1* mutants in response to severe salinity, while wild-type plants were only slightly impaired. Water-limiting conditions further led to an increased phosphorylation of At5g39570.1 in the wild type and propagated At5g39570.1 expression levels in *plda1* mutants. Similar observations were reported from orthologs in previous studies, suggesting a role of the protein in response to abiotic stress.

A yeast-two-hybrid assay identified potential interacting candidates that are involved in various RNA-associated processes. Repetitive identification of members of the MORF family suggests a function of At5g39570.1 in RNA-editing processes. The mRNA-splicing protein U1-70K was also identified repeatedly in the yeast-two-hybrid assay and was additionally found by the DELTA blast analysis of At5g39570.1. Although *in silico* analysis supports a function of At5g39570.1 in RNA-binding events, additional protein-protein interaction methods could not yet confirm the candidate interacting partners. Further experiments are required to classify At5g39570.1 as a genuine protein involved in RNA-processing.

Two-dimensional gel analysis could not detect prominent, novel candidate proteins under the control of selected members of the PLD family.

7. Supplementary data



Supplementary figure 1: Amino acid composition of protein fragments.
 Blue: full-size At5g39570.1; Red: Nt-At5g39570.1; Green: Ct-At5g39570.1.

At5g39570.1:

MPYYTRDDNDVDDFDEFDPTPYSGGYDITVIYGRPIPPSDETCYPLSSGVDDDFEYER
PEFTQIHEPSAYGDEALNTEYSSYSRPKPRPAFRPDSGGGGHVQGERPNPGYGSESGY
GRKPESEYGSYGGQTEVEYGRRPEQSYGSGYGGRTETESEYGSGGGRTEVEYGR
RPESGLGSGYGGRSESEYERKPSYGRSEEQEEGYRKPSYGRSEEQEEGYRKPSYGRSE
EQEEGYRKPSYGRSEEEQEEGYRKPSYGRSEEQEEGSYRKPSYGRSDDQVESYIKPSY
GRSEEQEEGSYRKPSYGRSEEQEEGSYRKQPSYGRGNDDDDDEQRRNRSGSGDDEE
GSYGRKKYGGNDSDEDEEKKKHRHKHHHQKRRDEDDE

At5g39570.2

MRLVILSHLVSMNISNTRDLNLLRSMSLLLTVMKLLTQSTVAILDPSHDPHFDPIQVV
VVMFKVKDQILVMDLNPVMGGNRNLSTDLAMVDKRRWSMVGDLSRVMDLVMVE
GRRLNRSMDLVVVEELRLSMVGDNLQGLDLVMVGDRSLSMSVSLAMEGLRNKKKVV
IGSLAMEDLKNKRKVTGSQVMEDLRSRKKDIESLAMEDLRRNKRKVIGSLAMEDLR
NKRKEVTGNLVMGGLMIRWRVTLSLAMEDLRNRRREVTGSLVMGGLRNKRKRGVTG
SSLAMAVAMTMMMMSSVGTVLVLMMRKGAAMAARNMVAMTLMRMRRRRSTVT
SITTRS VVTKTMSKLNPLCARECNENVCLLSLKNLLNKELSHIPFYIISSDVG VVFV

Full-size construct At5g39570.1

MAYYTRDDNDVDDFDEFDPTPYSGGYDITVIYGRPIPPSDETCYPLSSGVDDDFEYER
PEFTQIHEPSAYGDEALNTEYSSYSRPKPRPAFRPDSGGGGHVQGERPNPGYGSESGY
GRKPESEYGSYGGQTEVEYGRRPEQSYGSGYGGRTETESEYGSGGGRTEVEYGR
RPESGLGSGYGGRSESEYERKPSYGRSEEQEEGYRKPSYGRSEEQEEGYRKPSYGRSE
EQEEGYRKPSYGRSEEEQEEGYRKPSYGRSEEQEEGSYRKPSYGRSDDQVESYIKPSY
GRSEEQEEGSYRKPSYGRSEEQEEGSYRKQPSYGRGNDDDDDEQRRNRSGSGDDEE
GSYGRKKYGGNDSDEDEEKKKHRHKHHHQKRRDEDLEHHHHHH

N-terminal construct of At5g39570.1 (Nt-At5g39570.1)

MPYYTRDDNDVDDFDEFDPTPYSGGYDITVIYGRPIPPSDETCYPLSSGVDDDFEYERPEFTQI
HEPSAYGDEALNTEYSSYSRPKPRPAFRPDSGGGGHVQGERPNPGYGSESGYGRKPESEYGS
YGGQTEVEYGRRPEQSYGSGYGGRTETESEYGSGGGRTEVEYGRRPESGLGSGYGGRSESE
YERKPSYHHHHHH

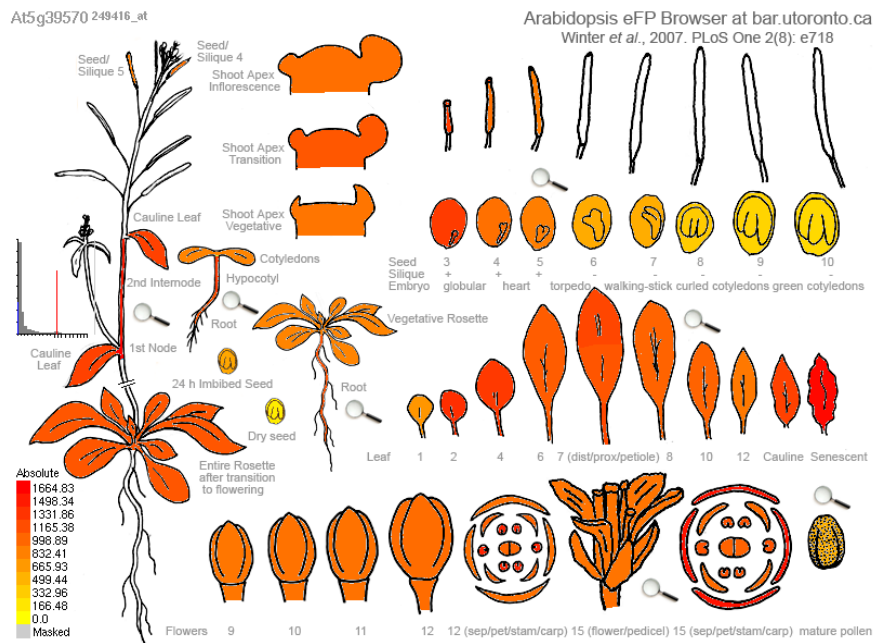
C-terminal construct of At5g3957.1 (Ct-At5g39570.1)

MGSSHHHHHHSSGLVPRGSHMASRPESGLGSGYGGRSESEYERKPSYGRSEEQEEGY
RKPSYGRSEEQEEGYRKPSYGRSEEQEEGYRKPSYGRSEEEQEEGYRKPSYGRSEEQEE
EGSYRKPSYGRSDDQVESYIKPSYGRSEEQEEGSYRKPSYGRSEEQEEGSYRKQPSY
RGNDDDDDDEQRRNRSGSGDDEEGSYGRKKYGGNDSDEDEEKKKHRHKHHHQKRR
DEDDE

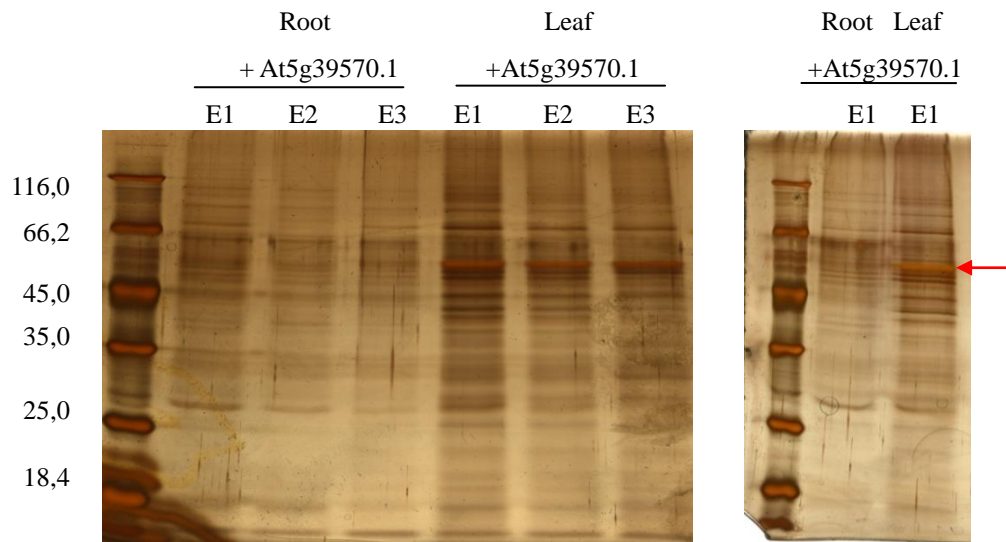
Supplementary figure 2: Overview of protein sequences from constructs and proteins.

		1	10	20	30	44	Section 1
At5g39570.1	(1)	MPYYTRDDNDVDDFDEFDPTFVSGGYDITVIYGRFIPPSDETCY					
At5g39570.1 - C-terminal	(1)	-----					
At5g39570.1 - N-terminal	(1)	MPYYTRDDNDVDDFDEFDPTFVSGGYDITVIYGRFIPPSDETCY					
		45	50	60	70	88	Section 2
At5g39570.1	(45)	PLSSGVDDDFEYERPEFTQIHEPSAYGDEALNTEYSSYSRKPFR					
At5g39570.1 - C-terminal	(1)	-----					
At5g39570.1 - N-terminal	(45)	PLSSGVDDDFEYERPEFTQIHEPSAYGDEALNTEYSSYSRKPFR					
		89	100	110	120	132	Section 3
At5g39570.1	(89)	FAFRPDSGGGGHVOGERPNIPGYGSESGYGRKPESEYSGYGGOT					
At5g39570.1 - C-terminal	(1)	-----					
At5g39570.1 - N-terminal	(89)	FAFRPDSGGGGHVOGERPNIPGYGSESGYGRKPESEYSGYGGOT					
		133	140	150	160	176	Section 4
At5g39570.1	(133)	EVEYGRRPEOSYGSYGGRTEIETSEYGSGGGRTEVYVGRRPES					
At5g39570.1 - C-terminal	(1)	-----METGSSHHHHHSGLVPRG-----HMTLSRPPES					
At5g39570.1 - N-terminal	(133)	EVEYGRRPEOSYGSYGGRTEIETSEYGSGGGRTEVYVGRRPES					
		177	190	200	210	220	Section 5
At5g39570.1	(177)	GLGSGYGRSESEYERKPSYGRSEEOEGYRKPYSYGRSEEOEFG					
At5g39570.1 - C-terminal	(32)	GLGSGYGRSESEYERKPSYGRSEEOEGYRKPYSYGRSEEOEFG					
At5g39570.1 - N-terminal	(177)	GLGSGYGRSESEYERKPSYHHHHH-----					
		221	230	240	250	264	Section 6
At5g39570.1	(221)	YRKPSYGRSEEOEGYRKPYSYGRSEEOEGYRKPYSYGRSEEOE					
At5g39570.1 - C-terminal	(76)	YRKPSYGRSEEOEGYRKPYSYGRSEEOEGYRKPYSYGRSEEOE					
At5g39570.1 - N-terminal	(203)	-----					
		265	270	280	290	308	Section 7
At5g39570.1	(265)	EGSYRKPYSYGRSDDOVESYIKPSYGRSEEOEGSYRKPYSYGRSE					
At5g39570.1 - C-terminal	(120)	EGSYRKPYSYGRSDDOVESYIKPSYGRSEEOEGSYRKPYSYGRSE					
At5g39570.1 - N-terminal	(203)	-----					

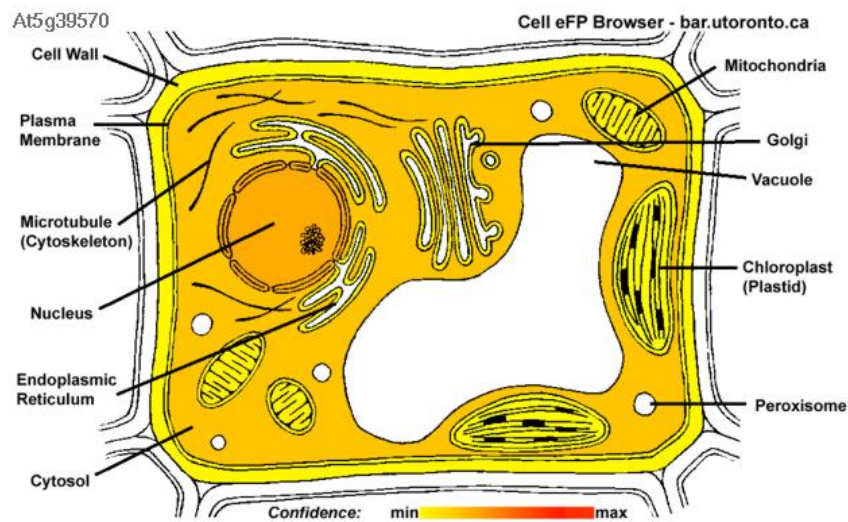
Supplementary figure 3: Alignment of At5g39570.1, Nt-At5g39570.1 and Ct-At5g39570.1. Alignment was conducted with VectorNTI.



Supplementary figure 4: Expression analysis of At5g39570.1 based on micro-array data in *A. thaliana*. Data and picture were obtained from the Arabidopsis eFP Browser.



Supplementary figure 5: Silver stains of Ni-NTA affinity chromatography. Total proteins from leaf and root extracts with (+At5g39570.1) bait protein. Red arrow: At5g39570.1.



Supplementary figure 6: Silver Prediction of sub-cellular localization for At5g39570.1. Data obtained from SUBA (Heazlewood *et al.*, 2007).

caagaaacaaaagagtaaacaacacagagaagcttctttaaaccgactactataaccagagatgacaacgacgtcgacgatttcgatga
gtttgatccaacgccgtacagtggtgttacgacatcacggtgatctacggccgtccgattccacctccgatgagacttggtatcctctcatctggtg
tcgaTGATGAttcgaatacagagagacCTGAatttactcagatccatgagccttctgcttacggTGATGAagctctaacacagagtac
agtagctattctcgaccaagccacgaccgcatttcgaccggattcaggtggtggtgcatgttcaaggtgaaagaccaaactcgtggtatggatC
TGAatccggttatgggaggaaccggaatCTGAgtacggatctggctatggtggacaaacggaggtggagtatggtcggagacCTGA
gagagttatggatctggtatggtggaaggacggagaCTGAatcggagtatggatctggtggtggtggaagaaCTGAggttgagtatggtag
gagacCTGAatcagggcttggatctggtatggtggagatcggagtCTGAgtatgagcgtaaacc
tagctatggaaggtCTGAgaacaagaagaaggtataggaagcctagctatggaagatCTGAagaacaagaggaaggttacaggaagcc
aagttatggaagatCTGAaggagcaggaagaaggatataagaaagcctagctatggaagatCTGAaggaggaacaagaggaaggttatagga
agcctagctatggaagatCTGAaggaacaagaggaaggaaggttacaggaacctagttatgggaggtCTGATGAtcaggtggagagttac
attaagcctagctatggaagatCTGAaggaacaggagggaggaagttacaggaagcctagttatgggaggtCTGAaggaacaggaagaggg
gagttacaggaagcagcctagctatggccgtggcaatgacgaTGATGATGATGAgcagcgtaggaaccgttctggttctggTGAT
GAtgaggaagggagctatggccgcaagaaatattggtggcaatgactCTGATGAggatgaggagaagaagaagcaccgtcacaagcatc
accaccagaagcgtcgtgacgaagacgatgactaaaccctctctgtgctagagagttaatagagaatgtgtgttgcctagcctcaaaaatct
actaaataaagagctaagtcacatacctttctacataataatctccgacgttggtgtgtgtttgtaattctctgtattactacagagcttcgactgg
ttcataataagaccttaagtgtattgggtccacctgtaactgttctactctgtttcgtttctatctatcgtttgtgttatgattactttctatcctataaa
ttaTGATGAtcatttcgttaataatcagaatgtttttgcatgaattggaattagatggaactttgtttaagg

Supplementary figure 7: Putative C-/D-box elements in *At5g39570.1*.

Red: C-Box sequence; Yellow: D-Box sequence. Grey: Position of putative antisense fragments a & b; Green: Start/ stop codon.

Supplementary table 1: Species with putative orthologs of At5g39570.1 (e-value < 10⁻⁵)

Family or phylum	Selected identified species with e-value < 10 ⁻⁵	
Amaranthaceae	XP_010665793.1	<i>Beta vulgaris</i>
Amborellaceae	XP_006827331.1	<i>Amborella trichopoda</i>
Arecaceae	XP_008800496.1	<i>Phoenix dactylifera</i>
Brassicaceae	KFK33197.1	<i>Arabidopsis thaliana</i>
Cucurbitaceae	KGN64592.1	<i>Cucumis sativus</i>
Euphorbiaceae	AAP46157.1	<i>Hevea brasiliensis</i>
Fabaceae	XP_003543859.2	<i>Glycine max</i>
Malvaceae	KJB11082.1	<i>Gossypium raimondii</i>
Moraceae	XP_010088125.1	<i>Morus notabilis</i>
Musaceae	XP_009419095.1	<i>Musa acuminata</i>
Myrtaceae	KCW56276.1	<i>Eucalyptus grandis</i>
Pinaceae	AAU_87303.1	<i>Pinus halepensis</i>
Poaceae	ACF88189.1	<i>Zea mays</i>
Rosaceae	XP_004304279.1	<i>Fragaria vesca</i>
Rubiaceae	CDO99684.1	<i>Coffea canephora</i>
Rutaceae	XP_006431210.1	<i>Citrus clementina</i>
Salicaceae	XP_006384339.1	<i>Populus trichocarpa</i>
Solanaceae	XP_006338424.1	<i>Solanum tuberosum</i>
Vitaceae	XP_002283932.1	<i>Vitis vinifera</i>
Lycophytes	XP_002979763.1	<i>Selaginella moellendorffii</i>
Cyanobacteria	EPG67155.1	<i>Leptospira wolffii</i>
Cnidaria	XP_001628456.1	<i>Nematostella vectensis</i>
Spirochaetes	WP017295764	<i>Geminocystis herdmanii</i>
Mollusca	XP_005101488.1	<i>Aplysia californica</i>
Mammals	XP_007616887.1	<i>Cricetulus griseus</i>

The e-value represents indicates significance of sequence identities.

Supplementary table 2: Top results of protein blast for At5g39570.1

Species	Query cover	E-value	Ident.	Accession
<i>Arabidopsis thaliana</i>	100%	0.0	100%	NP_568565.2
<i>Capsella rubella</i>	100%	0.0	90%	XP_006283824.1
<i>Arabidopsis lyrata</i>	100%	0.0	93%	XP_002870774.1
<i>Capsella rubella</i>	100%	0.0	85%	XP_006283825.1
<i>Camelina sativa</i>	100%	0.0	86%	XP_010441070.1
<i>Eutrema salsugineum</i>	100%	0.0	75%	XP_006405620.1
<i>Camelina sativa</i>	100%	3e-171	83%	XP_010435878.1
<i>Capsella rubella</i>	100%	1e-169	77%	XP_006283826.1
<i>Arabidopsis thaliana</i>	100%	5e-136	71%	KFK33197.1
<i>Eutrema salsugineum</i>	100%	1e-125	64%	XP_006405619.1
<i>Brassica rapa</i>	100%	2e-121	69%	XP_009139903.1
<i>Brassica napus</i>	100%	2e-115	65%	CDY30254.1
<i>Brassica napus</i>	100%	4e-105	62%	CDX74447.1
<i>Tarenaya hassleriana</i>	92%	1e-86	53%	XP_010552803.1
<i>Brassica napus</i>	100%	1e-84	54%	CDX95231.1
<i>Medicago truncatula</i>	95%	5e-68	47%	XP_003618539.1
<i>Malus domestica</i>	99%	2e-66	48%	XP_008353427.1
<i>Malus domestica</i>	99%	2e-64	47%	XP_008341598.1
<i>Medicago truncatula</i>	92%	2e-64	47%	KEH25017.1
<i>Tarenaya hassleriana</i>	100%	5e-63	52%	XP_010528357.1
<i>Pyrus x bretschneideri</i>	99%	7e-57	46%	XP_009360594.1
<i>Cicer arietinum</i>	100%	8e-56	45%	XP_004489417.1
<i>Ricinus communis</i>	94%	1e-54	44%	XP_002530006.1
<i>Cicer arietinum</i>	99%	1e-53	45%	XP_012568118.1

continues

Species	Query cover	E-value	Ident.	Accession
<i>Prunus mume</i>	93%	2e-52	43%	XP_008230802.1
<i>Fragaria vesca subsp. vesca</i>	99%	1e-51	45%	XP_004304279.1
<i>Populus trichocarpa</i>	100%	3e-51	46%	XP_006384339.1
<i>Vitis vinifera</i>	99%	1e-50	47%	XP_002283932.1
<i>Malus domestica</i>	100%	7e-49	41%	XP_008379385.1
<i>Solanum lycopersicum</i>	92%	1e-48	47%	XP_004232206.1
<i>Citrus sinensis</i>	79%	2e-47	51%	XP_006482634.1
<i>Nicotiana tomentosiformis</i>	95%	3e-47	43%	XP_009608846.1
<i>Arabis alpina</i>	40%	6e-47	63%	KFK33783.1
<i>Citrus sinensis</i>	63%	2e-46	55%	KDO36693.1
<i>Arabidopsis thaliana (At3g29075)</i>	40%	4e-46	60%	AA576703.1
<i>Populus euphratica</i>	100%	6e-46	44%	XP_011014107.1
<i>Arabidopsis thaliana</i>	40%	1e-45	60%	NP_189551.1
<i>Brassica rapa</i>	51%	3e-45	57%	XP_009151796.1
<i>Arabidopsis lyrata</i>	46%	4e-45	55%	XP_002877154.1
<i>Citrus clementina</i>	95%	7e-45	46%	XP_006431210.1
<i>Cucumis melo</i>	94%	7e-45	44%	XP_008443383.1
<i>Solanum tuberosum</i>	96%	1e-44	45%	XP_006338424.1
<i>Jatropha curcas</i>	63%	1e-44	47%	XP_012084739.1
<i>Nicotiana sylvestris</i>	95%	2e-44	42%	XP_009781780.1
<i>Populus euphratica</i>	100%	3e-44	42%	XP_011008581.1
<i>Populus trichocarpa</i>	92%	4e-44	46%	XP_006389469.1
<i>Solanum lycopersicum</i>	75%	4e-44	44%	XP_010317109.1
<i>Solanum tuberosum</i>	75%	5e-44	43%	XP_006363410.1
<i>Citrus sinensis</i>	49%	8e-44	59%	KDO36694.1
<i>Brassica napus</i>	51%	2e-43	57%	CDX85244.1
<i>Populus euphratica</i>	100%	1e-42	40%	XP_011008580.1
<i>Cucumis sativus</i>	95%	3e-42	44%	XP_004136693.1
<i>Sesamum indicum</i>	70%	4e-42	47%	XP_011098657.1
<i>Populus euphratica</i>	100%	6e-42	41%	XP_011008579.1
<i>Nelumbo nucifera</i>	100%	6e-42	41%	XP_010258396.1
<i>Brassica napus</i>	36%	8e-42	61%	CDY04054.1
<i>Phaseolus vulgaris</i>	49%	2e-41	53%	XP_007151256.1
<i>Nicotiana tomentosiformis</i>	99%	4e-41	36%	XP_009628950.1
<i>Nelumbo nucifera</i>	87%	9e-41	44%	XP_010258398.1
<i>Camelina sativa</i>	40%	1e-40	64%	XP_010425710.1
<i>Gossypium raimondii</i>	79%	2e-40	46%	KJB11098.1
<i>Brassica napus</i>	36%	2e-40	61%	CDY44410.1
<i>Solanum lycopersicum</i>	75%	5e-40	42%	XP_010317110.1
<i>Gossypium raimondii</i>	95%	6e-40	44%	XP_012441353.1
<i>Camelina sativa</i>	40%	6e-40	64%	XP_010502930.1
<i>Erythranthe guttatus</i>	63%	1e-39	48%	XP_012851132.1
<i>Brassica rapa</i>	36%	1e-39	61%	XP_009129332.1
<i>Camelina sativa</i>	41%	2e-39	62%	XP_010495864.1
<i>Theobroma cacao</i>	83%	2e-39	48%	XP_007032610.1
<i>Populus euphratica</i>	100%	9e-39	42%	XP_011035800.1
<i>Coffea canephora</i>	95%	9e-39	39%	CDP02257.1
<i>Populus trichocarpa</i>	74%	2e-38	47%	XP_006389471.1
<i>Medicago truncatula</i>	43%	2e-37	55%	AFK48716.1
<i>Glycine max</i>	71%	3e-37	46%	XP_003543859.2
<i>Jatropha curcas</i>	87%	3e-37	43%	XP_012084738.1
<i>Glycine soja</i>	71%	1e-36	47%	KHN13204.1
<i>Populus euphratica</i>	72%	2e-36	46%	XP_011035798.1
<i>Genlisea aurea</i>	57%	5e-36	48%	EPS71766.1
<i>Gossypium arboreum</i>	95%	4e-35	46%	KHG07281.1
<i>Morus notabilis</i>	95%	9e-35	41%	XP_010088125.1

E-value: The expectation value defines the likeliness that the sequence identity is based on chance, rather than homology. A low e-value ($E < 10^{-10}$) represents a significant sequence identity.

Supplementary table 3: Results of blast for the full length cDNA of *At5g39570.1* in *A. thaliana*

Description	Query cover	E- value	Ident.	Accession
AT5g39570/MIJ24_40	99%	0.0	100%	AY058080.1
At3g29075 gene	34%	3e-46	76%	BT012216.1
AT3g29075/MXE2_1	34%	3e-46	76%	AY125517.1
nuclear protein X1	2%	0.090	89%	NM_125727.5
uncharacterized protein	2%	0.090	84%	NM_001160924.1
chromosome 4 sequence	5%	0.31	90%	CP002687.1
chromosome 2, sequence	7%	0.31	93%	CP002685.1
AT4G15880	1%	0.31	90%	AK316760.1
tracheary element differentiation-like protein 7	1%	0.31	93%	NM_124269.2
ubiquitin-like-specific protease ESD4	1%	0.31	90%	NM_117680.3
myb domain protein 110	1%	0.31	90%	NM_001084751.1
AAA-ATPase 1	1%	0.31	100%	NM_123364.1
At5g48920 gene	1%	0.31	93%	BT011316.1
At5g48920	1%	0.31	93%	BT010840.1
At5g22310/MWD9_9	1%	0.31	96%	AY133525.1
clone F13P17 map ve016	1%	0.31	93%	AC004481.3
unknown protein (Z97339.45) ,	1%	0.31	90%	AY081548.1
uncharacterized protein ,	1%	0.31	96%	NM_122136.1
Unknown protein (Z97339.45) ,	1%	0.31	90%	AF386934.1
DNA chromosome 4, contig fragment No. 42	1%	0.31	90%	AL161542.2
DNA chromosome 4, ESSA I FCA fragment	1%	0.31	90%	Z97339.2
genomic DNA, chromosome 3, TAC	1%	0.31	90%	AB025615.1
genomic DNA, chromosome 5,	1%	0.31	96%	AB007651.1
RH1, TC1, G14587-5/6 , and PRL1 genes	1%	0.31	90%	Y11187.1
SUMO protease (esd4 gene)	1%	0.31	90%	AJ582719.1
hypothetical protein (1189 bp)	1%	0.31	90%	Y11155.1
chromosome 1 sequence	5%	1.1	92%	CP002684.1
reticulon-like protein B17	1%	1.1	93%	NM_201759.2
uncharacterized protein	1%	1.1	96%	NM_112352.3
RAFL09-89-L14	1%	1.1	96%	AK227180.1
hypothetical protein (At2g20590)	1%	1.1	93%	AY649311.1
(At2g20590/F23N11.9) ,	1%	1.1	93%	AY219046.1
chromosome 2 clone F23N11	1%	1.1	93%	AC007048.5

E-value: The expectation value defines the likeliness that the sequence identity is based on chance, rather than homology. A low e-value ($E < 10^{-10}$) represents a significant sequence identity.

Supplementary table 4: Blast result for ribosomal fragment a

Description	Query	Ident.	Accession
<i>Spirometra erinaceieuropaei</i> genome assembly	100%	100%	LN161904.1
predicted: <i>Cynoglossus semilaevis</i> receptor-type tyrosine-protein phosphatase F	100%	100%	XM_008334621.1
<i>Drosophila melanogaster</i> 3L BAC RP98-2C22	100%	100%	AC010017.5
<i>Gongylonema pulchrum</i> genome assembly	100%	100%	LL787056.1
<i>Echinostoma caproni</i> genome assembly	100%	100%	LL234345.1
<i>Solanum pennellii</i>	100%	100%	HG975442.1

Supplementary table 5: Blast result for ribosomal fragment b.

Description	Accession	Query coverage	Ident.	Accession
<i>Camelina sativa</i> uncharacterized protein At5g39570-like		100%	100%	XM_010442768.1
chromosome 5 sequence		100%	100%	CP002688.1
Zebra fish DNA sequence in linkage group 10		100%	100%	CR925781.6
uncharacterized protein		100%	100%	NM_123319.2

Supplementary table 6: *Arabidopsis*-specific nucleotide blast result for *At5g39570.1*-fragment a.

Description	Accession
At1g80960	BT030468.1
protein kinase	NM_103590.3
chromatin remodeling 31	NM_100428.3
myb domain protein 110	NM_001084751.1
protein kinase	NM_001084210.1
At5g61510	BT029771.1
F-box protein	NM_202465.1
GroES-like zinc-binding alcohol dehydrogenase family protein	NM_125544.3
pirin-1	NM_115784.2
UDP-glucosyl transferase 85A4	NM_106476.3
chromosome 2 clone F21P24	AC004401.3
pirin (PRN1)	AF353716.1
protein EMBRYO DEFECTIVE 1211	NM_001203438.1
myo-inositol monophosphatase like 2	NM_120072.4
eukaryotic translation initiation factor 3 subunit C	NM_001203173.1
DUO pollen 3 (DUO3)	FJ461625.1
aldose 1-epimerase-like protein	NM_121518.3
uncharacterized protein	NM_121329.5
universal stress protein PHOS34	NM_118866.4
phosphoinositide phospholipase C 2	NM_111686.5
uncharacterized protein	NM_121198.3
emp24/gp25L/p24 family/GOLD domain-containing protein	NM_113829.2
specific DNA binding transcription factor	NM_111947.3
kinase interacting (KIP1-like) protein	NM_100844.2
cysteine/histidine-rich C1 domain-containing protein	NM_127874.3
zinc finger CCCH domain-containing protein 21	NM_127587.2
eukaryotic translation initiation factor 3 subunit C	NM_115473.2
DNA-binding storekeeper protein-related transcriptional regulator	NM_128124.2
IBR domain containing protein	NM_127714.1
phosphoinositide phospholipase C 2	NM_001035583.1
phosphoinositide phospholipase C 7	NM_115452.1
AT4g27320/M4I22_130	AY123998.1
protein EMBRYO DEFECTIVE 1211	NM_122170.2
At2g32760/F24L7.10	AY075661.1
AT3g11100/F11B9_105	AY064137.1

Supplementary table 7: *Arabidopsis*-specific nucleotide blast result for *At5g39570.1*-fragment b.

Description	Accession
18S pre-ribosomal assembly protein gar2-related protein	NM_201683.2
alpha/beta-Hydrolases superfamily protein	NM_116124.2
At3g62590/F26K9_20	BT002305.1
AAA-ATPase 1	NM_123364.1
3-epi-6-deoxocathasterone 23-monooxygenase	NM_119801.3
ubiquitin-like-specific protease ESD4	NM_117680.3
At4g36380	BT029220.1
sequence-specific DNA binding transcription factor	NM_112274.3
calcium dependent protein kinase 6	NM_127284.2
unknown protein (At3g14180)	AY113853.1
putative calmodulin-domain protein kinase CPK6 (At2g17290)	AY140007.1
Unknown protein (Z97339.45)	AF386934.1
RH1, TC1, G14587-5, G14587-6, and PRL1 genes	Y11187.1
calmodulin-domain protein kinase CDPK isoform 6 (CPK6)	U31835.1
for SUMO protease (esd4 gene)	AJ582719.1
for cytochrome P450,	AB008097.1
fructose-bisphosphate aldolase 3	NM_126176.4
triacylglycerol lipase	NM_128726.1
At2g01140 (At2g01140/F10A8.2)	AF325014.2
genomic DNA, 3, P1 clone: MAG2	AP000600.1
calnexin2	NM_001203320.1
GC-rich sequence DNA-binding factor-like protein with Tuftelin interacting domain	NM_001084572.2
ecotype Landsberg erecta 3 genomic sequence	HQ698308.1
DNA primase	NM_001161303.1
peptidyl-prolyl cis-trans isomerase-like 1	NM_129172.5
60S acidic ribosomal protein P1-1	NM_179238.3
zinc finger CCCH domain-containing protein 17	NM_126276.3
reticulon-like protein B18	NM_118985.2
transcription factor MYB98	NM_117993.3
leucine-rich repeat receptor-like protein kinase (LRR-RLK), partial cds	FJ708737.1
Rossmann-fold NAD(P)-binding domain-containing protein	NM_115389.3

Supplementary table 8: Overview of literature and large-scale studies that identified At5g39570.1.

Identified in	Effect	Notes	Species	Reference
mature pollen		protein identification	<i>A. thaliana</i> <i>landsberg</i>	(Sheoran <i>et al.</i> , 2006)
seeds	up-regulation	protein accumulation	<i>A. thaliana</i>	(Fu <i>et al.</i> , 2005)
plant		identification of a putative 2 nd reading frame	<i>A. thaliana</i>	(Baerenfaller <i>et al.</i> , 2008)
zygotical/ somatic embryos		protein identification	<i>Theobroma cacao</i>	(Niemenak <i>et al.</i> , 2015)
microsomes	phosphorylation of peptides	salt stress	<i>A. thaliana</i>	(Chang <i>et al.</i> , 2012)
germinating plant	differential expression	salt stress	<i>Glycine max</i>	(Yin <i>et al.</i> , 2014)
buds/young plant	differential expression	decreased expression in off-crops (crops with reduced fruits) increased expression in on-crops	<i>Clementine mandarin</i>	(Muñoz-Fambuena <i>et al.</i> , 2013)
seedlings	up-regulation	photoreceptor - mutant <i>phyA/phyB/cry1/cry2</i>	<i>A. thaliana</i>	(Fox <i>et al.</i> , 2015)
roots	up-regulation	Zn-accumulating plants	<i>A. thaliana</i>	(Filatov <i>et al.</i> , 2006)
roots / leaves	differential gene expression	competitive neighboring plants	<i>Centaurea maculosa Lam</i>	(Broz <i>et al.</i> , 2008)
seedlings	high transcript levels	In etiolated seedlings “candidate sequence for involvement in vicine / covicine pathway”	<i>Vicia faba</i>	(Ray <i>et al.</i> , 2015)
roots	down-regulation	long-term boron deficiency associated with the MUTE promoter	<i>Citrus sinensis</i> <i>A. thaliana</i>	(Yang <i>et al.</i> , 2013) (Williams, 2013)
plant/ leaves				
plant	up-regulation	long-day conditions	<i>A. thaliana</i>	(Baerenfaller <i>et al.</i> , 2015)
plant	up-regulation	<i>In silico</i> analysis by MASS (Mapping and alignment with short sequences): candidate gene for UVB-induced root-growth arrest.	<i>A. thaliana</i>	(Brar, 2013)
leaves	differential expression	identified by comparing light and dark harvested plants	<i>Glycine max</i>	(Lee, 2013)
plant		identified as a target of CPK3	<i>A. thaliana</i>	(Mehlmer, 2008)
leaves/buds	differential regulation		<i>Camellia sinensis</i>	(Li <i>et al.</i> , 2015)
seedlings	down-regulation	in response to space conditions	<i>A. thaliana</i>	(Mazars <i>et al.</i> , 2014)
leaves	down-regulation	infection with Las “down-regulation of photosynthesis-related genes”	<i>A. thaliana</i>	(Nwugo <i>et al.</i> , 2013)
leaves		Identification of a phosphorylation site	<i>A. thaliana</i>	(Laugesen <i>et al.</i> , 2006)
leaves	differential regulation	up-regulation upon salt stress and down-regulation upon spermidin treatment	<i>Cucumber</i>	(Li <i>et al.</i> , 2013)
leaves		identification of phosphopeptides	<i>A. thaliana</i>	(Wang <i>et al.</i> , 2009)
root	down-regulation	In response to <i>Fusarium oxysporum</i>	<i>Solanum lycopersicum</i>	Silva, 2012 (Master thesis)

Supplementary table 9: Arabidopsis-specific nucleotide-blast of At5g39570.1-fragments with antisense complementarity.

Description	Locus	Sequence identity	Fragment
phosphoinositide phospholipase C 2	AT3G08510	19/19	A
phosphoinositide phospholipase C 7	AT3G55940	19/19	A
		14/14	B
sequence-specific DNA binding transcription factor	AT3G11100	19/19	A
eukaryotic translation initiation factor 3 subunit C	AT3G56150	19/19	A
F-box/LRR-repeat protein	AT3G59220	19/19	A
F-box protein	AT3G60790	19/19	A
myb domain protein 110	AT3G29020	19/19	A
emp24/gp25L/p24 family/GOLD	AT3G29070	19/19	A
pentatricopeptide repeat-containing protein	AT3G59040	18/18	A
pentatricopeptide repeat-containing protein	AT3G29230	18/19	A
sequence-specific DNA binding transcription factor	AT3G14180	17/17	B
58671 bp at 5' side: uncharacterized protein 26598 bp at 3' side: putative F-box protein	AT2G11165	16/16	B
zinc finger CCCH domain-containing protein 17	AT2G02160	16/16	B
CLAVATA1-related receptor kinase-like protein	AT3G49670	16/16	B
Rossmann-fold NAD(P)-binding domain-containing protein	AT3G55310	16/16	B
DNase I-like superfamily protein	AT1G40390	16/16	B
receptor protein kinase like protein	At3g49670	16/16	B
myb-like HTH transcriptional regulator-like	AT2G20400	16/16	B
Chloroplast protein enhancing stress tolerance	AT5G44650	16/16	B
pentatricopeptide repeat-containing protein	AT5G55840	15/15	B

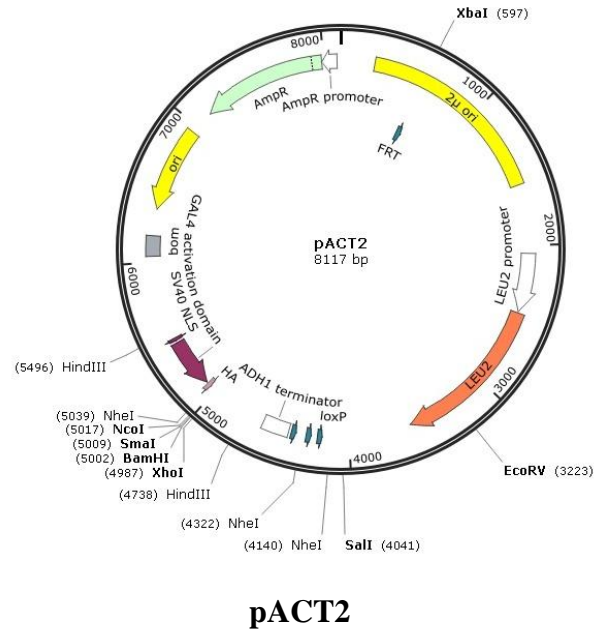
Supplementary table 10: DELTA BLAST At5g39570.1

Description	Query	E-value	Ident.	Accession
THO complex subunit 2	69%	6e-10	13%	NP_173871.6
F5A9.21	69%	2e-09	13%	AAG03122.1
DEAD-box ATP-dependent RNA helicase 26	70%	9e-09	13%	NP_196478.2
MIF4G and MA3 domain-containing protein	64%	1e-08	12%	NP_178208.1
RNA helicase-like protein	70%	3e-08	13%	BAB10010.1
Protein kinase superfamily protein	57%	2e-05	13%	NP_563928.3
formin binding protein-like	27%	4e-05	20%	BAB02553.1
RNA helicase	60%	2e-04	12%	CAA09213.1
Splicing factor U2af large subunit A	49%	3e-04	21%	NP_849509.1
protein kinase family protein	27%	4e-04	11%	NP_190932.1
pre-mRNA-processing protein 40B	27%	5e-04	20%	NP_188601.4
serine/threonine-protein kinase PRP4	64%	5e-04	11%	NP_189213.2
RNA recognition motif-containing protein RRC1	60%	5e-04	10%	NP_568464.1
Dicer	40%	7e-04	15%	AEZ02177.1
endoribonuclease Dicer-like 1	40%	7e-04	15%	NP_171612.1
T25K16.4	40%	7e-04	15%	AAF26461.1
putative TPR repeat nuclear phosphoprotein	49%	7e-04	13%	AAM15237.1
RNA polymerase IV largest subunit	64%	7e-04	14%	AAAY89362.1
Splicing factor U2af large subunit A	40%	8e-04	13%	NP_1190937.1
nuclear RNA polymerase D1B	64%	8e-04	14%	NP_181532.2
Dicer	40%	9e-04	15%	AEZ02176.1
protein early flowering 8	49%	0.001	13%	NP_178674.6
DEAD-box ATP-dependent RNA helicase 31	40%	0.001	14%	NP_201168.2
SWAP/Supr domain-containing protein	71%	0.002	12%	NP_568820.1
CAF protein	44%	0.002	15%	AAF03534.1
DNA ligase 4	43%	0.002	10%	NP_568851.2
putative clathrin interactor EPSIN 2	76%	0.003	13%	NP_850386.1
SWAP/Supr domain-containing protein	71%	0.003	12%	NP_851194.1
At2g43170/F14B2.11	76%	0.004	13%	AAK91471.1
F14N23.20	61%	0.004	11%	AAD32882.1
RecName: Full=DEAD-box ATP-dependent RNA helicase 31	40%	0.004	14%	Q9FFQ1.2
putative clathrin interactor EPSIN 2	62%	0.005	13%	NP_1031535.1
ania-6a type cyclin	46%	0.006	8%	AAK49036.1
Splicing factor U2af large subunit A	49%	0.007	21%	NP_195387.1
Pre-mRNA-splicing factor 3	24%	0.009	21%	NP_174127.1
RNA recognition motif-containing protein	66%	0.016	16%	NP_200378.1
Similar to RNA helicases	19%	0.040	20%	AAF98437.1
plant mobile domain family protein	39%	0.052	12%	NP_175490.1
nucleolar GTP-binding protein 1	32%	0.080	12%	NP_175505.1
multiple organellar RNA editing factor	60%	0.081	16%	NP_193735.1
DEAD-box ATP-dependent RNA helicase 50	51%	0.11	11%	NP_187354.1
U1 snRNP 70K protein - <i>Arabidopsis thaliana</i> (fragment)	50%	0.12	14%	S28147

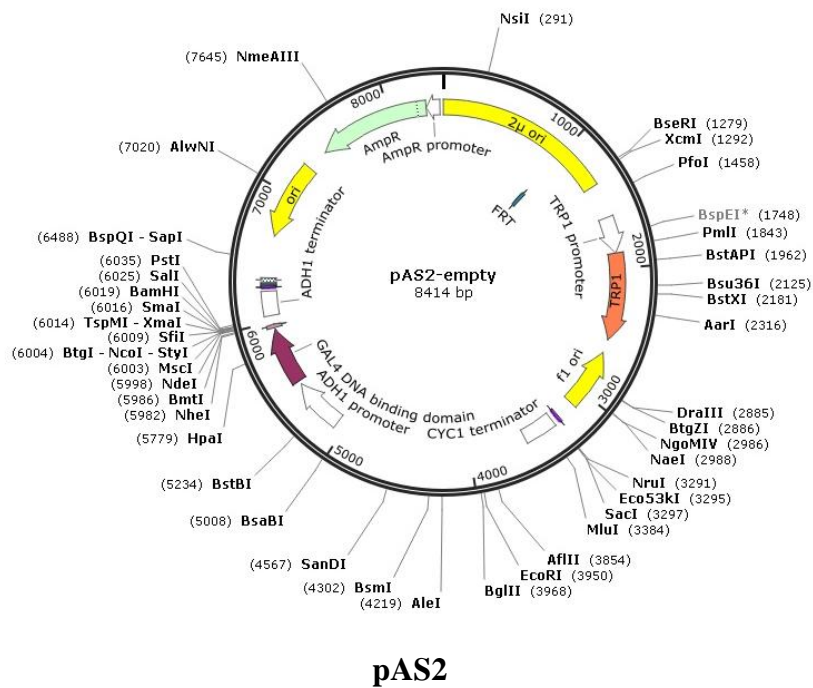
E-value: The expectation value defines the likeliness that the sequence identity is based on chance, rather than homology. A low e-value ($E < 10^{-10}$) represents a significant sequence identity.

Vector maps

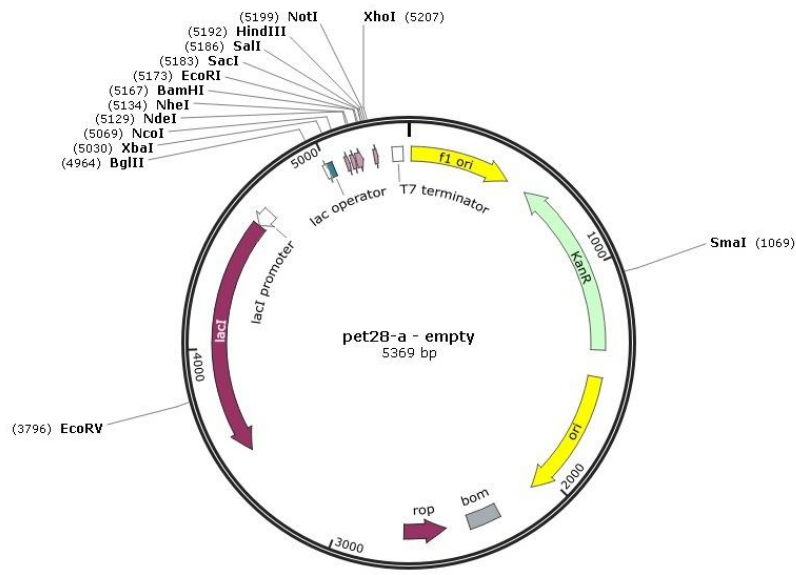
For more information see section 2.1.6.



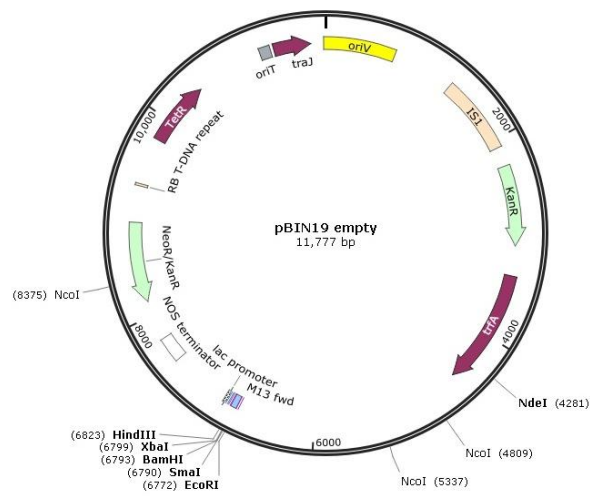
pACT2



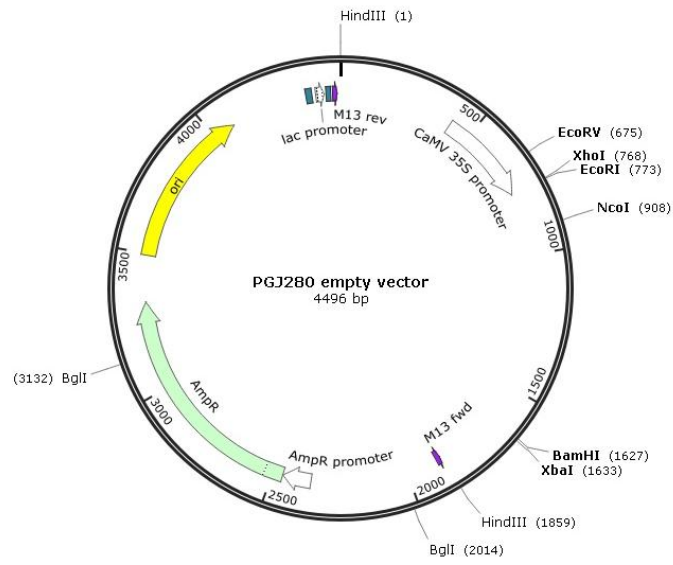
pAS2



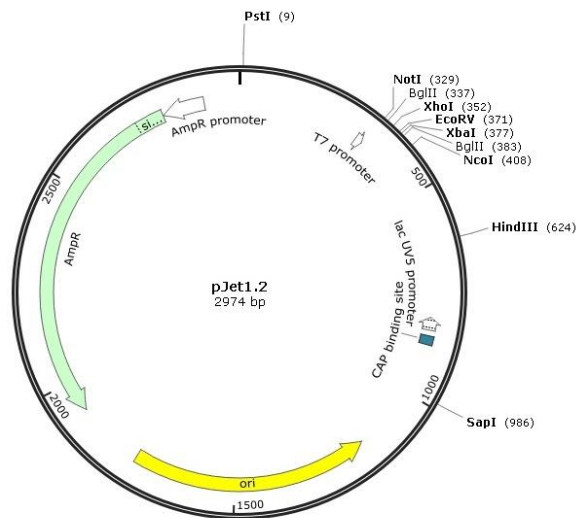
pet28-a



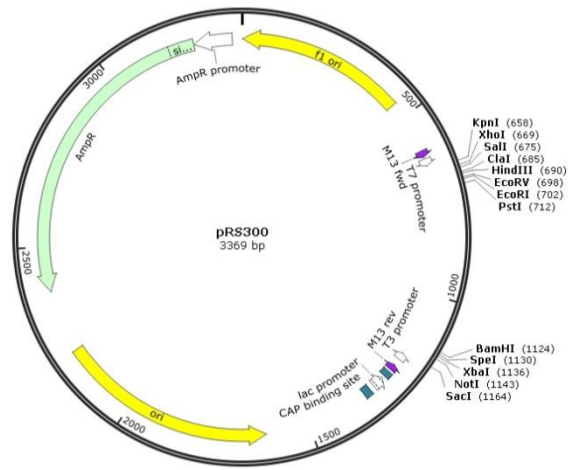
pBIN19



PGJ280



pJET1.2



pRS300

8. References

- Adkins S. & Burmeister M. (1996) Visualization of DNA in agarose gels as migrating colored bands: applications for preparative gels and educational demonstrations. *Analytical biochemistry*, **240**, 17-23.
- Ahmad K. & Henikoff S. (2002) Epigenetic Consequences of Nucleosome Dynamics. *Cell*, **111**, 281-284.
- Alvarez-Venegas R., Sadler M., Hlavacka A., Baluška F., Xia Y., Lu G., . . . Dubrovsky J.G. (2006) The Arabidopsis homolog of trithorax, ATX1, binds phosphatidylinositol 5-phosphate, and the two regulate a common set of target genes. *Proceedings of the National Academy of Sciences*, **103**, 6049-6054.
- Andrews S.J. & Rothnagel J.A. (2014) Emerging evidence for functional peptides encoded by short open reading frames. *Nat Rev Genet*, **15**, 193-204.
- Anfinsen C.B. (1972) The formation and stabilization of protein structure. *Biochemical Journal*, **128**, 737-749.
- Anthony R.G., Khan S., Costa J., Pais M.S. & Bögre L. (2006) The Arabidopsis protein kinase PTII-2 is activated by convergent phosphatidic acid and oxidative stress signaling pathways downstream of PDK1 and OXII. *Journal of Biological Chemistry*, **281**, 37536-37546.
- Arimura G.-i. & Sawasaki T. (2010) Arabidopsis CPK3 plays extensive roles in various biological and environmental responses. *Plant Signaling & Behavior*, **5**, 1263-1265.
- Arisz S.A., Testerink C. & Munnik T. (2009) Plant PA signaling via diacylglycerol kinase. *Molecular and Cell Biology of Lipids*, **1791**, 869-875.
- Bachelier J.-P., Cavaillé J. & Hüttenhofer A. (2002) The expanding snoRNA world. *Biochimie*, **84**, 775-790.
- Baerenfaller K., Grossmann J., Grobei M.A., Hull R., Hirsch-Hoffmann M., Yalovsky S., . . . Baginsky S. (2008) Genome-Scale Proteomics Reveals *Arabidopsis thaliana* Gene Models and Proteome Dynamics. *Science*, **320**, 938-941.
- Baerenfaller K., Massonnet C., Hennig L., Russenberger D., Sulpice R., Walsh S., . . . Gruissem W. (2015) A long photoperiod relaxes energy management in Arabidopsis leaf six. *Current Plant Biology*, **2**, 34-45.
- Bah A., Vernon R.M., Siddiqui Z., Krzeminski M., Muhandiram R., Zhao C., . . . Forman-Kay J.D. (2015) Folding of an intrinsically disordered protein by phosphorylation as a regulatory switch. *Nature*, **519**, 106-109.
- Barford D., Hu S.H. & Johnson L.N. (1991) Structural mechanism for glycogen phosphorylase control by phosphorylation and AMP. *Journal of Molecular Biology*, **218**, 233-260.
- Bargmann B.O., Laxalt A.M., ter Riet B., van Schooten B., Merquiol E., Testerink C., . . . Munnik T. (2009) Multiple PLDs required for high salinity and water deficit tolerance in plants. *Plant and Cell Physiology*, **50**, 78-89.
- Bargmann B.O.R. & Munnik T. (2006) The role of phospholipase D in plant stress responses. *Current Opinion in Plant Biology*, **9**, 515-522.
- Barrangou R., Fremaux C., Deveau H., Richards M., Boyaval P., Moineau S., . . . Horvath P. (2007) CRISPR provides acquired resistance against viruses in prokaryotes. *Science*, **315**, 1709-1712.
- Bentolila S., Oh J., Hanson M.R. & Bukowski R. (2013) Comprehensive High-Resolution Analysis of the Role of an Arabidopsis Gene Family in RNA Editing. *PLoS Genet*, **9**, e1003584.
- Blobel G. & Dobberstein B. (1975) Transfer of proteins across membranes. I. Presence of

- proteolytically processed and unprocessed nascent immunoglobulin light chains on membrane-bound ribosomes of murine myeloma. *The Journal of Cell Biology*, **67**, 835-851.
- Bockmühl D.P., Krishnamurthy S., Gerads M., Sonneborn A. & Ernst J.F. (2001) Distinct and redundant roles of the two protein kinase A isoforms Tpk1p and Tpk2p in morphogenesis and growth of *Candida albicans*. *Molecular Microbiology*, **42**, 1243-1257.
- Boratyn G., Schaffer A., Agarwala R., Altschul S., Lipman D. & Madden T. (2012) Domain enhanced lookup time accelerated BLAST. *Biology Direct*, **7**, 12.
- Bradford M.M. (1976) A rapid and sensitive method for the quantitation of microgram quantities of protein utilizing the principle of protein-dye binding. *Analytical Biochemistry*, **72**, 248-254.
- Brar A. (2013) Dissecting DNA Damage Responses in Arabidopsis: A High-Throughput Sequencing Approach. *Oregon State University*.
- Braun H.-P. & Schmitz U.K. (1999) The protein-import apparatus of plant mitochondria. *Planta*, **209**, 267-274.
- Broz A.K., Manter D.K., Callaway R.M., Paschke M.W. & Vivanco J.M. (2008) A molecular approach to understanding plant-plant interactions in the context of invasion biology. *Functional Plant Biology*, **35**, 1123-1134.
- Bu Z. & Callaway D.J.E. (2011) Chapter 5 - Proteins MOVE! Protein dynamics and long-range allostery in cell signaling. *Advances in Protein Chemistry and Structural Biology*, pp. 163-221.
- Cai S., He F., Samra H.S., de la Maza L.M., Bottazzi M.E., Joshi S.B. & Middaugh C.R. (2009) Biophysical and Stabilization Studies of the Chlamydia trachomatis Mouse Pneumonitis Major Outer Membrane Protein. *Molecular pharmaceuticals*, **6**, 1553-1561.
- Cameron I. (2012) Acidic proteins of the nucleus. *Elsevier*.
- Camoni L., Di Lucente C., Pallucca R., Visconti S. & Aducci P. (2012) Binding of phosphatidic acid to 14-3-3 proteins hampers their ability to activate the plant plasma membrane H⁺-ATPase. *IUBMB life*, **64**, 710-716.
- Capelluto D.G. (2013) Lipid-mediated Protein Signaling. *Springer*.
- Cevik V.J., (2015) Einfluss verschiedener Stressoren auf die Expression des Proteins At5g39570.1 in *Arabidopsis thaliana*. Bachelor thesis. *Unpublished*.
- Chandran D., Tai Y.C., Hather G., Dewdney J., Denoux C., Burgess D.G., . . . Wildermuth M.C. (2009) Temporal Global Expression Data Reveal Known and Novel Salicylate-Impacted Processes and Regulators Mediating Powdery Mildew Growth and Reproduction on Arabidopsis. *Plant Physiology*, **149**, 1435-1451.
- Chang I.-F., Hsu J.-L., Hsu P.-H., Sheng W.-A., Lai S.-J., Lee C., . . . Chen C.-C. (2012) Comparative phosphoproteomic analysis of microsomal fractions of *Arabidopsis thaliana* and *Oryza sativa* subjected to high salinity. *Plant Science*, **185-186**, 131-142.
- Cheever M.L., Sato T.K., de Beer T., Kutateladze T.G., Emr S.D. & Overduin M. (2001) Phox domain interaction with PtdIns(3)P targets the Vam7 t-SNARE to vacuole membranes. *Nat Cell Biol*, **3**, 613-618.
- Chevallet M., Luche S. & Rabilloud T. (2006) Silver staining of proteins in polyacrylamide gels. *Nature Protocols*, **1**, 1852-1858.
- Ciuzan O., Hancock J., Pamfil D., Wilson I. & Ladomery M. (2015) The evolutionarily conserved multifunctional glycine-rich RNA-binding proteins play key roles in development and stress adaptation. *Physiologia Plantarum*, **153**, 1-11.
- Clough S.J. & Bent A.F. (1998) Floral dip: a simplified method for *Agrobacterium*-mediated transformation of *Arabidopsis thaliana*. *The Plant Journal*, **16**, 735-743.
- Darwish E., Testerink C., Khalil M., El-Shihy O. & Munnik T. (2009) Phospholipid signaling

- responses in salt-stressed rice leaves. *Plant and Cell Physiology*, **50**, 986-997.
- Deak M., Casamayor A., Currie R.A., Downes C.P. & Alessi D.R. (1999) Characterisation of a plant 3-phosphoinositide-dependent protein kinase-1 homologue which contains a pleckstrin homology domain. *FEBS letters*, **451**, 220-226.
- Demarse N.A., Ponnusamy S., Spicer E.K., Apohan E., Baatz J.E., Ogretmen B. & Davies C. (2009) Direct binding of glyceraldehyde 3-phosphate dehydrogenase to telomeric DNA protects telomers against chemotherapy-induced rapid degradation. *Journal of molecular biology*, **394**, 789-803.
- Devaiah S.P., Roth M.R., Baughman E., Li M., Tamura P., Jeannotte R., . . . Wang X. (2006) Quantitative profiling of polar glycerolipid species from organs of wild-type Arabidopsis and a phospholipase D α 1 knockout mutant. *Phytochemistry*, **67**, 1907-1924.
- DeWald D.B., Torabinejad J., Jones C.A., Shope J.C., Cangelosi A.R., Thompson J.E., . . . Hama H. (2001) Rapid accumulation of phosphatidylinositol 4, 5-bisphosphate and inositol 1, 4, 5-trisphosphate correlates with calcium mobilization in salt-stressed Arabidopsis. *Plant physiology*, **126**, 759-769.
- Distéfano A., Scuffi D., García-Mata C., Lamattina L. & Laxalt A. (2012) Phospholipase D δ is involved in nitric oxide-induced stomatal closure. *Planta*, **236**, 1899-1907.
- Domínguez-González I., Vázquez-Cuesta S., Algaba A. & Diez-Guerra F. (2007) Neurogranin binds to phosphatidic acid and associates to cellular membranes. *Biochem. J*, **404**, 31-43.
- Dunker A.K., Romero P., Obradovic Z., Garner E.C. & Brown C.J. (2000) Intrinsic Protein Disorder in Complete Genomes. *Genome Informatics*, **11**, 161-171.
- Durfee T., Becherer K., Chen P.L., Yeh S.H., Yang Y., Kilburn A.E., . . . Elledge S.J. (1993) The retinoblastoma protein associates with the protein phosphatase type 1 catalytic subunit. *Genes & Development*, **7**, 555-569.
- Edwards K., Johnstone C. & Thompson C. (1991) A simple and rapid method for the preparation of plant genomic DNA for PCR analysis. *Nucleic Acids Research*, **19**, 1349.
- Elias M., Potocky M., Cvrckova F. & Zarsky V. (2002) Molecular diversity of phospholipase D in angiosperms. *BMC Genomics*, **3**, 2.
- Fields S. & Song O.-k. (1989) A novel genetic system to detect protein-protein interactions. *Nature*, **340**, 245-246.
- Filatov V., Dowdle J., Smirnoff N., Ford-Lloyd B., Newbury H.J. & Macnair M.R. (2006) Comparison of gene expression in segregating families identifies genes and genomic regions involved in a novel adaptation, zinc hyperaccumulation. *Molecular Ecology*, **15**, 3045-3059.
- Fire A., Xu S., Montgomery M.K., Kostas S.A., Driver S.E. & Mello C.C. (1998) Potent and specific genetic interference by double-stranded RNA in *Caenorhabditis elegans*. *Nature*, **391**, 806-811.
- Fox A.R., Barberini M.L., Ploschuk E.L., Muschiatti J.P. & Mazzella M.A. (2015) A proteome map of a quadruple photoreceptor mutant sustains its severe photosynthetic deficient phenotype. *Journal of Plant Physiology*, **185**, 13-23.
- Frank W., Munnik T., Kerkmann K., Salamini F. & Bartels D. (2000) Water Deficit Triggers Phospholipase D Activity in the Resurrection Plant *Craterostigma plantagineum*. *The Plant Cell*, **12**, 111-123.
- Fraser J.S., Clarkson M.W., Degan S.C., Erion R., Kern D. & Alber T. (2009) Hidden alternative structures of proline isomerase essential for catalysis. *Nature*, **462**, 669-673.
- Fu Q., Wang B., Jin X., Li H., Han P., Wei K.-h., . . . Zhu Y. (2005) Proteomic analysis and extensive protein identification from dry, germinating Arabidopsis seeds and young

- seedlings. *Journal of biochemistry and molecular biology*, **38**, 650.
- Gietz R.D. & Schiestl R.H. (2007) High-efficiency yeast transformation using the LiAc/SS carrier DNA/PEG method. *Nat. Protocols*, **2**, 31-34.
- Glisovic T., Bachorik J.L., Yong J. & Dreyfuss G. (2008) RNA-binding proteins and post-transcriptional gene regulation. *FEBS Letters*, **582**, 1977-1986.
- Goldstein A., Baertlein D. & Danon A. (1989) Phosphate starvation stress as an experimental system for molecular analysis. *Plant Molecular Biology Reporter*, **7**, 7-16.
- Golemis E. (2002) Protein-protein interactions : a molecular cloning manual. *Cold Spring Harbor Laboratory Press*.
- Golovkin M. & Reddy A.S. (1996) Structure and expression of a plant U1 snRNP 70K gene: alternative splicing of U1 snRNP 70K pre-mRNAs produces two different transcripts. *The Plant Cell*, **8**, 1421-1435.
- Gozani O., Karuman P., Jones D.R., Ivanov D., Cha J., Lugovskoy A.A., . . . Lessnick S.L. (2003) The PHD finger of the chromatin-associated protein ING2 functions as a nuclear phosphoinositide receptor. *Cell*, **114**, 99-111.
- Gsponer J. & Madan Babu M. (2009) The rules of disorder or why disorder rules. *Progress in Biophysics and Molecular Biology*, **99**, 94-103.
- Guo L., Devaiah S.P., Narasimhan R., Pan X., Zhang Y., Zhang W. & Wang X. (2012a) Cytosolic Glyceraldehyde-3-Phosphate Dehydrogenases Interact with Phospholipase D δ to Transduce Hydrogen Peroxide Signals in the Arabidopsis Response to Stress. *The Plant Cell*, **24**, 2200-2212.
- Guo L., Mishra G., Markham J.E., Li M., Tawfall A., Welti R. & Wang X. (2012b) Connections between Sphingosine Kinase and Phospholipase D in the Abscisic Acid Signaling Pathway in Arabidopsis. *Journal of Biological Chemistry*, **287**, 8286-8296.
- Guo L., Mishra G., Taylor K. & Wang X. (2011) Phosphatidic acid binds and stimulates Arabidopsis sphingosine kinases. *Journal of Biological Chemistry*, **286**, 13336-13345.
- Gustavsson J., Cederberg C., Sonesson U., Van Otterdijk R. & Meybeck A. (2011) Food losses and food waste: extent, causes and prevention. *FAO, Rome*.
- Hanahan D. (1983) Studies on transformation of Escherichia coli with plasmids. *Journal of Molecular Biology*, **166**, 557-580.
- He X.-J., Ma Z.-Y. & Liu Z.-W. (2014) Non-Coding RNA Transcription and RNA-Directed DNA Methylation in Arabidopsis. *Molecular Plant*, **7**, 1406-1414.
- Heazlewood J.L., Verboom R.E., Tonti-Filippini J., Small I. & Millar A.H. (2007) SUBA: the Arabidopsis Subcellular Database. *Nucleic Acids Research*, **35**, D213-D218.
- Hejgaard J. & Boisen S. (1980) High-lysine proteins in Hiproly barley breeding: Identification, nutritional significance and new screening methods. *Hereditas*, **93**, 311-320.
- Hengen P.H. (1997) Methods and reagents: False positives from the yeast two-hybrid system. *Trends in Biochemical Sciences*, **22**, 33-34.
- Hirayama T., Ohto C., Mizoguchi T. & Shinozaki K. (1995) A gene encoding a phosphatidylinositol-specific phospholipase C is induced by dehydration and salt stress in *Arabidopsis thaliana*. *Proceedings of the National Academy of Sciences*, **92**, 3903-3907.
- Hong H. (2014) Toward understanding driving forces in membrane protein folding. *Archives of Biochemistry and Biophysics*, **564**, 297-313.
- Hong Y., Zhang W. & Wang X. (2010) Phospholipase D and phosphatidic acid signalling in plant response to drought and salinity. *Plant, Cell & Environment*, **33**, 627-635.
- Hong Y., Zheng S. & Wang X. (2008) Dual functions of phospholipase D α 1 in plant response to drought. *Molecular Plant*, **1**, 262-269.
- Hou Q. (2015) Comparative studies of selected stress responsive DREB and ALDH genes in *Arabidopsis thaliana*, *Eutrema salsugineum* and *Hordeum vulgare*. *Universitäts-und*

- Landesbibliothek Bonn.*
- Hou Q., Ufer G. and Bartels D. (2015) Lipid signalling in plant responses to abiotic stress. *Plant, cell & environment*.
- Huang S., Gao L., Blanchoin L. & Staiger C.J. (2006) Heterodimeric capping protein from *Arabidopsis* is regulated by phosphatidic acid. *Molecular Biology of the Cell*, **17**, 1946-1958.
- Innis M.A., Gelfand D.H., Sninsky J.J. & White T.J. (2012) PCR protocols: a guide to methods and applications. *Academic press*.
- Izumi Y., Chibata I. & Itoh T. (1978) Herstellung und Verwendung von Aminosäuren. *Angewandte Chemie*, **90**, 187-194.
- Jackson A.O. & Larkins B.A. (1976) Influence of Ionic Strength, pH, and Chelation of Divalent Metals on Isolation of Polyribosomes from Tobacco Leaves. *Plant physiology*, **57**, 5-10.
- Jandl J. (2012) Zelluläre Lokalisierung und Expressionsanalyse des Proteins At5g39570.1 aus *Arabidopsis thaliana*. Diploma thesis. *Unpublished*.
- Jang J.-H., Lee C.S., Hwang D. & Ryu S.H. (2012) Understanding of the roles of phospholipase D and phosphatidic acid through their binding partners. *Progress in Lipid Research*, **51**, 71-81.
- Jeffares D.C., Poole A.M. & Penny D. (1998) Relics from the RNA World. *Journal of Molecular Evolution*, **46**, 18-36.
- Jenkins G.H., Fiset P.L. & Anderson R.A. (1994) Type I phosphatidylinositol 4-phosphate 5-kinase isoforms are specifically stimulated by phosphatidic acid. *Journal of Biological Chemistry*, **269**, 11547-11554.
- Jia M., Wu H., Clay K., Jung R., Larkins B. & Gibbon B. (2013) Identification and characterization of lysine-rich proteins and starch biosynthesis genes in the opaque2 mutant by transcriptional and proteomic analysis. *BMC Plant Biology*, **13**, 60.
- Johnson Louise N. (2009) The regulation of protein phosphorylation. *Biochemical Society Transactions*, **37**, 627-641.
- Joint W. (2007) Protein and amino acid requirements in human nutrition. *World health organization technical report series*, 1.
- Jorda J., Xue B., Uversky V.N. & Kajava A.V. (2010) Protein tandem repeats – the more perfect, the less structured. *FEBS Journal*, **277**, 2673-2682.
- Jose Lopez-Andreo M., Gomez-Fernandez J.C. & Corbalan-Garcia S. (2003) The Simultaneous Production of Phosphatidic Acid and Diacylglycerol Is Essential for the Translocation of Protein Kinase C ϵ to the Plasma Membrane in RBL-2H3 Cells. *Molecular Biology of the Cell*, **14**, 4885-4895.
- Julkowska M.M., McLoughlin F., Galvan-Ampudia C.S., Rankenberg J.M., Kawa D., Klimecka M., . . . Testerink C. (2015) Identification and functional characterization of the *Arabidopsis* Snf1-related protein kinase SnRK2. 4 phosphatidic acid-binding domain. *Plant, cell & environment*, **38**, 614-624.
- Karathanassis D., Stahelin R.V., Bravo J., Perisic O., Pacold C.M., Cho W. & Williams R.L. (2002) Binding of the PX domain of p47(phox) to phosphatidylinositol 3,4-bisphosphate and phosphatidic acid is masked by an intramolecular interaction. *The EMBO Journal*, **21**, 5057-5068.
- Karlova R., Boeren S., Russinova E., Aker J., Vervoort J. & de Vries S. (2006) The *Arabidopsis* somatic embryogenesis receptor-like kinase1 Protein Complex Includes brassinosteroid-insensitive1. *The Plant Cell*, **18**, 626-638.
- Katagiri T., Takahashi S. & Shinozaki K. (2001) Involvement of a novel *Arabidopsis* phospholipase D, AtPLD δ , in dehydration-inducible accumulation of phosphatidic acid in stress signalling. *The Plant Journal*, **26**, 595-605.
- Keegan L., Gill G. & Ptashne M. (1986) Separation of DNA binding from the transcription-

- activating function of a eukaryotic regulatory protein. *Science*, **231**, 699-704.
- Kelly S.M., Jess T.J. & Price N.C. (2005) How to study proteins by circular dichroism. *Biochimica et Biophysica Acta (BBA) - Proteins and Proteomics*, **1751**, 119-139.
- Kim D.-Y., Scalf M., Smith L.M. & Vierstra R.D. (2013a) Advanced Proteomic Analyses Yield a Deep Catalog of Ubiquitylation Targets in Arabidopsis. *The Plant Cell*, **25**, 1523-1540.
- Kim S.-C., Guo L. & Wang X. (2013b) Phosphatidic acid binds to cytosolic glyceraldehyde-3-phosphate dehydrogenase and promotes its cleavage in Arabidopsis. *Journal of Biological Chemistry*, **288**, 11834-11844.
- Klenova E., Chernukhin I., Inoue T., Shamsuddin S. & Norton J. (2002) Immunoprecipitation techniques for the analysis of transcription factor complexes. *Methods*, **26**, 254-259.
- Klimecka M., Szczegieliński J., Godecka L., Lewandowska-Gnatowska E., Dobrowolska G. & Muszynska G. (2011) Regulation of wound-responsive calcium-dependent protein kinase from maize (ZmCPK11) by phosphatidic acid. *Acta Biochim Pol*, **58**, 589-595.
- Kocourková D., Krčková Z., Pejchar P., Veselková Š., Valentová O., Wimalasekera R., . . . Martinec J. (2011) The phosphatidylcholine-hydrolysing phospholipase C NPC4 plays a role in response of Arabidopsis roots to salt stress. *Journal of Experimental Botany*, **62**, 3753-3763.
- König S., Ischebeck T., Lerche J., Stenzel I. & Heilmann I. (2008) Salt-stress-induced association of phosphatidylinositol 4, 5-bisphosphate with clathrin-coated vesicles in plants. *Biochem. J*, **415**, 387-399.
- Kooijman E. & Testerink C. (2010) Phosphatidic Acid: An Electrostatic/Hydrogen-Bond Switch? In: *Lipid Signaling in Plants*, pp. 203-222. Springer Berlin Heidelberg.
- Kooijman E.E., Chupin V., de Kruijff B. & Burger K.N.J. (2003) Modulation of Membrane Curvature by Phosphatidic Acid and Lysophosphatidic Acid. *Traffic*, **4**, 162-174.
- Kooijman E.E., Tieleman D.P., Testerink C., Munnik T., Rijkers D.T., Burger K.N. & De Kruijff B. (2007) An electrostatic/hydrogen bond switch as the basis for the specific interaction of phosphatidic acid with proteins. *Journal of Biological Chemistry*, **282**, 11356-11364.
- Kopka J., Pical C., Gray J.E. & Müller-Röber B. (1998) Molecular and Enzymatic Characterization of Three Phosphoinositide-Specific Phospholipase C Isoforms from Potato. *Plant Physiology*, **116**, 239-250.
- Kuhn A. (2009) Molekulare Analysen von Phospholipase D (PLD) Mutanten. Diploma thesis. *Unpublished*.
- Kusner D.J., Barton J.A., Qin C., Wang X. & Iyer S.S. (2003) Evolutionary conservation of physical and functional interactions between phospholipase D and actin. *Archives of Biochemistry and Biophysics*, **412**, 231-241.
- Kyte J. & Doolittle R.F. (1982) A simple method for displaying the hydropathic character of a protein. *Journal of Molecular Biology*, **157**, 105-132.
- Laemmli U.K. (1970) Cleavage of Structural Proteins during the Assembly of the Head of Bacteriophage T4. *Nature*, **227**, 680-685.
- Larrieu A. & Vernoux T. (2015) Comparison of plant hormone signalling systems. *Essays In Biochemistry*, **58**, 165-181.
- Laugesen S., Messinese E., Hem S., Pichereaux C., Grat S., Ranjeva R., . . . Bono J.-J. (2006) Phosphoproteins analysis in plants: A proteomic approach. *Phytochemistry*, **67**, 2208-2214.
- Law Y.-S., Zhang R., Guan X., Cheng S., Sun F., Duncan O., . . . Lim B.L. (2015) Phosphorylation and Dephosphorylation of the Presequence of Precursor multiple organellar rna editing factor3 during Import into Mitochondria from Arabidopsis. *Plant Physiology*, **169**, 1344-1355.
- Lee H. (2013) Identifying Molecular Functions of Heliotropic Motor Tissue Through

- Proteomic Analysis of Soybean Pulvini. *Doctoral dissertation*.
- Lemmon M. & Ferguson K. (2000) Signal-dependent membrane targeting by pleckstrin homology (PH) domains. *Biochem. J.*, **350**, 1-18.
- Li B., He L., Guo S., Li J., Yang Y., Yan B., . . . Li J. (2013) Proteomics reveal cucumber Spd-responses under normal condition and salt stress. *Plant Physiology and Biochemistry*, **67**, 7-14.
- Li M., Hong Y. & Wang X. (2009) Phospholipase D- and phosphatidic acid-mediated signaling in plants. *Molecular and Cell Biology of Lipids*, **1791**, 927-935.
- Li M., Qin C., Welti R. & Wang X. (2006) Double Knockouts of Phospholipases D ζ 1 and D ζ 2 in Arabidopsis Affect Root Elongation during Phosphate-Limited Growth But Do Not Affect Root Hair Patterning. *Plant Physiology*, **140**, 761-770.
- Li Q., Li J., Liu S., Huang J., Lin H., Wang K., . . . Liu Z. (2015) A Comparative Proteomic Analysis of the Buds and the Young Expanding Leaves of the Tea Plant (*Camellia sinensis* L.). *International Journal of Molecular Sciences*, **16**, 14007-14038.
- Li X., Lin H., Zhang W., Zou Y., Zhang J., Tang X. & Zhou J.-M. (2005) Flagellin induces innate immunity in nonhost interactions that is suppressed by *Pseudomonas syringae* effectors. *Proceedings of the National Academy of Sciences of the United States of America*, **102**, 12990-12995.
- Lin S.-L., Miller J.D. & Ying S.-Y. (2006) Intronic MicroRNA (miRNA). *Journal of Biomedicine and Biotechnology*, **2006**, 13.
- Lindsay A.J. & McCaffrey M.W. (2004) The C2 domains of the class I Rab11 family of interacting proteins target recycling vesicles to the plasma membrane. *Journal of Cell Science*, **117**, 4365-4375.
- Lorow D. & Jessee J. (1990) Max efficiency DH10BTM: a host for cloning methylated DNA. *Focus*, **12**, 19.
- Lunde B.M., Moore C. & Varani G. (2007) RNA-binding proteins: modular design for efficient function. *Nat Rev Mol Cell Biol*, **8**, 479-490.
- Lurin C., Andrés C., Aubourg S., Bellaoui M., Bitton F., Bruyère C., . . . Small I. (2004) Genome-Wide Analysis of Arabidopsis Pentatricopeptide Repeat Proteins Reveals Their Essential Role in Organelle Biogenesis. *The Plant Cell*, **16**, 2089-2103.
- Matilla A., Koshy B.T., Cummings C.J., Isobe T., Orr H.T. & Zoghbi H.Y. (1997) The cerebellar leucine-rich acidic nuclear protein interacts with ataxin-1. *Nature*, **389**, 974-978.
- Mazars C., Brière C., Grat S., Pichereaux C., Rossignol M., Pereda-Loth V., . . . Carnero-Diaz E. (2014) Microsome-associated proteome modifications of Arabidopsis seedlings grown on board the International Space Station reveal the possible effect on plants of space stresses other than microgravity. *Plant Signaling & Behavior*, **9**, e29637.
- McLoughlin F. & Testerink C. (2013) Phosphatidic acid, a versatile water-stress signal in roots. *Frontiers in Plant Science*, **4**, 525.
- Mehlmer N. (2008) Ca²⁺ dependent protein kinases in *Arabidopsis thaliana*. *Doctoral dissertation*.
- Missihoun T.D., Schmitz J., Klug R., Kirch H.-H. & Bartels D. (2011) Betaine aldehyde dehydrogenase genes from Arabidopsis with different sub-cellular localization affect stress responses. *Planta*, **233**, 369-382.
- Mullis K.B. & Faloona F.A. (1987) Specific synthesis of DNA in vitro via a polymerase-catalyzed chain reaction. *Methods in enzymology*, **155**, 335.
- Munnik T. (2001) Phosphatidic acid: an emerging plant lipid second messenger. *Trends in Plant Science*, **6**, 227-233.
- Munnik T. (2014) PI-PLC: Phosphoinositide-phospholipase C in plant signaling. In: *Phospholipases in Plant Signaling*, pp. 27-54. Springer.
- Munnik T., Meijer H.J.G., Ter Riet B., Hirt H., Frank W., Bartels D. & Musgrave A. (2000)

- Hyperosmotic stress stimulates phospholipase D activity and elevates the levels of phosphatidic acid and diacylglycerol pyrophosphate. *The Plant Journal*, **22**, 147-154.
- Muñoz-Fambuena N., Mesejo C., Reig C., Agustí M., Tárraga S., Lisón P., . . . González-Mas M.C. (2013) Proteomic study of 'Moncada' mandarin buds from on- versus off-crop trees. *Plant Physiology and Biochemistry*, **73**, 41-55.
- Murashige T. & Skoog F. (1962) A Revised Medium for Rapid Growth and Bio Assays with Tobacco Tissue Cultures. *Physiologia Plantarum*, **15**, 473-497.
- Nakanishi H., Morishita M., Schwartz C.L., Coluccio A., Engebrecht J. & Neiman A.M. (2006) Phospholipase D and the SNARE Sso1p are necessary for vesicle fusion during sporulation in yeast. *Journal of Cell Science*, **119**, 1406-1415.
- Nasr A (2015) Isolation and characterization of the unknown protein At3g29075 from *Arabidopsis thaliana*. Master thesis. *Unpublished*.
- Németh K, Salchert K, Putnoky P, Bhalerao R, Koncz-Kálmán Z, Stankovic-Stangeland B, . . . Koncz C (1998) Pleiotropic control of glucose and hormone responses by PRL1, a nuclear WD protein, in *Arabidopsis*. *Genes & Development* **12** (19):3059-3073.
- Niemenak N., Kaiser E., Maximova S.N., Laremore T. & Gultinan M.J. (2015) Proteome analysis during pod, zygotic and somatic embryo maturation of *Theobroma cacao*. *Journal of Plant Physiology*, **180**, 49-60.
- Nwugo C.C., Duan Y. & Lin H. (2013) Study on Citrus Response to Huanglongbing Highlights a Down-Regulation of Defense-Related Proteins in Lemon Plants Upon 'Ca. Liberibacter asiaticus' Infection. *PLoS ONE*, **8**, e67442.
- Ohlrogge J. & Browse J. (1995) Lipid biosynthesis. *The Plant Cell*, **7**, 957-970.
- Palmer I. & Wingfield P.T. (2001) Preparation and Extraction of Insoluble (Inclusion-Body) Proteins from *Escherichia coli*. *Current Protocols in Protein Science*.
- Pandey B. (2012) Construction of TAP vectors for ALDH3H1 and At5g39570. Project work. *Unpublished*.
- Pappan K., Austin-Brown S., Chapman K.D. & Wang X. (1998) Substrate Selectivities and Lipid Modulation of Plant Phospholipase D α , - β , and - γ . *Archives of Biochemistry and Biophysics*, **353**, 131-140.
- Pappan K. & Wang X. (1999) Molecular and biochemical properties and physiological roles of plant phospholipase D. *Biochimica et Biophysica Acta (BBA) - Molecular and Cell Biology of Lipids*, **1439**, 151-166.
- Peters C., Li M., Narasimhan R., Roth M., Welti R. & Wang X. (2010) Nonspecific phospholipase C NPC4 promotes responses to abscisic acid and tolerance to hyperosmotic stress in *Arabidopsis*. *The Plant Cell*, **22**, 2642-2659.
- Petersen J., Eriksson S.K., Harryson P., Pierog S., Colby T., Bartels D. & Röhrig H. (2012) The lysine-rich motif of intrinsically disordered stress protein CDeT11-24 from *Craterostigma plantagineum* is responsible for phosphatidic acid binding and protection of enzymes from damaging effects caused by desiccation. *Journal of experimental botany*.
- Porath J., Carlsson J.A.N., Olsson I. & Belfrage G. (1975) Metal chelate affinity chromatography, a new approach to protein fractionation. *Nature*, **258**, 598-599.
- Potocký M., Pleskot R., Pejchar P., Vitale N., Kost B. & Žárský V. (2014) Live-cell imaging of phosphatidic acid dynamics in pollen tubes visualized by Spo20p-derived biosensor. *New Phytologist*, **203**, 483-494.
- Qin C., Li M., Qin W., Bahn S.C., Wang C. & Wang X. (2006) Expression and characterization of *Arabidopsis* phospholipase D γ 2. *Biochimica et Biophysica Acta (BBA) - Molecular and Cell Biology of Lipids*, **1761**, 1450-1458.
- Qin C. & Wang X. (2002) The *Arabidopsis* Phospholipase D Family. Characterization of a Calcium-Independent and Phosphatidylcholine-Selective PLD ζ 1 with Distinct Regulatory Domains. *Plant Physiology*, **128**, 1057-1068.

- Ray H., Bock C. & Georges F. (2015) Faba Bean: Transcriptome Analysis from Etiolated Seedling and Developing Seed Coat of Key Cultivars for Synthesis of Proanthocyanidins, Phytate, Raffinose Family Oligosaccharides, Vicine, and Convicine. *The Plant Genome*, **8**.
- Reinders J. & Sickmann A. (2007) Modificomics: Posttranslational modifications beyond protein phosphorylation and glycosylation. *Biomolecular Engineering*, **24**, 169-177.
- Rodriguez M.C.S., Edsgård D., Hussain S.S., Alquezar D., Rasmussen M., Gilbert T., . . . Mundy J. (2010a) Transcriptomes of the desiccation-tolerant resurrection plant *Craterostigma plantagineum*. *The Plant Journal*, **63**, 212-228.
- Rodriguez M.C.S., Petersen M. & Mundy J. (2010b) Mitogen-Activated Protein Kinase Signaling in Plants. *Annual Review of Plant Biology*, **61**, 621-649.
- Röhrig H., Colby T., Schmidt J., Harzen A., Facchinelli F. & Bartels D. (2008) Analysis of desiccation-induced candidate phosphoproteins from *Craterostigma plantagineum* isolated with a modified metal oxide affinity chromatography procedure. *Proteomics*, **8**, 3548-3560.
- Röhrig H., Schmidt J., Colby T., Brautigam A., Hufnagel P. & Bartels D. (2006) Desiccation of the resurrection plant *Craterostigma plantagineum* induces dynamic changes in protein phosphorylation. *Plant, cell and environment*, **29**, 1606-1617.
- Röhrig U.F., Awad L., Grosdidier A., Larrieu P., Stroobant V., Colau D., . . . Michielin O. (2010) Rational Design of Indoleamine 2,3-Dioxygenase Inhibitors. *Journal of Medicinal Chemistry*, **53**, 1172-1189.
- Romero P., Obradovic Z., Li X., Garner E.C., Brown C.J. & Dunker A.K. (2001) Sequence complexity of disordered protein. *Proteins: Structure, Function, and Bioinformatics*, **42**, 38-48.
- Roston R., Gao J., Xu C. & Benning C. (2011) Arabidopsis chloroplast lipid transport protein TGD2 disrupts membranes and is part of a large complex. *The Plant Journal*, **66**, 759-769.
- Ruano M.L.F., Pérez-Gil J. & Casals C. (1998) Effect of Acidic pH on the Structure and Lipid Binding Properties of Porcine Surfactant Protein a: potential role of acidification along its exocytic pathway. *Journal of Biological Chemistry*, **273**, 15183-15191.
- Ruelland E., Cantrel C., Gawer M., Kader J.-C. & Zachowski A. (2002) Activation of Phospholipases C and D Is an Early Response to a Cold Exposure in Arabidopsis Suspension Cells. *Plant Physiology*, **130**, 999-1007.
- Sachetto-Martins G., Franco L.O. & de Oliveira D.E. (2000) Plant glycine-rich proteins: a family or just proteins with a common motif? *Biochimica et Biophysica Acta (BBA) - Gene Structure and Expression*, **1492**, 1-14.
- Sagaram U.S., El-Mounadi K., Buchko G.W., Berg H.R., Kaur J., Pandurangi R.S., . . . Shah D.M. (2013) Structural and functional studies of a phosphatidic acid-binding antifungal plant defensin MtDef4: identification of an RGFRRR motif governing fungal cell entry. *PLoS ONE* 8(12): e82485
- Sambrook J., Fritsch E.F. & Maniatis T. (1989) Molecular cloning (vol. 2). *Cold spring harbor laboratory press New York*.
- Sanford J.C., Smith F.D. & Russell J.A. (1993) Optimizing the biolistic process for different biological applications. *Methods in enzymology* **217** (1993): 483-509.
- Schwab R., Ossowski S., Riester M., Warthmann N. & Weigel D. (2006) Highly Specific Gene Silencing by Artificial MicroRNAs in Arabidopsis. *The Plant Cell*, **18**, 1121-1133.
- Selvy P.E., Lavieri R.R., Lindsley C.W. & Brown H.A. (2011) Phospholipase D - enzymology, functionality, and chemical modulation. *Chemical reviews*, **111**, 6064-6119.
- Serber Z. & Ferrell Jr J.E. (2007) Tuning Bulk Electrostatics to Regulate Protein Function.

- Cell*, **128**, 441-444.
- Sheoran I., Sproule K., Olson D.H., Ross A.S. & Sawhney V. (2006) Proteome profile and functional classification of proteins in *Arabidopsis thaliana* (Landsberg erecta) mature pollen. *Sexual Plant Reproduction*, **19**, 185-196.
- Shen J. (2008) Untersuchungen an Phospholipase D Mutanten in *Arabidopsis thaliana*. Diploma thesis. *Unpublished*.
- Silva T.D.d., Correia M.T.d.S.O. & Silva M.V.d.C. (2012) Análise do perfil protéico em raiz de tomateiro submetido à inoculação com *Fusarium oxysporum* f. sp. *lycopersici*. *Doctoral dissertation*.
- Singh A., Bhatnagar N., Pandey A. & Pandey G.K. (2015) Plant phospholipase C family: Regulation and functional role in lipid signaling. *Cell calcium*.
- Speranza A., Scoccianti V., Crinelli R., Calzoni G.L. & Magnani M. (2001) Inhibition of Proteasome Activity Strongly Affects Kiwifruit Pollen Germination. Involvement of the Ubiquitin/Proteasome Pathway as a Major Regulator. *Plant Physiology*, **126**, 1150-1161.
- Stiti N., Triki S. & Hartmann M.-A. (2007) Formation of triterpenoids throughout *Olea europaea* fruit ontogeny. *Lipids*, **42**, 55-67.
- Sukumaran S. (2015) unknown title. Project work. *Unpublished*.
- Takenaka M., Verbitskiy D., Zehrmann A. & Brennicke A. (2010) Reverse Genetic Screening Identifies Five E-class PPR Proteins Involved in RNA Editing in Mitochondria of *Arabidopsis thaliana*. *Journal of Biological Chemistry*, **285**, 27122-27129.
- Takenaka M., Zehrmann A., Verbitskiy D., Kugelmann M., Härtel B. & Brennicke A. (2012) Multiple organellar RNA editing factor (MORF) family proteins are required for RNA editing in mitochondria and plastids of plants. *Proceedings of the National Academy of Sciences*, **109**, 5104-5109.
- Tanabe N., Kimura A., Yoshimura K. & Shigeoka S. (2009) Plant-specific SR-related protein atSR45a interacts with spliceosomal proteins in plant nucleus. *Plant Molecular Biology*, **70**, 241-252.
- Tasma I.M., Brendel V., Whitham S.A. & Bhattacharyya M.K. (2008) Expression and evolution of the phosphoinositide-specific phospholipase C gene family in *Arabidopsis thaliana*. *Plant Physiology and Biochemistry*, **46**, 627-637.
- Testerink C. & Munnik T. (2011) Molecular, cellular, and physiological responses to phosphatidic acid formation in plants. *Journal of experimental botany*, err079.
- The-Arabidopsis-genome-project (2000) Analysis of the genome sequence of the flowering plant *Arabidopsis thaliana*. *Nature*, **408**, 796-815.
- Thore S., Mayer C., Sauter C., Weeks S. & Suck D. (2003) Crystal Structures of the *Pyrococcus abyssi* Sm Core and Its Complex with rna: common features of rna binding in archaea and eukarya. *Journal of Biological Chemistry*, **278**, 1239-1247.
- Tompa P. (2002) Intrinsically unstructured proteins. *Trends in biochemical sciences*, **27**, 527-533.
- Towbin H., Staehelin T. & Gordon J. (1979) Electrophoretic transfer of proteins from polyacrylamide gels to nitrocellulose sheets: procedure and some applications. *Proceedings of the National Academy of Sciences*, **76**, 4350-4354.
- Tsien R.Y. (1998) the green fluorescent protein. *Annual Review of Biochemistry*, **67**, 509-544.
- Tung W.L. & Chow K.-C. (1995) A modified medium for efficient electrotransformation of *E. coli*. *Trends in Genetics*, **11**, 128-129.
- Ufer G. (2011) Isolierung und Charakterisierung des unbekanntes Proteins At5g39570.1 aus *Arabidopsis thaliana*. Diploma thesis. *Unpublished*.
- Uraji, Misugi, et al. "Cooperative function of PLD δ and PLD α 1 in abscisic acid-induced stomatal closure in *Arabidopsis*." *Plant physiology* 159.1 (2012): 450-460.
- Uversky V.N., Oldfield C.J. & Dunker A.K. (2008) Intrinsically Disordered Proteins in

- Human Diseases: Introducing the D2 Concept. *Annual Review of Biophysics*, **37**, 215-246.
- Valenzuela-Avendaño J., Mota I.E., Uc G., Perera R., Valenzuela-Soto E. & Aguilar J.Z. (2005) Use of a simple method to isolate intact RNA from partially hydrated *Selaginella lepidophylla* plants. *Plant Molecular Biology Reporter*, **23**, 199-200.
- Vaultier M.-N., Cantrel C., Vergnolle C., Justin A.-M., Demandre C., Benhassaine-Kesri G., . . . Ruelland E. (2006) Desaturase mutants reveal that membrane rigidification acts as a cold perception mechanism upstream of the diacylglycerol kinase pathway in *Arabidopsis* cells. *FEBS Letters*, **580**, 4218-4223.
- Vergnolle C., Vaultier M.-N., Taconnat L., Renou J.-P., Kader J.-C., Zachowski A. & Ruelland E. (2005) The Cold-Induced Early Activation of Phospholipase C and D Pathways Determines the Response of Two Distinct Clusters of Genes in *Arabidopsis* Cell Suspensions. *Plant Physiology*, **139**, 1217-1233.
- Wang C.-R., Yang A.-F., Yue G.-D., Gao Q., Yin H.-Y. & Zhang J.-R. (2008) Enhanced expression of phospholipase C 1 (*ZmPLC1*) improves drought tolerance in transgenic maize. *Planta*, **227**, 1127-1140.
- Wang X. (1997) Molecular analysis of phospholipase D. *Trends in Plant Science*, **2**, 261-266.
- Wang X., Guo L., Wang G. & Li M. (2014) PLD: phospholipase Ds in plant signaling. *Springer*, 3-26.
- Wang Z., Dong G., Singh S., Steen H. & Li J. (2009) A simple and effective method for detecting phosphopeptides for phosphoproteomic analysis. *Journal of Proteomics*, **72**, 831-835.
- Wartenberg H. & Blumöhr T. (1966) Untersuchungen der Hyperchlorophyllierung und der Chloroplastenstruktur phosphatmangelkranker Tomatenpflanzen. *Journal of Phytopathology*, **55**, 101-116.
- Weirauch M.T. (2011) Gene Coexpression Networks for the Analysis of DNA Microarray Data. In: *Applied Statistics for Network Biology*, pp. 215-250.
- Williams A.F. (2013) Identification of proteins that putatively bind the promoter of the stomatal master regulator gene, MUTE. Master thesis. *Washington university*.
- Williamson L.C., Ribrioux S.P.C.P., Fitter A.H. & Leyser H.M.O. (2001) Phosphate Availability Regulates Root System Architecture in *Arabidopsis*. *Plant Physiology*, **126**, 875-882.
- Wright P.E. & Dyson H.J. (1999) Intrinsically unstructured proteins: re-assessing the protein structure-function paradigm. *Journal of Molecular Biology*, **293**, 321-331.
- Xue B., Dunbrack R.L., Williams R.W., Dunker A.K. & Uversky V.N. (2010) PONDR-FIT: A meta-predictor of intrinsically disordered amino acids. *Biochimica et Biophysica Acta (BBA) - Proteins and Proteomics*, **1804**, 996-1010.
- Yamaryo Y., Dubots E., Albrieux C., Baldan B. & Block M.A. (2008) Phosphate availability affects the tonoplast localization of PLD ζ 2, an *Arabidopsis thaliana* phospholipase D. *FEBS Letters*, **582**, 685-690.
- Yang J.-S., Gad H., Lee S.Y., Mironov A., Zhang L., Beznoussenko G.V., . . . Hsu V.W. (2008) A role for phosphatidic acid in COPI vesicle fission yields insights into Golgi maintenance. *Nat Cell Biol*, **10**, 1146-1153.
- Yang L.-T., Qi Y.-P., Lu Y.-B., Guo P., Sang W., Feng H., . . . Chen L.-S. (2013) iTRAQ protein profile analysis of *Citrus sinensis* roots in response to long-term boron-deficiency. *Journal of Proteomics*, **93**, 179-206.
- Yao H., Wang G., Guo L. & Wang X. (2013) Phosphatidic acid interacts with a MYB transcription factor and regulates its nuclear localization and function in *Arabidopsis*. *The Plant Cell*, **25**, 5030-5042.
- Yin Y., Yang R. & Gu Z. (2014) Organ-Specific Proteomic Analysis of NaCl-Stressed

- Germinating Soybeans. *Journal of Agricultural and Food Chemistry*, **62**, 7233-7244.
- Young V.R. & Pellett P.L. (1994) Plant proteins in relation to human protein and amino acid nutrition. *The American Journal of Clinical Nutrition*, **59**, 1203S-1212S.
- Yu L., Nie J., Cao C., Jin Y., Yan M., Wang F., . . . Zhang W. (2010) Phosphatidic acid mediates salt stress response by regulation of MPK6 in *Arabidopsis thaliana*. *New Phytologist*, **188**, 762-773.
- Zegzouti H., Li W., Lorenz T.C., Xie M., Payne C.T., Smith K., . . . Christensen S.K. (2006) Structural and functional insights into the regulation of Arabidopsis AGC VIIIa kinases. *Journal of Biological Chemistry*, **281**, 35520-35530.
- Zehr B.D., Savin T.J. & Hall R.E. (1989) A one-step, low background Coomassie staining procedure for polyacrylamide gels. *Analytical Biochemistry*, **182**, 157-159.
- Zehrmann A., Verbitskiy D., van der Merwe J.A., Brennicke A. & Takenaka M. (2009) A DYW Domain-Containing Pentatricopeptide Repeat Protein Is Required for RNA Editing at Multiple Sites in Mitochondria of *Arabidopsis thaliana*. *The Plant Cell*, **21**, 558-567.
- Zhang J. (2003) Evolution by gene duplication: an update. *Trends in Ecology & Evolution*, **18**, 292-298.
- Zhang T., Faraggi E., Li Z. & Zhou Y. (2013a) Intrinsically Semi-disordered State and Its Role in Induced Folding and Protein Aggregation. *Cell Biochemistry and Biophysics*, **67**, 1193-1205.
- Zhang W., Qin C., Zhao J. & Wang X. (2004) Phospholipase D α 1-derived phosphatidic acid interacts with ABI1 phosphatase 2C and regulates abscisic acid signaling. *Proceedings of the National Academy of Sciences of the United States of America*, **101**, 9508-9513.
- Zhang X.D., Wang R.P., Zhang F.J., Tao F.Q. & Li W.Q. (2013b) Lipid profiling and tolerance to low-temperature stress in *Thellungiella salsuginea* in comparison with *Arabidopsis thaliana*. *Biologia Plantarum*, **57**, 149-153.
- Zhang Y., Zhu H., Zhang Q., Li M., Yan M., Wang R., . . . Wang X. (2009) Phospholipase D α 1 and phosphatidic acid regulate NADPH oxidase activity and production of reactive oxygen species in ABA-mediated stomatal closure in Arabidopsis. *The Plant Cell*, **21**, 2357-2377.
- Zhao J. (2015) Phospholipase D and phosphatidic acid in plant defence response: from protein-protein and lipid-protein interactions to hormone signalling. *Journal of Experimental Botany*.
- Zhao J. & Wang X. (2004) Arabidopsis Phospholipase D α 1 Interacts with the Heterotrimeric G-protein α -Subunit through a Motif Analogous to the DRY Motif in G-protein-coupled Receptors. *Journal of Biological Chemistry*, **279**, 1794-1800.
- Zhu J.-K. (2002) Salt and Drought Stress Signal Transduction in Plants. *Annual review of plant biology*, **53**, 247-273.